

**Romanian Society of
Biochemistry & Molecular Biology**

BIOLOGIA

Volume 68 (2023), December, No. 2/2023

**STUDIA
UNIVERSITATIS BABEȘ-BOLYAI
BIOLOGIA**

**2 / 2023
July – December**

©Studia Universitatis Babeș-Bolyai Biologia. Published by Babeș-Bolyai University.
ISSN (online): 2065-9512 | ISSN-L: 2065-9512
Licensed under a Creative Commons Attribution-NonCommercial-
NoDerivatives 4.0 International License.

EDITORIAL BOARD

STUDIA UNIVERSITATIS BABEȘ-BOLYAI BIOLOGIA

JOURNAL EDITOR:

Lecturer **Karina P. Battes**, Babeș-Bolyai University, Cluj-Napoca, Romania.

Contact: studies.ubb.biologia@gmail.com

EDITOR-IN-CHIEF STUDIA BIOLOGIA:

Professor **Manuela Banciu**, Babeș-Bolyai University, Cluj-Napoca, Romania.

SUBJECT EDITORS:

Professor **Nicolae Dragoș**, Babeș-Bolyai University, Cluj-Napoca, Romania (Algology);
Professor **László Gallé**, Member of the Hungarian Academy, University of Szeged, Hungary
(Entomology);

Professor **Michael Moustakas**, Aristotle University, Thessaloniki, Greece (Botany);

Professor **Leontin Ștefan Péterfi**, Associate Member of the Romanian Academy,
Babeș-Bolyai University, Cluj-Napoca, Romania (Algology);

Professor **László Rakosy**, Babeș-Bolyai University, Cluj-Napoca, Romania (Entomology);

Senior Researcher **Anca Sima**, Associate Member of the Romanian Academy,
Institute of Citology and Cellular Pathology, Bucharest, Romania (Cellular Biology);

Professor **Helga Stan-Lötter**, University of Salzburg, Salzburg, Austria (Microbiology);

Associate Professor **Anca Butiuc-Keul**, Babeș-Bolyai University, Cluj-Napoca, Romania
(Biotechnologies);

Associate Professor **Ioan Coroiu**, Babeș-Bolyai University, Cluj-Napoca, Romania (Vertebrates);

Associate Professor **Beatrice Kelemen**, Babeș-Bolyai University, Cluj-Napoca, Romania
(Human Genetics, Bioarcheology);

Lecturer **Mirela Cîmpean**, Babeș-Bolyai University, Cluj-Napoca, Romania (Hydrobiology);

Lecturer **Cristina Craioveanu**, Babeș-Bolyai University, Cluj-Napoca, Romania
(Entomology, Terrestrial invertebrates);

Lecturer **Irina Goia**, Babeș-Bolyai University, Cluj-Napoca, Romania (Plant communities);

Lecturer **Andre Jakob**, Babeș-Bolyai University, Cluj-Napoca, Romania
(Molecular biology, microbiology);

Lecturer **Anca Stoica**, Babeș-Bolyai University, Cluj-Napoca, Romania (Animal physiology);

Lecturer **Vlad Alexandru Toma**, Babeș-Bolyai University, Cluj-Napoca, Romania
(Histology, Biochemistry);

Teaching Assistant **Adorjan Cristea**, Babeș-Bolyai University, Cluj-Napoca, Romania (Vertebrates).

SITE ADMINISTRATOR:

Bogdan Hărăștășan, Babeș-Bolyai University, Cluj-Napoca, Romania.

LIST OF ASSOCIATE REVIEWERS:

Associate Professor **Eszter Ruprecht**, Babeș-Bolyai University, Cluj-Napoca, Romania;

Lecturer **Alin David**, Babeș-Bolyai University, Cluj-Napoca, Romania;

Lecturer **Anca Farkas**, Babeș-Bolyai University, Cluj-Napoca, Romania;

Lecturer **Alexandru N. Stermin**, Babeș-Bolyai University, Cluj-Napoca, Romania;

Lecturer **Lucian Alexandru Teodor**, Babeș-Bolyai University, Cluj-Napoca, Romania;

Biologist **Octavian Craioveanu**, Babeș-Bolyai University, Cluj-Napoca, Romania.

YEAR
MONTH
ISSUE

Volume 68 (LXVIII), 2023
DECEMBER
2

PUBLISHED ONLINE: 2023-12-28
ISSUE DOI: 10.24193/subbbiol.2023.2
ISSN (online): 2065-9512
<https://studiabiologia.reviste.ubbcluj.ro/>

STUDIA
UNIVERSITATIS BABEŞ-BOLYAI
BIOLOGIA
2

SUMAR – CONTENT – SOMMAIRE – INHALT

*ABSTRACTS OF THE ANNUAL INTERNATIONAL CONFERENCE OF THE
ROMANIAN SOCIETY OF BIOCHEMISTRY AND MOLECULAR BIOLOGY,
SEPTEMBER 13-15, 2023, CLUJ-NAPOCA, ROMANIA*

S.M. Petrescu, Deciphering endoplasmic reticulum associated protein degradation: EDEM proteins.....	11
A. Filimon, G. Negroiu, New molecular mechanisms involved in melanoma cell resistance to nutritional and chemotherapeutic stress.....	13
D. Cruceriu, L. Gavrilaş, O. Sava, Curcumin reverses the irinotecan acquired resistance in colorectal cancer cells, in vitro.....	15
T. Stratulat, R. Tecucianu, C. Coman, A. Ionescu, C. Trif, A.S. Anghel, R. Badea, A. Babes, S. Petrescu, S. Tunaru, GPR75, an unusual and mesmerizing novel therapeutic target.....	17
M.D. Copolovici, A. Gostăviceanu, C. Popa, C. Moisa, A.I. Lupitu, O. Gavriliuc, F. Bojin, L. Copolovici, New cell-penetrating peptides with antimicrobial properties.....	19

O.L. Pop, C. Ciont, D.C. Vodnar, A. Mesaros, Iron oxide nanoparticles carried by probiotics in iron absorption	21
V.F. Rauca, L. Pătraș, G. Negrea, E. Licărete, A. Porfire, L. Barbu, L. Lupuț, A. Sesărman, M. Banciu, The use of functionalized liposomes and extracellular vesicles as drug delivery systems with high cancer-targeting efficacy.....	23
N. Nichita, A.M Pantazica, M.O Dobrica, C. Lazara, C. Tucureanu, I. Caras, I. Ionescu, A. Costache, A. Onu, J. Liu-Clarke, C. Stavaru, Production of chimeric subviral particles with enhanced immunogenicity for the development of next-generation HBV vaccines.....	25
A. Juncu, D. Ion, P. Forian, G. Chiritoiu, T. Sulea, A. Borota, L. Crisan, A. Bora, S. Avram, O. Vlaicu, D. Otelea, U. Bilitewski, L. Spiridon, L. Pacureanu, C.I. Popescu, Novel HTS cell based assay for cis acting protease activity identifies Hepatitis C Virus NS2 cysteine protease inhibitors with antiviral activity.....	27
M.A. Socaciu, D. Rugina, Z. Diaconeasa, M. Nistor, C. Socaciu, Multifunctional complexes nanolipid - microbubbles for a targeted delivery of antitumor drugs by ultrasonography-assisted procedures.....	29
A. Roseanu, M. Icriverzi, P. E. Florian, L. Sima, O. Gherasim, V. Gurmazescu, G. Socol, F. Ionita, C. Coman, Medical devices for skin-wound healing; from bench to in vivo study	31
M.O Dobrica, A. van Erde, C. Tucureanu, A. Onu, L. Paruch, I. Caras, E. Vlase, H. Steen, S. Haugslie, D. Alonzi, N. Zitzmann, R. Bock, C.I. Popescu, C. Stavaru, J. Liu-Clarke, N. Nichita, Plant-produced Hepatitis C Virus E2-derived glycoproteins for vaccine development.....	33
M. Sarbu, R. Ica, A.D. Zamfir, Identification of novel potentially active chondroitin/dermatan sulfate domains in human decorin by ion mobility mass spectrometry	35
D.M. Buda, H.L. Banciu, Transcriptomic profiling of halophilic archaeon <i>Haloferax alexandrinus</i> DSM 27206T grown under silver stress.....	37
L.E. Sima, M. Tudor, C. Munteanu, G. Chiritoiu, F. Jipa, S. Orobeti, F. Sima, S.M. Petrescu, G.E. Schiltz, D. Matei, Targeting tumor cells and ovarian tumor microenvironment using tissue transglutaminase inhibitors.....	39
L. Spiridon, T.A, Șulea, V. G. Ungureanu, E.C. Martin, A.J. Petrescu, Robosample: Harnessing the Power of Constrained Molecular Dynamics and Gibbs Sampling to Investigate Macromolecules.....	41
A.J. Petrescu, Computational Assisted Investigation of Two Key Protein Families of the Immune System	43
A. Pintea, P. Muntean, A. Bunea, Francis V. Dulf, M. Focșan, C. Coman, D. Rugină, Zeaxanthin oil-in-water nanoemulsions as delivery systems for food or nutraceuticals applications	44
D. Rugină, M. Nistor, Z. Diaconeasa, M. Focșan, L.Găină, M. Cenariu, R. Pop, C. Socaciu, A. Pintea, Crimson serenade: anthocyanins orchestrating melanoma defense, revealing oxidative stress and mitochondrial membrane potential through the enchantment of fluorescence free molecules and encapsulated brilliance	46

R.S. Boiangiu, E. Bagci, G. Dumitru, L. Hritcu, E. Todirascu-Ciornea, The neurological effects of <i>Glaucosciadium cordifolium</i> (Boiss.) Burt & Davis essential oil in a zebrafish model of cognitive impairment.....	48
C. Ciont, G. Difonzo, A. Pasqualone, S.M.Chis, F. Ranga, K. Szabo, E. Simon, A. Naghiu, L. Barbu-Tudoran, D.C. Vodnar, O.L. Pop, Phenolic profile of micro- and nano-encapsulated olive leaf extract in biscuits during <i>in vitro</i> gastrointestinal digestion.....	49
L.M. Cucuș, T.A. Șulea, L. Spiridon, I. Caras, I. Ionescu, A. Costache, C. Stavaru, N. Nichita, C.I. Popescu, Hepatitis C Virus Envelope Protein E2 Antigen Design and Characterization for Vaccine Development.....	50
A.M. Tripon, A. Cristea, H.L. Banciu, Reacting to stress: upregulating the genes involved in polyhydroxybutyrate synthesis during nutrient starvation by <i>Halomonas elongata</i> DSM 2581T.....	52
B. Dume, A. Sesărman, M. Banciu, E. Licărete, Overcoming doxorubicin resistance in B16.F10 melanoma cells by targeting Hypoxia-Inducible Factor-1 alpha	54
A.M. Pantazică, A. van Eerde, M.O. Dobrică, I. Caras, I. Ionescu, A. Costache, C. Tucureanu, H. Steen, C. Lazăr, I. Heldal, S. Haugslie, A. Onu, C. Stăvaru, J. Liu-Clarke, N. Nichita, “Humanization” of the N-glycosylation pathway in <i>Nicotiana benthamiana</i> via CRISPR/Cas9 technology significantly improves the immunogenicity of HBV antigens and the virus- neutralizing antibody response in vaccinated mice.....	56
G. Negrea, S. Meszaros, S. Drăgan, V.A. Toma, B. Dume, V.F.Rauca, L. Pătraș, E. Licărete, M. Banciu, A. Sesărman, 3D tumor spheroids as a model to unriddle the complexity of tumor microenvironment chemoresistance	58
I. Honceriu, I. Brinza, R.S. Boiangiu, L. Hritcu, Anti-dementia effects of mansorin A, mansonone G, and 6-paradol in zebrafish (<i>Danio rerio</i>).....	60
I. Brinza, A.B. Stache, R.S. Boiangiu, O. Eldahshan, D.L.Gorgan, M. Mihasan, L. Hritcu, Baicalein 5,6-dimethyl ether prevent scopolamine-induced memory impairment in zebrafish by increasing the creb1 protein level and the mRNA expression of bdnf and creb1 gene	61
P. Miron, B. Boșca, A.D. Andreicuț, A. Parvu, A.C. Moț, Advancing selenium analysis: method optimization, validation, and its application in assessing selenium levels in selenate-treated rats.....	63
A.R. Lazăr, A.M. Mocan, A. Pușcaș, A.E. Mureșan, F. Ranga, A.M. Truță, V. Mureșan, Evaluation of phenolic compounds from the morphological parts of beechnut (<i>Fagus sylvatica</i> L.).....	65
V.G. Ungureanu, I. Popa, C. Tănase, L. Spiridon, <i>In-silico</i> study of RAGE-S100B Inhibitors	67
A. S. Podar, C.A. Semeniuc, F. Ranga, M.I. Socaciu, M. Fogarasi, A.C. Fărcaș, D.C. Vodnar, S.R. Ionescu, S.A. Socaci, Preliminary results on the recovery of coenzyme Q10 from vegetable and animal waste	69
T.A. Șulea, N. Papadopoulous, S.N. Constantinescu, L. Spiridon, A.J. Petrescu, Unraveling molecular basis of myeloproliferative neoplasms (MPN) by experimentally constrained modelling and simulation.....	70

A. El-Sabeh, M. Mihășan, Long-read direct RNA nanopore sequencing of the nicotine-related transcriptome of <i>Paenarthrobacter nicotinovorans</i> ATCC 49919	72
A.M. Dăescu, M. Nistor, M. Focșan, R. Pop, A. Pinte, M. Suci, D. Rugină, pH-responsive nanocapsules for anthocyanins encapsulation, delivery, intracellular tracking, and controlled release inside B16-F10 melanoma cells.....	74
A.B. Tigu, C.S. Constantinescu, P. Teodorescu, D. Kegyes, R. Munteanu, R. Feder, M. Peters, I. Pralea, C. Iuga, D. Cenariu, A. Marcu, A. Tanase, A. Colita, R. Drula, J.T. Bergthorsson, V. Greiff, D. Dima, C. Selicean, I. Rus, M. Zdrenghia, D. Gulei, G. Ghiaur, C. Tomuleasa, Design and preclinical testing of an anti-CD41 CAR T cell for the treatment of acute Megakaryoblastic leukemia.....	76
A.M. Negrescu, V. Mitran, F. Miculescu, A. C. Mocanu, A.E. Constantinescu, A. Cimpean, <i>In vitro</i> biological performance of 3D-printed PLA-based composites as bone scaffolds	78
A.D. Lazăr (Popa), L. Slemain, M.M. Marin, M.G. Albu-Kaya, M. Costache, S. Dinescu, Novel biohybrid enriched with curcumin and quercetin displays favorable properties as potential active wound dressing for biomedical applications.....	80
B. Galateanu, A. Cowell, V. Uivarosi, M. Charitaki, K. Velonia, A. Hudita, La(Nal) ₃ loaded PDMAEMA NPs induce HT-29 adenocarcinoma cells apoptosis <i>in vitro</i>	82
B. Stoean, I. Lupan, Luiza Găină, Novel photosensitizing methylene blue analogues for antimicrobial photodynamic therapy	84
M.P. Ciurlic, A.M. Colpoș, M. Ștefan, M. Mihășan, Building a 3D printed microscope – the OpenFlexure@BioIASI project.....	85
D. Cenariu, A.B. Tigu, D. Kegyes, M. Peters, J.T. Bergthorsson, V. Greiff, M. Cenariu, G. Ghiaur, C. Tomuleasa, MDS cells maturation induced by ATRA differentiating agent in myelodysplastic syndromes.....	86
G. Negrea, S. Meszaros, S. Drăgan, V.A. Toma, B. Dume, V.F. Rauca, L. Pătraș, E. Licărete, M. Banciu, A. Sesărman, 3D tumor spheroids as a model to unriddle the complexity of tumor microenvironment chemoresistance	88
L. Copolovici, A. Gostăviceanu, S. Gavrilaș, D.G. Radu, M. Dochia, C. Moisa, A.I. Lupitu, D.M. Copolovici, Peptide-based therapeutics	90
M. Icriverzi, P.E. Florian, A. Bonciu, N. Dumitrescu, L. Rusen, V. Dinca, A. Roseanu, Cell behaviour modulation by new polydimethylsiloxane (PDMS) modified interfaces	91
M.A. Matica, A. Năstasie, A. Tudor, T. Kelemen, R. Alicu, D.L. Roman, Biodegradable chitosan-based films for biomedical applications	93
M.S. Meszaros, G.G. Negrea, V.A. Toma, V.F. Rauca, E. Licărete, L. Pătraș, M. Banciu, A. Sesărman, Development of a 3D Model for immunotherapy evaluation in melanoma	95

M. Moruz, A. Campu, S. Astilean, M. Focsan, Miniaturized electrochemical biosensor for troponin i protein - cardiac biomarker detection.....	97
I.T. Munteanu, M. Mihășan, Develop a genetic engineering tool for <i>Paenarthrobacter nicotinotans</i> ATCC 49919	98
P. Muntean, A. Pinte, A. Bunea, F.V. Dulf, M. Focșan, D. Rugină, Carotenoid loaded nanocarriers – preparation and evaluation	100
P.E. Florian, M. Icriverzi, A. Bonciu, L.N. Dumitrescu, D. Pelinescu, C. Munteanu, L.E. Sima, V. Dinca, L. Rusen, A. Roseanu, Synthesis, characterization and in vitro evaluation of a new smart responsive pNIPAM –based biopolimer with antimicrobial and antitumoral activity.....	102
R. Nachawati, P. Florian, A. Roseanu, C.I. Popescu, A new design of Hepatitis C Virus E2 chimeric protein oligomer as a vaccine candidate....	104
R. Pop, A. Boldianu, M. Nistor, M. Suci, A. Pinte, M. Focsan, D. Rugină, Resveratrol: NIR-responsive microcarrier-based polymeric delivery system to enhance its therapeutic potential towards diabetic retina cells	106
A. Ghionescu, M. Uță, C. Lazăr, P. Alexandru, N. Nichita, The endoplasmic reticulum (ER) degradation-enhancing alpha-mannosidase-like protein 3 is a host cell regulator of HBV infection.....	108
A.A.M. Botezatu, D.I. Băcioiu, F. Piciu, D. Cucu, Roles of transient receptor potential melastatin 8 (TRPM8) and epidermal growth factor receptor (EGFR) in glioblastoma.....	110
R.A. Badea, A.S. Anghel, T. Stratulat, S. Tunaru, SREB receptor family members differentially regulate protein expression and processing	111
G. Ágoston, K. Boros, R.B. Tomoioagă, L.C. Bencze, Data mining and protein engineering for aromatic ammonia-lyases with enhanced activity towards challenging substrates	113
M. Nistor, M. Focsan, L. Gaina, M. Cenariu, A. Pinte, C. Socaciu, D. Rugina, Fluorescence imaging in real-time employed to visualize the presence of anthocyanins complexed with diphenylboric acid 2-aminoethyl inside B16-F10 melanoma cells.....	115
M.Ș. Dobrescu, D.A. Țoc, A. Butiuc-Keul, Integrins and HGT – How do integrins affect HGT in multidrug resistant Gram-negative ESKAPE pathogens.....	117
M. Płóciennik, L. Kiczak, U. Paśławska, W. Gozdzik, B. Adamik, M. Zielinska, S. Zieliński, K. Nowak, J. Bania, M. Nowak, R. Paśławski, C. Frostell, Unchanged amount, localization and activity of glucocorticoid receptor in combination therapy - inhaled nitric oxide and intravenous hydrocortisone in porcine endotoxemia model	119
A.I. Moatăr, A.R. Chiș, D. Nitusca, C. Marian, C. Oancea, I.O. Sîrbu, Altered expression of microRNA-195 might contribute to a severe outcome in SARS-CoV-2 infection.....	121
A.A. Rus, I. Militaru, I. Popa, Ș. Petrescu, NPC1 regulates specific cargo traffic to lysosome related organelles and melanosome biogenesis	123

S.A. Anghel, C. Trif, R.A. Badea, A.E. Ionescu, T. Stratulat, C. Triță, S. Tunaru, Ș.M. Petrescu, GPR27, insulin secretion regulator and beyond.....	124
S. Buzatoiu, S. Tunaru, N. Nichita, GPR27 inhibits Hepatitis B Virus internalisation and replication	126
Ș.M. Drăgan, V.A. Toma, Analytical differences between hemoglobin peroxidase and enzyme-based peroxidase activity in tissue lysates	127
A. El-Sabeh, A.M. Mlesnita, I.T. Munteanu, I. Honceriu, F. Kallabi, R.Ș. Boiangiu, M. Mihășan, A highly syntenic nic-genes cluster is present in several related bacterial strains.....	129
D. Iordache, M. Dobrescu, A. Fita, A. Butiuc-Keul, The intricate relationship between the CRISPR-Cas system and antibiotic-resistance genes in <i>Klebsiella pneumoniae</i>	130
M.R. Biricioiu, M. Sarbu, R. Ica, A.D. Zamfir, Ion mobility mass spectrometry of human cerebellum gangliosides.....	132
M. Mernea, C. Mares, S. Avram, The pharmacological profile of natural compounds from <i>Aconitum</i> sp.....	134
M. Sarbu, D.E. Clemmer, Ž. Vukelić, A.D. Zamfir, Glicolipidomics of human glioblastoma multiforme by ion mobility mass spectrometry	136
M. Tudor, C. Munteanu, G. Chiritoiu, F. Jipa, Ș.M. Petrescu, G.E. Schiltz, D. Matei, L.E. Sima, New strategies for potentiating the effect of tissue transglutaminase-fibronectin small molecule inhibitors in ovarian cancer treatment.....	138
P.D. Ciordas, M. Romanescu, A.R. Chis, C. Marian, I.O. Sîrbu, Absolute and relative expression analysis of plasma microRNAs in patients with prostate cancer – a comparison.....	140
R. Ica, K. Mlinac-Jerković, S. Kalanj-Bognar, C.V.A. Munteanu, A.J. Petrescu, A.D. Zamfir, Profiling and structural characterization of gangliosides in human temporal lobe epilepsy	142
A. Varadi, C. Cimpoi, A.C. Mot, Evaluation of total iodine uptake in biofortified chilli peppers	144
C.A. Gîlcescu (Florescu), G. Bica, E.C. Stănciulescu, L. Colhon, C.G. Pisoschi, <i>In vitro</i> and <i>in vivo</i> assessment of the antioxidant properties of <i>Apis mellifera</i> venom	145
C.A. Faur, M. Zăhan, G. Roman, C.I. Bunea, E. Hârșan, A. Bunea, Antioxidant and antiproliferative activity of anthocyanin rich extract from roses (<i>Rosa</i> L.).....	146
C. Gherasim, A. Pintea, Valorization of carotenoid from sea buckthorn pomace using green solvents and ultrasound-assisted extraction	148
F.V. Scurtu, D. Clapa, F. Ranga, V. Coman, A.C. Moț, S.A. Socaci, L.F. Leopold, C. Coman, Toxicity of Gadolinium on <i>Stevia rebaudiana</i> grown <i>in vitro</i>	150
I.A. Barbu, A. Ciorîță, R. Carpa, A.C. Moț, A. Butiuc-Keul, M. Pârveu, <i>Allium sativum</i> and <i>Allium ursinum</i> extracts: antimicrobial activity and phytochemical characterization.....	152

L.F. Leopold, F.V. Scurtu, D. Clapa, N. Leopold, S.D. Iancu, F. Ranga, S.A. Socaci, C. Coman, Assessing the risks of nanoplastic exposure to plants: Implications for growth and steviol glycoside production.....	154
M. Aurori, D. Hanganu, E. Pall, M. Cenariu, S. Andrei, Antioxidant and cytoprotective effects of <i>Sorbus aucuparia</i> L. fruit extract in gentamicin-induced nephrotoxicity on mice renal cells	155
M. Iakab, E. Domokos, C. Albert, B. Biró-Janka, F.V. Dulf, The Effect of <i>Rhizophagus irregularis</i> on Phenolics and Essential Oil of the <i>Echinacea purpurea</i> (L.) Moench.....	157
M. Cotul, D.A. Dumitraş, A. Dreancă, A.P. Ungur, S. Andrei, Antioxidant supplementation and its impact on inflammatory and oxidative stress parameters in diet-induced obesity rats	159
L.F. Popovici, L.A. Oprică, The impact of silica nanoparticles (SiNPs) on some biochemical parameters in <i>Silybum marianum</i> seedlings	161
R. Tripon, C. Gaşpar, D. Camen, M. Enea, R. Romănu, C. Tulcan, The GC-MS analysis of some volatile oils and the evaluation of their antibacterial properties against <i>S. aureus</i> and <i>E. coli</i> bacterial strains.....	163
A.C. Tocai, S.I. Vicas, Polyphenols and antimicrobial activity in glycerol <i>Sanguisorba officinalis</i> L. and <i>Sanguisorba minor</i> Scop. Roots extracts.....	165
S.I. Vicas, V. Laslo, E. Klezken, A.R. Memete, T.E. Fertig, D.S. Marta, <i>In vitro</i> antioxidant and antigenotoxic potential of <i>Viscum album</i> L. subsp. <i>Album</i>	167
C. Trif, S. Tunaru, Strategy for deorphanizing G-protein coupled receptor 75 using brain extract fractions.....	169
D.I. Băcioiu, F. Piciu, A.A.M. Botezatu, D. Cucu, Interactions between transient receptor potential subfamily ankyrin member 1 (TRPA1) and the epidermal growth factor receptor (EGFR) in glioblastoma	170
E. Matei, A. Filip, C.G. Floare, A. Pirnau, M. Mic, Molecular aggregation pathway of cataract-associated γ D-crystallin p23T congenital defect	172
F.S. Bectaş, T.A. Şulea, L. Spiridon, A.J. Petrescu, Modelling of MHC-I Peptide Loading Complex.....	174
I. Popa, C. Tanase, B. Ellinger, J. Reinshagen, P. Gribbon, High-throughput screening to identify inhibitors of RAGE-S100B interaction.....	176
L.M. Stănescu, C. Aramă, Ş. Petrescu, C.V.A. Munteanu, RP-HPLC studies on chiral separations of racemic nonapeptides sulfoxides.....	178
M. Lehene, R. Silaghi-Dumitrescu, The first complex of cobalamin with an organic peroxide	180
R.M. Tecucianu, S. Tunaru, Ş.M. Petrescu, Synthesis, degradation and trafficking processes of the GPR75 receptor.....	181
R. Szabó, C.P. Rácz, F.V. Dulf, Study on the interactions between icaraside II and whey protein concentrate	183

REGULAR ARTICLES

- N. Chaabane, S. Chafaa, F. Naama, Y. Nouidjem, F. Mimeche, Population dynamics of *Euphyllura olivina* Costa, 1857 (Psyllidae: Hemiptera) in olive trees in the semi-arid region of Djelfa (Algeria) 185
- R. Rechid, M. Laamari, A. Goldarazena, First notes on plant diversity, finding sites and sex ratio in natural populations of *Thrips tabaci* Lindeman (Thysanoptera: Thripidae) in Algeria (Biskra province)..... 197
- S.-D. Covaciu-Marcov, D.-M. Pop, F.-N. Sucea, G.-A. Ile, A.-Ş. Cicort-Lucaciu, S. Ferenţi, Good news from newts: distribution, population size, and dynamics of two protected newt species in the Jiu Gorge National Park, Romania 219
- L. Benhalima, S. Amri, M. Bensouilah, Dual resistance to heavy metals and antibiotics of *Aeromonas hydrophila* isolated from *Carassius carassius* (Linnaeus, 1758) in Lake Tonga, Algeria..... 235

All authors are responsible for submitting manuscripts in comprehensible US or UK English and ensuring scientific accuracy.

Original picture on front cover:
Logo of the Romanian Society of Biochemistry and Molecular Biology
© <https://srbbm.biochim.ro/>

Deciphering endoplasmic reticulum associated protein degradation: EDEM proteins

Stefana M. Petrescu¹✉

¹*Institute of Biochemistry, Romanian Academy, Bucharest, Romania,*

✉ *Corresponding author, E-mail: stefana.petrescu@biochim.ro*

Introduction: Endoplasmic reticulum associated protein degradation, ERAD, is a highly regulated process that clears the crowded ER lumen of polypeptides with fatal folding errors, leaving the ER in a folding competent state. EDEM proteins are able to recognize some misfolded glycoproteins and to trim the Man9 N-glycans in order to target the glycoproteins to degradation by proteasomes. Despite many advances in the field and the validation of a number of mutants that are EDEM substrates there is still unclear what is the physiological role of this family of proteins and whether there are endogenous proteins targeted by EDEM during ERAD. EDEM family includes three proteins, EDEM-1, EDEM-2 and EDEM3, highly conserved from *C.elegans* to mammalian. We addressed the role of EDEMs in *C.elegans* in order to understand their physiological role in an organism. We also aimed to identify EDEMs interactors in mammalian systems and endogenous proteins that are targeted to degradation by EDEMs.

Materials and methods: We used CRISPR/Cas technology to obtain cell lines depleted in genes involved in ERAD. *C.elegans* was used to investigate the ERAD at an organismal level. To identify interactors and ERAD substrates we used mass spectrometry based proteomics.

Results: Using the model organism *C.elegans*, we found that there are distinctive differences in the roles of the three EDEMs, with EDEM2 validated as physiologically crucial in maintaining protein homeostasis. The other two EDEMs are required to protect the organism during acute ER stress. We also report the discovery of a number of endogenous substrates for EDEM2 whose half-life determined using SILAC high performance mass spectrometry was regulated by EDEM2. EDEM3, one of the most active EDEM mannosidase has four consecutive modules that we were able to model and address their individual roles. We also identified a particular sensitivity of EDEM3 towards the ER redox environment, suggesting a mechanism involving rearrangements of disulfide bridges.

Conclusions: EDEM proteins are involved in the quality control of endogenous proteins in mammals and the role of the three proteins is significantly different under physiological ER stress conditions.

Acknowledgements: This work was funded from Romanian Academy projects, PN-III-P1-1.1-PD-2016-1528, PN-III-P1-1.1-PD-2019-1242, PN-III-P1-1.1-PD-2019-1278, PNCDI-III-PCCDI-2018-1.

New molecular mechanisms involved in melanoma cell resistance to nutritional and chemotherapeutic stress

Anca Filimon¹✉ and Gabriela Negroiu¹

^{1,2} *Institute of Biochemistry of Romanian Academy, Bucharest, Romania,*
✉ *Corresponding author, E-mail: anca_m_filimon@yahoo.com*

Introduction: During tumor development cancer cells are subjected to various stress conditions due to high proliferation rates, limited levels of oxygen, glucose, amino acids or the presence of reactive oxygen species. Tumor expansion and metastasis can be successful only if cancer cells can adapt to these stressful conditions through activation of signaling cascades and transcriptional programs which determine the expression of the necessary adaptive genes. Activating transcription factor 4 (ATF4) is the master regulator of cellular stress responses triggered by multiple signaling pathways that form the integrated stress response (ISR). The phosphorylation of the alpha subunit of eukaryotic translation initiation factor 2 (eIF2 α) on serine 51 is the core event of the ISR that leads to a marked reduction in global protein synthesis while allowing the translation of selected genes including ATF4. Besides the canonical induction by ISR recent studies have shown that ATF4 is activated by the mechanistic target of rapamycin complex 1 (mTORC1) as a part of an anabolic program initiated by pro-growth signals. While translational regulation of ATF4 is one of the main mechanisms for ATF4 expression, transcriptional control is also important for ATF4 mediated cellular processes. Besides stress conditions generated by a rapid tumor growth and anabolic processes, ATF4 is also induced by chemotherapeutic stress and can be a major player in tumor cell resistance to chemotherapy. Dopachrome tautomerase (DCT) is an enzyme involved in the distal step of melanin biosynthesis in melanocytes and melanoma cells and has been shown to reduce melanoma cells sensitivity to oxidative stress and protect cells from UV or X ray induced apoptosis. So far, the molecular mechanisms through which DCT modulates cellular stress responses have not been elucidated. Moreover, DCT expression assessed in melanoma FFPE specimens has been associated with unfavorable clinical parameters (ulceration and a high number of mitoses) and biomarkers indicative of metastatic progression.

Materials and methods: melanoma primary and metastatic cell lines (WM35, WM39, MJS, SKMel23, SKMel28), cell culture media, supplements and sterile plasticware, siRNAs, CRISPR/Cas9, LC/MS, RT-qPCR, Western Blot.

Results: ATF4 and DCT expressions are correlated in MJS growing cell cultures at protein and mRNA levels and respond to variations in the concentrations of non essential aminoacids.

Downregulation of DCT expression through siRNAs or CRISPR/Cas9 determines a marked reduction in the expression of ATF4 and its target gene asparagin synthetase (ASNS) at protein and mRNA levels.

DCT protein levels are upregulated in BRAF mutated V600E melanoma cells treated with Vemurafenib or in BRAF WT cells where BRAF expression is silenced with siRNAs.

Conclusions: DCT is a novel protein associated with ATF4 expression either as part of the ISR or in anabolic processes controlled by mTOR signalling.

DCT is a novel regulator of ATF4 and its target gene ASNS at mRNA and protein levels in multiple BRAF WT and BRAF mutated melanoma cell lines.

DCT is upregulated as a result of signalling blockade on RAS-RAF-MAPK-ERK pathway and is a novel candidate player in the resistance to chemotherapy through regulating ATF4 expression levels. ***The decipheration of DCT-ATF4 axis is important for a better understanding of melanoma molecularity and possibly for development of novel therapeutical approaches in some tumor subtypes.***

Acknowledgements: This work was funded from PCCDI project nr. 61/2018.

Curcumin reverses the irinotecan acquired resistance in colorectal cancer cells, *in vitro*

Daniel Cruceriu^{1,2✉}, Laura Gavrița³ and Oana Sava²

¹ Department of Molecular Biology and Biotechnology, Babes-Bolyai University, Cluj-Napoca, Romania; ² Department of Genetics, Genomics and Experimental Pathology, The Oncology Institute "Prof. Dr. Ion Chiricuta", Cluj-Napoca, Romania; ³ Department of Bromatology, Hygiene, Nutrition, "Iuliu Hatieganu" University of Medicine and Pharmacy, Cluj-Napoca, Romania
✉ Corresponding author, E-mail: daniel.cruceriu@ubbcluj.ro

Introduction: A major problem in the management of colorectal cancer (CRC) is represented by the tumor acquired resistance to conventional chemotherapy, including irinotecan, a compound usually administrated in advanced CRC, as a first- or second-line chemotherapeutic drug. Specific plant-derived compounds have the potential to resensitize chemoresistant cancer cells to certain drugs. Curcumin, the major bioactive compound found in *Curcuma longa* is one such promising compound. Therefore, the purpose of this study was to assess curcumin's capacity to reverse the acquired resistance to irinotecan of CRC cells and provide novel insights into the cellular and molecular processes associated with it.

Materials and methods: An irinotecan-resistant cell line (DLD1_IRI-R) was obtained through successive exposures of DLD1 cells to increasing concentrations of irinotecan, until cells would survive and proliferate in culture medium containing the drug at a concentration of 20 μ M, the concentration at which irinotecan is found in the blood stream of CRC patients. The MTT assay was used to evaluate the sensitivity of both cell lines to irinotecan and curcumin, administered alone or in combination at different concentrations, at 48h after exposure. The nature of the interaction between the two compounds was determined by the Chou-Talalay method, whereas curcumin's capacity to reverse the irinotecan-acquired resistance was evaluated based on the Reversal Fold (RF) parameter. Flow-cytometry was used to assess apoptosis, whereas clonogenicity assays were used to monitor proliferation in all experimental settings. Whole- genome transcriptional profiling of the irinotecan-sensitive, irinotecan-resistant and curcumin-treated irinotecan-resistant cell lines was performed by microarray technology, whereas the functional analysis of the data was performed in IPA (Ingenuity Pathway Analysis) and GESA (Gene Set Enrichment Analysis).

Results: DLD1_IRI-R cells were 7.17X more resistant to irinotecan than the parental cells. Based on the whole transcriptome data, as well as the clonogenicity assays, one of the main mechanisms by which CRC cells acquire resistance to irinotecan is by slowing down the cell cycle, several molecular pathways involved in proliferation being inhibited. Interestingly, the resistance to curcumin also increased (3.2X) in the irinotecan-resistant cell line, suggesting the activation of more general drug-induced resistance mechanisms. When a combinatorial treatment of irinotecan in successive concentration and curcumin at a constant low concentration (IC10) was administered on DLD1_IRI-R cells, a significant decrease in the irinotecan specific IC50 was observed, demonstrating a resistance reversal fold of 3.74X. Furthermore, the combined treatment was characterized by synergistic effects on the resistant cell line according to the Chou-Talalay analysis ($CI < 1$) for every tested combination of concentrations, both in experiments with a constant-dose ratio and in combinations of irinotecan with curcumin at IC5, IC10, IC15 or IC20. The observed synergistic effects are most likely due to the different mechanisms by which the compounds affect cells: irinotecan triggers cell cycle arrest, while curcumin induces apoptosis, as demonstrated by flow-cytometry. Besides inducing apoptosis, curcumin also reactivated several signaling pathways which promote proliferation and triggered the inhibition of several genes known to be involved in drug efflux, increasing the overall sensitivity of the tumor cells.

Conclusions: Curcumin might be capable of reversing the acquired resistance to irinotecan in CRC cells by inducing apoptosis, retriggering cell proliferation and sensitizing cells to irinotecan, whereas the combinatorial therapy could increase the conventional treatment efficacy.

Acknowledgements: This work was funded by the Romanian Ministry of Education and Research, No. PN-III-P1-1.1-PD-2019-0468.

GPR75, an unusual and mesmerizing novel therapeutic target

Teodora Stratulat^{1,3}, Ramona Tecucianu¹, Cristin Coman²,
Aura Ionescu¹, Cosmin Trif¹, Anghel S. Andreea¹, Rodica Badea¹,
Alexandru Babes³, Stefana Petrescu⁴ and Sorin Tunaru¹✉

¹ Cell Signalling Research Group, Institute of Biochemistry of the Romanian Academy, Bucharest, Romania; ² National Institute of Research and Development for Microbiology and Immunology "Cantacuzino", București, Romania; ³ Department of Anatomy, Physiology, and Biophysics, Faculty of Biology, University of Bucharest, Bucharest, Romania; ⁴ Molecular Cell Biology Department, Institute of Biochemistry of the Romanian Academy, Bucharest, Romania;
✉ **Corresponding author, E-mail:** sorin.tunaru@googlemail.com

Introduction: GPR75 belongs to the largest superfamily of membrane receptors, G-protein coupled receptors (GPCRs). The particularity of GPR75 is that no ligand or biological roles have been clearly assigned to it, despite several studies pointing to its implication in the regulation of human and mouse metabolism. In mouse and humans, GPR75 is highly expressed in brain, pancreas, liver and retina. Large scale human exome analysis associated GPR75 presence with increased sensitivity of individuals to obesity.

Materials and methods: HEK293T, COS-7, HeLa cell lines were transiently transfected with plasmids containing the cDNA of human GPR75, muscarinic acetyl-choline receptors (hM1-hM5) and genetic probes sensitive and specific for intracellular calcium and cAMP. Forty-eight hours after the transfection, cells were loaded with HBSS buffer containing luciferases and determination of agonists-induced messenger accumulation was performed by using a 96-well plate reader (Flexstation 3, Molecular Devices). Phylogenetic analyses were carried out by using MEGA11 software. GPR75 deficient mice were generated by homologous recombination in ES cells. Groups of wild-type and GPR75 deficient mice were subjected to high-fat diet for more than six month. Body weight, food and water consumption was recorded on a daily base.

Results: Our results indicate that GPR75 is an ancient receptor that resembles no sequence similarity to any known GPCR. Studies performed by expressing human GPR75 in HEK293T and other cell lines demonstrated a potential role in the modulation of other GPCRs and ion channels, heterologously or endogenously expressed. Cellular biochemistry assays identified several unusual interacting proteins that contribute to GPR75 expression at the cell surface. To examine GPR75 role *in vivo*, mouse model of *Gpr75* gene deficiency was

generated and analyzed. The results proved that GPR75 receptor has important metabolic roles as evidenced by its contribution in models of diet-induced obesity and type-2 diabetes.

Conclusions: At cellular level, GPR75 appears to modulate the function of specific targets by an yet-to-be-identified mechanism. *In vivo*, GPR75 seems to play major roles in the regulation of metabolism, being a significant factor in obesity and diabetes.

Acknowledgements: This work was funded from "EEA-RO-NO-2018-0535 - New Generation of Drug Targets for Schizophrenia (NEXTDRUG)".

New cell-penetrating peptides with antimicrobial properties

Dana Maria Copolovici¹✉, Andreea Gostăviceanu^{1,2}, Carmen Popa^{1,2},
Cristian Moisa¹, Andreea Ioana Lupitu¹, Oana Gavriiliuc^{1,3,4},
Florina Bojin^{1,3,4} and Lucian Copolovici¹

¹"Aurel Vlaicu" University of Arad, Faculty of Food Engineering, Tourism and Environmental Protection and Institute of Technical and Natural Sciences Research-Development-Innovation of "Aurel Vlaicu" University, Arad, Romania; ² University of Oradea, Biomedical Sciences Doctoral School, Oradea, Romania; ³ "Victor Babes" University of Medicine and Pharmacy, Department of Functional Sciences, Immuno-Physiology and Biotechnologies Center, Timisoara, Romania; ⁴ Timis County Emergency Clinical Hospital "Pius Brînzeu" Timisoara, Center for Gene and Cellular Therapies in the Treatment of Cancer—OncoGen, Timisoara, Romania;
✉Corresponding author, E-mail: dana.copolovici@uav.ro

Introduction: Modern lifestyles and longer lifespans necessitate treatment for cancer, neurological diseases, and viral infections. Thus, innovative, effective, and reliable methods with higher target cell specificity, low cost, and little impacts on healthy tissues are needed. Peptide-based systems could deliver drugs and genes. Cell-penetrating peptides (CPPs) are small molecules that may cross cell plasma membranes and carry cargo (drugs, nucleic acids, imaging agents, etc.) into the cytosol or nucleus. They are chemically changeable, stable, and non-immunogenic molecules.

Materials and methods: Solid-phase peptide synthesis (SPPS) and the labile fluorenylmethyloxycarbonyl group (Fmoc chemistry) strategy with solid Rink-amide resin were used to synthesize six peptides, three without stearyl moiety group, and three stearylated homologous peptides. The peptides were purified by preparative HPLC and their purity was determined using analytical HPLC and MALDI-TOF-MS analysis. Minimum inhibitory concentration (MIC) values were used to evaluate the antibacterial efficacy of the newly obtained peptides. Following Wiegand *et al.*'s (2008) published technique, the MIC of the peptides was determined in two bacteria (*Staphylococcus aureus* and *Klebsiella pneumoniae*) using the broth microdilution method. The cytotoxicity, cell proliferation and cellular metabolic activity was determined by microscopy and Alamar Blue assay at divers concentrations.

Results: Six peptides, named CPP-1 – CPP-6, were obtained. The antimicrobial activity against *Staphylococcus aureus* and *Klebsiella pneumoniae* is depended both on the peptides' sequence and peptides concentration. The

majority of the peptides are not toxic in MDA-MB-231 and MCF-7 breast cancer cell lines, while all six peptides are not toxic on mesenchymal stem cells.

Conclusions: Designing peptides that can, among other things, break through the cell membrane or pass biological barriers, stay in circulation longer, and are not toxic or immunogenic to humans is crucial for the rapid development of peptide-based therapeutic systems.

Acknowledgements: This work was supported by a grant of the Ministry of Research, Innovation and Digitization, CNCS - UEFISCDI, project number PN-III-P4-PCE-2021-0639, within PNCDI III.

Iron oxide nanoparticles carried by probiotics in iron absorption

Oana Lelia Pop^{1✉}, Călina Ciont¹, Dan Cristian Vodnar¹ and Amalia Mesaros⁴

¹ Department of Food Science, University of Agricultural Sciences and Veterinary Medicine, Cluj-Napoca, Romania; ² Institute of Life Sciences, University of Agricultural Sciences and Veterinary Medicine, Cluj-Napoca, Romania; ³ Molecular Nutrition and Proteomics Laboratory, Institute of Life Sciences, University of Agricultural Sciences and Veterinary Medicine, Cluj-Napoca, Romania; ⁴ Physics and Chemistry Department, CAS Centre, Technical University of Cluj-Napoca, Cluj-Napoca, Romania; ✉ **Corresponding author, E-mail:** oana.pop@usamvcluj.ro

Introduction: Recently, newly generated iron oxide nanoparticles (IONPs) carried by probiotics have been recommended as innovative iron supplements due to their low reactivity and high bioavailability compared to conventional anemia treatments. Due to the probiotic's capacity to connect with the intestinal walls, IONPs-bacteria incorporate into the enterocyte, where nanoparticles are given, providing an adequate iron content. The present study aimed to investigate the beneficial effect of IONPs with probiotics (average size 10 nm) as new iron supplements for iron deficiency in anemic rats compared with the conventional treatment (FeSO₄).

Materials and methods: The research included a comprehensive set of tests, including *in vitro* MRI, electronic microscopy investigations on the CaCO₂ human cell line after treatment, and magnetic examination of the various rat tissues following administration of IONPs and IONPs with probiotics. Also, the restoration of healthy levels of blood parameters and iron-related protein expressions were investigated to confirm the efficiency of this material as a new drug for anemia.

Results: The efficiency of IONPs for the treatment of anemia was sensibly higher when nanoparticles were incorporated into the probiotic bacterium *Lactobacillus fermentum* than the conventional treatment (FeSO₄). Plasma iron and hemoglobin, intestine expression of divalent metal transporter 1 (DMT1) and duodenal cytochrome B (DcytB), as well as hepatic expression of the hormone hepcidin, was fully restored to healthy levels after administration of IONPs with probiotic.

Conclusions: The collective analysis of results points out that *L. fermentum* is an excellent carrier to overcome the stomach medium and drive IONPs to the intestine, where iron absorption occurs.

Acknowledgments: This research was supported by grants from the Romanian Ministry of Education and Research, CCCDI-UEFISCDI, project number PN-III-P4-ID-PCE-2020-2126, within PNCDI 541 III.

The use of functionalized liposomes and extracellular vesicles as drug delivery systems with high cancer-targeting efficacy

Valentin Florian Rauca^{1✉}, Laura Pătraș¹, Giorgiana Negrea², Emilia Licărete¹, Alina Porfire³, Lucian Barbu⁴, Lavinia Luput¹, Alina Sesărman¹ and Manuela Banciu¹

¹Department of Molecular Biology and Biotechnology, and Center of Systems Biology, Biodiversity and Bioresources, Faculty of Biology and Geology, Babes-Bolyai University, Cluj-Napoca, Romania;

²Doctoral School in Integrative Biology, Faculty of Biology and Geology, Babes-Bolyai University, Cluj-Napoca; ³Department of Pharmaceutical Technology and Biopharmaceutics, Faculty of Pharmacy, University of Medicine and Pharmacy "Iuliu Hatieganu", Cluj-Napoca, Romania;

⁴"C. Craciun" Electron Microscopy Center, Faculty of Biology and Geology, "Babes-Bolyai" University, Cluj-Napoca, Romania; ✉**Corresponding author, E-mail:** valentin.rauca@ubbcluj.ro

Introduction: To be considered efficient, Nanoparticle-based Drug Delivery Systems (NDDSs) face tremendous challenges related to toxicity, controlled release, stability, physical barrier penetration, clearance, and finally, enrichment at tumor sites in order to elicit desired therapeutic effects. Increasingly more studies focus on designing engineered nanoformulations with specific properties related to molecular level pathogenesis. Among the most efficient delivery systems developed by our group are tumor cell-derived extracellular vesicles "sterically stabilized" with poly(ethylene glycol) (PEG) and loaded with doxorubicin (PEG-EV-DOX) to selectively target melanoma cells, and long circulating liposomes functionalized with IL-13 to ensure simvastatin (IL-13-LCL-SIM) or prednisolone (IL-13-LCL-PLP) drug delivery to tumor microenvironment cells such as tumor associated macrophages (TAMs).

Materials and methods: We used spectrofluorimetric and fluorescence microscopy methods to assess cellular uptake of our rhodamine-tagged engineered nanoformulations. To assess the antiproliferative potential of the drug-loaded delivery systems we used ELISA BrdU-colorimetric immunoassay. The antitumor effect of our NDDSs was investigated on C57BL6 mice bearing B16.F10 s.c melanoma tumors and molecular mechanisms with regard to major hallmarks of tumor progression (angiogenesis, oxidative stress, resistance to apoptosis, invasion) were surveilled by protein array, WB, HPLC and IHC.

Results: Experimental data has shown that PEG-EV-DOX were more efficient to inhibit B16.F10 murine melanoma growth than clinically applied long-circulating liposomal DOX (LCL-DOX) and reduced significantly melanoma

aggressiveness and tumor angiogenesis. Furthermore, both functionalized liposomal formulations (IL-13-LCL-SIM, IL-13-LCL-PLP) showed higher antitumor potential than their nonfunctionalized counterparts (LCL-SIM, LCL-PLP). Thus, we proposed novel sequential or simultaneous administration therapies based on PEG-EV-DOX to precisely target melanoma cells and on IL-13-LCL-SIM or IL-13-LCL-PLP to ensure targeting of tumor microenvironment cells such as tumor associated macrophages (TAMs).

Conclusion: The novel NDDSs showed high efficiency in potentiating antitumor effects of all chemotherapeutic agents tested. The drug delivery strategy based on combined active targeting of both cancer cells and immune cells was able to induce a potent antitumor effect by disruption of the reciprocal interactions between TAMs and melanoma cells.

Acknowledgements: This work was funded by UEFISCDI under Grant PN-III-P4-ID-PCE-2016-0342 (No. 91/2017) and under Grant PN-III-P2-2_1-PED-2021-0411 (No.659PED/2022)

Production of chimeric subviral particles with enhanced immunogenicity for the development of next-generation HBV vaccines

Norica Nichita¹✉, Ana-Maria Pantazica¹, Mihaela-Olivia Dobrica¹, Catalin Lazar^a, Catalin Tucureanu², Iuliana Caras², Irina Ionescu², Adriana Costache², Adrian Onu², Jihong Liu- Clarke³ and Crina Stavaru²

¹ Institute of Biochemistry of the Romanian Academy, Bucharest, Romania;

² Cantacuzino" Medico-Military National Research Institute, Bucharest, Romania;

³ NIBIO - Norwegian Institute for Bioeconomy Research, Ås, Norway;

✉ **Corresponding author, E-mail:** norica70@yahoo.co.uk

Introduction: Chronic infection with Hepatitis B virus (HBV) is a major health issue world-wide accounting for more than 800.000 deaths annually, while a curable treatment is still missing. The development of HBV vaccines based on expression of the small (S) envelope protein in yeast has significantly reduced the morbidity and mortality associated with this disease. However, up to 10% of vaccinated adults fail to develop a protective immune response and virus mutations resistant to current vaccines continue to emerge, prompting further research into developing more immunogenic HBV antigens.

The large (L) envelope protein plays a critical role in HBV attachment to hepatocytes and is the target for virus neutralizing antibodies, which makes it a promising immunogen for inclusion in novel vaccine formulations. However, efficient expression of the L protein in recombinant systems is very difficult to achieve due to a significant cellular toxicity induced by its retention in the endoplasmic reticulum.

In this work we took advantage of the S protein ability to self-assemble into highly immunogenic sub-viral particles (SVP's) and used this molecular scaffold to create chimeric antigens which contain relevant structural and functional epitopes of the L and S proteins.

Materials and methods: By using molecular biology tools, the newly designed S/L chimeric HBV antigens were cloned in expression vectors and produced in mammalian cells. Their antigenic and immunogenic properties were characterised in molecular detail by ELISA, immunoprecipitation and western blot. The antigen candidate with the highest expression and secretion levels, which retained the ability to assemble in SVP, was selected for further studies *in vivo*.

Results: Analysis of the immune response induced in mice vaccinated with S/L chimeric antigens demonstrated improved immunogenicity and superior activation of humoral and cellular immune responses when compared with the S protein. This combined activation resulted in production of neutralizing antibodies against both wild-type and vaccine-escape HBV variants.

Conclusions: Our results validate the design of chimeric HBV antigens and promote the novel S/L protein as a promising strategy for immunization of poor-responders to current HBV vaccines.

Acknowledgements: This work was funded from the EEA Project 1/2019 (SmartVac).

Novel HTS cell based assay for cis acting protease activity identifies Hepatitis C Virus NS2 cysteine protease inhibitors with antiviral activity

Andrei Juncu¹, Daniel Ion¹, Paula Forian¹, Gabi Chiritoiu¹, Teodeor Sulea¹, Ana Borota², Luminita Crisan², Alina Bora², Sorin Avram², Ovidiu Vlaicu³, Dan Otelea³, Ursula Bilitewski⁴, Laurentiu Spiridon¹, Liliana Pacureanu² and Costin-Ioan Popescu¹✉

¹ Institute of Biochemistry of the Romanian Academy, Bucharest, Romania; ² Institute of Chemistry "Coriolan Dragulescu" of the Romanian Academy, Timisoara, Romania; ³ National Institute for Infectious Disease "Prof. Matei Bals", Bucharest, Romania; ⁴ Helmholtz Centre for Infection Research, Braunschweig, Germany; ✉ **Corresponding author, E-mail:** pop@biochim.ro; popescu80@hotmail.ro

Introduction: Proteases represent major drug targets for various viruses. Cis acting proteases play important roles in different viral families life cycle. Due to the available assays most of the protease inhibitors are targeting trans-acting protease. Hepatitis C Virus (HCV) poses a significant global health challenge, infecting approximately 58 million individuals worldwide. One promising drug target is the HCV NS2 cysteine protease which is an exclusive autoprotease. Our understanding of the precleavage form of HCV NS2 is limited and no cell based HTS assay is available to identify potent inhibitors.

Materials and methods: Advanced bioinformatic techniques were used for compound library selection. A cell based assay was optimized using heterologous protein expression from plasmids obtained by basic molecular biology techniques. High-throughput screening was performed by robotic liquid handling and hit confirmation followed in HCV cell culture system. Mode of action was explored by new bioinformatics techniques which sample the conformational space of the precleavage form of HCV NS2 protease at high speed.

Results: Potential HCV NS2 inhibitors were prioritized "in silico" in a targeted cysteine inhibitors library. In parallel, we optimized and automatized for HTS screening a cell based assay for HCV NS2 cis-protease activity. The false positive hits were filtered by a counterscreen. A secondary screen performed in HCV cell cultured system identified several chemical scaffolds with IC₅₀s in the low micromolar range to pursue. Series of structure – activity relationship (SAR), bicistronic replicons and rapid sampling of the NS2-NS3 protease precleavage form informed about the hit mode of action. Moreover, a novel insight in the dynamics of HCV NS2 precleavage form was achieved.

Conclusions: Herein, we present a new HTS assay for HCV NS2 protease which may be extrapolated to other cis- acting proteases and innovative bioinformatics methods to investigate the conformational space of the precleavage form of a cis-acting protease helping to design new compounds targeting this family of enzymes.

Multifunctional complexes nanolipid - microbubbles for a targeted delivery of antitumor drugs by ultrasonography-assisted procedures

Mihai Adrian Socaciu^{1,2}, Dumitrita Rugina^{2,3},
Zorita Diaconeasa^{2,3}, Madalina Nistor^{2,3}, Carmen Socaciu^{2,3}✉

¹Faculty of Medicine, University of Medicine and Pharmacy "Iuliu Hatieganu" Cluj-Napoca Romania;

²University of Agricultural Sciences and Veterinary medicine, Cluj-Napoca, Romania;

³BIODIATECH- Research Centre for Applied Biotechnology in Diagnosis and Molecular Therapy, Cluj-Napoca, Romania; ✉Corresponding author, E-mail: csocaciudac@gmail.com

Introduction: New exploratory directions in nanomedicine involves a multidisciplinary knowledge regarding functional nanostructures which incorporate anticancer agents, new solutions for a targeted delivery, including ultrasonography for improved theranostics. Innovative solutions were recently focused on multifunctional complexes which include antitumor molecules into nanolipid structures (liposomes, nanolipid complexes) which are attached to microbubbles, as optimal vehicles, and best contrast agents to deliver such molecules to tumor targets.

Materials and methods: Experimental data including different protocols applied to incorporate plant-derived anticancer molecules, betulinic acid (BA) and a standardized triterpenoid extract (TT) comparative to Doxorubicin (as a gold standard) in liposomes and lipid nanospheres (NLC) are presented, as well their physical and chemical linkage to microbubbles. These supramolecular structures were used for a targeted delivery to Walker256 tumor cells *via* sonoporation, either *in vitro* or *in vivo*. The characteristics of such complexes are described considering their size and composition by DLS size measurements, UV-Vis spectrometry and LC-MS, cytotoxicity on Walker tumor cells, as well their stability. Protocols for sonoporation experiments *in vitro* and *in vivo* will be also presented

Results: The review combines the updated information and experimental data obtained in our laboratory: adapted recipes and experimental protocols to optimize the critical ratios between the nanolipid/anticancer molecules, the incorporation rate of anticancer molecules inside nanolipids, the ratios between the nanolipid complexes and microbubbles, their stability in time, for an improved delivery and efficiency against tumor cells *in vitro* and *in vivo*.

Conclusions: Current opportunities and challenges are presented, related to the future developments for improved targeted drug delivery *via* ultrasonography, to be applied using such multifunctional complexes in clinical therapy, valorizing the innovative solutions offered by nanobiotechnology.

Acknowledgements: This Research is funded by the Romanian National Authority for Scientific Research (UEFISCDI), PN-III-P4-PCE-2021-0378

Medical devices for skin-wound healing; from bench to *in vivo* study

Anca Roseanu¹✉, Madalina Icriverzi¹, Paula Ecaterina Florian¹,
Livia Sima¹, Oana Gherasim², Valentina Gurmazescu², Gabriel Socol²,
Fabiola Ionita³ and Cristin Coman³

¹ Institute of Biochemistry of the Romanian Academy, Bucharest, Romania;

² National Institute for Lasers, Plasma, and Radiation Physics, Măgurele, Romania;

³ 'Cantacuzino' National Medico-Military Institute for Research and Developmen, Bucharest, Romania ✉ **Corresponding author, E-mail:** roseanua@gmail.com

Introduction: The skin wound healing is among the most complex physiological process in the human body. It is governed by sequential yet overlapping phases, including homeostasis, inflammatory, angiogenesis, growth, re-epithelisation, and tissue remodelling. Any aberration in the process may lead to excessive wound healing or chronic wound, thus hindering the normal physical function of skin. While several therapies for wound healing are available, these are only moderately effective. From a clinical point of view, topical application is attractive for full-thickness wound, due to reducing adverse effects on other organs. A promising strategy for a more efficient action is to develop/design patches with the capability of promoting dermis regeneration and provide support for epithelial skin. In this context, we have proposed a new formulation based on chitosan and loaded with anti-inflammatory, antioxidant and antimicrobial compounds and evaluated the wound healing potential *in vitro* and *in vivo*.

Materials and methods: The effect of proposed patches on the viability of THP-1 differentiated macrophages was assessed by MTS colorimetric assay. The anti-inflammatory potential was investigated using an experimental model of inflammation, macrophages stimulated with bacterial endotoxins and the level of pro-inflammatory cytokines (IL-6, PGE2) determined by ELISA method. *In vivo* effect on wound healing process was investigated on rats for 14 days. As a control, Hartmann standardised silver and unloaded patches were used. The average wound area was measured every 48h. Samples of wounds/ scars were collected on the 7th and 14th postoperative days and evaluated histological and immunohistochemically (H&E, Masson's Trichrome, collagen, α -SMA, CD31).

Results: No cytotoxic effect on cells was found in the presence of the new patches. Moreover, the new formulation was able to reduce LPS-induced inflammation by suppressing pro-inflammatory cytokine production *in vitro*. The *in vivo* studies showed that on day 14, healing process was similar for the animal groups treated either with new or standard Hartmann patches, respectively. Haematological analysis of blood samples and histopathological examination of skin samples collected on day 14 revealed a reduced number of inflammatory cells and no bacterial colonization. An almost complete wound closure and skin normal architecture was observed. Topical application of coated patches on the wounds of rats increased collagen synthesis, stimulated re-epithelialisation, fibroblast proliferation, accelerating wound healing process in rats.

Conclusions: Collectively, our study provides evidence that the topical application of proposed patches can promote the cutaneous wound healing process and represents a promising candidate for skin tissue therapy.

Acknowledgements: This research was funded by grant of the Romanian Ministry of Education and Research, CCCDI-UEFISCDI, project number PN-III-P1-1.2-PCCDI-2017-0728. A.R. acknowledge and thanks the partial support of Project no. 5 of the Structural and Functional Proteomics Research Program of the Institute of Biochemistry of the Romanian Academy.

Plant-produced Hepatitis C Virus E2-derived glycoproteins for vaccine development

Mihaela-Olivia Dobrica¹✉, Andre van Eerde², Catalin Tucureanu³, Adrian Onu³, Lisa Paruch², Iuliana Caras³, Ene Vlase³, Hege Steen², Sissel Haugslie², Dominic Alonzi⁴, Nicole Zitzmann⁴, Ralph Bock⁵, Costin-Ioan Popescu¹, Crina Stavaru³, Jihong Liu Clarke² and Norica Nichita¹

¹Department of Viral Glycoproteins, Institute of Biochemistry of the Romanian Academy, Splaiul Independentei 296, Bucharest, Romania; ²NIBIO - Norwegian Institute for Bioeconomy Research, Høgskoleveien 8, 1433, Ås, Norway; ³"Cantacuzino" Medico-Military National Research Institute, Bucharest, Romania; ⁴Institute of Glycobiology, Department of Biochemistry, University of Oxford, Oxford, UK; ⁵Max Planck Institute of Molecular Plant Physiology, Potsdam-Golm, Germany;

✉Corresponding author, E-mail: olivia@biochim.ro, mihaelaolivia.dobrica@yahoo.com

Introduction: Infections with Hepatitis C Virus (HCV) represent a major global health burden with 58 million chronically infected people and 290,000 deaths/year caused by severe liver complications. An efficient antiviral therapy has been recently developed, however, the access to diagnosis and treatment is limited. In these circumstances, prevention by vaccination remains the most effective way to control HCV infections. Currently, there is no commercial vaccine against HCV infection. Our study aims to develop and characterize HCV antigens as vaccine candidates in a cost-effective manner. We previously published the production in premiere of an HCV antigen in plants as an alternative system, by expressing the E1E2 envelope heterodimer in lettuce leaves. We describe here the expression and characterization of glyco-engineered antigens derived from E2 protein, the major HCV vaccine candidate, in *Nicotiana benthamiana*, to investigate the impact of N-glycan composition on their immunogenic properties.

Materials and methods: E2 envelope protein was transiently expressed in *N. benthamiana* and in mammalian cells, as control, and purified by lectin affinity followed by size exclusion chromatography. N-glycans were released by glycosidases treatment and analysed by NP-HPLC. The purified E2 conformation was assessed by binding to either specific antibodies or the HCV receptor, CD81, and its immunogenicity was studied following vaccination of BALC/c mice. The neutralizing capacity of the E2-induced antibodies was verified using the HCV pseudoparticle (pp) system. We further designed a histidine tagged E2-derived construct lacking the transmembrane domain and the hypervariable region I. The novel antigen was expressed in *N. benthamiana*

wild-type (in presence/absence of KDEL signal) and CRISPR/Cas9-edited to lack β -1,2-xylosyltransferase and α -1,3-fucosyltransferase activities (FX-KO). Antigens were purified by Ni affinity chromatography and used for N-glycan profile analysis by LC/MS.

Results: Our data indicate similar expression of the E2 antigen in plant leaves and mammalian cells. The comparative HPLC glycan analysis shows a different extent in the N-glycan trimming between the two systems. Plant-produced HCV E2 acquired the native conformation required for CD81 binding and triggered specific IgM and IgG response in mice, with significant neutralizing activity against HCV1a pp. The truncated E2 antigens presented an improved expression yield in plants (up to 200 μ g/g FW) and displayed similar electrophoretic mobility irrespective of the plant type, indicating that the N-glycan pattern is not grossly altered by the host. The N-glycosylation profiles of E2-derived antigens in wild-type and FX-KO plants are currently being analysed by mass spectroscopy.

Conclusions: Our results promote plants as suitable host and biotechnological platforms for cost-efficient production of functional complex antigens for vaccine development.

Acknowledgements: The research leading to these results has received funding from the EEA Grants 2014-2021, within the GreenVac and SmartVac Projects, contracts no. 5/2014 and no. 1/2019.

Identification of novel potentially active chondroitin/dermatan sulfate domains in human decorin by ion mobility mass spectrometry

Mirela Sarbu¹, Raluca Ica² and Alina D. Zamfir^{1,2}✉

¹*Department of Condensed Matter, National Institute for Research and Development in Electrochemistry and Condensed Matter, Timisoara, Romania;* ²*Department of Technical and Natural Sciences, "Aurel Vlaicu" University of Arad, Arad, Romania;*

✉*Corresponding author, E-mail: alina.zamfir@uav.ro*

Introduction: Decorin (DCN), an ubiquitous component of the extracellular matrix, is a proteoglycan consisting of a core protein linked to a single hybrid glycosaminoglycan chain in which chondroitin sulfate (CS) and dermatan sulfate (DS) domains are interspersed. Hence, DCN-CS/DS chain is characterized by sequences of different lengths, epimerization, sulfation patterns and binding functions. This structural and functional diversity gave rise to development of approaches for the identification of the biologically active motifs. In this context, we report here on the introduction of ion mobility (IMS) MS and MS/MS for structural analysis of DCN-CS/DS and discovery of novel potentially active domains.

Materials and methods: The hybrid CS/DS chain, released by β -elimination from DCN prepared from conditioned media of cultured human skin fibroblasts, was depolymerization by chondroitin AC I lyase and fractionated by size-exclusion chromatography. The collected oligosaccharide fractions, purified and dissolved in methanol were infused by (-)nanoESI into a Synapt G2S mass spectrometer and subjected to IMS MS and CID MS/MS. The signal was acquired at 1.4 kV ESI and 15 V cone voltage. IMS wave velocity was set at 650 m/s and IMS wave height at 40 V. CID was performed using collision energies of 30 eV.

Results: The IMS MS separation and screening in the negative ion mode allowed: i) the discrimination of CS/DS isobaric species by their separation according to the mobilities of their corresponding ions and ii) the detection in the DCN-derived CS/DS domains of novel over- and undersulfated CS/DS sequences which, in view of their sulfation status are, more likely, biologically active. Moreover, by IMS CID MS/MS, the new potentially active domains were structurally characterized in details in terms of epimerization and sulfation pattern. Fragmentation analysis data indicated that even misregulations in the

sulfate distribution along the CS/DS chain could be discovered; CS/DS domains, placed initially in the category of regularly sulfated sequences due to the number of sulfates that equals the number of disaccharide repeats, were found to correspond, in fact, to abnormally sulfated structures.

Conclusions: Considering these results, we believe that the concept of the present IMS MS-based approach addresses to a better extent the needs of glycosaminoglycomics for faster, more reliable and more sensitive methodologies on one side and a few of the many questions still open, related to the structure and sulfation status of biologically active CS/DS domains in human decorin.

Acknowledgements: This work was supported by the Romanian National Authority for Scientific Research, UEFISCDI, PN-III-P4-ID-PCE-2020-0209 granted to A.D.Z

Transcriptomic profiling of halophilic archaeon *Haloferax alexandrinus* DSM 27206T grown under silver stress

Doriana Mădălina Buda^{1✉}, Horia Leonard Banciu^{2,3}

¹Doctoral School of Integrative Biology, Faculty of Biology and Geology, Babeș-Bolyai University, Cluj-Napoca, Romania; ² Department of Molecular Biology and Geology, Faculty of Biology and Geology, Babeș-Bolyai University, Cluj-Napoca, Romania; ³Centre for Systems Biology, Biodiversity and Bioresources, Faculty of Biology and Geology, Babeș-Bolyai University, Cluj-Napoca, Romania; ✉Corresponding author, E-mail: doriana.buda@gmail.com

Introduction: Organisms living in high salt environments face multiple challenges including the incidental presence of high heavy metal levels. The present study focuses on the mechanisms of silver tolerance in the halophilic archaeon *Haloferax (Hfx.) alexandrinus* DSM 27206^T through transcriptome analysis. Gaining insights into metal-cell interactions in halophilic prokaryotes can contribute to the development of effective strategies for mitigating metal contamination of saline systems.

Materials and methods: The physiological response of *Hfx. alexandrinus* DSM 27206^T to silver ions was assessed in saline (20% NaCl w/v) liquid cultures with 0.1, 0.25, and 0.5 mM AgNO₃. Scanning electron microscopy coupled with energy dispersive spectrometry (SEM-EDS) analysis was employed to reveal the produced silver nanoparticles. Genomic sequencing was performed on *Hfx. alexandrinus* cells, while RNA extraction was conducted for transcriptomic analysis. The RNA-Seq data was validated using reverse transcription quantitative PCR (RT-qPCR).

Results: Optical density (OD₆₂₃) measurements showed a slight delay in archaeal cells cultivated with increasing AgNO₃ concentrations compared to the control (no silver) cultures. SEM-EDS analysis revealed the presence of extracellular silver-containing nanoparticles in cells exposed to 0.5 mM AgNO₃. Gene set enrichment analysis (GSEA) indicated that genes associated with basic cellular metabolism, genetic and environmental information processing were significantly altered in silver-stressed cells. Metal transporters and metal-related genes were strongly induced in response to silver exposure, suggesting their involvement in silver detoxification. Moreover, multiple genes involved in oxidative stress management, basic metabolism, and cellular motility were also

differentially expressed in response to elevated Ag⁺ levels. The RT-qPCR results confirmed the reliability and consistency of RNA-Seq data in identifying candidate gene responsive to heavy metal exposure.

Conclusions: The present study employed RNA-Seq analysis to uncover a specific response to silver-stressed *Hfx alexandrinus* cells, involving differential gene expression across various cellular processes. The essential role of the CopA copper ATPase in surviving silver exposure was identified, providing novel insights into the cellular components and mechanisms underlying heavy-metal tolerance in halophilic archaea.

Acknowledgements: This work was supported by a grant of the Ministry of Research, Innovation and Digitization, CNCS/CCCDI – UEFISCDI, project number PN-III-P4-ID-PCE-2020-1559, within PNCDI III.

Targeting tumor cells and ovarian tumor microenvironment using tissue transglutaminase inhibitors

Livia E. Sima¹✉, Monica Tudor¹, Cristian Munteanu¹,
Gabriela Chiritoiu¹, Florin Jipa², Stefana Orobeti^{1,2}, Felix Sima²,
Stefana M. Petrescu¹, Gary E. Schiltz³ and Daniela Matei^{3,4}

¹ Institute of Biochemistry of the Romanian Academy, Bucharest, Romania;

² National Institute of Laser Plasma and Radiation Physics, Bucharest-Magurele, Romania;

³ Northwestern University, Chicago, USA; ⁴ Jesse Brown VA Medical Center, Chicago, USA;

✉ **Corresponding author, E-mail:** lsima@biochim.ro

Introduction: Tissue transglutaminase (TG2) is a multifunctional protein that was found overexpressed in many solid tumors, including ovarian cancer. Extracellular TG2 forms a molecular complex with fibronectin (FN) and integrin $\beta 1$ ($I\beta 1$) thereby modulating “outside-in” signaling controlling adhesion. Our proposed inhibitor MT4 interferes with ovarian cancer (OC) cell adhesion by binding to TG2 and inhibiting its interaction with FN. TG2 is a non-toxic druggable target. However, treatment with TG2-FN small molecule inhibitors (SMIs) sensitizes cancer cells to chemotherapy. Here we present the results obtained during testing of new MT-4 analogues. Also, we recently pursued a new approach to co-target TG2 with inhibitors blocking signaling pathways involved in cellular adaptation to MT-4. Further, we characterized the effects of TG2 targeting in 3D co-cultures of OC cells and normal ovarian fibroblasts (NOF). Next, CD8⁺ T cell killing activity was measured upon inhibiting different TG2 activities.

Materials and methods: We used proximity ligation assay (PLA) to test TG2- $I\beta 1$ disruption by MT-4 analogues and immunofluorescence microscopy for cell adhesion analysis. Flow cytometry was employed to characterize pFAK expression and cell cycle profile in WT and TG2KO OC cells treated with inhibitors. We developed new phosphoproteomics protocols on SILAC-labeled cells to identify key pathways differentially upregulated in cells attaching on FN in the presence of MT-4. Tumor microarrays were used for multiplex IHC (mIHC) using TSA labeling for assessing TG2 expression by multiple lineages in tumors. DiI/DiO labeled OC cells and NOFs were used for heterosphere formation. NOF secretome was assessed by mass spectrometry, upon activation in the presence of SMI-exposed OC cells. Mouse spleen isolated CD8⁺ T cells were treated with TG2 inhibitors and used in T cell killing assays in live cell imaging conditions.

Results: Out of the 5 new analogues, compound #3002 produced the highest destabilization of TG2- I β 1 interaction. Consequently, OC cells showed decreased adhesion onto FN, an attenuated pFAK signaling and cell cycle arrest. Phosphoproteomic analyses revealed upregulation of members of cell adhesion and survival pathways, upon adhesion to FN in the presence of MT4. Pharmacological co-targeting of TG2 and identified signaling proteins decreases CFU count, while increasing apoptosis in OC cells and spheroids. CompuSyn analyses showed synergistic effects for several combinations of TG2-FN SMIs and signaling pathway inhibitors. Next, we detected TG2 in α -SMA⁺ stroma of OC tumors using mIHC. *In vitro*, MT-4 prevented OVCAR5-NOF heterospheroids formation, and increased CCL2 and CXCL12 secretion by NOFs. Also, MT-4 did not interfere with *in vitro* T cell killing activity, which together with the enhanced immune response observed in TG2KO mice supports TG2 as potential therapeutic target in OC.

Conclusions: These results encourage the development of TG2 inhibitors for translational applications and underline the importance of this protein in OC metastatic process.

Acknowledgements: This work was supported by US Department of Veterans Affairs (I01 BX000792-06), Robert H Lurie Comprehensive Cancer Center and UEFISCDI (PN-III-P2-2.1-PED-2019-1543; PN-III- P1-1.1-TE- 2019-0670).

Robosample: Harnessing the Power of Constrained Molecular Dynamics and Gibbs Sampling to Investigate Macromolecules

Laurentiu Spiridon¹✉, Teodor Asvadur Șulea¹, Victor Gabriel Ungureanu¹, Eliza Cristina Martin¹ and Andrei Jose Petrescu¹

¹*Institute of Biochemistry of the Romanian Academy, Bucharest, Romania;*

✉ *Corresponding author, E-mail: spiridon.laurentiu@gmail.com*

Introduction: Simulation of macromolecules enables the investigation of the behavior, properties, and interactions of biomolecules. However, all the simulation techniques face a persistent obstacle posed by molecules' intricate potential energy landscape, arising from the interplay of high dimensionality and functional complexity. Within this work, we introduce Robosample, a software package that synergistically combines the efficiency of robot mechanics algorithms for rapid constrained simulations, with the ability of Gibbs sampling to jump across subspaces, making it capable to achieve statistical convergence hundreds of times faster.

Materials and methods: Robosample represents molecules as articulated rigid bodies, which offers a notable advantage in expediting macromolecule simulations primarily attributed to the ease of solving for constraints. An illustrative example is observed in torsional dynamics, wherein the system is transformed into Bond-Angle-Torsion coordinates, and then disregards the motion of bonds and angles. The equations of motion are efficiently solved within linear time, using robot mechanics algorithms with reduced coordinates. This eliminates the need for overdetermination, coordinate transformation, and mass matrix tensor inversion that would typically require cubic time complexity.

The employed sampling technique, known as Gibbs sampling coupled with Hamiltonian Monte Carlo (GCHMC), selectively maps random variables across molecular degrees of freedom. Within GCHMC, specific rigid molecule segments are chosen to be subsampled, while soft degrees of freedom, such as torsions are oversampled. At the end, all degrees of freedom are sampled, interleaving fully flexible Cartesian Monte Carlo proposals.

Results: The method was successfully employed across a diverse range of molecules, encompassing both small compounds and large macromolecules. The method's validity was demonstrated on small systems, including a model

four-bead linear system and alanine dipeptide, accurately reproducing their free energy landscapes. Subsequently, the efficiency of the method was evaluated by subjecting it to rigorous testing with macrocycle-containing molecules and complex glycan structures. These challenging systems provided a robust assessment of the method's performance in handling larger and structurally diverse molecules.

To assess the scalability of the method for larger biological systems, GCHMC was subsequently tested on various challenging targets, including the HCV pre-cleavage viral glycoprotein NS2-NS3, human apelin APJR GPCR receptor, human Receptor for Advanced Glycation Endproducts (RAGE), and other important molecular structures. Simulation efficiency was assessed through comparative RMSD analysis with state-of-the-art available molecular simulation programs.

Conclusions: These diverse and complex biological systems served as robust benchmarks to evaluate the method's ability to effectively handle and accurately capture the dynamics and interactions within such large-scale systems.

Acknowledgements: This work was funded from: PNCDIII P4, code PN-III-P4-ID-PCE-2020-2444, acronym CYBORG.

Computational assisted investigation of two key protein families of the immune system

Andrei-J. Petrescu¹✉

*¹Department of Bioinformatics and Structural Biochemistry,
Institute of Biochemistry of the Romanian Academy, Bucharest, Romania;*

✉Corresponding author, E-mail: petrescuaj@gmail.com

Introduction: Over the past decade our group have actively investigated by intertwining experiment with Bioinformatics and Biocomputing the structure-function relations in two major protein families of the immune system: (a) NOD like receptors - the key intracellular constituents of innate immunity and (b) the advent and evolution of the RAG system - found at the core of adaptive immunity.

Materials and methods: In order to predict the structure of the main modules and components we have developed intricate remote homology, ab-initio and constrained modelling techniques given the low level or absence of sequence similarity. Model based predictions were then validated by crystallography, FRET, cryoEM or point mutation analysis in collaboration with well established experimental groups in the field. Machine learning and bioinformatic techniques were further used to identify structural invariants and motifs; and to gain an overall structured view of these highly diverse protein classes.

Results: Model based predictions combined with experiment were key to understanding the processes and functioning cycles of these proteins as well as the determinant factors driving their properties. The work also resulted in useful computational tools and bioinformatic resources at hand now for the scientific community involved in immune system research.

Conclusions: Results presented herein clearly demonstrate that intertwining experiment with heuristic molecular modeling, simulation and bioinformatics is able to crack down highly complex problems in structural biology which are out of reach to the most recent automatic approaches even if these are based on state of the art artificial intelligence methods.

Zeaxanthin oil-in-water nanoemulsions as delivery systems for food or nutraceuticals applications

Adela Pintea¹✉, Patricia Muntean¹, Andrea Bunea¹, Francis V. Dulf¹,
Monica Focșan², Cristina Coman¹ and Dumitrița Rugină¹

¹University of Agricultural Sciences and Veterinary Medicine Cluj-Napoca, Cluj-Napoca, Romania;

²Nanobiophotonics and Laser Microspectroscopy Center, Interdisciplinary Research Institute in Bio-Nano-Sciences, Babes-Bolyai University, Cluj-Napoca, Romania;

✉Corresponding author, E-mail: apintea@usamvcluj.ro

Introduction: Zeaxanthin and lutein, also known as the macular carotenoids are important contributor to eye and brain health and function. Due to their lipophilic character, the overall bioaccessibility of carotenoids from food or nutraceuticals is low. The lipid components in food are essential for the absorption of carotenoids and can modulate their bioaccessibility, depending on the concentration, unsaturation degree and chain length. The aim of our work was to develop oil-in-water nanoemulsions containing zeaxanthin (Zea) and zeaxanthin dipalmitate (ZeaDP) and to examine their impact on the bioaccessibility and cellular uptake of carotenoids.

Materials and methods: Four vegetable oils (coconut MCT, olive, sunflower, linseed and palm oils) were characterized in terms of fatty acids and carotenoid composition by GC-MS. Zea and ZeaDP were isolated and purified from plant sources using chromatographic techniques. Zea and ZeaDP oil in water (O/W; 1:9 v/v) nanoemulsions doped with carotenoids (0.05 mg/ml in the final emulsion) were obtained by probe ultrasonic emulsification, in the presence of emulsifier at 1 % (Tween 20). Bioaccessibility of carotenoids was determined by the INFOGEST standardized in vitro digestion protocol. Cellular uptake in Caco-2 and RPE cells was determined by C30-HPLC-PDA and visualized using a Raman microspectrometer (InVia, Renishaw). Raman spectra were recorded with a 532 nm laser at a spectral resolution of ~4 cm⁻¹. All data were analyzed using the QUASAR software and principal component analysis (PCA) was used to identify multiple cellular components.

Results: Very good incorporation yield (up to 98 %) of carotenoids in nanoemulsions were obtained for all vegetable oils. The average hydrodynamic diameter ranged between 100-200 nm (PDI < 0.3), depending on the type of oil (chain length, unsaturation degree). Nanoemulsions with ZeaDP had a larger diameter than those with free Zea, regardless of the type of fat used. The bioaccessibility of free zeaxanthin was higher than that of ZeaDP, regardless of

the oil used, and higher for nanoemulsions compared to non-emulsified oils doped with carotenoids. Nanoemulsions with Zea obtained with coconut oil and those with ZeaDP and olive oil showed the highest bioaccessibility, with 60 % and 42%, respectively, which is far superior to the bioaccessibility of Zea from known food matrices. Cellular uptake and secretion of Zea in intestinal and retinal cells was superior from nanoemulsions compared to solvent delivery (DMSO), and dependent on the type of emulsions. The highest values were obtained for nanoemulsions with unsaturated oils. The presence of Zea in the cytosol of RPE cells, near the nucleus, was qualitatively confirmed by Raman mapping, based on specific and intense signals.

Conclusions: Oil-in water nanoemulsions doped with zeaxanthin shows better bioaccessibility and cellular uptake compared to non-emulsified oils supplemented with zeaxanthin. Both the esterification of zeaxanthin and the type of oil impact the bioaccessibility of pigments. Zea nanemulsions represent promising delivery systems for food or nutraceuticals applications.

Acknowledgements: This work was supported by a grant of the Romanian Ministry of Education and Research, CNCS - UEFISCDI, project number PN-III-P4-ID-PCE-2020-1172, number 243/2021 within PNCDI III.

Crimson serenade: anthocyanins orchestrating melanoma defense, revealing oxidative stress and mitochondrial membrane potential through the enchantment of fluorescence free molecules and encapsulated brilliance

Dumitrița Rugină¹✉, Mădălina Nistor¹, Zorita Diaconeasa¹,
Monica Focșan¹, Luiza Găină³, Mihai Cenariu¹, Roxana Pop¹,
Carmen Socaciu¹ and Adela Pinteă¹

¹ *Biochemistry Department, University of Agricultural Sciences and Veterinary Medicine Cluj-Napoca, Cluj-Napoca, Romania;* ² *Nanobiophotonics and Laser Microspectroscopy Center, Interdisciplinary Research Institute in Bio-Nano-Sciences, Babes-Bolyai University;* ³ *Babes-Bolyai University, Faculty of Chemistry and Chemical Engineering, Cluj-Napoca, Romania;*
✉ *Corresponding author, E-mail: dumitrita.rugina@usamvcluj.ro*

Introduction: Anthocyanins (AnTs) are natural pigments that orchestrate a captivating display of color during autumn's leaf senescence, enchanting us with the sight of vibrant forests. Acting as protectors of vegetal tissues exposed to direct light, these remarkable molecules hold aesthetic beauty and profound health benefits. Humans have been consuming AnTs for centuries, effortlessly ingesting due to their presence in roots, fruits, leaves, juices, and extracts, embracing their presence without any concerns. However, the full journey of AnTs within cells once they are internalized remains partially veiled, therefore understanding of the AnTs intracellular path once they are uptaken by the cells needs more attention.

Methods and Results: Specifically, we have selected fruit extracts with a distinct chemical pattern (containing glucosylated derivatives or glycosylated) were selected to be tested on normal and melanoma cell lines, proving no detrimental effects on healthy cells, but reducing proliferation, increasing oxidative stress biomarkers, and diminishing the mitochondrial membrane potential in melanoma cells. The path we tread throughout our research was not without challenges like the intricate detection and monitoring of anthocyanins within the cells. In this light, diphenylboric acid 2-aminoethyl (DPBA), a non-fluorescent reagent, was successfully used to form fluorescent complexes with AnTs (aglycon and the glycosylated compounds as extract formula). According to NMR (nuclear magnetic resonance) spectroscopy and HRMS (high-resolution mass spectrometry) analysis, it was proven that DPBA and cyanidin are forming

a complex, cyanidin@DPBA. Notably, *in vitro* tests the non-toxic nature of cyanidin@DPBA complex on B16-F10 melanoma cells. To further illuminate, the sub-cellular visualization of all AnTs, fluorescence microscopy and flow cytometry were employed, yielding detectable signals of non-metabolized cyanidin and glycosylated cyanidin within melanoma cells. Unfortunately, anthocyanins are very sensitive to environmental factors such as pH, light, and oxygen, and consequently are easily degraded. To counteract this challenge, an architectural structure was crafted, having a spherical shape, 1080 nm diameter, and a solid groundwork of CaCO₃ (PAH), on which rhodamine B isothiocyanate fluorophore was firstly added, was developed to counteract the anthocyanin's susceptibility to environmental factors. AnTs were entrapped between polyelectrolyte layers of the microcapsule (loading efficiency 94.6%). Moreover, these microcapsules offer the opportunity to trace the internalization and trafficking of AnTs, granting us glimpses into their mysterious journey after 24 hours of treatment.

Conclusions: Anthocyanins may inhibit melanoma cell proliferation and increase the level of oxidative stress, with opposite effect on normal cells. The effective technique to imaging AnTs is required in drug delivery development and mechanisms related to their metabolism. Through the artistry of encapsulation technology, we unveil valuable insights into the intricate delivery of anthocyanins within melanoma cells, presenting a strategic pathway that holds promise for enhancing tumor therapies.

Acknowledgements: This research was funded by the Romanian National Authority for Scientific Research, CNDI- UEFISCDI, project number PN-III-P1-1.1-TE-2019-1276.

The neurological effects of *Glaucosciadium cordifolium* (Boiss.) Burt & Davis essential oil in a zebrafish model of cognitive impairment

Răzvan Ștefan Boianțiu¹✉, Eyup Bagci², Gabriela Dumitru¹,
Lucian Hritcu¹ and Elena Todirascu-Ciornea¹

¹Department of Biology, Alexandru Ioan Cuza University of Iasi, Iasi, Romania;

² Department of Biology, Faculty of Science, Firat University, Elazig, Turkey;

✉Corresponding author, E-mail: razvan.boianțiu@uaic.ro

Introduction: Alzheimer's disease (AD), the most common form of dementia, is characterized by progressive cognitive decline accompanied by mood changes, such as anxiety and depression. *Glaucosciadium cordifolium* has been used in traditional medicine for stomach ailments and as an aphrodisiac and appetizer and was proven to possess antimicrobial and antioxidant properties. This study aims to investigate the *G. cordifolium* essential oil (GCEO) effects on anxiety and learning and memory impairment induced by scopolamine (SCOP) in zebrafish.

Materials and methods: The GCEO chemical composition was analyzed by GC-MS. The dementia model was induced by SCOP (100 μ M), whereas GCEO (25 and 150 μ L/L) and galantamine (GAL, 1 mg/L) were delivered to the SCOP-induced model. The anxiety-like behavior and cognitive performances of the animals were assessed using specific in vivo tasks, such as the novel tank diving test (NTT) and Y-maze and novel object recognition (NOR) tasks respectively. Post analysis, the animals were euthanized and the brains were used to measure the oxidative status and the acetylcholinesterase activity.

Results: The GC-MS analysis showed that the highest content was limonene followed by α - and β -pinene, p-cymene and α -phellandrene. It was found that GCEO significantly improved memory impairment and anxiety-like response induced by SCOP through the Y-maze, novel object recognition (NOR) test, and novel tank diving tests (NTT). Biochemical analyses showed that GCEO reduced SCOP-induced oxidative damage. Additionally, the cholinergic system activity was improved in the SCOP-induced model by decreasing the acetylcholinesterase (AChE) activity following the exposure to GCEO.

Conclusions: It was clear that as a mixture, GCEO displays positive action in improving memory impairment through restoring cholinergic dysfunction and brain antioxidant status.

Acknowledgements: This work was supported by a grant of the "Alexandru Ioan Cuza" University of Iasi, within the Research Grants program, Grant UAIC, code GI-UAIC-2022-08.

Phenolic profile of micro- and nano-encapsulated olive leaf extract in biscuits during *in vitro* gastrointestinal digestion

Călina Ciont¹, Graziana Difonzo², Antonella Pasqualone², Simona Maria Chis¹, Florica Ranga¹, Katalin Szabo¹, Elemer Simon¹, Anca Naghiu³, Lucian Barbu-Tudoran³, Dan Cristian Vodnar¹ and Oana Lelia Pop¹✉

¹ Department of Food Science, University of Agricultural Sciences and Veterinary Medicine, Cluj-Napoca, Romania; ² Department of Soil, Plant and Food Science (DISSPA), University of Bari Aldo Moro, Bari, Italy; ³ Research Institute for Analytical Instrumentation, National Institute of Research and Development for Optoelectronics INOE 2000, Cluj-Napoca, Romania;

✉ **Corresponding author, E-mail:** oana.pop@usamvcluj.ro

Introduction: Olive leaf was characterized by a high content of phenols and flavonoids (oleuropein, luteolin, and their derivatives), presenting functional and health-related properties. The chemical instability of phenolics through technological processes and their bioavailability may negatively impact them, leading to lower absorption. This research aims to appraise the evolution of the phenolic extract from olive leaves and assess their stability and bioaccessibility through incorporation in biscuits matrix, using *in vitro* digestion model.

Materials and methods: The extraction process of olive leaves was ultrasound-assisted, and a binary blend of gum arabic and maltodextrin (1:1 w/w) was used for its encapsulation, confirmed through TEM and SEM microscopy.

Results: Applying the micro- and nano-capsules in biscuits showed significant protection of phenolic compounds. According to the *in vitro* results, the biscuits enriched with olive leaf extract can be considered a proposal for functional food products.

Conclusions: The present study has the opportunity to contribute significantly to the vast field of functional foods. It provides new options for producing healthier foods while optimizing the valorization of olive by-products.

Acknowledgments: This work was supported by a grant granted by the Ministry of Research and Innovation, C.N.C.S. UEFISCDI, project number PN-III-P4-ID-PCE-2020-2306 and PN-III-P4-IDPCE 2020-2126 PNCDI III.

Hepatitis C Virus Envelope Protein E2 Antigen Design and Characterization for Vaccine Development

Lia-Maria Cucos¹✉, Teodor Asvadur Șulea¹, Laurențiu Spiridon¹, Iuliana Caras², Irina Ionescu², Adriana Costache², Crina Stavaru², Norica Nichita¹ and Costin-Ioan Popescu¹

¹*Institute of Biochemistry of the Romanian Academy, Bucharest, Romania;*

²*“Cantacuzino” Medico-Military National Research Institute, Bucharest, Romania;*

✉*Corresponding author, E-mail: lia@biochim.ro; liamcucos@gmail.com*

Introduction: With over 58 million individuals infected with Hepatitis C Virus (HCV) worldwide and costly antiviral drugs, the need for a vaccine is even more pressuring. The main target in vaccine development is the viral envelope protein E2, which binds to CD81 receptor functioning as an entry factor for HCV. HCV E2 412-423 epitope is involved in CD81 binding and it is targeted by broadly neutralizing antibodies (nAbs). HCV E2 412-423 epitope presents in different conformations due to protein flexibility and a beta hairpin conformation was found to co-crystallize with a nAb. The objective of our study was to construct and characterize novel HCV E2 derived antigens that elicit a potent neutralizing humoral response by stabilizing the 412-423 epitope in a beta hairpin conformation.

Materials and methods: Advanced bioinformatics tools were used to predict mutations stabilizing this epitope. Briefly, starting from a homology model built using Modeller, a conformational ensemble was generated using Hamiltonian Monte Carlo coupled with Gibbs Sampling (GCHMC), implemented in Robosample and followed by implicit solvent molecular dynamics (using OpenMM) to test mutant stability. A subset of HCV E2 mutants were expressed in HEK 293T cells and their biochemical and antigenical properties were investigated by Western Blot, ELISA, and glycan digestion. A vaccine candidate was expressed in Expi293 cells and the monomeric form was purified by IMAC (Immobilized metal affinity chromatography) followed by size exclusion chromatography to over 95% purity. The candidate was used to immunize BALB-C mice and obtained sera was used to neutralize HCVpp infection.

Results: Screening results provided us with an antigen candidate showing decreased binding for an antibody recognizing the open structure of the epitope. This antigen was successfully purified in the monomeric form. A mass spectrometry assay was optimized for further structure confirmation. The

antigen was not able to bind CD81. Preliminary immunization studies revealed similar immunogenicity of the new antigen comparing to HCV E2 protein. Moreover, a potentially higher neutralization capacity of the immune sera was observed for the conformationally stabilized antigen using the HCV pseudotype system.

Conclusions: The presented data suggest that by de-novo antigen design, HCV E2 412-423 epitope can be stabilized in a desired conformation with potential impact on its immunogenicity.

Acknowledgements: This work was funded from EEA Grants 2014-2021, SmartVac SEE1/2019

Reacting to stress: upregulating the genes involved in polyhydroxybutyrate synthesis during nutrient starvation by *Halomonas elongata* DSM 2581T

Andreea-Melisa Tripon^{1✉}, Adorján Cristea² and Horia Leonard Banciu³

¹Doctoral School of Integrative Biology, Faculty of Biology and Geology, Babeș-Bolyai University, Cluj-Napoca, Romania; ² Department of Taxonomy and Ecology, Faculty of Biology and Geology, Babeș-Bolyai University, Cluj-Napoca, Romania; ³ Department of Molecular Biology and Biotechnology, Faculty of Biology and Geology, Babeș-Bolyai University, Cluj-Napoca, Romania; ✉Corresponding author, E-mail: andreea.tripon@ubbcluj.ro

Introduction: Nutrient starvation in some prokaryotes triggers a series of molecular events that culminate in the activation of polyhydroxyalkanoate synthase (PhaC), which is responsible for the synthesis of polyhydroxyalkanoates (PHAs). Among the PHAs, polyhydroxybutyrate (PHB) is the most abundant polyester. PHB serves as intracellular carbon and energy reserve in the extremely halotolerant bacterium *Halomonas elongata* DSM 2581^T during nitrogen limitation and abundant carbon availability. Despite its prospective relevance as bioplastics precursor, the molecular mechanisms underlying PHB synthesis in *H. elongata* is poorly understood. Therefore, the objective of our study is to investigate the molecular processes involved in the synthesis and depolymerization of PHB in *H. elongata* DSM 2581^T.

Materials and methods: *H. elongata* was cultivated in rich and nutrient-limited saline media (8% NaCl, w/v) followed by biomass collection at 24, 96, and 120 hrs. Total RNA extraction was performed using the RNeasy PowerSoil Total RNA kit (Qiagen). The extracted RNA was prepared for RNA-Seq at Macrogen. The raw sequences underwent quality checking with FastQC v0.11.7, followed by trimming using Trimmomatic 0.38. Short RNA reads were mapped to the reference genome using Bowtie 1.1.2 and gene expression levels from the RNA-seq data were assessed using HTSeq version 0.10.0. The accumulation of PHB during the experiments was monitored using the spectrophotometric-based crotonic acid assay.

Results: PHB synthesis in *H. elongata* was induced under nutrient-limiting conditions, with the number of upregulated genes increasing over time as follows: 583 genes (24 hrs), 660 genes (96 hrs), and 716 genes (120 hrs). PHB production is relatively low (0.2 g/L ± 0.02) at 24 hours. Nevertheless, the expression of *phaC* and other genes associated with sugar transport and glucose metabolism, is increased compared to the control. In contrast, expression of

phaA (coding for acetyl-CoA C-transferase) is downregulated. At 96 hrs, a significant increase in PHB is observed ($1.8 \text{ g/L} \pm 0.06$). *phaC* and genes related to sugar transport remain upregulated, while genes associated with glucose metabolism are downregulated. At 120 hrs, when PHB production plateaus ($2 \text{ g/L} \pm 0.05$), *phaC* remains upregulated while genes associated with sugar transport and metabolism are downregulated.

Conclusions: Our results suggest a redirection of metabolic resources towards PHB production in *H. elongata* grown under nutrient limitation. Further investigations, such as metabolic reconstruction, are needed to fully comprehend the regulation of sugar metabolism and other pathways involved in PHB synthesis. Overall, our study enhances understanding of PHB synthesis in *H. elongata* and provides a basis for future optimization of PHB production in halophilic bacteria.

Acknowledgements: This work was funded by grants from CNCS-UEFISCDI project number PN-III-P4-ID-PCE-2020-1559 and by the Research Starting Grants UBB contract number 32913/22.06.2023.

Overcoming doxorubicin resistance in B16.F10 melanoma cells by targeting Hypoxia-Inducible Factor-1 alpha

Bogdan Dume¹✉, Alina Sesărman², Manuela Banciu² and Emilia Licărete²

¹Doctoral School in Integrative Biology, Faculty of Biology and Geology, "Babes-Bolyai" University, Cluj-Napoca, Romania; ²Department of Molecular Biology and Biotechnology, Center of Systems Biology, Biodiversity and Bioresources, Faculty of Biology and Geology, "Babes-Bolyai" University, Cluj-Napoca, Romania; ✉Corresponding author, E-mail: bogdan.dume@ubbcluj.ro

Introduction: Hypoxia plays a critical role in promoting cancer progression and conferring resistance to conventional therapies. Among various malignancies, melanoma stands out as a particularly challenging cancer to treat, owing to its inherent resistance to both tumour cell and microenvironment-mediated drug resistance mechanisms. Adaptation to hypoxia is primarily regulated by the activity of Hypoxia-Inducible Factor-1 (HIF-1). HIF-1 serves as a central mediator in the cellular response to hypoxia and acts as a key regulator of O₂ homeostasis, controlling the expression of numerous genes involved in various aspects of oncogenesis. In this study, we used an *in vitro* approach to investigate the effects of HIF-1 inhibition on sensitizing B16.F10 murine melanoma cells to the cytotoxic drug doxorubicin to which melanoma cells have intrinsic resistance.

Materials and methods: Subconfluent B16.F10 murine melanoma cells were reverse transfected with HIF-1 α specific siRNA and incubated in hypoxia (1% O₂) for 24 hours. On the second day, the cells were treated with doxorubicin and subsequently incubated for an additional 24 hours. Gene knockdown was verified by quantitative RT-PCR. Then, cell proliferation, migration and invasion capacity were quantified. Protein levels of HIF-1 α and other pro-survival proteins were examined by Western blot analysis. Intratumour angiogenesis related protein production was determined by protein microarray. Total RNA was extracted and sent for transcriptome sequencing. MDA, a lipid peroxidation marker, was measured using HPLC to evaluate cell oxidative stress.

Results: The specific siRNA significantly decreased both gene and protein expression levels of HIF-1 α , leading to an increased sensitivity of the cells to doxorubicin. Combined therapy showed a greater reduction of cell proliferation, migration and invasion capacity than cells treated with doxorubicin alone.

Also, concomitant administration of HIF-1 α siRNA and doxorubicin promoted apoptosis, induced oxidative stress and showed a modest inhibitory effect on angiogenesis.

Conclusions: HIF-1 α knockdown emerges as a promising future treatment strategy in melanoma as it has shown significant results in its ability to overcome B16.F10 murine melanoma cell resistance to doxorubicin.

Acknowledgements: This work was funded by UEFISCDI (Romanian Ministry of Research and Innovation), under Grant PN-III-P1-1.1-TE-2019-1320.

“Humanization” of the N-glycosylation pathway in *Nicotiana benthamiana* via CRISPR/Cas9 technology significantly improves the immunogenicity of HBV antigens and the virus- neutralizing antibody response in vaccinated mice

Ana-Maria Pantazică¹✉, André van Eerde², Mihaela-Olivia Dobrică¹, Iuliana Caras³, Irina Ionescu³, Adriana Costache³, Cătălin Tucureanu³, Hege Steen², Cătălin Lazăr¹, Inger Heldal², Sissel Haugslieen², Adrian Onu³, Crina Stăvaru³, Jihong Liu Clarke² and Norica Nichita¹

¹*Institute of Biochemistry of the Romanian Academy, Bucharest, Romania;*

²*NIBIO - Norwegian Institute of Bioeconomy Research, Ås, Norway;*

³*“Cantacuzino” Medico-Military National Research Institute, Bucharest, Romania;*

✉*Corresponding author, E-mail: pantazicaanamaria@gmail.com*

Introduction: Hepatitis B Virus (HBV) infection affects over 290 million people worldwide, with more than 800 000 annual deaths due to HBV-related complications. Vaccination remains the best approach to mitigate HBV infections and meet the World Health Organization goal to eliminate viral hepatitis by 2030. Development of more immunogenic HBV antigens is crucial to overcome the disadvantages of the current vaccine, based on the small (S) envelope protein produced in yeast, such as non-responsiveness and lack of protection against “vaccine-escape” mutants. We have previously shown that combination of relevant immunogenic epitopes of the S and large (L) envelope proteins significantly increased the anti-HBV immune response. However, protein production in mammalian cells is costly and limits large scale production. Plants are an attractive alternative for protein production, as they are versatile and rapidly scalable. The recent generation of plants lacking β -1,2-xylosyltransferase and α -1,3-fucosyltransferase activities (FX-KO), by CRISPR/Cas9 genome editing, enables production of proteins with “humanized” N-glycosylation. In this study, we investigated the impact of plant N-glycosylation on the immunogenic properties of a chimeric HBV S/L vaccine candidate produced in wild-type and FX-KO *Nicotiana benthamiana*.

Materials and methods: Wild-type and FX-KO *N. benthamiana* plants were transformed by Agrobacterium infiltration with a vector encoding the chimeric S/preS1 antigen, followed by antigen extraction, molecular characterisation and

purification. The N-glycosylation patterns of the HBV antigens were determined via UPLC-FLD/MS and antigenicity was determined via ELISA using a panel of conformation dependent anti-S antibodies. The antigens were used for immunization in mice and the humoral and cellular immune response was quantified by ELISA and ELISpot. The neutralization capacity of the obtained anti-sera was tested against wild-type and “vaccine escape” HBV by using an *in vitro* infection system.

Results: We found that the absence of β -1,2-xylose and α -1,3-fucose from the HBV antigen obtained in FX-KO *N. benthamiana* significantly impacted its antigenicity when compared to the wild-type counterpart. Moreover, the “humanized” glycosylation pattern increased the immune response in mice, as compared with the wild-type plant-produced antigen. Notably, the antibodies triggered by the FX-KO- produced antigen neutralized more efficiently both wild-type HBV and a clinically relevant vaccine escape mutant.

Conclusions: Our study validates in premiere the glyco-engineered *Nicotiana benthamiana* as a substantially improved host for plant production of glycoprotein vaccines and illustrates the importance of antigen glycosylation for the immunogenic properties of vaccine candidates.

Acknowledgements: This research was funded by the EEA Grants 2014-2021, SmartVac project no. 1SEE/2019.

3D tumor spheroids as a model to unriddle the complexity of tumor microenvironment chemoresistance

Giorgiana Negrea¹✉, Szilvia Meszaros², Stefan Drăgan², Vlad-Alexandru Toma^{2,3}, Bogdan Dume¹, Valentin-Florian Rauca², Laura Pătraș², Emilia Licărete², Manuela Banciu² and Alina Sesărman²

¹ Doctoral School in Integrative Biology, Faculty of Biology and Geology, "Babes-Bolyai" University, Cluj-Napoca, Romania; ² Department of Molecular Biology and Biotechnology, Center of Systems Biology, Biodiversity and Bioresources, Faculty of Biology and Geology, "Babes-Bolyai" University, Cluj-Napoca, Romania; ³ Department of Experimental Biology and Biochemistry, Institute of Biological Research, Branch of NIRDBS Bucharest, Cluj-Napoca, Romania;

✉ **Corresponding author, E-mail:** giorgiana.negrea@ubbcluj.ro

Introduction: Recent oncology advances emphasize the tumor microenvironment (TME) critical role in drug resistance. Therefore, accurate models reflecting TME complexity are essential. 3D models offer greater tumor heterogeneity compared to 2D cell cultures, making them a pioneering tool for cancer research. Our aim was to create 3D in vitro models with B16.F10 murine melanoma cells combined with endothelial cells (2H11) and/or primary macrophages, to mimic the chemoresistant melanoma microenvironment, and to validate them using doxorubicin.

Materials and methods: Macrophages were isolated from C57BL6 mice bone marrows. Spheroids were created using the liquid overlay technique, co-culturing B16.F10 murine melanoma cells with endothelial cells or macrophages in non-adherent 96-well plates with 1.5% commercial extracellular matrix (ECM). Characterization of the 3D cocultures included morphology analysis by light microscopy, as well as immunohistochemistry using specific antibodies for component cells. To assess the models' ability to mimic melanoma microenvironment chemoresistance, spheroids were treated with DOX (IC30), a chemotherapeutic drug to which melanoma patients fail to respond. Parameters like HIF-1 α , VEGF and leptin expression, total antioxidant capacity and peroxidase activity were evaluated using western blot, protein micro-array and spectrophotometry.

Results: The developed models displayed some of the chemoresistance traits. After DOX treatment, the 3D coculture with B16.F10 melanoma cells and macrophages showed significant increases in total antioxidant capacity (TAC) and catalase activity ($p < 0.05$) compared to the control group (untreated spheroids). Immunohistochemistry analysis indicated no changes in peroxidase

activity ($p>0.05$) in DOX-treated spheroids compared to control. Moreover, the chemoresistant profile persisted when B16.F10 melanoma cells were 3D cocultured with endothelial cells and treated with DOX, as key angiogenesis promoters (HIF-1 α , VEGF and leptin) remained unchanged compared to the control group ($p>0.05$). These findings demonstrate that the cells involved in the 3D coculture models, exhibit a deliberate mechanism to evade substantial molecular alterations when exposed to DOX treatment, suggesting a strategic approach in preserving protumor processes crucial for driving tumor growth.

Conclusions: Our results indicate the reliability of our models in reflecting chemoresistance characteristics of the melanoma microenvironment. To better understand the complex cellular interactions driving melanoma's chemoresistant profile, further investigation with additional cell types and analysis of other key parameters is needed.

Acknowledgements: This work was funded from UEFISCDI grant PN-III-P2-2_1-PED-2021-0411 (No. 659PED/2022) granted to Alina Sesarman.

Anti-dementia effects of mansorin A, mansonone G, and 6-paradol in zebrafish (*Danio rerio*)

Iasmina Honceriu¹✉, Ion Brinza¹, Răzvan Ștefan Boianțiu¹ and Lucian Hritcu¹

¹“Alexandru Ioan Cuza” University of Iasi, Department of Biology, Iași, Romania;

✉ **Corresponding author, E-mail:** iasmina.honceriu@student.uaic.ro

Introduction: Alzheimer’s disease (AD) is the most common form of dementia. The patients manifest memory and cognitive impairments accompanied by depression and anxiety. The main pathologies are β -amyloid plaque accumulation, neurofibrillary tangles, and the death of cholinergic neurons, followed by neuroinflammation and increased oxidative stress. AD is fatal yet incurable and a priority in research. Natural bioactive compounds show promising anti-AD potential. That may be the case for mansorin A and mansonone G from *Mansonia gagei* and 6-paradol from *Zingiber officinale*. This study aims to determine whether mansorin A, mansonone G, and 6-paradol have anti-dementia effects.

Materials and methods: Mansorin A, mansonone G, and 6-paradol were chronically administered to adult zebrafish (*Danio rerio*) by immersion. Anxiety-like behavior was assessed using specific *in vivo* tasks: the Novel Tank Diving test (NTT) and Novel Object Approach (NOA) test, while memory performances were determined using the Novel Object Recognition (NOR) and Y-maze tasks. The specific activities of the antioxidant enzymes such as superoxide dismutase, catalase, glutathione peroxidase, and glutathione reductase along with carbonylated proteins and malondialdehyde levels were also determined. The cholinergic status was evaluated by acetylcholinesterase activity.

Results: The used bioactive compounds improve spatial and recognition memory in zebrafish as indicated by NOR and Y-maze tasks and reduce anxiety-like behavior in NTT and NOA tests. They also improve the antioxidant status in zebrafish brain, as indicated by biochemical analysis.

Conclusions: Mansorin A, mansonone G, and 6-paradol exhibited promnesic and anxiolytic effects in zebrafish and show anti-dementia potential.

Acknowledgements: This work is supported by CNS-UEFISCDI, project number PN-III-P4-PCE-2021-1692, within PNCDI III.

Baicalein 5,6-dimethyl ether prevent scopolamine-induced memory impairment in zebrafish by increasing the creb1 protein level and the mRNA expression of bdnf and creb1 gene

Ion Brinza¹✉, Alexandru Bogdan Stache^{1,2}, Răzvan Ștefan Boianțiu¹, Omayma Eldahshan³, Dragos Lucian Gorgan¹, Marius Mihasan¹ and Lucian Hritcu¹

¹ Department of Biology, Alexandru Ioan Cuza University of Iasi, Iasi, Romania; ²Department of Molecular Genetics, Center for Fundamental Research and Experimental Development in Translation Medicine-TRANSCEND, Regional Institute of Oncology, Iasi, Romania;

³ Department of Pharmacognosy, Ain Shams University, Egypt;

✉Corresponding author, E-mail: ion.brinza@student.uaic.ro

Introduction: Baicalein 5,6-dimethyl ether (Baic), is a natural flavonoid, which was isolated for the first time from the roots of the plant *Scutellaria baicalensis*, variety, Georgi. Numerous studies have shown that Baic has many pharmacological properties and a variety of important biological activities such as its anti-inflammatory, anticancer and neuroprotective activity. However, its effects on the neuropathology of Alzheimer's disease (AD) have not been well studied. AD is a neurodegenerative, multifactorial, progressive, and irreversible disorder, which involves various mechanisms of disease onset and progression. The disease is associated with memory disorders and cognitive decline that ultimately affect thought, reason, video-spatial orientation, and behavior. Neurovascular dysfunction, cholinergic changes, inflammatory processes, and oxidative stress are critical factors in the pathogenesis and development of the disease. Decreased autophagy and the ability to regulate the production of brain-derived neurotrophic factor (BDNF), nuclear factor erythroid 2-related factor 2 α (*nrf2* α) and cAMP response binding protein (CREB) are also reported as emerging disease factors. In the final stage of the disease, the affected people become unconscious and stiff.

Materials and methods: Baic (1, 3 and 5 $\mu\text{g} / \text{L}$) was administered by immersion to zebrafish once a day for 16 days. To assess the anxiety-like behavior of zebrafish, the novel tank diving test (NTT) was used. For assessing the spatial memory and the recognition memory, the Y maze test, and the novel object recognition test (NOR) were used. To evaluate the effects of Baic on the oxidative and cholinergic status in the zebrafishes brain, the specific activity of

superoxide dismutase (SOD), catalase (CAT), malondialdehyde (MDA) level and acetylcholinesterase (AChE) activity were evaluated. Also, in this study the effects of Baic on *bdnf*, *nrf2 α* and *creb1* mRNA expression were investigated and the level of CREB1 protein by the immunoblotting technique was quantified.

Results: Baic can improve cognitive dysfunction of the amnesic zebrafish by increasing the absolute gene expression of *bdnf*, *nrf2 α* and *creb1*, and inhibiting AChE activity and restoring the antioxidant status, which is also correlated with improved memory parameters, as shown in behavioral approaches (NTT, Y-maze and NOR).

Conclusions: Our results suggest that Baic may be a novel active therapeutic drug for the amelioration of memory degradation.

Acknowledgements: Ion Brinza, Razvan Stefan Boiangiu, Marius Mihasan and Lucian Hritcu were supported by a grant of the Ministry of Research, Innovation and Digitization, CNCS-UEFISCDI, project number PN-III-P4-PCE-2021-1692, within PNCDI III.

Advancing selenium analysis: method optimization, validation, and its application in assessing selenium levels in selenate-treated rats

Petruț Miron¹✉, Bogdan Boșca¹, Andra-Diana Andreicuț²,
Alina Parvu² and Augustin C. Moț¹

¹*ANALYTICA Research Center, Faculty of Chemistry and Chemical Engineering, Babeș-Bolyai University, Cluj-Napoca, Romania;* ²*Department of Pathophysiology, "Iuliu Hațieganu" University of Medicine and Pharmacy, Cluj-Napoca, Romania;*
✉ *Corresponding author, E-mail: petrut.miron@stud.ubbcluj.ro*

Introduction: Selenium is an essential trace element with diverse environmental forms, and it plays a vital role in biological systems. Inorganic selenium compounds, including selenite and selenate, facilitate its incorporation into the food chain, while organic selenium compounds, such as selenomethionine and selenocysteine, contribute to essential protein functions. The fluorescence properties of certain selenium compounds have attracted attention in bioimaging and biomedical research, enabling precise detection and real-time monitoring of molecules and structures in living systems. In our study, we introduce an optimized method to quantify selenium absorption in rat organs, providing insights into selenium metabolism and its health implications.

Materials and Methods: Targeted organs (heart, liver, and kidney) were mineralized in concentrated nitric acid and hydrogen peroxide. Selenate was chemically reduced to selenite, and the resulting selenite quantity was determined by measuring the fluorescence of piaszelenol compound produced after the reaction with 2,3-diaminonaphthalene at 520 nm. Measurements were performed using a fluorescence spectrometer, and a calibration curve was established using known selenite standards. The study followed statistical analysis, included replicates and controls, and adhered to ethical guidelines.

Results: The absorption of selenite demonstrated a proportional relationship with the quantity of ingested selenate across multiple experimental lots. The developed method allowed for clear signal detection without interference from other fluorescent species in the samples. This reliable methodology enables the quantification of selenite levels and investigation of the relationship between selenate ingestion and selenite assimilation in the examined organs.

Conclusions: Our findings highlight the influence of different selenium compounds, particularly selenate ingestion, on the overall assimilation of selenite in organs such as the kidney, heart, and liver. The optimized method provides a comprehensive understanding of selenium metabolism and opens avenues for further research on its impact on overall health and disease.

Keywords: selenium, fluorescence, quantification, piaszelenol compounds.

Acknowledgements: This work was supported by a grant from the Ministry of Research, Innovation and Digitization, CNCS/CCCDI—UEFISCDI, project number TE-2019-1396, within PNCDI III.

Evaluation of phenolic compounds from the morphological parts of beechnut (*Fagus sylvatica* L.)

Alexandra R. Lazăr¹✉, Andrei M. Mocan², Andreea Pușcaș¹, Andruța E. Mureșan¹, Floricuța Ranga³, Alina M. Truță⁴ and Vlad Mureșan¹

¹ Food Engineering Department, Faculty of Food Science and Technology, University of Agricultural Sciences and Veterinary Medicine Cluj-Napoca, Cluj-Napoca, Romania; ²Department of Pharmaceutical Botany, "Iuliu Hațieganu" University of Medicine and Pharmacy, Cluj-Napoca Romania; ³Department of Food Science, University of Agricultural Sciences and Veterinary Medicine Cluj-Napoca, Cluj-Napoca, Romania; ⁴ Faculty of Horticulture, University of Agricultural Sciences and Veterinary Medicine of Cluj-Napoca, Cluj-Napoca, Romania;

✉Corresponding author, E-mail: alexandra-raluca.lazar@student.usamvcluj.ro

Introduction: The Plant Kingdom is an unlimited supply of natural bioactive substances that may be used in a variety of sectors, including food, medicine, and cosmetics. The European beech (*Fagus sylvatica* L.) is one of the most significant tree species in the northern hemisphere, with a kernel that is a triangular, reddish-brown achene that is 1-1.5 cm long and encased in an involucre. The current study attempted to determine the biologically active compounds found in the involucre, achene, skin, and cotyledon of the beechnut seeds.

Materials and methods: The raw materials were harvested from the production unit (U.P.III. Chelița, Maramureș), from the landscaping unit (u.a. 71 A) and subjected to the drying process at a temperature of approximately 15°C. About 1 g of each sample – the involucre, achene, skin, and cotyledon – was weighed and ground using a coffee grinder until a powder was obtained. Each sample was transferred into stoppered Erlenmeyer beakers and approximately 200 mL of methanol was added. The samples were then subjected to the sonication process (Bandelin SONOREX, Sigma Aldrich, Berlin, Germany) at a frequency of 80 Hz for 10 minutes.

A concentration step was also performed at a temperature of 35°C under low pressure using a Heidolph Rotovapor. 10 ml of HPLC methanol were used for sample recovery, after which they were filtered through 0.45 μm Millipore nylon filters and used for HPLC-MS analysis. HPLC analysis was performed on Agilent 1200 system equipped with a quaternary pump, a degasser DGU-20 A3 (Prominence), an autosampler, an UV-VIS detector with a photodiode (DAD), coupled with a single-quadrupole Mass Detector Agilent model 6110 (Agilent Technologies, Santa Clara, CA, USA). The phenolic compound separation was

conducted on the Eclipse XDB C18 column (5 µm, 4.6 × 150 mm). The gradient program was adapted from (Weisz, Kammerer and Carle, 2009), as follows: 10% B to 17.2% B (18 min), 17.2% B to 23% B (12 min), 23% B isocratic (10 min), 23% B to 31.3% B (13 min), 31.3% B to 46% B (12 min), 46% B to 55% B (5 min), 55% B to 100% B (5 min), 100% B isocratic (8 min), 100% B to 10% B (2 min), 10% B isocratic (5 min). The total run time was 90 min. The injection volume for all samples was 5 µL. Phenolic compounds were monitored separately at 280 nm (hydroxybenzoic acids) and 320 nm (hydroxycinnamic acids) at a flow rate of 0.4 mL/min. The chromatograms were monitored at 280 and 340 nm, respectively. The mass spectrometric data were obtained using a single-quadrupole 6110 mass spectrometer (Agilent Technologies, Chelmsford, MA, USA) equipped with an ESI probe. The measurements were performed in the positive mode with an ion-spray capillary voltage of 3000 V and a temperature of 300°C. The nitrogen flow rate was 7 L/min. Data were collected in full scan mode within 100 to 1200 m/z. The data reading and acquisition were made using Agilent ChemStation software.

Results: Results revealed 2065.26 mg / 100 g dw phenolic compounds in the involucre, among them, epicatechin (231.84 mg / 100 g dw) and procyanidin trimer isomer 1 (231.08 mg / 100 g dw) being more prevalent, followed by procyanidin trimer isomer 2 (228.45 mg / 100 g dw) and procyanidin trimer isomer 3 (226.90 mg / 100 g dw). Other compounds found in considerable amounts are catechin (216.66 mg / 100 g dw) and ellagic acid-arabioside (213.17 mg / 100 g dw). Quercetin, kaempferol, kaempferol-di p-coumaroyl-glucoside, tiliroside, hydroxybenzoic acid, and procyanidin dimer isomer 2 are other compounds identified in the involucre.

Eight phenolic compounds were identified in the achene - epicatechins, catechins, isomer 2 of the dimer and trimer of procyanidin, hydroxybenzoic acid, and in much smaller quantities naringenin-glucoside, tiliroside and kaempferol. Hydroxybenzoic acid was predominant in the beechnut skin (297.88 mg / 100 g dw), while in the cotyledon it was 54.18 mg / 100 g dw. The most significant proportion was provided by kaempferol-p-coumaroyl-glucoside (85.76 mg / 100 g dw), hydroxybenzoic acid-glucoside (83.77 mg / 100 g dw), and kaempferol-rutinoside (73.21 mg / 100 g dw) from the overall concentration of phenolic compounds in the cotyledon (627.07 mg / 100 g dw).

Conclusions: The four samples contained 24 phenolic compounds, the majority of which belonged to the flavanol subclass. Hydroxybenzoic acid and tiliroside were among the compounds discovered in varying levels in all four samples, with the rest being part-specific compounds. Phenolic compounds identified in the morphological parts of the *Fagus sylvatica* L. might represent a potential source of natural antioxidants for the food industry.

***In-silico* study of RAGE-S100B Inhibitors**

Victor Gabriel Ungureanu^{1✉}, Ioana Popa¹, Carmen Tănase¹ and
Laurențiu Spiridon¹

¹*Institute of Biochemistry of the Romanian Academy, Bucharest, Romania;*

[✉]*Corresponding author, E-mail: victorungu99@gmail.com*

Introduction: RAGE (Receptor for Advanced Glycation Endproducts) is a transmembrane receptor which comprises a V-type domain, two C-type Ig-like domains (C1 and C2), a transmembrane helix, and a cytosolic domain. It is known to bind a wide variety of ligands, including the S100 calcium-binding protein B (S100B). Based on predictions from native and cross-linking mass spectrometry, it is suggested that these proteins form a multimeric complex through concurrent interactions between RAGE-RAGE and RAGE-S100B. The inhibition of RAGE activation could be the key to preventing the progression of multiple diseases such as Alzheimer's, inflammatory complications of diabetes and tumor progression. In this study, molecular docking was employed to identify potential inhibitors of the RAGE-S100B complex formation, from a commercially available library of 137 natural and small-molecule compounds, hereafter referred to as the "target set".

Materials and methods: RAGE and S100B receptor structural models were generated via homology modeling using Modeller. Protonation at the physiological pH of 7.4 and charge assignment were performed with *pdb2pqr* using the AMBER force field.

Prior to the docking and scoring of the target set, we created a "method selection set" by combining known BindingDB database RAGE binders with decoys generated through DeepCoy. Subsequently, the method selection set underwent molecular docking using multiple programs, including AutoDock4, Vina, Vinardo, DLigand2, GNINA, DrugScoreX and dkoes. We systematically evaluated each program and handpicked those that demonstrated superior discrimination between binders and decoys. We assume that an optimal score, by its very nature, would inherently indicate the correct pose. Following the docking of the method selection set, AutoDock was chosen for pose prediction, while dkoes was employed for ranking purposes.

Molecular docking search space was limited to four surfaces on VC1 that are known to be involved in the interaction between RAGE and S100B. The first surface consisted of amino acids already established to be involved in S100B

binding, while the other three surfaces were suggested by previous studies as key binding sites for different inhibitors.

Results: Our predictions indicate that the target set encompasses a range of mechanisms of action. Specifically, certain compounds bind to the RAGE-S100B interface, while others interact with the RAGE-RAGE interface. This observation suggests that the prevention of receptor oligomerization and inhibition of RAGE-S100B interaction are distinct mechanisms employed by different compounds to exert their inhibitory effects. Understanding these distinct mechanisms is crucial for comprehending the inhibitory action of specific compounds on cellular RAGE. The results of the *in silico* screen were compared with the *in vitro* binding results with purified proteins and cellular RAGE.

Conclusions: In this study, we have undertaken the optimization of a method specifically designed for the *in silico* detection and characterization of inhibitors that target the RAGE receptor. This optimized method serves as a valuable tool for virtual screening of larger compound libraries, enabling the identification of potential therapeutic candidates for RAGE-associated disorders.

Acknowledgements: This work was funded from: PNCDIII P4, cu codul PN-III-P4-ID-PCE-2020-2444, acronym CYBORG.

Preliminary results on the recovery of coenzyme Q10 from vegetable and animal waste

Andersina Simina Podar¹✉, Cristina Anamaria Semeniuc¹, Floricuța Ranga¹, Maria-Ioana Socaciu¹, Melinda Fogarasi¹, Anca Corina Fărcaș¹, Dan Cristian Vodnar¹, Simona Raluca Ionescu¹ and Sonia Ancuța Socaci¹

¹ Faculty of Food Science and Technology, University of Agricultural Sciences and Veterinary Medicine from Cluj-Napoca, Cluj-Napoca;

✉ **Corresponding author, E-mail:** andersina-simina.podar@usamvcluj.ro

Introduction: Most foods of animal origin, such as meat, eggs and dairy products, are rich sources of coenzyme Q10 (CoQ10); other available food sources include vegetable oil, fish, bee pollen and microorganisms. This work aims to recover CoQ10 from plant and animal waste, in order to use it as a food supplement.

Materials and methods: Six types of scraps, resulting from the cold extraction process of rapeseed, sunflower, pumpkin, linseed, walnut and hemp oils, minced samples of whole fish and chicken hearts, were studied to determine the content of CoQ10. CoQ10 extraction was performed by ultrasound-assisted extraction using 2-propanol as solvent.

Results: Among the studied plant extracts, pumpkin extract has the highest CoQ10 content (84.80 µg CoQ10/g material), and among the animal samples, the highest amount was determined in chicken hearts (114.39 µg CoQ10/g material).

Conclusions: Ultrasound-assisted extraction using 2-propanol as solvent is an effective method for the recovery of CoQ10 from both plant and animal matrix; the optimized CoQ10 recovery method has the advantage of being a simple and ecological method.

Acknowledgements: This work was supported by two grants from the Ministry of Research and Innovation, CNCS - UEFISCDI, project number PN-III-P1-1.1-TE-2016-0973 and PN-III-P1-1.1-PD-2016-0869, within PNCDI III.

Unraveling molecular basis of myeloproliferative neoplasms (MPN) by experimentally constrained modelling and simulation

Teodor A. Șulea^{1✉}, Nicolas Papadopoulos², Stefan N. Constantinescu²,
Laurentiu Spiridon¹, and Andrei J. Petrescu¹

¹*Department of Bioinformatics and Structural Biochemistry, Institute of Biochemistry of the Romanian Academy, Bucharest, Romania;* ²*Université catholique de Louvain and de Duve Institute, Brussels, Belgium;* ✉*Corresponding author, E-mail: teodor.sulea@biochim.ro*

Introduction: CALR is an ER-resident chaperone involved in glycoprotein folding quality control. In its wildtype form, this transitory protein holds glycoproteins in ER until their proper folding. However myeloproliferative neoplasms (MPN) were shown to result from several frameshift mutations in CALR which then permanently binds the Thrombopoietin receptor (TpoR) and disrupts its proper function. We aimed here to model the interaction between TpoR and mutant CALR in an effort to uncover the mechanism behind this specificity.

Materials and methods: Interaction between the distal Cytokine Receptor Module (CRM) of TpoR and the frameshift region of CALR was investigated by docking followed by Molecular Dynamics (MD) based Molecular Mechanics Generalised Born & Surface Area Solvation (MM-GBSA) and Time-lagged Independent Component Analysis (TICA) to identify conformational microstates. The overall tetrameric system (2 CALR-2 TpoR) system was then built incorporating Hydrogen-Deuterium Exchange data. This glycoproteic model was further inserted into a POPC lipid bilayer, accommodating the transmembrane region of the TpoR using known NMR constraints resulting in an overall model of ~1,000,000 atoms including water & ions which was then subjected to stability test via MD simulation.

Results: Relying exclusively on an EpoR template, the automated AlphaFold2 model of TpoR-CRM fails to identify its true 4/5 β -sandwich nature due to its tendency to overfit with the closest template EpoR which displays a 3/4 β -sandwich architecture leaving a ~60aa sequence stretch unassigned. This was corrected by manual heuristic modelling. Interaction studies demonstrate that the frameshift CALR region tightly binds TpoR in a large number of configurations. This protein-protein interaction adds up to the lectin type interactions between the globular CALR region with TpoR immature glycans attached to N117.

Conclusions: During folding the N117 TpoR glycan is recognized by CALR-del52 mutant by the lectin mechanism. This brings TpoR-CRM to come in contact with the positively charged frameshift region of CALR-del52 stabilizing the formation of robust 2xTpoR-2xmCALR tetramer which prevents TpoR from working properly. Hence this work suggests on how mutations in CALR have pathological effects and lays the foundation for possible inhibitory therapies as identifying the specific residues of CRM1 involved in CALR-del52 interaction might help in the development of inhibitors targeting this interaction.

Long-read direct RNA nanopore sequencing of the nicotine-related transcriptome of *Paenarthrobacter nicotinovorans* ATCC 49919

Amada El-Sabeh¹✉ and Marius Mihășan¹

Department of Biochemistry and Molecular Biology, Alexandru Ioan Cuza University, Iasi, Romania; ✉Corresponding author, E-mail: amadaelsabeh@gmail.com

Introduction: *Paenarthrobacter nicotinovorans* ATCC 49919 is a soil nicotine-degrading bacterium that harbours the pAO1 catabolic megaplasmid. Although the nicotine catabolic genes have been sequenced, there is a gap in knowledge regarding the interplay between the degradation pathway and the general metabolism of the cell. A better understanding of the mechanisms which regulate nicotine catabolism would unlock the strain's potential in converting the toxic alkaloid into valuable precursors for drug synthesis and green chemicals. Here, long-read direct RNA nanopore sequencing was used to study the transcriptome of *P. nicotinovorans* ATCC 49919 grown in the presence and absence of nicotine.

Materials and methods: The bacterium was grown on citrate medium with and without nicotine. Cells were harvested at three timepoints correlated with nicotine catabolism (~5, 10 and 24 h after inoculation). Native RNA was extracted with the Promega SV Total RNA Isolation System. Because library preparation was performed with the Oxford Nanopore Technologies (ONT) Direct RNA sequencing kit (SQK-RNA002) designed for eukaryotes, adenine tails are required for ONT sequencing adapter ligation. Therefore, using the Lucigen Poly(A) Polymerase Tailing Kit, the extracted *P. nicotinovorans* native RNA was incubated with the *E. coli* poly(A) polymerase I to provide the necessary adenine tails for adapter ligation and sequencing. The applied library prep protocol and data acquisition parameters were adjusted for use with the ONT Flongle instead of the SpotON flow cell. Direct RNA sequencing was performed with the ONT MinION Mk1B device equipped with Flongle flow cells and controlled via the MinKNOW software. Raw data was basecalled with the Guppy_6.3.2 high accuracy algorithm. The resulting RNA sequences were quality controlled and analysed for differential gene expression between control and nicotine-treatment using the nf-core/nanoseq pipeline v3.1.0.

Results: A total of 24 sequencing runs were performed, representing 4 replicates per timepoint and treatment, with a yield of 1 million reads totalling over 1 Gb, 80% of which had quality scores above 7. The longest read measured ~12 kb and the average read length was 1.2 kb. Differential expression (DE) analyses were performed with DESeq2. Over 40 genes with nicotine-related expression ($p_{adj} < 0.1$; $abs(\log_2\text{FoldChange}) > 1$) were identified: 15 were previously known to be involved in nicotine catabolism and the remaining genes are reported here first. Time-based analyses indicated the presence of nicotine-related transcripts up to ten hours after inoculation. 24 h after inoculation there was only one statistically significant ($p_{adj} < 0.1$) DE transcript between control and nicotine-treatment, encoding for a universal stress protein previously linked to resistance to oxidative stress.

Conclusions: This study represents the first transcriptomic analysis of *P. nicotinovorans* ATCC 49919. Differential expression analyses identified over 20 novel genes which are suggested here first as having nicotine-related expression.

Acknowledgements: This work was supported by a grant from the Romanian Ministry of Education and Research, CNCS-UEFISCDI, project number PN-III-P4-ID-PCE-2020-0656, within PNCDI III.

pH-responsive nanocapsules for anthocyanins encapsulation, delivery, intracellular tracking, and controlled release inside B16-F10 melanoma cells

Adela Maria Dăescu¹, Mădălina Nistor¹, Monica Focșan², Roxana Pop¹,
Adela Pinteă¹, Maria Suciuc^{3,4} and Dumitrița Rugină¹✉

¹Faculty of Veterinary Medicine, University of Agricultural Sciences and Veterinary Medicine, Cluj-Napoca, Romania; ²Sciences, Babes-Bolyai University, Cluj-Napoca, Romania; ³Electron Microscopy Centre "C. Craciun", Biology and Geology Faculty, Babes-Bolyai University, Cluj-Napoca, Romania; ⁴National Institute for Research and Development of Isotopic and Molecular Technologies, Cluj-Napoca, Romania; ✉**Corresponding author, E-mail: dumitrita.rugina@usamvcluj.ro**

Introduction: Melanoma, the most lethal form of skin cancer, is characterized by the accumulation of a large load of mutations in melanocytes, mainly due to prolonged exposure to ultraviolet rays. Due to the multiple effects demonstrated by anthocyanins (AntS) in suppressing the expansion of melanoma, they can be considered promising sources of therapeutic molecules. The present article aimed to manufacture a fluorescent pH-sensitive polymeric nanosystem (Nano@AntS), capable of encapsulating the AntS extracted from *Aronia melanocarpa* fruits, that travels through the cellular environment and resists at a continuous decrement of pH, thus maintaining the AntS's stability.

Materials and methods: The extracted anthocyanins were purified using the solid phase extraction (SPE) technique and then subjected to HPLC chromatography. The purified anthocyanins were nano-encapsulated. The synthesis of Nano@AntS was done using a layer-by-layer technique, their morphology was examined by scanning and transmission electron microscopy (SEM/TEM) and the mean size was determined by DLS analysis. The presence and arrangement of fluorophores RBITC (561nm) and FTIC (468 nm) in the structure of the nanocapsules were verified using conventional fluorescence microscopy, confocal microscopy with double scanning RCM-VIS, and fluorescence microscopy (FLIM). WST-1 viability assay was used to determine the viability of the B16-F10 murine melanoma cell line after nanocapsules treatment. The FLIM and TEM microscopy techniques were used for the delivery, internalization, and intracellular localization of Nano@AntS in melanoma cells.

Results: Nano@AntS was successfully constructed by layer-by-layer technique with a final size between 50-200 nm and an encapsulation efficiency of AntS of 63%. The optimal release of AntS was obtained in solution at a pH

value of 4.5 and 6.5. The system also induced maximal cytotoxicity of 40% on the tested cells, and the effect of AntS as a pure extract was highly cytotoxic in a dose-dependent manner. The localization and internalization of Nano@AntS were mostly observed in the cytoplasm.

Conclusions: This research successfully proposed and described a novel targeted drug delivery nanosystem with a modulated pH response, offering a potentially effective treatment for melanoma, adequate intracellular delivery of anthocyanins, and controlled response in the internal pH environment of melanocytes.

Acknowledgments: This research was funded by the Romanian National Authority for Scientific Research, CNDI- UEFISCDI, project number PN-III-P1-1.1-TE-2019-1276.

Design and preclinical testing of an anti-CD41 CAR T cell for the treatment of acute Megakaryoblastic leukemia

Adrian Bogdan Tigu^{1✉}, Catalin Sorin Constantinescu^{1,2,3}, Patric Teodorescu^{2,4}, David Keygyes^{1,2}, Raluca Munteanu¹, Richard Feder¹, Mareike Peters^{1,2}, Ioana Pralea¹, Cristina Iuga¹, Diana Cenariu¹, Andra Marcu^{5,6}, Alina Tanase^{5,6}, Anca Colita^{5,6}, Rares Drula¹, Jon Thor Bergthorsson^{7,8}, Victor Greiff⁹, Delia Dima¹⁰, Cristina Selicean¹⁰, Ioana Rus¹⁰, Mihnea Zdrenghea¹⁰, Diana Gulei¹, Gabriel Ghiaur^{1,4} and Ciprian Tomuleasa^{1,2,10}

¹ Medfuture Research Center for Advanced Medicine, Iuliu Hatieganu University of Medicine and Pharmacy, Cluj-Napoca, Romania; ² Department of Hematology, Iuliu Hatieganu University of Medicine and Pharmacy, Cluj-Napoca, Romania; ³ Intensive Care Unit, Emergency Clinical Hospital, Cluj-Napoca, Romania; ⁴ Department of Leukemia, Sidney Kimmel Cancer Center at Johns Hopkins, Johns Hopkins University School of Medicine, Baltimore, MD, United States; ⁵ Department of Pediatrics, Carol Davila University of Medicine and Pharmacy, Bucharest, Romania; ⁶ Department of Stem Cell Transplantation, Fundeni Clinical Institute, Bucharest, Romania; ⁷ Stem Cell Research Unit, Biomedical Center, School of Health Sciences, University of Iceland, Reykjavik, Iceland; ⁸ Department of Laboratory Hematology, Landspítali, University Hospital, Reykjavik, Iceland; ⁹ Department of Immunology, University of Oslo and Oslo University Hospital, Oslo, Norway; ¹⁰ Department of Hematology, Ion Chiricuta Clinical Cancer Center, Cluj Napoca, Romania; ✉ **Corresponding author, E-mail:** adrianbogdantigu@gmail.com

Introduction: Acute Megakaryoblastic leukemia (AMkL) is a rare subtype of acute myeloid leukemia (AML) representing 5% of all reported cases, and frequently diagnosed in children with Down syndrome. Patients diagnosed with AMkL have low overall survival and have poor outcome to treatment, thus novel therapies such as CAR T cell therapy could represent an alternative in treating AMkL. In the last decades, significant progress has been made in the field of novel immunotherapeutic agents that can be used as treatments for hematological malignancies. Chimeric antigen receptor T cells (CAR T cell) are the T cells modified to recognize specific antigen. Currently, five FDA-approved CAR-T cell therapies are used in the clinic. This is the case for the antiCD19 CAR T cells tisagenlecleucel, brexucabtagene autoleucel, lisocabtagene maraleucel and axicabtagene ciloleucel, as well as the anti-BCMA idecabtagene vicleucel. Thus, the existing CAR T cells are mostly targeting CD19, which is a specific antigen for B cells, with impressive for B-cell acute lymphoblastic leukemia and B-cell non-Hodgkin lymphomas.

Materials and methods: The cell populations were evaluated by Flow cytometry, cytokine evaluation by ELISA Assays and LDH using a colorimetric test.

Results: The performed flow cytometry evaluation highlighted a percentage of 93.8% CAR T cells eGFP- positive and a limited acute effect on lowering the target cell population. However, the interaction between effector and target (E:T) cells, at a low ratio, lowered the cell membrane integrity, and reduced the M7-AMkL cell population after 24h of co-culture, while the cytotoxic effect was not significant in groups with higher E:T ratio. The cells were maintained in sterile conditions during the experiment.

Conclusions: Our findings suggest that the anti-CD41 CAR T cells are efficient for a limited time spawn and the cytotoxic effect is visible in all experimental groups with low E:T ratio.

Acknowledgements: This work was funded from Young Research Teams (PN-III-PI-1.1-TE-2019-0271 --“Supporting a team of young researchers to create an independent research program based on the use of Sleeping Beauty protocol for the development of CAR T Cells - SEATTLE”).

***In vitro* biological performance of 3D-printed PLA-based composites as bone scaffolds**

Andreea Mariana Negrescu^{1✉}, Valentina Mitran¹, Florin Miculescu²,
Aura Catalina Mocanu², Andreea Elena Constantinescu² and
Anisoara Cimpean¹

¹*Department of Biochemistry and Molecular Biology, Faculty of Biology, University of Bucharest, Bucharest, Romania;* ²*Department of Metallic Science, Physical Metallurgy, University Politehnica of Bucharest, Bucharest, Romania;* ✉**Corresponding author, E-mail:** andreea.ne94@gmail.com

Introduction: The positive outcome of an implant depends mainly on the functionality of the biomaterial, therefore the development of new scaffold materials with favourable mechanical and biological properties is imperative for an efficient regeneration process. Due to their favourable biocompatibility and biodegradability, polylactic acid (PLA) based materials are frequently used in various medical applications, such as sutures or orthopaedic fixation devices. However, PLA alone has an insufficient mechanical strength and osteoconductivity, therefore the incorporation of different particles such as hydroxyapatite (HA) into the PLA matrix constitutes a promising strategy towards an enriched composite material. Moreover, having just expanded into the biomedical field, graphene (GnP) and its derivatives continues to attract interest due to their unique characteristics and numerous efforts have been made to employ their exceptional properties for the regeneration of different tissues, particularly bone. In this context, we developed 3D printed composite products, based on PLA, GnP, and naturally derived HA.

Materials and methods: The composite substrates were fabricated through the incorporation of different ratios of HA (0–50%) and GnP (0–5%) into the PLA matrix. For each sample, the mixing process required the following steps: (1) mechanical homogenization; (2) thermal homogenization at a constant temperature (~200 °C); (3) flattening of the viscous slurry between two ceramic plates to a thin lamella/film of 1 ± 0.05 mm thickness; (4) cutting the lamella into small pieces to facilitate the extrusion procedure. In the end, the extruded filaments were transformed into 3D printed plates via the Fused deposition modelling (FDM) technique. *In vitro* performance of the novel composite scaffolds was explored through direct contact assays using the MC3T3-E1 pre-osteoblasts and RAW 264.7 macrophages. The cellular behaviour of the pre-osteoblasts was assessed in terms of cell viability/proliferation,

morphology and osteogenic differentiation, while the inflammatory response of the RAW 264.7 cells was investigated via cell viability/proliferation and morphological features analysis, and also through the quantification of specific inflammatory mediators and foreign body giant cells (FBFCs) formation.

Results: The results suggested that all samples, in various degrees, supported cell survival/proliferation, for both cell lines. Similar, the cytoskeletal examination revealed typical cellular morphologies; however, with significant differences in cell density (a reduced number of cells on 5% GnP and 4% GnP samples). Likewise, the differentiation study demonstrated their ability to promote new bone formation. Nonetheless, the supports led to the formation of FBGCs even in the lipopolysaccharide (LPS) absence in the next order: 5%GnP < 4%GnP < 1%GnP < 2%GnP < 3 %GnP < 1%GnP. This surprising result could be explained by the low number of cells found on the 5%GnP and 4%GnP samples as compared to the rest.

Conclusions: Taken together, our results demonstrate that all analyzed samples, with the exception of 4% GnP and 5% GnP and to a different extent, meet the strict requirements of a biomimetic material for bone tissue engineering applications.

Acknowledgements: This work was funded by CNCS—UEFISCDI (PN-III-P2-2.1-PED-2021-1650).

Novel biohybrid enriched with curcumin and quercetin displays favorable properties as potential active wound dressing for biomedical applications

Andreea-Daniela Lazăr (Popa)¹, Lea Sleiman¹✉, Maria Minodora Marin^{3,4}, Mădălina Georgiana Albu-Kaya³, Marieta Costache^{1,2} and Sorina Dinescu^{1,2}

¹ Department of Biochemistry and Molecular Biology, University of Bucharest, Bucharest, Romania;

² Research Institute of the University of Bucharest (ICUB), Bucharest, Romania; ³ Collagen Department, Leather and Footwear Research Institute, Bucharest, Romania; ⁴ Politehnica University of Bucharest, Advanced Polymer Materials Group, Bucharest, Romania;

✉ **Corresponding author, E-mail:** sleiman.lea@s.bio.unibuc.ro

Introduction: Chronic wounds require repetitive treatments, incur considerable medical costs and can lead to other dangerous medical conditions, such as diabetic ulcers, which precede amputations. Thus, much effort has been focused on developing wound dressings with intrinsic beneficial properties that could facilitate the impaired healing process of acute lesions. Among the natural agents considered for severe wound healing are phytochemicals, such as curcumin (C) and quercetin (Q). In this study, we evaluated if the addition of novel encapsulated CQ improved the properties of collagen-sericin (Coll-SS) materials in terms of biocompatibility, cell adhesion, anti-inflammatory and antioxidant effects.

Materials and methods: Coll-SS tridimensional materials, enriched or not with CQ microcapsules (Coll-SS- CQ) were developed and characterized using scanning electron microscopy (SEM). The compositions were seeded with keratinocytes from an adult human skin cell line and cultivated for up to 7 days. During biocompatibility assessment, MTT assay was used for cell viability and proliferation evaluation, LDH assay to investigate the biohybrids' cytotoxicity, and Live/Dead staining was performed to visualize the extent of live and dead cells, comparing Coll-SS-CQ to a pure Coll-SS matrix. Immunolabeling and confocal microscopy allowed observation of cytoskeleton distribution. The levels of proinflammatory mediators in response to CQ anti-inflammatory effect were evaluated after induced macrophages were put in contact with the materials, at gene and protein level. Activated macrophages exposed to no other treatment were considered positive reference in analysis. Moreover, ROS production was quantified to assess the antioxidant effect.

Results: All samples exhibited a uniform porous structure with interconnected pores, beneficial for cell growth and migration, as shown by representative SEM images. After one week of *in vitro* culture, the biohybrids presented good biocompatibility, without significant cytotoxic effects. Highest cell viability and proliferation were registered for Coll-SS-CQ material, as compared to the controls. Cytoskeleton staining revealed proper adhesion of skin cells to the substrates and highlighted an elongated cell morphology of actin microfilaments. Results indicated a clear decrease in proinflammatory cytokine levels secreted by cells in contact with Coll-SS-CQ, as well as ROS production, suggesting that the encapsulation and gradual release of CQ results in a more efficient anti-inflammatory and antioxidant response.

Conclusions: In conclusion, the novel Coll-SS biohybrid enriched with encapsulated CQ can be considered as a potential active wound dressing for biomedical applications.

Acknowledgements: This work was funded by CNCS-UEFISCDI, project no. PN-III-P2-2.1-PED-2021-2917/HEALSKIN.

La(Nal)₃ loaded PDMAEMA NPs induce HT-29 adenocarcinoma cells apoptosis in vitro

Bianca Galateanu¹✉, Alexandra Cowell², Valentina Uivarosi²,
Mirto Charitaki³, Kelly Velonia³ and Ariana Hudita¹

¹ University of Bucharest, Bucharest, Romania; ² University of Medicine and Pharmacy Carol Davila from Bucharest, Bucharest, Romania; ³ University of Crete, Crete, Greece;
✉Corresponding author, E-mail: bianca.galateanu@bio.unibuc.ro

Introduction: Recent statistics rank colorectal cancer (CRC) as the second cause of cancer-related deaths and third as incidence and highlight the emerging need to improve the currently available therapeutic approaches. In the context of increasing resistance and dose-limiting side effects to traditional chemotherapy, a current strategy in bringing the activity of 'older' drugs back into clinical use for purposes that are outside the scope of the original medical indication (drug repositioning). With this respect, we intend to shift the 'old' antibacterial quinolones to anticancer compounds via coordination with appropriate metal ions such as La. In this study, we investigated the anticancer activity on HT-29 adenocarcinoma cells of the complex La(Nal)₃ (HNal = nalidixic acid) and of the complex-loaded poly[2-(N,N-dimethyl amino) ethyl methacrylate (PDMAEMA) based nanoparticles(NPs).

Materials and methods: The IC₅₀ dose of the La(Nal)₃ - loaded PDMAEMA NPs on HT-29 adenocarcinoma cells was previously determined by using the MTT spectrophotometric assay. This dose was further used to investigate the pro-apoptotic potential of the pristine and La(Nal)₃ - loaded PDMAEMA NPs. Briefly, HT-29 adenocarcinoma cells were seeded at an initial cell density of 5 x 10³ cells/cm² in 6 well plates and allowed 24h to adhere to the culture surface in standard conditions of culture (37 °C, humidified atmosphere and 5% CO₂). Then, the monolayers were treated with pristine NPs, La(Nal)₃ - loaded PDMAEMA NPs and La(Nal)₃ and incubated for another 6h and 24h. An untreated control monolayer was kept for each time point. Apoptosis was investigated by annexin-V/PI test using flow cytometry (Cytoflex, Beckman Coulter)

Results: Our results show that both the control and the cells treated with pristine NPs remained viable and negative for annexin V and PI, while the cells treated with La(Nal)₃ and La(Nal)₃ - loaded PDMAEMA NPs entered apoptosis after 6h of treatment.

Conclusions: In conclusion, the novel $\text{La}(\text{Nal})_3$ – loaded PDMAEMA NPs exert pro-apoptotic effects *in vitro* and could be further used for *in vivo* studies to investigate their bio distribution and delivery efficacy.

Acknowledgements: This work was supported by the Ministry of Research, Innovation and Digitization, CNCS UEFISCDI through grant number PN-III-P1-1.1-TE-2021-1660 within PNCDI III (104TE/2022).

Novel photosensitizing methylene blue analogues for antimicrobial photodynamic therapy

Bianca Stoean¹✉, Iulia Lupan² and Luiza Găină¹

¹ Research Center on Fundamental and Applied Heterochemistry, Faculty of Chemistry and Chemical Engineering, Babeș-Bolyai University, Cluj-Napoca, Romania; ² Department of Molecular Biology and Biotechnology, Babeș-Bolyai University, Cluj-Napoca, Romania;

✉Corresponding author, E-mail: bianca.stoean@ubbcluj.ro

Introduction: Photodynamic therapy (PDT) is based on the principle of administering a photosensitizer, followed by irradiation with visible light (using the wavelength specific to the absorption of the photosensitizer molecule). In the presence of molecular oxygen in the cells, the photosensitizer forms cytotoxic species ($^1\text{O}_2$ -oxygen singlet, free radicals-ROS) that result in cell death through various mechanisms, such as apoptosis, angiogenesis or autophagy. Used in the last two decades as a treatment against malignant and benign tumors, photodynamic therapy seems to be a good alternative in the fight against bacteria that have become resistant to existing antibiotics.

Materials and methods: Broth dilution method were performed in order to test the inhibition effects of tested MB compounds against *Escherichia coli* ATCC 25922; *Staphylococcus aureus* ATCC 25923; *Pseudomonas aeruginosa* ATCC 27853; *Deinococcus radiodurans* (DSM no. 20539). The tested bacterial strain was cultivated in Mueller-Hinton Broth (*P. aeruginosa* and *S. aureus*) and Luria Broth (*E. coli*) at 37°C or TGY medium (*D. radiodurans*) at 28°C. Minimum inhibitory concentration (MIC) was determined for both the scenario where methylene blue (MB) analogues were not irradiated and the case where the compounds were irradiated with 660 nm wavelength light of 1,2 mW power coming from a LED lamp (M660L4-C1) leading to the singlet oxygen formation.

Results: For all studied methylene blue analogues, the minimum inhibitory concentration for all tested bacterial strains (gram-positive and gram-negative) were remarkably lower with 660 nm light LED irradiation, demonstrating the efficacy of using photodynamic therapy against resistant bacteria.

Conclusions: In this work we examine the ROS production capacity and the potential for use in antimicrobial photodynamic therapy for a series of MB analogues recently reported by our group covering auxochromic alteration by steric and electronic factors affecting the position of their absorption wavelength maxima, aggregation and hydrophilic/lipophilic balance.

Acknowledgements: This work was supported by a grant of Romanian Ministry of Research and Innovation, CNCS – 788 UEFISCDI, project number PN-III-P4-ID-PCCF-2016-0142, within PNCDI III.

Building a 3D printed microscope – the OpenFlexure@BioIASI project

Maria Paula Ciurlic¹✉, Andreea Monica Colpoș¹, Marius Ștefan¹ and Marius Mihășan¹

¹*BioActive research group, Department of Biology, Alexandru Ioan Cuza University of Iași, Romania;* ✉ **Corresponding author, E-mail:** ciurlicmp@gmail.com

Introduction: The OpenFlexure project (<https://openflexure.org>) aims to provide an open-source, 3D-printed microscope with applications in both medical and teaching environment. OpenFlexure@BioIASI is a student-based project that kicked off in 2021 with the goal of building and evaluating the real costs of a 3D printed OpenFlexure microscope and its applications in the practicals taking place at the Department of Biology, Alexandru Ioan Cuza University of Iași.

Materials and methods: All parts required were sourced from local and overseas distributors (Aliexpress and alike) at a total cost of about 200 euros. All objectives were sourced from old or not working microscopes. All printed parts were fabricated from PLA using an Creality Ender-5 printer at a total cost of 5 euro.

Results: Following the instructions available, a fully motorized, single objective microscope was built which uses a Raspberry Pi camera to acquire images and a Raspberry Pi single board computer running the specialized Raspbian OpenFlexure Lite OS to control the motors. The microscope was configured to generate its own Wi-Fi network and hence a simple laptop with a browser is all that is required to control it. Its optical performance was so far tested in different settings and it was shown that it provides images that are comparable with other microscopes such as: Leica DM 1000 LED, Lacerta BIM 151 T-LED, Optika B-157R-PL, Optika B-350 PL and Olympus BX41. Some drawbacks were nevertheless recorded, such as a low power light supply, poor condenser lenses and low overall robustness of the build.

Conclusions: In a controlled environment, the 3D printed microscope could replace professional microscopes and provide good-enough images.

MDS cells maturation induced by ATRA differentiating agent in myelodysplastic syndromes

Diana Cenariu¹✉, Adrian Bogdan Tigu¹, David Kegyes¹, Mareike Peters¹, Jon Thor Berghthorsson⁶, Victor Greiff⁷, Cenariu Mihai⁵, Gabriel Ghiaur^{1,8} and Ciprian Tomuleasa^{1,2,3,4}

¹Medfuture Research Center for Advanced Medicine, Iuliu Hatieganu University of Medicine and Pharmacy Cluj Napoca, Cluj Napoca, Romania; ²Department of Hematology, Iuliu Hatieganu University of Medicine and Pharmacy Cluj Napoca, Cluj Napoca, Romania; ³Department of Hematology, Ion Chiricuta Clinical Cancer Center Cluj Napoca, Cluj Napoca, Romania; ⁴Department of Chemotherapy, Ion Chiricuta Clinical Cancer Center, Cluj Napoca, Romania; ⁵Univ Agr Sci & Vet Med, Dept Anim Reprod & Reprod Pathol, Cluj Napoca Romania; ⁶Univ Iceland, Biomed Ctr, Sch Hlth Sci, Stem Cell Res Unit, Reykjavik, Iceland; ⁷Univ Oslo, Dept Immunol, Oslo, Norway; ⁸ Johns Hopkins University, Baltimore, USA; ✉Corresponding author, E-mail: diacenariu@gmail.com

Introduction: Myelodysplastic syndromes (MDS) are heterogeneous hematopoietic stem cell (HSC) disorders characterized by bone marrow (BM) dysplasia and peripheral cytopenias. CYP26 activity in the BME protects normal and malignant HSCs from ATRA-induced differentiation and contributes to drug resistance. Malignant cells can hijack control of stromal CYP26 activity to create permissive microenvironments.

Materials and methods: In vitro cultivation of MDS92 cells and OP9 cells, treated with different ATRA concentrations (10e-9M, 3x10e-9M, 10e-8M, 3x10e-8M, 10e-7M) to induce differentiation. Talarozol (R115866), an inhibitor that blocks CYP26 was added to the ATRA treatment in the experimental design, at 1nM concentration. Flow cytometry evaluation. The processed experimental samples are labelled with 4 antibodies: CD45PerCP-Cy5.5: CD38APC-H7: CD11b APC: GlyA-PE and the mean fluorescence intensity is calculated. Colony forming units are performed to evaluate and validate the maturation of MDS cells following ATRA treatment, by counting the number of colonies formed in each plate. 2.000 cells from each combination MDS92 no stroma and MDS92 co-cultivated with stromal OP9 on 6 well plates on methylcellulose for 14 days, have been counted.

Results: CD45 staining isolates the leucocyte population out of the analyzed cells; from here, specific antibodies that prove maturation of MDS92 cells are used: CD38, CD11b and Gly A. There is a shift in the positive population of mature cells dependent of the ATRA treatment concentration. Best results are observed at 10e-8M ATRA. The number of colonies formed is counted in

triplicate for all wells and compared in Graph Prism 8.0. The number of colonies formed decreases, once the differentiation of MDS92 cells is induced due to the retinoic acid treatment, in the presence/absence of stroma.

Conclusions: Since myelodysplastic cells mature slower in the presence of stroma than those grown without stroma by the addition of Talarozol to the experimental design we could prove that R115866 blocks Cyp26, thus therapy resistance can be eliminated in vitro. The ATRA inactivation is stronger on MDS92 in the presence of stroma OP9, which proves that Cyp26 is involved in limiting the production of the active ATRA.

Acknowledgements: The research was financed by an international collaborative grant of the European Economic Space between Romania, Iceland and Norway 2014–2021, “Continuous Flow Interchange of Communication and Knowledge in Biomedical University Research” (grant number 21-COP-0034).

3D tumor spheroids as a model to unriddle the complexity of tumor microenvironment chemoresistance

Giorgiana Negrea¹✉, Szilvia Meszaros², Stefan Drăgan²,
Vlad-Alexandru Toma^{2,3}, Bogdan Dume¹, Valentin-Florian Rauca²,
Laura Pătraș², Emilia Licărete², Manuela Banciu² and Alina Sesărman²

¹ Doctoral School in Integrative Biology, Faculty of Biology and Geology, "Babes-Bolyai" University, Cluj-Napoca, Romania; ² Department of Molecular Biology and Biotechnology, Center of Systems Biology, Biodiversity and Bioresources, Faculty of Biology and Geology, "Babes-Bolyai" University, Cluj-Napoca, Romania; ³ Department of Experimental Biology and Biochemistry, Institute of Biological Research, Branch of NIRDBS Bucharest, Cluj-Napoca, Romania;
✉ **Corresponding author, E-mail:** giorgiana.negrea@ubbcluj.ro

Introduction: Recent oncology advances emphasize the tumor microenvironment (TME) critical role in drug resistance. Therefore, accurate models reflecting TME complexity are essential. 3D models offer greater tumor heterogeneity compared to 2D cell cultures, making them a pioneering tool for cancer research. Our aim was to create 3D in vitro models with B16.F10 murine melanoma cells combined with endothelial cells (2H11) and/or primary macrophages, to mimic the chemoresistant melanoma microenvironment, and to validate them using doxorubicin.

Materials and methods: Macrophages were isolated from C57BL6 mice bone marrows. Spheroids were created using the liquid overlay technique, co-culturing B16.F10 murine melanoma cells with endothelial cells or macrophages in non-adherent 96-well plates with 1.5% commercial extracellular matrix (ECM). Characterization of the 3D cocultures included morphology analysis by light microscopy, as well as immunohistochemistry using specific antibodies for component cells. To assess the models' ability to mimic melanoma microenvironment chemoresistance, spheroids were treated with DOX (IC30), a chemotherapeutic drug to which melanoma patients fail to respond. Parameters like HIF-1 α , VEGF, and leptin expression, total antioxidant capacity, and peroxidase activity were evaluated using western blot, protein microarray, and spectrophotometry.

Results: The developed models displayed some of the chemoresistance traits. After DOX treatment, the 3D coculture with B16.F10 melanoma cells and macrophages showed significant increases in total antioxidant capacity (TAC) and catalase activity ($p < 0.05$) compared to the control group (untreated spheroids). Immunohistochemistry analysis indicated no changes in peroxidase

activity ($p>0.05$) in DOX-treated spheroids compared to control. Moreover, the chemoresistant profile persisted when B16.F10 melanoma cells were 3D cocultured with endothelial cells and treated with DOX, as key angiogenesis promoters (HIF-1 α , VEGF, and leptin) remained unchanged compared to the control group ($p>0.05$). These findings demonstrate that the cells involved in the 3D coculture models, exhibit a deliberate mechanism to evade substantial molecular alterations when exposed to DOX treatment, suggesting a strategic approach in preserving protumor processes crucial for driving tumor growth.

Conclusions: Our results indicate the reliability of our models in reflecting chemoresistance characteristics of the melanoma microenvironment. To better understand the complex cellular interactions driving melanoma's chemoresistant profile, further investigation with additional cell types and analysis of other key parameters is needed.

Acknowledgements: This work was funded from UEFISCDI grant PN-III-P2-2_1-PED-2021-0411 (No. 659PED/2022) granted to Alina Sesarman.

Peptide-based therapeutics

Lucian Copolovici¹✉, Andreea Gostăviceanu^{1,2}, Simona Gavrilaș¹,
Dana G. Radu¹, Mihaela Dochia¹, Cristian Moisa¹, Andreea Ioana Lupitu¹,
Dana Maria Copolovici¹

¹"Aurel Vlaicu" University of Arad, Faculty of Food Engineering, Tourism and Environmental Protection and Institute of Technical and Natural Sciences Research-Development-Innovation of "Aurel Vlaicu" University, Arad, Romania; ² University of Oradea, Biomedical Sciences Doctoral School, Oradea, Romania;
✉ **Corresponding author, E-mail:** lucian.copolovici@uav.ro

Introduction: Traditional treatments for cancer have very bad side effects. Peptide-based therapy as a complementary choice for treating cancer has shown promising results because it is selective, and is safe. The goal of this study was to explain the different ways that peptides are used in cancer therapy, as well as the engineering techniques that are used to improve the effectiveness of peptides, and to look at the current state and future trends of publications about anticancer peptides.

Materials and methods: For the bibliometric study, we searched articles published in PubMed, ScienceDirect, and Web of Science, Clarivate, in the last two decades.

Results: Information was gathered about how peptides work in anticancer treatment. Anticancer peptides may get rid of cancerous cells in more than one way. Engineering techniques have been used successfully to improve the effectiveness of peptides by making them more bioavailable. The bibliometric study depicts how important anticancer peptides have become in the treatment of cancer in the last 20 years.

Conclusions: Biopharmaceutical peptides have led to new ways to treat and prevent many diseases, including cancer. Peptide-based therapeutics have opened up new ways to control drug delivery and improve clinical results in cancer by using innovative peptide-based assembly. Like some common polymeric formulations, these macromolecules may be able to greatly slow the rate at which a drug is released. Peptides, unlike many polymeric formulations, can be made to fit a specific sequence by using genetic engineering. This makes them an interesting option to traditional formulations. Combinations of peptide-based strategies and conventional therapies are being investigated for their potential synergistic effects in the development of anticancer drugs.

Acknowledgements: This work was supported by a grant of the Ministry of Research, Innovation and Digitization, CNCS - UEFISCDI, project number PN-III-P4-PCE-2021-0639, within PNCDI III.

Cell behaviour modulation by new polydimethylsiloxane (PDMS) modified interfaces

Madalina Icriverzi¹✉, Paula Ecaterina Florian¹, Anca Bonciu²,
Nicoleta Dumitrescu², Laurentiu Rusen², Valentina Dinca²,
Anca Roseanu¹

¹ Institute for Biochemistry of Romanian Academy, Bucharest, Romania;

² National Institute for Laser, Plasma and Radiation Physics, Măgurele, Romania;

✉ **Corresponding author, E-mail:** mradu@biochim.ro

Introduction: Different strategies for improved efficiency of implanted devices are developed. Surface texturing and chemical modifications are important strategies to allow medical-devices to improve biocompatibility and also minimizing adverse responses. Here we present our results regarding polydimethylsiloxane (PDMS) modified interfaces, their physical-chemical characteristics and *in vitro* effect on cell behaviour.

Materials and methods: Matrix-Assisted Laser Evaporation (MAPLE) method was used to create the newly proposed functionalized scaffold and physical-chemical characteristics were evaluated by Scanning Electron Microscopy, Atomic Force Microscopy, Contact angle, Surface energy, Fourier Transform Infrared Spectroscopy and X-ray Photoelectron Spectroscopy. Cell adhesion, proliferation and morphology of cells grown on Polydimethylsiloxane (PDMS) surfaces were evaluated in *in vitro* studies, using human macrophages and fibroblasts, cells paying an important role in foreign body reaction.

Results: Physical and chemical properties of the new coatings revealed that the MAPLE technique has the advantage of achieving homogeneous, stable and moderate hydrophilic thin layers onto hydrophobic PDMS. In addition, the proposed approach does not require any pre-treatment, therefore avoiding the major disadvantage of hydrophobicity recovery. Statistically significant reduction of the adhesion and proliferation of human macrophages and of human fibroblasts grown on PDMS with modified surfaces compared to unmodified scaffold was revealed by *in vitro* biological investigations. These findings evidence the capacity of the newly PDMS modified surfaces to modulate cell behaviour and thus to overcome undesired cell responses such as inflammation and fibrosis.

Conclusions: Our data highlighted the potential for the new PDMS modified interfaces obtained by MAPLE to develop PDMS-based implants able to mitigate foreign body response and thus to be used in the biomedical field.

Acknowledgements: This research was funded by a grant of the Romanian Ministry of Education and Research, project number project PN-III-P4-ID-PCE-2020-2375. P.F., M.I. and A.R. acknowledge and thank the partial support of Project No.5 of the Structural and Functional Proteomics Research Program of the Institute of Biochemistry of the Romanian Academy.

Biodegradable chitosan-based films for biomedical applications

Mariana-Adina Matica^{1✉}, Alexandra Năstasie², Alexandra Tudor²,
Timea Kelemen², Ramona Alicu² and Diana-Larisa Roman^{2,3}

¹ Department of Chemistry-Biology, Institute for Advanced Environmental Research, West University of Timisoara, Timisoara, Timiș, Romania; ² Department of Biology-Chemistry, Faculty of Chemistry, Biology, Geography, West University of Timisoara, Timisoara, Timiș, Romania; ³ Advanced Environmental Research Laboratories, West University of Timisoara, Timisoara, Timiș, Romania; ✉ **Corresponding author, E-mail:** mariana.matica@e-uvt.ro

Introduction: Chitosan is a cationic polymer, widely found in nature, and used in biomedical application due to its numerous advantages such as biodegradability, biocompatibility, antimicrobial and wound healing properties, as well as low toxicity. The film-forming capacity of chitosan makes it a suitable polymer for wound dressing development. The use of chitosan combined with antimicrobial peptides (AMPs) is a common practice adopted in order to overcome the increase of antibiotic resistance to conventional antibiotics. Nisin is a polycyclic cationic peptide classified as a Type A (I) lantibiotic molecule and a GRAS (Generally Recognized As Safe) molecule, mainly used in food industry, but recent approaches indicate its use biomedical fields, as an alternative to common antibiotics. The purpose of this study was to design chitosan-based films with enhanced antibacterial effect against most common pathogenic bacteria, using nisin as a potential antimicrobial compound.

Materials and methods: A medium molecular weight chitosan was used to prepare chitosan-based films containing different concentration of nisin (5 mg/mL and 10 mg/mL). Chitosan films were prepared via solvent casting method and glycerol was added as a plasticizer. Physico-chemical properties of the films were determined, as well as the microbiological properties, using most common pathogens strains (*Escherichia coli*, *Pseudomonas aeruginosa* and *Staphylococcus aureus*). Moreover, biodegradable studies were carried out by testing chitosan-based films degradation in soil and in order to observe the impact of the polymeric materials, the total microbial count and enzymatic activity of soil microbiome was analyzed.

Results: Chitosan-based films are suitable materials for the sustained delivery of antimicrobial compounds. The results have shown that the release of nisin from chitosan matrix happens at a slow and sustained rate, at a pH value

similar to the most common wound environment. Such properties such as swelling, water-vapor permeability and optical properties of the films indicate that the biomaterials are suitable as wound dressing starting material. Moreover, the microbial permeation studies and microbiological analysis reveal that the addition of nisin increases the antibacterial effect of the films, while the biodegradability studies show that these type of materials are safe for the environment.

Conclusions: Chitosan plays an important role in biomedical application as it offers a safer and environmentally friendly alternative in creating drug-delivery platforms, with slow and sustained drug release. The use of AMPs in order to enhance the pristine antibacterial effect of chitosan, can be favorable and can help overcome the main drawback represented by the use of conventional antibiotics. Moreover, the availability of chitosan as a waste byproduct generated by the seafood processing industry is a topic that lines up with the interest of current scientific research, which is to enhance exploitable resources in the context of the circular and sustainable economy.

Acknowledgements: This work was funded from CNFIS-FDI-2022-0246 „Consolidarea capacității instituționale a Universității de Vest din Timișoara în domeniul cercetării științifice de excelență” and the ERA-Net COFASP Project “Biotechnological tools implementation for new wound-healing applications of byproducts from the crustacean seafood processing industry-Chitowound (project no. PN3-P3-284/4/2017 program H2020, financed by the Romanian National Authority for Scientific Research UEFISCDI).

Development of a 3D Model for immunotherapy evaluation in melanoma

Marta-Szilvia Meszaros¹, Giorgiana-Gabriela Negrea², Vlad-Alexandru Toma^{2,3}, Valentin-Florian Rauca¹, Emilia Licărete¹, Laura Pătraș¹, Manuela Banciu¹ and Alina Sesărman¹✉

¹Department of Molecular Biology and Biotechnology, Center of Systems Biology, Biodiversity and Bioresources, Faculty of Biology and Geology, "Babes-Bolyai" University, Cluj-Napoca, Romania

²Doctoral School in Integrative Biology, Faculty of Biology and Geology, "Babes-Bolyai" University, Cluj-Napoca, Romania; ³ Department of Experimental Biology and Biochemistry, Institute of Biological Research, Branch of NIRDBS Bucharest, Cluj-Napoca, Romania;

✉ **Corresponding author, E-mail:** alina.sesarman@ubbcluj.ro

Introduction: Previous research has shown that immunotherapies are a promising treatment opportunity for many types of cancer. Melanoma is regarded as a great candidate for immune checkpoint inhibitors due to the immunogenicity caused by a high tumor mutational burden. However, some melanoma patients do not respond well to immunotherapy. To address this, improved preclinical models are needed, particularly 3D models that accurately represent the tumor microenvironment's elements, spatial arrangement, and treatment response. This study aimed to generate heterocellular spheroids consisting of B16.F10 melanoma cells, dendritic cells, and CD8⁺ T cells to investigate the combined effects of anti-PD-L1 antibody and curcumin, as an immunotherapy strategy.

Materials and methods: Spheroids were formed using the "liquid overlay" technique by seeding B16.F10 melanoma cells, bone marrow-derived dendritic cells, and CD8⁺ T cells isolated from C57BL6 mice's lymph nodes, onto non-adherent plates. The spheroids' morphology was examined using light and fluorescent microscopy. Immunohistochemistry was used to assess the presence of immune cells within the spheroids using specific antibodies. The acid phosphatase assay determined the impact of the immunomodulatory treatments on the viability of the spheroid cells. Additionally, the western blot technique was employed to investigate the treatment's influence on HIF-1 α , pNF-k β p65, pAP-1 c-Jun, and Akt expression levels.

Results: The administration of curcumin resulted in decreased cell viability within heterocellular spheroids. The IC₅₀ value of curcumin was determined to be 15 μ M. This effect was accompanied by a decrease in the

expression levels of HIF-1 α , while no significant changes were observed in pNF-kBp65 or pAP-1c-Jun protein expression levels. Notably, when combined with anti-PD-L1 antibodies, a concentration of 25 μ M curcumin led to nearly complete inhibition (almost 100%) of cell viability in heterocellular spheroids.

Conclusions: In conclusion, our team has developed a new 3D cell culture platform which enables the incorporation of diverse cell types and facilitates testing with a broad spectrum of immunotherapeutics.

Acknowledgements: This work was funded from **UEFSCDI project PN-III-P1-1_1-TE-2021-0366** "Targeted therapy for the treatment of melanoma based on co-administration of anti-PD-L1 antibodies and curcumin-loaded extracellular vesicles", granted to Alina Sesarman.

Miniaturized electrochemical biosensor for troponin I protein – cardiac biomarker detection

Mihnea Moruz¹, Andreea Campu², Simion Astilean² and
Monica Focsan²

¹*Faculty of Physics, 'Babeș-Bolyai' University, Cluj-Napoca, România;* ²*Nanobiophotonics and Laser Microspectroscopy Center, Interdisciplinary Research Institute in Bio- Nano-Sciences, 'Babeș-Bolyai' University, Cluj-Napoca, România;*  **Corresponding author, E-mail:** moruz.mihnea@yahoo.com

Introduction: The cardiovascular category of diseases, a major contributor to global mortality, accounts for 31% of worldwide deaths, with an expected 10% increase in affected individuals over the next decade. Researchers have focused on studying biomarkers, such as Troponin I, to prevent acute myocardial infarction, which is recognized by the European Society of Cardiology as the most suited.

Materials and methods: In the current work, the development of a novel and efficient electrochemical immunosensor device was targeted, through the synergistic combination of a sensor that integrates plasmonic electrodes of desired shape and size on paper with a portable electrochemical system. The electrodes realised by deposition of thin gold films on a paper substrate were characterized both optical and morphological. Then, the electrodes were placed on a PDMS substrate, conferring both stability, and elasticity to the fully realised device. The validation of the device to detect Troponin I was confirmed using Surface-Enhanced Raman Spectroscopy (SERS) and Cyclic Voltammetry (CV) methods.

Results: A 90 nm thick continuous gold layer, characterized by a rugosity of 3.2 nm, was used as active area for detection purposes. In order to calibrate the detection method using Differential Pulse Voltammetry (DPV), we tested different concentrations of Troponin I in a biologically simulated environment and finally in plasma samples from patients.

Conclusions: In conclusion, it is anticipated that a miniaturized and electrochemical nanodevice will be provided, which is adapted for specific portable detection of the cardiac biomarker Troponin I. Furthermore, the device can be easily customized and optimized for a wide range of medical and environmental applications of interest. The unique properties of the proposed immunosensor can potentially offer a real advantage in the early diagnosis of cardiovascular diseases, thereby positioning our device as an excellent candidate for potential technology transfer.

Acknowledgements: Mihnea Moruz acknowledges the financial support from the Special Scholarship for Scientific Activity, grant awarded by STAR-UBB (Babeș-Bolyai University).

Develop a genetic engineering tool for *Paenarthrobacter nicotinovorans* ATCC 49919

Iustin-Tiberius Munteanu¹✉ and Marius Mihășan¹

¹BioActive Research Group, Faculty of Biology, "Alexandru Ioan-Cuza" University of Iasi, Romania;
✉Corresponding author, E-mail: tibimunteanu897@gmail.com

Introduction: *Paenarthrobacter nicotinovorans* ATCC 49919 is a nicotine degrading microorganism (NDM) with biotechnological potential for the production of compounds of industrial and pharmaceutical importance like 6-hydroxy-L-nicotine, methylamine, succinic acid or gamma-amino-butyric-acid. The nicotine catabolism is related to the presence of pAO1 plasmid. In the present study we aim to develop a genetic engineering tool based on the CRISPR system that would allow fast and easy editing of the *P. nicotinovorans* genome to increase its biotechnological potential. Our aim is to inactivate or drastically reduce the expression of 6-hydroxy-L-nicotine oxidase (*6hlnO*), the key enzyme that catabolizes the conversion of 6-hydroxy-L-nicotine (6-HLN) to 6-hydroxy-methylmyosmine (6-HMM).

Materials and methods: Plasmid DNA have been isolated using QIAprep Spin Miniprep Kit. CRISPR-Cpf1 genes from pJYS3-ΔcrtYF plasmid have been isolated by PCR using the following primers set: For: TCCGACGTCGTCGACTTTGCTGTTTACAATTAATCATCGTGTGG; Rev: ACCACTAGTCCTAGGTTTTTGACAGCTAGCTCAGTCCT and cloned into the DraI linearized pART2 vector using Gibson Assembly (NEBuilder HiFi DNA Assembly Master Mix). Positive recombinant plasmids were selected following digestions with SpeI and ApaLI.

1. A 20 bp spacer targeting the gene of interest was obtained by annealing two 5' phosphorylated synthetic oligonucleotides (For: GAAAAAGTTGCAGCATCCAAAGCG and Rev: AAACCGCTTTGGATGCTGCAACTT) by incubating at 95°C for 3 minutes and then gradually cooling the mixture by 0.010°C every 10 seconds for 2 hours. The spacer was cloned using Golden-Gate assembly (NEBridge Golden Gate Assembly Kit BsaI-HF[®]v2) into pCasiART. Positive colonies have been selected by blue-white screening. Positive recombinant plasmids have been electroporated into the *P. nicotinovorans* following the protocol described by Zhang *et al.* (2011). DNA concentrations were routinely evaluated using agarose gel electrophoresis and a Quantus[™] Fluorometer.

Results: Two distinct approaches have been used to inactivate the gene of interest. One is based on the CRISPR-Cpf1 system and aims to completely knock-out the *6hlnO* gene by deleting it. Genes containing the CRISPR-Cpf1 system from plasmid pJYS3- Δ crtYF (AddGene #85542) have been transferred into the pART2 plasmid using Gibson assembly, resulting the pART2-Cpf1 plasmid. We are in the process of targeting the CRISPR-Cpf1 system for *6hlnO* by cloning a crRNA sequence and corresponding protospacers into the pART2-Cpf1.

The second approach is based on the CRISPR/dCasi9 system and allows partial and controlled inactivation of the *6hlnO* gene transcription. Thus, the CRISPR/dCasi9 system has been targeted to the gene of interest by cloning a 20 bp spacer with the sequence complementary to the *6hlnO* gene into the pCasiART plasmid using the Golden-Gate assembly method and the pCasiART- Δ 6hlnO have been obtained. The resulting plasmids have been introduced into *Paenarthrobacter nicotinovorans* by electroporation.

Experiments are underway for evaluating the efficiency of *6hlnO* gene inactivation of the two constructs: pART2-Cpf1- Δ 6hlnO and pCasiART- Δ 6hlnO. For this, cultures in liquid-broth will be performed and samples at regular intervals will be analyzed by HPLC for quantification of nicotine and 6HLN levels.

Conclusions: At this stage, pCasiART- Δ 6hlnO and pART2-Cpf1 plasmids were obtained, and tests are underway for evaluating the efficiency of these genetic engineering tools.

Acknowledgements: This work was supported by a grant from the Romanian Ministry of Education and Research, CNCS – UEFISCDI, project number PN-III-P4-ID-PCE-2020-0656, within PNCDI II.

Carotenoid loaded nanocarriers- preparation and evaluation

Patricia Muntean¹✉, Adela Pinteaa¹, Andrea Bunea¹, Francis V. Dulf¹,
Monica Focșan¹ and Dumitrița Rugină¹

¹University of Agricultural Sciences and Veterinary Medicine Cluj-Napoca, Cluj-Napoca, Romania;

²Nanobiophotonics and Laser Microspectroscopy Center, Interdisciplinary Research Institute in Bio-Nano-Sciences, Babes-Bolyai University, Cluj-Napoca, Romania; ✉**Corresponding author,**
E-mail: patricia-andreea-lia.muntean@usamvcluj.ro

Introduction: Zeaxanthin is a xanthophyll carotenoid that is widely distributed in tissues and is the primary carotenoid in the eye lens and retinal macular region. Zeaxanthin has antioxidant effects and can be employed as a bioactive molecule because of its favorable effects on human health. Plants, bacteria, and microalgae all create this beneficial pigment, but because of their hydrophobicity, their bioavailability and effectiveness in biological systems is limited. Moreover, zeaxanthin has a low thermal and photostability. As a consequence, it is essential to overcome such problems to gain access to the high proficiency of beneficial capacities of zeaxanthin. Nanoencapsulation provides an advantageous environment for the bioactive contents of foods to be protected from stressful conditions.

Materials and methods: Zeaxanthin with a 95% purity was obtained from plant material by solvent extraction and purification using TLC and column chromatography. Four vegetal oils (coconut MCT, olive, sunflower, and linseed) were profiled for fatty acids composition using GC-MS and for carotenoids using C30-HPLC-PDA. In the presence of a 1% emulsifier (Tween 20), ultrasonic emulsification was used to produce zeaxanthin O/W nanoemulsions (NE) (1:9 v/v) loaded with carotenoids (0.05 mg/ml). DLS, z-potential, and SEM were used to characterize NEs, which were then subjected to a 30-day stability study under various conditions (temperature, salt content, and pH). Temperature stress test was performed by storing the NEs in vials at various temperatures (4, 20, 37, 50, and 60°C) in the dark. NEs were diluted with increasing amounts of aqueous NaCl solution to produce a series of samples with the same particle dosage but different salt concentrations (0, 25, 50, 100, and 250 mM NaCl). HCl 0.1N and NaOH 1N solutions were used to adjust the pH to the desired range (pH 3 to 8). Except for the temperature stability test, all samples were stirred before being transferred into vials and stored in a dark place at room temperature.

Results: Vegetal oils have a high rate of carotenoids incorporation into nanoemulsions (up to 98%). The surface was negatively charged (zeta potential ranging from -2 to -30 mV) and the PDI was less than 0.3. Depending on the oil type, average diameters ranged from 100 to 300nm. The stability investigation indicated that under specific stress situations, NEs might become unstable. Temperature was shown to be the most stressful factor; the NEs became unstable in the first few days after the experiment started, beginning from 37°C. High concentrations of NaCl starting at the halfway point of the experiment were the only concentrations that had an impact on NEs stability. The stability of NEs loaded with zeaxanthin was not significantly impacted by pH.

Conclusions: According to preliminary testing, the NE in which linseed oil was used as the lipidic matrix was the most stable, followed by coconut MCT, sunflower and olive oil based NEs.

Acknowledgements: This work was supported by a grant of the Romanian Ministry of Education and Research, CNCS - UEFISCDI, project number PN-III-P4-ID-PCE-2020-1172, number 243/2021 within PNCDI III.

Synthesis, characterization and *in vitro* evaluation of a new smart responsive pNIPAM –based biopolimer with antimicrobial and antitumoral activity

Paula Ecaterina Florian¹✉, Madalina Icriverzi¹, Anca Bonciu², Luminita Nicoleta Dumitrescu², Diana Pelinescu³, Cristian Munteanu¹, Livia Elena Sima¹, Valentina Dinca², Laurentiu Rusen² and Anca Roseanu¹

¹ Institute of Biochemistry of the Romanian Academy, Bucharest, Romania;

² National Institute for Lasers, Plasma, and Radiation Physics, Măgurele, Romania;

³ Faculty of Biology University of Bucharest, Department of Genetics, Bucharest, Romania;

✉Corresponding author, E-mail: florian@biochim.ro

Introduction: Obtaining new smart biomaterials with pH and thermo-sensitive properties relevant for applications in implantology and tissue engineering domains represents one of the main challenges in biomedical field. The aim of our work was to investigate whether Poly-Nisopropylacrylamide-butyl acrylat (pNIPAM-BA) co-polymer porous coatings prepared by Matrix-Assisted Pulsed Laser Evaporation (MAPLE) technique and subsequently loaded with cationic peptides belonging to antimicrobial peptide family resulted in a new and more efficient scaffold with antibacterial and anticancer action.

Materials and methods: The influence of various solvents and laser fluences on the physical-chemical characteristics of the pNIPAM-BA based coatings were evaluated by atomic force microscopy, scanning electron microscopy (SEM), contact angle measurements, Fourier-transform-IR spectroscopy and X-ray photoelectron spectroscopy. The antimicrobial effect of the new developed biomaterials was investigated using clinical relevant bacteria such as *Staphylococcus aureus* (Gram+), a human pathogen typically found in post-surgical infections, *Escherichia coli* (Gram-) and *Pseudomonas aeruginosa*, a highly antibiotic resistant pathogen associated with nosocomial infections. The capacity of pNIPAM-BA scaffolds, loaded or unloaded with different active compounds, to inhibit cell proliferation and cell cycle progression as well as to induce an apoptotic effect was investigated *in vitro*, in human normal cells and melanoma cell lines.

Results: pNIPAM-BA porous polymeric platforms were obtained by MAPLE technique using DMSO as solvent and 72 k pulses fluence. Our study revealed that the pNIPAM-BA coatings featuring nanopores were suitable

substrates for incorporation of cationic peptides exhibiting antibacterial and anti tumoral properties. The embedded scaffolds with peptides demonstrated the capacity to impair *in vitro* bacterial growth and to significantly reduce cancer cell proliferation, by increasing the number of apoptotic and necrotic cells.

Conclusions: Our data are promising considering how a smart stimuli-responsive scaffold loaded with active compounds could point towards a positively impact for treatment of key pathological conditions, such as cancer and bacterial infection.

Acknowledgements: This research was funded by grant of the Romanian Ministry of Education and Research, CCCDI-UEFISCDI, project number PN-III-P2-2.1-PED-2019-2695. V.D acknowledge partial support of project PN-III-P4-ID-PCE-2020-2375. P.F., M.I., C.M., S.L.E and A.R. acknowledge and thank the partial support of Project no. 5 of the Structural and Functional Proteomics Research Program of the Institute of Biochemistry of the Romanian Academy.

A new design of Hepatitis C Virus E2 chimeric protein oligomer as a vaccine candidate

Raed Nachawati¹✉, Paula Florian¹, Anca Roseanu¹ and Costin-Ioan Popescu¹

¹*Institute of Biochemistry of the Romanian Academy, Bucharest, Romania;*

✉ *Corresponding author, E-mail: nachawati.raed98@gmail.com*

Introduction: Hepatitis C virus (HCV) is a positive sense, single-stranded RNA virus that causes liver disease, including liver cirrhosis and hepatocellular carcinoma. Around 71 million people worldwide suffer from chronic HCV infection. Direct-acting antiviral agents developed in recent years can cure HCV infection in most patients, but they do not prevent reinfection and are costly in some parts of the world. Moreover, a vaccine against HCV is not yet available. The viral envelope glycoprotein E2 is the main target of neutralizing antibodies and has been used as the basis for vaccine design strategies. Most vaccine development efforts have been focusing on monomeric forms of HCV E2 but with little success. It was previously reported that multivalent display of HCV E2 antigens may improve the potency of the humoral immune response. In this study, we present a new strategy to potentially enhance the immunogenicity of E2 by designing a fusion protein comprising E2 and an oligomerization motif which self-assembles into trimers. Our hypothesis is that the oligomerization domain could also increase the uptake of the fusion protein in antigen-presenting cells by receptor-mediated endocytosis.

Materials and methods: A naturally occurring oligomerization motif was genetically fused to the HCV E2 ectodomain (residues 405-661). HEK293T cells were transfected with the construct encoding the fusion protein, followed by protein purification via affinity chromatography using Ni-NTA resin. The identity, purity and oligomerization profile of the recombinant protein were evaluated by SDS-PAGE followed by Coomassie Blue staining and Western Blot. For large-scale protein production, the fusion protein was expressed in Expi293 cells following the manufacturer's instructions. The recombinant protein was then labeled with Alexa Fluor 647, and its internalization in macrophages differentiated from the monocytic cell line THP-1 pretreated or not with chlorpromazine (a clathrin-mediated endocytosis inhibitor) was assessed by FACS analysis.

Results: A fusion protein between HCV E2 and an oligomerization domain was expressed and purified in a mammalian recombinant system. Western Blot analysis revealed that the secreted form of the recombinant protein self-assembles into trimers. Preliminary results strongly suggest that the multimeric form of HCV E2 presents is uptaken by macrophage-like THP-1 cells by receptor-mediated endocytosis.

Conclusions: The new protein design strategy which we are developing may allow the assembly of HCV E2 trimers to be tested as a vaccine candidate against HCV. Future work will aim at combining this strategy with other methods of multivalent antigen display to potentially further increase the immunogenicity of the vaccine candidates.

Resveratrol: NIR-responsive microcarrier-based polymeric delivery system to enhance its therapeutic potential towards diabetic retina cells

Roxana Pop¹✉, Adrian Boldianu¹, Mădălina Nistor¹, Maria Suciuc², Adela Pinteală¹, Monica Focsan³ and Dumitrița Rugină¹

¹ University of Agricultural Sciences and Veterinary Medicine Cluj-Napoca, Cluj-Napoca, Romania;

² Electron Microscopy Centre "C. Craciun", Biology and Geology Faculty, Babes-Bolyai University, Cluj-Napoca, Romania; ³ Nanobiophotonics and Laser Microspectroscopy Center, Interdisciplinary Research Institute in Bio-Nano-Sciences, Cluj-Napoca, Romania;

✉ **Corresponding author, E-mail:** roxana.pop@usamvcluj.ro

Introduction: Diabetic retinopathy (DR) is the leading cause of vision impairment and blindness in the world. Resveratrol (RSV) has been proposed as a potential therapeutic agent for DR owing to its anti-angiogenic and antioxidant properties. However, RSV encapsulation in a delivery system is needed to improve its bioavailability and bioaccessibility.

Materials and methods: After RSV was attached to a CaCO₃ template, negative poly(sodium styrene sulfonate) and positive polyethylenimine polymers were alternately added using the layer-by-layer technique, whereas fluorescein isothiocyanate and gold nanoparticles were trapped between the layer. The microsystem's surface was decorated with anti-vascular endothelial growth factor (VEGF) antibodies. Morphological characterization and internalization in human retinal pigmented epithelial (RPE) D407 cells were performed using electron and fluorescence microscopy. High-performance liquid chromatography (HPLC) was used to measure the encapsulation efficiency of RSV and its release under near-infrared (NIR) laser irradiation at 785 and 808 nm. Cell viability was analyzed using the WST-1 reagent.

Results: A stable spherical shape and an average diameter of 2.5 μm were recorded through electron microscopic analysis. According to the HPLC analysis, RSV was encapsulated with an efficiency of over 90% (29.81 ± 0.04 μg/ml). Its release from the microsystem after 785 nm laser irradiation was 12.83 ± 0.21 μg/ml (43%) and after 808 nm laser irradiation was 3.89 ± 0.07 μg/ml (13,04%). Successful internalization in D407 cells was observed by fluorescence microscopy after 4–24 h of treatment with 10 microcapsules/cell. No cytotoxic effect on cells was detected. Following 808 nm irradiation, changes in cellular viability were observed.

Conclusions: This novel as-developed hybrid polymeric microcarrier able to release RSV by laser-induced thermoplasmonic effect could have an important translational potential for the treatment of DR.

Acknowledgements: This research was funded by the Romanian National Authority for Scientific Research, CNDI - UEFISCDI, project number PN-III-P2-2.1-PED-2019-4558, contract no. PED 369/2020.

The endoplasmic reticulum (ER) degradation-enhancing alpha-mannosidase-like protein 3 is a host cell regulator of HBV infection

Alina Ghionescu^{1✉}, Mihaela Uță¹, Cătălin Lazăr¹, Petruța Alexandru¹ and Norica Nichita¹

¹ *Institute of Biochemistry of the Romanian Academy, Department of Viral Glycoproteins Bucharest, Romania; ✉Corresponding author, E-mail: alinaghionescu@yahoo.com*

Introduction: Hepatitis B virus (HBV) infection remains a serious health problem, with approximately 296 million people chronically infected worldwide. HBV is a DNA virus of the Hepadnaviridae family, that contains relaxed circular partially double-stranded DNA – rcDNA packed into a nucleocapsid enveloped by lipid bilayer embedding the small (S), medium (M), and large (L) surface glycoproteins. These proteins are synthesized in the endoplasmic reticulum (ER), where glycosylation, folding, and oligomerization, occur and are thought to induce an unfolded protein response (UPR) in HBV-infected cells. Growing evidence indicates that the ER-associated degradation (ERAD), and autophagy, two UPR pathways, are modulated by viruses in order to facilitate their replication. Indeed, non-degradative autophagy is required for nucleocapsid assembly and HBV replication. We have previously reported that HBV upregulates EDEM3 expression in hepatic cells. This ERAD lectin is involved in the degradation of the excess proteins accumulating in the ER, including the viral glycoproteins. However, the role played by EDEM3 in HBV infection is not known. The aim of this study was to investigate at the molecular level the complex interplay between UPR and the HBV life-cycle, with a focus on EDEM proteins.

Materials and methods: We established new HepaRG cell lines that constitutively modulate EDEM3 expression using a retroviral virus for EDEM3 overexpression and CRISPR/Cas9 technology for EDEM3 depletion. In these cells, viral infection, autophagy, and UPR markers were quantified with specific methods, including qPCR, western blotting, and ELISA.

Results: Our data indicate that HBV infection increases significantly in EDEM3-overexpressing HepaRG cells. Moreover, we observed that EDEM3 increases the secretory autophagy by microtubule-associated protein 1A/1B-light chain 3 (LC3) up-regulation and mammalian target of rapamycin (mTOR) inhibition. Additionally, EDEM3 decreases UPR markers such as protein kinase RNA-like ER kinase (PERK), inositol-requiring enzyme 1 (IRE1), and glucose-

regulated protein 78 (GRP78/BiP), likely contributing to the alleviation of the ER stress during viral infection. EDEM3 depletion in HepaRG cells resulted in opposite effects, confirming the specificity of EDEM3 regulation of HBV infection.

Conclusions: Our results suggest that EDEM3 increases HBV infection by activating secretory autophagy, through modulation of the UPR signaling. Further investigation of this molecular pathway will be carried out in HBV-infected patients to potentially validate EDEMs as novel antiviral targets.

Acknowledgments: This work was funded by the Viral Glycoproteins Department, Institute of Biochemistry of the Romanian Academy, and Ph.D. - School of Advanced Studies of the Romanian Academy (SCOSAAR).

Roles of transient receptor potential melastatin 8 (TRPM8) and epidermal growth factor receptor (EGFR) in glioblastoma

Alina-Ana-Maria Botezatu¹✉, David-Ionuț Băcioiu¹, Florentina Picu¹
and Dana Cucu¹

¹ Department of Anatomy, Animal Physiology and Biophysics, Faculty of Biology,
University of Bucharest, Bucharest, Romania;

✉ **Corresponding author, E-mail:** botezatu.alina-ana-maria22@s.bio.unibuc.ro

Introduction: Glioblastoma multiforme (GBM) is an extremely dangerous primary brain tumor with a low survival rate and characterized by nuclear atypia, cellular pleomorphism, mitotic activity, anaplasia, and rapid proliferation alternated with an aggressive invasion of the surrounding brain tissue. Numerous functions have been linked to members of the transient receptor potential (TRP) non-selective cation channel superfamily. In recent years, many reports have supported the theory that the transient receptor potential melastatin 8 (TRPM8) is a promising novel therapeutic target in cancer treatment. However, the precise methods by which TRPM8 operates in glioma cells as well as its roles in carcinogenesis are still not well understood. EGFRvIII, deletion of exons 2 through 7, is the most common EGFR mutation found in glioblastoma. However, the EGFRvIII mutant is classically considered low constitutively active. Also, EGFRvIII dimers can be as active as wild-type ligand-bound activated EGFR.

Materials and methods: We used flow cytometry to assess the influence of TRPM8 activation on cell cycle progression of U87 cells. And the wound healing technique was used to assess the roles of TRPM8 in cell migration. The experiments also follow whether the activation of EGFR influences the expression and function of TRPM8.

Results: We monitored cell migration under different conditions: activating TRPM8 by menthol and inhibition of Ca²⁺ entry using the antagonist N-(4-tertiarybutylphenyl)-4-(3-chloropyridin-2-yl)tetrahydropyrazine-1(2H)-carboxamide (BCTC). We performed cell cycle analysis with flow cytometry to determine whether TRPM8 may change the distribution of cell cycle phases, as noticed in our previous studies for TRPA1 in pancreatic cancer cells. Moreover, we quantify the influence of TRPM8 expression on cell apoptosis.

Conclusions: With this study we provide a preliminary analysis of TRPM8 expression and function in glioma cells U87 and its modulation by the EGFRvIII. TRPM8 channel may have functional implications for glioma survival, proliferation, apoptosis and local tumor invasion.

SREB receptor family members differentially regulate protein expression and processing

Rodica – Aura Badea¹✉, Andreea Sorina Anghel¹, Teodora Stratulat¹ and Sorin Tunaru¹

¹ Cell Signaling Research Group, Institute of Biochemistry of the Romanian Academy, Bucharest, Romania; ✉Corresponding author, E-mail: Rodica.Badea@biochim.ro

Introduction: The super-conserved receptors expressed in the brain (SREB) constitute a family of orphan G protein-coupled receptors (GPCRs) that include three members: GPR27 (SREB1), GPR85 (SREB2) and GPR173 (SREB3). They share some common features such as: high level of sequence conservation among vertebrates and predominant expression in the central nervous system. The SREB family has been postulated to play important roles in different physiologic processes and diseases, including pancreas β -cell insulin secretion and regulation, schizophrenia, autism and atherosclerosis. One of the ways in which these GPCRs could influence different cellular processes is by modulating the expression and processing of proteins with important cellular functions. Our present study focuses on a comparative evaluation of the involvement of the three members of SREB family in the regulation of the expression and processing of some proteins with important roles in cell signaling.

Materials and methods: HEK293T and HeLa cells were transiently transfected with plasmids containing the cDNA of human GPR27, GPR85, GPR173, GPR75, PTGIR, β 1-AR, GPR109A, a genetic probe specific for cAMP accumulation (pGloSensor), cDNA of vSrc, Lck and GRK kinases using either polyethyleneimine or Lipofectamin 2000. After 48h from transfection, cells were prepared for various investigations. The influence of GPR27, GPR173 and GPR85 on cell signaling through G-proteins was determined by a luminescence-based assay using pGloSensor (Promega) genetic probe. The impact of SREB family members on protein expression levels of some other GPCRs (GPR75, PTGIR, β 1-AR) and kinases (vSrc, Lck, GRKs) was assessed by western blotting, while their effect on gene transcription was performed by qPCR.

Results: Functional assays demonstrated an inhibitory effect of GPR27 and GPR173 on forskolin-induced cAMP accumulation in HEK293T and HeLa cells. Interestingly, these effects were insensitive to a Gi-specific blocker, pertussis toxin (PTX). Further on, the data obtained from immuno-blotting experiments have shown that both GPR27 and GPR173 specifically inhibit the expression of some co-expressed proteins, such as GPR75, β 1-adrenergic

receptor (β 1-AR) and prostacyclin receptor (PTGIR), protein tyrosine kinases (Src) and protein serin/threonin kinases (GRKs), whereas the expression of a Src-related kinase such as Lck was not affected. GPR85 did not have inhibitory effects on the aforementioned proteins. The overall results suggest that GPR27 and GPR173 play specific inhibitory effects on the expression of certain proteins while the GPR85 seems to not affect the protein expression. Further studies are required to clarify the role of SREB family receptors in cellular physiology.

Conclusions: GPR27 and GPR173 modulate various physiological processes by influencing the expression of some important proteins in cell signaling (GPCR, G protein subunits, kinases) by an yet unknown mechanism.

Acknowledgements: This work was funded from "EEA-RO-NO-2018-0535 - New Generation of Drug Targets for Schizophrenia (NEXTDRUG)".

Data mining and protein engineering for aromatic ammonia-lyases with enhanced activity towards challenging substrates

Gyopárka Ágoston¹✉, Krisztina Boros¹, Raluca Bianca Tomoiagă¹ and László-Csaba Bencze¹

¹*Enzymology and Applied Biocatalysis Research Center, Faculty of Chemistry and Chemical Engineering, Babeș-Bolyai University, Cluj-Napoca, Romania;*

✉ *Corresponding author, E-mail: gyoparka.agoston@stud.ubbcluj.ro*

Introduction: Phenylalanine ammonia-lyases (PALs) have emerged as a powerful tool in the production of optically pure L-phenylalanines, providing a greener approach with high conversion rates. Together with histidine and tyrosine ammonia-lyases (HALs and TALs), these enzymes harbour the catalytically indispensable 3,5-dihydro-5-methylidene-4H-imidazole-4-one (MIO) prosthetic group, thereby constituting the MIO enzyme family. A major limitation of PALs is their low activity towards electron donating poly-substituted substrates, a problem which so far could not be solved by the means of protein engineering. Recently, a new aromatic ammonia-lyase (AAL) was discovered, derived from *Loktanella atrilutea* (*LaAAL*) showing high activity in the production of 3,4-dimethoxy-L-phenylalanine, prominent as an intermediate in the synthesis of the anti-Parkinson drug L-DOPA. The focus of this study is the exploration of the natural role and substrate domain of *LaAAL*.

Materials and methods: Employing the Basic Local Alignment Search Tool (BLAST) homologues of *LaAAL* were selected, with the highest rates of coverage and identity values above 60%. The evolutionary lineage relationships between these homologues and known members of the MIO enzyme family were mapped through phylogenetic tree analysis, using the Molecular Evolutionary Genetics Analysis (MEGA11) program. Multiple Sequence Comparison by Log-Expectation (MUSCLE) was applied comparing the catalytic sites of the homologues and point mutations were introduced to *LaAAL* using megaprimer based polymerase chain reactions (PCR). Three mutant enzymes were transformed and expressed in *E. coli* competent cells. Their conversion-based activities were monitored with RP-HPLC and compared to the native enzyme within the ammonia addition and elimination reaction.

Results: While, the MIO prostetic group is present in all the selected AAL homologues, their catalytic site is unique compared to other characterized MIO-family members. On the generated phylogenetic diagram, the examined AALs form a distinct clade, having common ancestors with PALs and TALs of bacterial origin. Between the identified AALs, there are well-conserved residues specific to MIO-family members, but a vast diversity was observed amongst the residues defining the substrate selectivity. To assess how these distinct residues affect the activity, several mutations that interchange the catalytic sites of the AALs and of the known PALs were performed, testing the activity of the variant library towards a defined set of differently substituted substrates.

Conclusions: A phylogenetical analysis was performed on the novel aromatic ammonia-lyase from *Loktanella atrilutea* and its homologues together with known MIO-family representatives. The mutational strategy implemented by interchanging the catalytic sites of the different PAL homologues, provides knowledge for developing protein engineered PALs, capable of transforming lignin-derived monomers, including syringic acid and ferulic acid.

Fluorescence imaging in real-time employed to visualize the presence of anthocyanins complexed with diphenylboric acid 2-aminoethyl inside B16-F10 melanoma cells

Madalina Nistor¹✉, Monica Focsan², Luiza Gaina³, Mihai Cenariu¹, Adela Pinteaa¹, Carmen Socaciu¹ and Dumitrita Rugina¹

¹ University of Agricultural Sciences and Veterinary Medicine, Cluj-Napoca, Romania;

² Nanobiophotonics and Laser Microspectroscopy Center, Interdisciplinary Research Institute in Bio-Nano-Sciences, Cluj-Napoca, Romania; ³ Babes-Bolyai University, Faculty of Chemistry and Chemical Engineering, Cluj-Napoca, Romania;

✉ **Corresponding author, E-mail:** nistor.madalina@usamvcluj.ro

Introduction: Anthocyanins (AN) are natural antioxidant compounds regularly consumed by humans, that possess remarkable potential for therapeutic use when applied directly to melanoma pathology. However, the development of an effective therapy is still underway due to the limited understanding of how AN molecules behave within cells, once they are absorbed. A major obstacle in this endeavor is the requirement for an imaging technique that can accurately detect and locate AN molecules within cells. To address this challenge, a non-fluorescent reagent called diphenylboric acid 2-aminoethyl (DPBA) was utilized in this study to successfully create fluorescent complexes with AN, offering a solution for their intracellular detection and localization.

Materials and methods: The AN used in this study consisted of cyanidin aglycon as standard molecule (CY) and glycosylated compounds extracted, purified from chokeberry fruits (AE) and quantified by high-performance liquid chromatography with photodiode array detector (HPLC/PDA). Observation of CY/AN inside B16-F10 melanoma cells was done using flow cytometry and fluorescence microscopy. To enhance their fluorescence detectability, AN/CY were conjugated with DPBA, and formed fluorescent complexes, as proven by nuclear magnetic resonance (NMR) analysis. Additionally, their impact on cellular viability was also analysed through the colorimetric WST-1 assay.

Results: The results showed that AN form fluorescent complexes with DPBA within the melanoma cells, resulting in an enhanced fluorescent signal. After 24 hours, 62.9% of the B16-F10 cells treated with AE and 64.8% of cells treated with CY, emitted fluorescence. Fluorescence microscopy imaging and flow cytometry analysis validated the cellular uptake of the complex. Also, the

viability test showed that AN had cytotoxic effect on melanoma cells, on a dose-dependent manner, while DPBA showed no impact on viability, at the concentrations used in this study.

Conclusions: This study demonstrated that DPBA can be effectively utilized as a sensitive and non-invasive method for imaging AN intracellularly. The success of this approach opens up new possibilities for its application in various fields, such as drug development and the study of metabolism-associated mechanisms. The findings suggest that DPBA has the potential to significantly enhance our understanding of AN behavior within cells and can have broad implications for further research and applications in related areas.

Acknowledgements: This work was funded by the Romanian National Authority for Scientific Research, CNDI- UEFISCDI, project number PN-III-P1-1.1-TE- 2019-1276.

Integrans and HGT – How do integrans affect HGT in multidrug resistant Gram-negative ESKAPE pathogens

Matei-Ștefan Dobrescu^{1,2,3}✉, Dan Alexandru Țoc⁴, and Anca Butiuc-Keul^{1,2}

¹ Department of Molecular Biology and Biotechnology, Faculty of Biology and Geology, Babeș-Bolyai University, Cluj-Napoca, Romania; ² Centre for Systems Biology, Biodiversity and Bioresources, Babeș-Bolyai University, Cluj-Napoca, Romania; ³ Doctoral School of Integrative Biology, Babeș-Bolyai University, Cluj-Napoca, Romania; ⁴ Department of Microbiology, Iuliu Hatieganu University of Medicine and Pharmacy, Cluj-Napoca, Romania; ✉ **Corresponding author, E-mail:** matei.dobrescu@ubbcluj.ro

Introduction: Bacterial resistance to antibiotics is a public health problem due to the stress these substances place on bacteria, causing them to acquire antibiotic resistance genes (ARGs). Horizontal gene transfer (HGT) allows bacteria to obtain new genetic material from outside their own species or from individuals within the same species. Through HGT, bacteria can acquire new genes that confer characteristics that can be useful and help them to perpetuate the species in a given environment. ARGs can be obtained through HGT, one of the main ways these genes being acquired through mobile genetic elements (MGE), especially integrans. Through the acquisition of ARGs, some bacteria can become multidrug resistant (MDR). Over the years, a group of such bacteria have gained notoriety, being placed in a group named ESKAPE pathogens. In this group, we can find bacteria such as *Enterobacter* spp., *Klebsiella pneumoniae*, *Acinetobacter baumannii* and *Pseudomonas aeruginosa*.

Materials and methods: The clinical isolates used were isolated from patients from the Cluj County Emergency Hospital. We have analyzed 95 isolates from 4 different bacterial species: *Enterobacter* spp. (E), *Klebsiella pneumoniae* (K), *Acinetobacter baumannii* (A) and *Pseudomonas aeruginosa* (P). 40 ARGs and 3 integrase genes (intI, intII, intIII) were tested by using PCR and electrophoresis to identify which ARGs and which integran classes are present. The data was analyzed using Microsoft Excel and statistical tests (ANOVA; Mann–Whitney U and Kruskal–Wallis) were done using the R Studio software.

Results: Out of all 40 ARGs, we have only identified 20. These 20 ARGs are shared between 6 antibiotic classes: β -lactamases, macrolides, tetracyclines, sulphonamides, aminoglycosides and quinolones. Out of all 95 isolates, 23 of them can be considered MDR, meaning they are resistant to at least 3 antibiotic classes. Out of all the isolates, we have identified 41 isolates having integrans. Regarding

the MDR isolates, only 19 out of 23 have integrons. Regarding the integrons, the most present class was class I (36 isolates). Only 6 isolates have class II integrons and none have class III. We have analyzed the impact of integrons over each antibiotic class. In the case of sulphonamides, 25 out of 29 isolates present integrons (86,2%). For macrolides, 15 out of 27 present integrons (55,5%). For aminoglycosides, 8 out of 10 isolates present integrons (80%). For tetracyclines, 6 out of 23 present integrons (26%). For β -lactamases, 39 out of 77 isolates present integrons (50,64%). When looking at quinolones, there is only one isolate that has resistance to them and it also contains integrons. When analyzing the presence of integrons in MDR isolates, 20 out of 23 have only class I integrons (86,95%). After statistical analysis, we can observe a possible correlation between the dissemination of sulphonamides and the presence of integrons. Regarding the other classes, there isn't a significant correlation. However, there might be a correlation between integrons and the dissemination of macrolides in the case of *Enterobacter* spp as only the isolates with integrons present resistance to macrolides. When looking at the MDR isolates, there is a significant correlation between the presence of integrons and the MDR phenomena.

Conclusions: Integrons can facilitate the movement of certain antibiotic classes such as sulphonamides and macrolides. We can confirm that some antibiotic classes might move independently from integrons, such as β -lactamases which are known to move with the aid of plasmids. The MDR phenomena might be affected by integrons, helping the spread of ARGs to bacteria who are already resistant to multiple antibiotic classes.

Unchanged amount, localization and activity of glucocorticoid receptor in combination therapy – inhaled nitric oxide and intravenous hydrocortisone in porcine endotoxemia model

Michał Płóciennik^{1✉}, Liliana Kiczak¹, Urszula Paślawska^{2,3}, Waldemar Gozdzik⁴, Barbara Adamik⁴, Marzena Zielinska⁴, Stanisław Zieliński⁴, Kacper Nowak³, Jacek Bania⁵, Marcin Nowak⁶, Robert Paślawski² and Claes Frostell⁷

¹Department of Biochemistry and Molecular Biology, Faculty of Veterinary Medicine, Wrocław University of Environmental and Life Sciences, Wrocław, Poland; ²Veterinary Center, Nicolaus Copernicus University in Torun, Torun, Poland; ³Department of Internal Diseases and Clinic of Diseases of Horses, Dogs and Cats, Faculty of Veterinary Medicine, Wrocław University of Environmental and Life Sciences, Wrocław, Poland; ⁴Clinical Department of Anesthesiology and Intensive Therapy, Wrocław Medical University, Wrocław, Poland; ⁵Department of Food Hygiene and Consumer Health Protection, Faculty of Veterinary Medicine, Wrocław University of Environmental and Life Sciences, Wrocław, Poland; ⁶Department of Pathology, Faculty of Veterinary Medicine, Wrocław University of Environmental and Life Sciences, Wrocław, Poland; ⁷Department of Anesthesia and Intensive Care, Karolinska Institutet, Danderyd Hospital, Stockholm, Sweden; ✉ **Corresponding author, E-mail:** michal.plociennik@upwr.edu.pl

Introduction: Despite modern intensive care the hospital mortality in sepsis still varies between 30–45%. Multiple preclinical studies have proven the central role of endogenous glucocorticoids tolerance against sepsis by counteracting several of the sepsis characteristics i.a. excessive inflammation. Therefore, glucocorticoids (GCs) have been tested as an adjunctive therapy in sepsis and septic shock in different randomized clinical trials. Nonetheless, these studies produced conflicting results. Glucocorticoid resistance (inadequate response of the glucocorticoid receptor, GR) is a well-known manifestation in sepsis and may contribute to the failure of GCs to improve sepsis patients. On the other hand, a combination therapy - simultaneous administration of both a corticosteroid and an inhaled nitric oxide (iNO) in a porcine endotoxemia model (infusion of lipopolysaccharide, LPS) attenuated the inflammatory response and almost preserved or restored normal histology of both lung and systemic organs. Thus, we decided to evaluate the influence of this combination therapy on amount and localization of GR in lung, kidney and liver, using two complementary methods – immunohistochemistry and Western blotting (after protein subfractionation) as well as GR activity (expression of genes controlled by GR).

Materials and methods: A shock-like condition was established in 23 animals by continuous infusion of *E. coli* LPS for 10 hours. Then the animals were observed for 10 hours. 12 pigs received iNO and hydrocortisone (iNO treatment started 3 hours after the initial LPS infusion and continued until experiment end). 11 pigs were controls (with standard treatment). Cytoplasmic and nuclear protein fractions were extracted from lungs, liver, and kidney for Western blot analysis of GR. GR localization in porcine lungs, liver, and kidneys was analyzed using immunohistochemistry (IHC). Expression of proinflammatory genes (IL-1 β , TNF- α , IL-6, TGF- β) was measured by real-time PCR.

Results: Western blotting demonstrated that amount of GR in cytoplasmic and nuclear protein fractions in lungs, kidneys and livers remained on similar levels in **pigs treated with iNO** and hydrocortisone and in controls. The IHC image digital analysis with Image J program revealed that the cytoplasmic and nuclear staining pattern was comparable in both analyzed groups. **Expression of proinflammatory genes, controlled by GR, remained on similar level in all animals.**

Conclusions: **Animals treated with the combination of iNO and corticosteroid and controls represented similar amounts, localization, and activity of GR in pulmonary, hepatic and renal tissue. Our findings suggest that the combination therapy with GCs and iNO might prevent glucocorticoid resistance in sepsis therapy.**

Altered expression of microRNA-195 might contribute to a severe outcome in SARS-CoV-2 infection

Alexandra-Ioana Moatăr¹✉, Aimee Rodica Chiș¹, Diana Nitusca¹,
Cătălin Marian¹, Cristian Oancea² and Ioan-Ovidiu Sîrbu¹

¹ Department of Biochemistry, University of Medicine and Pharmacy "Victor Babeș",
E.Murgu Square no.2, Timișoara, Romania; ² Department of Pneumology,
University of Medicine and Pharmacy "Victor Babeș", E.Murgu Square no.2, Timișoara, Romania;
✉ **Corresponding author, E-mail:** moatar.alexandra@umft.ro

Introduction: While the infections with SARS-CoV-2 have reached a "steady state" globally, there is still a dire need to understand the molecular mechanisms that contribute to the long term effects of COVID-19. Human microRNAs, as important modulators of gene expression, are frequently dysregulated in response to viral infection. MicroRNA-195, in particular, was found to interact 'in silico' with the N gene of SARS-CoV-2 genome, however, it is not clear how this molecule associate to and impact the progression of COVID-19 disease. Here, we quantified the plasma levels of microRNA-195 in COVID-19 patients and evaluated its association with progressive stages of the disease.

Materials and methods: We used qRT-PCR to profile the expression of microRNA-195, in plasma samples of COVID-19 patients admitted to the Clinical Hospital of Infectious Diseases and Pneumophysiology, Timisoara. We used mirWalk 3.0 and STRING algorithms to evaluate the biological impact of microRNA-195 on lung, heart, lymph nodes, liver and kidneys transcriptomes. The statistical significance of changes in microRNA-195 expression was calculated using Kruskal Wallis test with Dunn's multiple corrections. Correlation analyses were performed using the two-tailed Spearman test (continuous variables), Point Biserial test (continuous vs. binary variables) and Phi test (binary variables). Receiver operating characteristics (ROC) analyses were performed with the standard parameters in Prism 9, using Wilson/Brown method for confidence interval calculation. All statistical analyses were two tailed and the threshold of statistical significance was set at 0.05.

Results: Plasma microRNA-195 is strongly downregulated in patients infected with SARS-CoV-2 virus compared to controls, an effect dependent on the severity of the SARS-CoV-2 infection. ROC curve analyses showed that plasma microRNA-195 has a high discriminative power (AUC>0.9, p<0.0001) for severe COVID-19 cases vs. controls and COVID-19 mild cases. Results from

the bioinformatic analysis showed that microRNA-195 significantly impacts the mitochondrial respiration in cardiac muscle. Furthermore, our correlation analysis revealed that plasma microRNA-195 is negatively correlated with exitus ($p=0.008$), D-dimers ($p=0.041$) and age ($p=0.018$).

Conclusions: Plasma microRNA-195 downregulation is strongly associated with early signs of COVID-19 disease severity. Our work points towards a previously unknown role of microRNA-195 host response to SARS-CoV-2 infection cases.

NPC1 regulates specific cargo traffic to lysosome related organelles and melanosome biogenesis

Adriana Alina Rus¹✉, Ioana Militaru¹, Ioana Popa¹ and Ștefana Petrescu¹

¹ Department of Molecular Cell Biology, Institute of Biochemistry, Bucharest, Romania;

✉ *Corresponding author, E-mail: rus.alinaa@yahoo.com*

Introduction: Niemann-Pick type C1 protein (NPC1) is a multi-spanning protein of lysosomes membrane that enables cholesterol and lipids transport. Mutations in the NPC1 protein can lead to Niemann-Pick type C1 disease, a lysosomal storage disorder, characterized by the accumulation of glycosphingolipids and cholesterol within lysosomes. NPC1 protein plays a major role in the endolysosomal pathway, therefore we have investigated its role in a lysosome-related organelle, the melanosome.

Materials and methods: We used CRISPR/CAS9 engineering method to generate a new cell line lacking NPC1 protein. Other methods such as Western blot, immunofluorescence staining, subcellular fractionation and flow cytometry were used to characterise the perturbed processes in cell lines deficient in NPC1 protein.

Results: We have generated a knock-out NPC1 melanoma cell line, MNT-1 NPC1-KO (NPC1-KO), and we found that the cellular phenotype is associated with a decreased pigmentation accompanied by low expression of the melanogenic enzyme tyrosinase. We investigated the pathway of tyrosinase and melanosome biogenesis. In the absence of NPC1 protein not just the expression of tyrosinase, but also the processing and the localization were affected. In contrast with the decrease in tyrosinase protein expression, we observed a significant intracellular accumulation of mature PMEL17, the structural protein of melanosomes. Therefore, in NPC1-KO cell line the melanosomal matrix generation is unable to lead to the maturation of melanosomes causing them to remain immature with a subcellular localization adjacent to the plasma membrane, in contrast to the dendritic melanosomal localization in wild type cells.

Conclusions: In conclusion, these findings suggest that NPC1 is involved in tyrosinase transport from the TGN to melanosomes and melanosome maturation, indicating a novel function for the NPC1 protein.

Acknowledgements: This work was funded by the Romanian Academy Project 1, 2019-2022 (SMP, AAR, IP), Horizon 2020 - Marie Skłodowska-Curie Research and Innovation Staff Exchange (RISE) (Lysomod) program, Grant Agreement no. 734825.

GPR27, insulin secretion regulator and beyond

Sorina-Andreea Anghel¹✉, Cosmin Trif¹, Rodica-Aura Badea¹,
Aura-Elena Ionescu¹, Teodora Stratulat¹, Cristiana Triță¹,
Sorin Tunaru¹ and Ștefana M. Petrescu²

¹Cell Signaling Research Group, Institute of Biochemistry of the Romanian Academy, Bucharest, Romania; ² Department of Molecular Cell Biology, Institute of Biochemistry of the Romanian Academy, Bucharest, Romania; ✉Corresponding author, E-mail: anghelsandreea22@gmail.com

Introduction: G-protein coupled receptors (GPCRs) are ubiquitously expressed in the human body and play essential roles in an array of physiological processes, including glucose homeostasis. Orphan GPCRs are receptors that lack endogenous ligands and biological functions, thus being potential novel targets for drug discovery. GPR27 is an orphan receptor belonging to the SREB family (Super-conserved Receptors Expressed in Brain) together with GPR85 and GPR173. Previously, GPR27 was linked with increased insulin production. We pursued to define GPR27 signaling in insulinoma cell line (INS1E) and beyond, in order to establish its role in insulin secretion.

Materials and methods: Secondary messengers were quantified by using cytosolic biosensors transiently expressed together with GPR27 in HEK293T cells or in INS1E cell line. cAMP levels were determined using pGlo22F system (Promega), while G5A (GFP-aequorin fusion protein) detected changes of intracellular calcium. The G-proteins activity was determined using TRUPATH biosensors. Expression of GPR27 in INS1E cells was performed by qPCR. Insulin secretion was measured by HTRF (Cisbio).

Results: We demonstrated that GPR27 is expressed in INS1E cells. Firstly, we sought to characterize GPR27 signaling in a heterologous expression system. In HEK293T cell line, GPR27 induced a decrease of cAMP in an agonist-independent manner suggesting a constitutive activity mediated by Gai/o proteins. However, pertussis toxin (PTX) or (OZITX), inhibitors of Gai/o proteins, did not affect the observed decline in cAMP levels. Moreover, GPR27 did not recruit any Gα protein as assessed by TRUPATH method. Next, by using a functional approach we demonstrated that GPR27 blocks the activity of free-fatty acids receptors (FFAR1, FFAR4) and muscarinic acetylcholine receptors (M1, M3, M5), well-known Gαq coupled receptors expressed in beta-cells. Furthermore, knockdown of GPR27 in INS1E cells by siRNA strategy resulted in elevated intracellular calcium signaling and augmented glucose-stimulated insulin secretion.

Conclusions: GPR27 exerts an inhibitory effect in an agonist-independent manner affecting the activity of free-fatty acids receptors (FFAR1, FFAR4) and muscarinic acetylcholine receptors (M1, M3, M5) via a G-protein independent pathway. Likewise, the SREB member seem to negatively regulate insulin secretion.

Acknowledgements: This work was funded from EEA-RO-NO-2018-0535 New Generation of Drug Targets for Schizpophrenia (NEXTDRUG)

GPR27 inhibits Hepatitis B Virus internalisation and replication

Stefania Buzatoiu¹✉, Sorin Tunaru¹ and Norica Nichita¹

¹*Institute of Biochemistry of the Romanian Academy, Splaiul Independenței 296, București 06003, Romania, ✉Corresponding author, E-mail: stefaniabuzatoiu@gmail.com*

Introduction: Hepatitis B Virus (HBV) is the cause of 800.000 annual deaths out of 296 million of chronically-infected patients worldwide, for whom no curative treatment is currently available. Previous studies have indicated that the HBV life-cycle and the host cell metabolism are tightly interdependent. Understanding the molecular details of these interactions may reveal novel antiviral targets and therapeutic strategies. G protein coupled receptors (GPCR) constitute the largest superfamily of human membrane receptors involved in signal transductions through activation of intracellular G proteins. GPCRs regulate various physiological processes and are one of the most important group of pharmacological targets. We have recently shown that a member of this family, GPR27 is expressed in hepatic cells. Our hypothesis is that GPR27 may regulate HBV infection through activation or inhibition of host cell pathways involved in the viral life-cycle.

Materials and methods: Transient overexpression of GPR27 in hepatoma cell lines. HepG2-NTCP cells were treated with 0,25 µg pcDNA-GPR27/pcDNA plasmids for 24; GPR27 overexpression was further confirmed by western blot and immunofluorescence assays. **In vitro HBV infection.** HepG2 NTCP cells were incubated with HBV at 300 MOI 24h post GPR27 overexpression and harvested after 24h or 7 days, respectively. **Quantification of HBV antigens secretion by ELISA.** The amount of HBV-SVPs released was quantified using the Monolisa HBsAg Ultra Kit according to the protocol recommended by the manufacturer. Secretion of the HBeAg was monitored by using the Monolisa HBe Ag-Ab PLUS. **Viral DNA extraction** was performed using Phenol/Chloroform/Isoamyl Alcohol Extraction protocol and qPCR reaction products were amplified using HBV primers.

Results: Our results suggest that GPR27 overexpression could inhibit HBV entry and replication, leading to a decreased infection rate.

Conclusions: In this study, we have established that GPR27 is a novel host factor involved in HBV infection. Future research will aim to determine the molecular mechanism of this inhibition and identify GPR27-targeting drugs with antiviral properties.

Analytical differences between hemoglobin peroxidase and enzyme-based peroxidase activity in tissue lysates

Ștefan-Mihai Drăgan¹✉ and Vlad-Alexandru Toma^{1,2,3}

¹ Department of Molecular Biology and Biotechnology, Faculty of Biology and Geology, Babeș-Bolyai University, Cluj-Napoca, Romania; ² Institute of Biological Research, Cluj-Napoca, the branch of NIRDBS Bucharest, Romania, ³ „Maya & Nicolae Simionescu” Fellow, Romanian Society for Cell Biology, Cluj-Napoca, Romania;
✉ Corresponding author, E-mail: stefan.dragan@stud.ubbcluj.ro

Introduction: The peroxidase-like activity of hemoglobin has been well described in the literature over the years, due to its hem prosthetic group which can catalyze the breakdown of peroxide into H₂O and ROS. Stroma-free hemoglobin can arise due to erythrocyte’s plasma membrane destruction, resulting in hemoglobin release, or from perfusion of hemoglobin-based blood substitutes. Since naturally when measuring the peroxide activity in a tissue, it is over-amplified in value by the other peroxidase activities as such of Hb but also other heme-containing proteins like cytoglobin, neuroglobin, and androglobin, the need for this discrimination becomes clear, to precisely measure the internal, intracellular peroxidase activity, and accounting for the external sources of influence on the cellular oxidative stress.

Materials and methods: Using the UV-Vis spectrophotometer, we managed to provide a method that relies on the oxidation state of σ -dianisidine (method 1) to register a color change proportional to the quantity of stroma-free Hb present in the sample. Other two methods are proposed to validate the method based on the oxidation state of σ -dianisidine. The ABTS colorimetric assay (method 2), in which the color change to the green of the solution can be measured at 410 nm will be proportional to peroxidase activity in the solution. The third approach is based on the reaction between the hydroxyl radicals generated by the Fenton reaction and compounds, that upon hydroxylation will produce a fluorescent signal that can be measured accordingly such as sodium terephthalate or coumarin, thus allowing the precise assessment of peroxidase activity related to Hb vs whole peroxidase activity in the tissue homogenate (method 3).

Results: We found that the additional peroxidase activity of Hb can be distinguished from the peroxidase activity of true peroxidase and can be easily calculated and subtracted for a more precise estimation of oxidative stress reduction in the sample. Accordingly, the hemoglobin concentration can be

calculated using Lambert-Beer law, $C (\mu\text{M}) = A_{410 \text{ nm}} / \epsilon$, ϵ having a value of $0.46 \mu\text{M}^{-1} \text{ cm}^{-1}$. To obtain the true values of native peroxidase present in the tissue, we sought to create a standard curve of peroxidase and a mathematical formula for defining the additional peroxidase activity of hemoglobin in the tissue lysates. The formula $C (U/mL) = \frac{\Delta\text{abs}+0,1203}{0,06295}$, gives us the exact value in units of true peroxidase, and the possibilities for this peroxidase activity to be subtracted from the total peroxidase activity in any given tissue lysates.

Conclusions: When measuring the peroxidase activity in a tissue lysates sample, the presence of Hb is a *bona fide* factor, which must be considered to properly estimate the oxidative stress in the sample, following a drug therapy applied. Usually, this pseudo-peroxidase activity is oversight, but nonetheless, it is present, and it should be considered. This activity is present in certain conditions, mainly pathological, in which both components are present, stroma-free Hb and hydrogen peroxide. Methods were comparable and the procedure based on the oxidation state of σ -dianisidine was the most reliable protocol. Future perspectives will take into account two other sensitive methods for determining the peroxidase activity of Hb in tissue homogenates such as RAMAN and EPR methods for heme detection and correlation to peroxidase values.

Acknowledgments: The authors are thankful for the materials supplied by the Institute of Biological Research, Republicii Street No. 48, 400016, Cluj-Napoca, the branch of NIRDBS Bucharest, Romania.

A highly syntenic *nic*-genes cluster is present in several related bacterial strains

Amada El-Sabeh¹, Andreea-Mihaela Mlesnita¹,
Iustin-Tiberius Munteanu¹, Iasmina Honceriu¹, Fakhri Kallabi^{1,2},
Razvan-Stefan Boiangiu¹ and Marius Mihasan¹✉

¹ BioActive Research Group, Faculty of Biology, Alexandru Ioan-Cuza University of Iasi, Blvd Carol I no. 20A, Iasi, Romania; ² Laboratory of Human Molecular Genetics, Faculty of Medicine of Sfax, University of Sfax, Tunisia; ✉ **Corresponding author, E-mail:** marius.mihasan@uaic.ro

Introduction: The pyridine-pathway for nicotine degradation present in *Paenarthrobacter nicotinovorans* ATCC 49919 can serve as a model for studying the molecular evolution of catabolic pathways. In this current study, the newly released genome of the strain was used as a reference and an extensive comparative genomics study was performed on a total of 65 related genomes.

Materials and methods: All pairwise comparisons among the set of genomes were conducted using GBDP available in TYGS, digital DNA-DNA hybridization (dDDH) values and confidence intervals were calculated using GGDC 3.0 and average nucleotide identity (ANI) values were calculated using the OrthoANI algorithm. Species clustering was done using a 70% dDDH cutoff. Comparative analysis of *nic*-genes cluster was performed with progressive Mauve using the HOXD scoring matrix.

Results: Five *Arthrobacter* strains showing both dDDH and ANI values over the species threshold when compared to *P. nicotinovorans* ATCC 49199 were identified. Five plasmids and two contigs belonging to *Arthrobacter* and *Paenarthrobacter* strains were shown to be virtually identical with the pAO1 plasmid of *Paenarthrobacter nicotinovorans* ATCC 49919. Moreover, a highly syntenic *nic*-genes cluster was identified on four plasmids, one contig and four chromosomes. The *nic*-genes cluster contains two major locally-colinear blocks (LCBs) that apparently form a putative catabolic transposon.

Conclusions: Although the origins of the *nic*-genes cluster, the putative transposon and the pAO1 megaplasmid still elude us, we hypothesise here that the ATCC 49919 strain most probably evolved from *Paenarthrobacter* sp. YJN-D or a very closely related strain by acquiring the pAO1 megaplasmid and the nicotine degradation pathway.

Acknowledgements: This work was supported by a grant from the Romanian Ministry of Education and Research, CNCS-UEFISCDI, project number PN-III-P4-ID-PCE-2020-0656, within PNCDI III.

The intricate relationship between the CRISPR-Cas system and antibiotic-resistance genes in *Klebsiella pneumoniae*

Dumitrana Iordache^{1,3}✉, Matei Dobrescu¹, Andreea Fita² and Anca Butiuc-Keul^{2,3}

¹Doctoral School of Integrative Biology, Babeș-Bolyai University, Cluj-Napoca, Romania;

²Department of Molecular Biology and Biotechnology, Faculty of Biology and Geology, Babeș-Bolyai University, Cluj-Napoca, Romania; ³Centre for Systems Biology, Biodiversity and Bioresources, Babeș-Bolyai University, Cluj-Napoca, Romania;

✉Corresponding author, E-mail: dumitrana.iordache@ubbcluj.ro

Introduction: *Klebsiella pneumoniae* has emerged as the predominant pathogen responsible for nosocomial infections and exhibits significant levels of antibiotic resistance. Bacteria employ the CRISPR-Cas system to restrict the intake of foreign genetic material, effectively maintaining an equilibrium between acquiring advantageous traits through horizontal gene transfer (HGT) and safeguarding against bacteriophage infections. Research has revealed the presence of Type I-E and subtype I-E* CRISPR-Cas systems within *K. pneumoniae* strains. This study aimed to assess the implication of the CRISPR-Cas system in the acquisition of antimicrobial resistance genes (ARG) by *K. pneumoniae* genomes.

Materials and methods: The current study employed a comprehensive approach to investigate *K. pneumoniae* genomes. A total of 100 complete genomes with CRISPR-Cas type I-E, 100 genomes with CRISPR-Cas type I-E*, and 100 genomes lacking CRISPR-Cas were downloaded from the CRISPRCasdb database. Subsequently, the CRISPR spacers within these genomes were scrutinized for potential matches against plasmids (RefSeq-Plasmid), viruses (IMGVR, RefSeq-Phage, RefSeq-Viral, and PHAST), as well as ARGs (Comprehensive Antibiotic Resistance Database) and integrons (INTEGRALL database), using the CRISPRTarget program and a custom Python script. Moreover, the presence of ARGs within the sequenced genomes was examined using the same script. The Kolmogorov-Smirnov test was conducted to evaluate normal distribution, followed by the Kruskal-Wallis test to assess parametric differences. Additionally, chi-square tests were utilized to investigate associations between counts or frequencies. For all statistical analyses, significance was determined at a p-value threshold of less than 0.05.

Results: In *K. pneumoniae*, the type I-E system has a single locus downstream of the Cas cluster, whereas the I-E* system typically exhibits two loci positioned both upstream and downstream of the Cas cluster. Notably, the number of spacers within the I-E system is generally higher than the combined spacers within the two I-E* CRISPR loci. Furthermore, the I-E* subtype is also distinguished from the I-E type by the sequence of the direct repeat. The spacers present in each locus are distinct, with no shared spacers observed among the three loci; however, instances of plasmids and viruses exhibiting a perfect match between spacers from both systems have been identified. The analysis demonstrated that most identified spacers originated from viral sources. While no spacers were found to correspond to antibiotic resistance genes (ARGs) or integrase sequences, certain spacers did target plasmids that may carry ARGs. Interestingly, genomes harbouring the I-E* system exhibited a significantly lower presence of ARGs compared to genomes possessing the I-E system ($p=0.0239$). Nevertheless, when compared to genomes lacking the CRISPR-Cas system, while a difference was observed, it was not statistically significant ($p=0.0587$).

Conclusions: These findings indicate that the CRISPR-Cas system in *K. pneumoniae* may primarily serve as a defence mechanism against bacteriophage infections rather than directly targeting ARGs or integrase sequences. However, the system could still indirectly impact the dissemination of ARGs by targeting plasmids carrying these genes. Although the I-E system does not impede the acquisition of ARGs, the I-E* system may possess a certain level of activity in this regard.

Ion mobility mass spectrometry of human cerebellum gangliosides

Maria-Roxana Biricioiu^{1,2}✉, Mirela Sarbu¹, Raluca Ica¹ and Alina D. Zamfir^{1,3}

¹ National Institute for Research and Development in Electrochemistry and Condensed Matter, Timisoara, Romania; ² Faculty of Physics, West University of Timisoara, Timisoara, Romania; ³ Department of Technical and Natural Sciences, "Aurel Vlaicu" University of Arad, Arad, Romania; ✉ **Corresponding author, E-mail:** maria.biricioiu99@e-uvt.ro

Introduction: Cerebellum represents a highly specialized region of the brain encompassing approximately 80% of the total brain neurons and regular arrays of neuronal units involved in motor control, learning, cognitive and emotional functions. In recent years, human cerebellum started to be investigated at the molecular level, in order to correlate its functions with the expression of various biomolecules, especially gangliosides, sialylated glycosphingolipids highly expressed in the central nervous system. Among the bioanalytical methods employed so far in the analysis of cerebellar biomolecules, mass spectrometry (MS) provided the most comprehensive information.

Materials and methods: We report here on the first introduction in cerebellum research of ion mobility separation (IMS) mass spectrometry for a systematic mapping of cerebellar gangliosides and determination of the species associated to development and aging. For this purpose, gangliosides extracted from post-mortem tissue biopsies of fetal -in the 15 and 40 gestational weeks (samples 15GW and 40GW)- and 65 years of age (sample 65Y) cerebellum were analyzed by nanoESI IMS MS in the negative ion mode under identical conditions.

Results: Altogether, no less than 694 molecular ions corresponding to 522 gangliosides, fucogangliosides and species modified by *O*-acetylation, *O*-GalNAc and CH₃COO⁻ were identified by IMS MS separation and screening, which represents almost five times more cerebellar structures than ever reported before.

Conclusions: The comparative analysis revealed for the first time that: i) 40GW contains the highest number of species (356), followed by 15GW (303) and 65Y (201); ii) fetal cerebellum gangliosidome is characterized by a much higher sialylation degree and species altered by carbohydrate and non-carbohydrate type of modifications than the gangliosidome of aged cerebellum; iii) significant developmentally- and age-regulated changes in the expression

and structure of cerebellum gangliosides exist. These variations are to be correlated in the future with the neurological diseases, leading to the discovery of pathways to more effective therapeutic schemes.

Acknowledgements: This work was funded by the Romanian National Authority for Scientific Research, UEFISCDI, project PN-III-P4-ID-PCE-2020-0209.

The pharmacological profile of natural compounds from *Aconitum* sp.

Maria Mernea¹✉, Catalina Mares¹ and Speranta Avram¹

¹ Department of Anatomy, Animal Physiology and Biophysics, Faculty of Biology, University of Bucharest, Bucharest, Romania; ✉Corresponding author, E-mail: maria.mernea@bio.unibuc.ro

Introduction: Plants from *Aconitum* genus are well known for their toxic effects. At the same time, their active compounds were shown to have beneficial effects like anticancer, antimicrobial, antifungal, or antioxidant. A thorough characterization of these compounds is needed in order to understand their pharmacokinetic, pharmacodynamic and toxicity profiles. Here we used bioinformatics methods to address these aspects in the case of 21 constituents of *Aconitum* sp that were identified by high performance liquid chromatography (HPLC).

Materials and methods: The SMILES structures of compounds were retrieved from PubChem database. MOE program was used to calculate the physico-chemical features of compounds relevant for their pharmacologic profile. The SMILES structures were loaded in ExPasy server to evaluate the drug-likeness profiles of compounds. AdmetSAR was used to predict their ADMET properties and SwissTarget was used to predict their targets.

Results: From the 21 compounds, 15 present drug-like features. Except for magnoforine, the compounds should present a good gastro-intestinal absorption. The oral bioavailability is increased for ferulic acid, caffeic acid, delphinidin and syringic acid. The blood brain barrier permeability is increased for aconitine, hyaconitine, mesaconitine, magnophorine, gallic acid, ferulic acid, malvidin and syringic acid.

In what concerns the toxicity of compounds, most compounds are not toxic for birds or bees, have no mutagenic potential, but are toxic for fish. The prediction show that most compounds are hepatotoxic, except for hyaconitine, catechin, ferulic acid, caffeic acid, chlorogenic acid, epicatechin, coumaric acid or syringic acid. Except for gallic acid, ferulic acid, caffeic acid, coumaric acid, syringic acid, rutin and naringenin, the compounds could present toxicity at the mitochondrial level. Most compounds are expected to present toxicity at the respiratory level, except for gallic acid, ferulic acid, caffeic acid, coumaric acid. The compounds were not predicted to be cardiotoxic.

The predicted targets of *Aconitum* sp compounds pointed toward carbonic anhydrases of different types. In addition, some compounds like coumaric acid, daidzein and genistein modulate estrogen receptors. Other compounds like genistein, hyaconitine and magnoflorine should modulate targets from the central nervous system.

Conclusions: The compounds from *Aconitum* sp appear as promising therapeutic agents, acting on carbonic anhydrases and other targets even from the central nervous system. Some compounds present favorable pharmacokinetic and toxicity profiles, but there are compounds presenting different types of toxicity like hepatotoxicity, respiratory or mitochondrial.

Acknowledgements: The study was supported by UEFISCDI through the project PN-III-P2-2.1-PED-2021-2866.

Glicolipidomics of human glioblastoma multiforme by ion mobility mass spectrometry

Mirela Sarbu¹✉, David E. Clemmer², Željka Vukelić³ and Alina D. Zamfir^{1,4}

¹ Department of Condensed Matter, National Institute for Research and Development in Electrochemistry and Condensed Matter, Timisoara, Romania; ² Department of Chemistry, The College of Arts & Science, Indiana University, Bloomington, Indiana, USA; ³ Department of Chemistry and Biochemistry, Faculty of Medicine, University of Zagreb, Croatia; ⁴ Department of Technical and Natural Sciences, "Aurel Vlaicu" University of Arad, Arad, Romania;

✉ **Corresponding author, E-mail:** mirela.sarbu86@yahoo.co.uk

Introduction: Glioblastoma multiforme (GBM) is the most widespread primary brain tumor in adults. With a rapid infiltration rate into the nearby tissue, GBM has drawn a significant attention because of its poor prognosis and the limited treatment options available. The research nowadays is focused on the determination of the molecular mechanisms related to GBM tumor invasion and the discovery of innovative approaches for invasiveness suppression. Since gangliosides (GGs) are tumor-associated antigens, we have introduced here IMS MS for the discovery of GBM-specific structures.

Materials and methods: GGs were extracted from a brain tumor localized in the frontotemporal cortex of the right hemisphere in a male patient, age 47. The histopathological analysis has shown that the tumor is GBM, grade IV. Ten μL of the working GBM GG solution in methanol were infused into a Synapt G2S instrument. To enhance the GG separation, the IMS parameters were set as follows: ESI voltage 1.5kV, cone voltage 45 V, IMS wave velocity 650 m/s, IMS wave height 40 V and collision energy 40 eV.

Results: The 2D data set of GBM GGs revealed the GG separation into mobility families based on their charge state, carbohydrate chain length, and the degree of sialylation. IMS MS offered a reliable separation, given the detection and identification in GBM of 215 ions, corresponding to no less than 160 distinct glycoforms, more than triple the number of GGs previously discriminated in GBM with no separation prior to MS. The tumor was found dominated in equal and high proportions by GD3 and GT1 forms, with a particular incidence of C24:1 fatty acids in the ceramide. By the occurrence of only one mobility feature and the diagnostic fragment ions, the IMS tandem MS conducted using collision-induced dissociation (CID) disclosed for the first time the presence of GT1c(d18:1/24:1) newly proposed here as a potential GBM marker.

Conclusions: By IMS MS and CID MS/MS various novel species could be identified and added to the currently existing panel of glioblastoma tissue-associated structures, since the number of the GGs identified here is three times higher than ever discovered in this tumor type.

Acknowledgements: This work was supported by the Romanian National Authority for Scientific Research, UEFISCDI, PN-III-P4-ID-PCE-2020-0209 granted to A.D.Z

New strategies for potentiating the effect of tissue transglutaminase-fibronectin small molecule inhibitors in ovarian cancer treatment

Monica Tudor¹✉, Cristian Munteanu¹, Gabriela Chirițoiu¹,
Florin Jipa², Ștefana M. Petrescu¹, Gary E. Schiltz^{3,4,5},
Daniela Matei^{4,5,6} and Livia E. Sima¹

¹ Institute of Biochemistry of the Romanian Academy, Bucharest, Romania;

² National Institute of Laser Plasma and Radiation Physics, Bucharest-Magurele, Romania;

³ Northwestern University, Chicago, USA; ⁴ Jesse Brown VA Medical Center, Chicago, USA;

✉ **Corresponding author, E-mail:** monica.tudor@biochim.ro

Introduction: Ovarian cancer (OC) is the 8th most common cancer in women. It is often diagnosed at late stages - 60% of cases are present with stage III or IV cancer and this affects the response to treatment. Tissue transglutaminase (TG2), an overexpressed protein in OC tumors, interacts with fibronectin (FN) and promotes OC intraperitoneal dissemination, which makes TG2 a promising target for treatment. We previously identified MT4 as a promising small molecule inhibitor (SMI) of TG2-FN protein-protein interaction. We recently 5 new MT4 analogues (#2997, #2998, #3002, #3010, #3011) and investigated their effect on OC cells. We used phosphoproteomics to analyze the adaptive signaling of OC cells treated with MT4 in order to identify new potential TG2 co-targets.

Materials and methods: We used MTS assay to evaluate SMIs cytotoxicity. Cells were seeded in 3D culture conditions to evaluate spheroid formation. For early attachment assessment, we determined DNA content of cells attached to FN within 45 min. Wound healing was performed to evaluate cell migration. SILAC labeled cells were used in a 30 minutes adhesion on FN. Both attached and suspension cells were collected, lysed and prepared for LC-MS/MS analysis using Easy nanoLC II coupled with LTQ- Orbitrap Velos Pro Mass Spectrometer. Data analysis was performed using Proteome Discoverer V 1.4, KEGG pathways and IPA. Synergy was evaluated using CompuSyn analysis. A gradient generating microfluidic chip was obtained using laser-based methods for testing the effect of various inhibitor concentrations or combinations thereof on OC cells or spheroids attachment onto FN. Live cell imaging of mesothelial clearance was performed using primary LP9 mesothelial cell monolayers and SKOV3 spheroids.

Results: To characterize the newly developed SMIs, we tested their effect on spheroid formation using OVCAR5 cell line and its *Tgm2* gene CRISPR knockout variant. Compound #3011 totally prevented sphere formation, similar to *Tgm2* gene excision. Early attachment assay revealed that SMIs #3002 and #3011 diminished cell adhesion. Wound healing assay showed that #2997 inhibited SKOV3 cell migration. We developed a microfluidic chip that allowed us to perform real-time visualization of mesothelial clearance. The results revealed that our proposed SMIs had an inhibitory effect on SKOV3 spheroids' capacity to displace mesothelial cells. Phosphoproteomic analysis revealed two classes of upregulated proteins – sirtuins and p21 activated kinases (PAKs). SIRT1 inhibitor molecules in combination with MT4 or #3011 affected 3D spheroid formation, number of 2D colonies formed, and had a cytotoxic effect on OVCAR5 cells. MT4-PAK1 inhibitors combinations enhanced OVCAR5 cell adhesion inhibitory effect of MT4.

Conclusions: We obtained new SMIs for TG2-FN interaction with improved capacity to inhibit spheroid formation and OC cell attachment. We then identified new promising molecular TG2 co-targets for OC treatment that induce cell death in both 2D and 3D conditions.

Acknowledgements: This work was funded from US Department of Veterans Affairs (I01 BX000792-06), Robert H Lurie Comprehensive Cancer Center and UEFISCDI (PN-III-P2-2.1-PED-2019-1543).

Absolute and relative expression analysis of plasma microRNAs in patients with prostate cancer – a comparison

Paula Diana Ciordas^{1,2}, Mirabela Romanescu^{1,2}, Aimee Rodica Chis², Catalin Marian² and Ioan Ovidiu Sirbu²

¹ Doctoral School, “Victor Babes” University of Medicine and Pharmacy, Timișoara, Romania;

² Discipline of Biochemistry, “Victor Babes” University of Medicine and Pharmacy, Timișoara, Romania;  **Corresponding author, E-mail:** paula.muntean@umft.ro

Introduction: Prostate cancer (PCa) is the second most common malignancy in men and a major source of male mortality. Due to their outstanding stability in various biological fluids, microRNAs are excellent diagnostic and prognostic biomarker candidates in various cancers (including PCa). Plasma microRNAs quantification involves real-time PCR, through either a relative or an absolute approach. Despite a rigorous methodology for choosing the right normalizer, relative quantification might lead to results drastically different from those obtained by absolute quantification. Herein we compared the findings from absolute (using standard curve) and relative quantification experiments conducted on both the guide and the passenger strand of 5 microRNAs known for their involvement in PCa.

Materials and methods: Total RNA was purified from plasma specimens collected from PCa patients and controls. *Caenorhabditis elegans* miR-39 mimic was spiked-in during the extraction procedure for subsequent external normalisation. Next, we used TaqMan assays to conduct singleplex qRT-PCR reactions for each microRNA of interest. For absolute quantification, standard curves were generated using 10 log dilutions of synthetic RNA oligonucleotides. Carrier RNA from bacteriophage MS2 was used to mimic the RNA plasma profile and improve the recovery of short and low-represented RNA species. Data analysis and visualizations were performed on RStudio integrated development environment.

Results: Our findings show that compared to absolute quantification, the results from relative quantification experiments are less consistent and more variable, most probably due to variability in the expression of reference genes. Furthermore, we present data indicating that the GC content of target microRNA could influence de quantification outcome and should be taken into consideration

when designing art-PCR quantification experiments. Thus, while more labour-intensive and time-consuming, standard-curve absolute quantification stands out as the more reliable method of measuring the plasma level of microRNAs.

Conclusions: Dysregulation of the circulating microRNAs profile of PCa patients could be exploited as potential diagnosis tool for the disease. Absolute quantification using a standard curve is a suitable technique for quantifying small RNA-based plasma biomarkers since it provides highly reproducible results and allows for the determination of the exact copy number of species of interest.

Acknowledgements: This work was funded from project PN-III-P2-2.1-PED2021-1171.

Profiling and structural characterization of gangliosides in human temporal lobe epilepsy

Raluca Ica¹✉, Kristina Mlinac-Jerković², Svjetlana Kalanj-Bognar², Cristian V.A. Munteanu³, Andrei J. Petrescu³ and Alina D. Zamfir^{1,4}

¹ Department of Condensed Matter, National Institute for Research and Development in Electrochemistry and Condensed Matter, Timisoara, Romania; ² Department for Chemistry and Biochemistry & Croatian Institute for Brain Research, School of Medicine, Zagreb University, Croatia; ³ Institute of Biochemistry of the Romanian Academy, Bucuresti, Romania; ⁴ Department of Technical and Natural Sciences, "Aurel Vlaicu" University of Arad, Romania; ✉Corresponding author, E-mail: raluca.ica@gmail.com

Introduction: Temporal lobe epilepsy (TLE) is one of the most common forms of epilepsy in humans. The molecular phenomena underlying seizures involve variations in membrane ion homeostasis leading to disturbances in neuronal excitability. Numerous pathophysiological effects of gangliosides have been demonstrated, but their potential role in the molecular pathogenesis of TLE has not been explored. We developed a high-resolution (HR) MSⁿ approach using Orbitrap MS nanoESI to assess changes in the ganglioside pattern in TLE-affected adult hippocampus compared to normal hippocampus, with the aim of detecting TLE-associated structures.

Materials and methods: The native ganglioside mixtures analyzed were purified from human hippocampus affected by TLE (sample HipE) and age-matched normal hippocampus tissue (sample Hip), used as the control. Gangliosides were extracted in chloroform: methanol: water (1:2:0.75 by vol.), separated, collected and purified. The MS experiments were conducted in the negative ion mode on a LTQ Orbitrap Velos equipped with nanoESI source. Multistage mass spectrometry (MSⁿ) was carried out by higher energy collision dissociation (HCD) at variable collision energies within 35-80 eV.

Results: The high sensitivity and the resolution employed in the present experiments enabled the detection and identification of no less than 99 different gangliosides in hippocampus affected by TLE and 75 in the normal adult hippocampus specimen, which represent 5 times more structures than ever reported in the adult tissue and the highest number of species identified in hippocampus solely on the basis of MS profiling. The results also showed marked differences of the ganglioside expression in TLE vs. control, particularly with respect to the sialylation degree of components, discovered as a general marker of TLE. Another major finding was the occurrence of tetrasialo-

fucogangliosides in TLE and species modified by either *O*-acetylation or CH₃COO-. Additional structural analysis by nanoESI high-energy collisional dissociation (HCD) MS/MS gave rise to fragmentation patterns supporting the presence of GQ1b (d18:1/18:0) isomer as a novel TLE marker.

Conclusions: In this study high resolution MS approach provided detailed data on altered hippocampal gangliosidome in TLE, establishing GQ1b as a specific TLE-related biomarker, and strongly supported the hypothesized association of gangliosides with disturbed ion homeostasis underlying seizures pathogenesis in humans.

Acknowledgements: Research funded by the Romanian National Authority for Scientific Research (UEFISCDI), PN-III-P4-ID-PCE-2020-0209 to ADZ.

Evaluation of total iodine uptake in biofortified chilli peppers

Ana Varadi¹✉, Claudia Cimpoi¹ and Augustin C. Mot¹

¹Faculty of Chemistry, Department of Chemistry, Babes-Bolyai University, Cluj-Napoca, Romania;

✉Corresponding author, E-mail: ana.varadi@ubbcluj.ro

Introduction: Among human micronutrient deficiencies, iodine is unique for the fact that its deficiency appears regardless of the economic status of the population, being prevalent in developing as well as developed countries. Iodized salt approach has several drawbacks, that is why other methods have to be used in order to supply the individuals with adequate amounts, one of them being iodine biofortification of vegetables. Considering that chilli peppers cannot be consumed in high quantities because of their pungency as well as either deficit or sudden iodine excess can be dangerous for human health, we decided to evaluate the amount of iodine that can be internalized in chili pepper fruits after iodine biofortification and without toxic effects for the plant.

Materials and Methods: Chili peppers varieties or cultivars of the *Capsicum annuum* and *Capsicum baccatum*, were biofortified with iodine as KI beginning with the 25th day from germination and were divided in two experimental approaches. For the first experimental design iodine was added in three doses namely 2.5, 6.5 and 16 mg iodine per kg soil, doses that were divided in 9 weeks. For the second design, iodine doses were 25, 50 and 100 mg I/kg soil and were divided in 4 weeks. When ripen, the fruits, leaves and roots were oven-dried at 45 °C for 72 h, milled into powder and iodine was analysed using the ferric thiocyanate-nitric acid catalytic kinetic method, following the sample combustion.

Results: The recovered iodine in soil was about 50% of the added amount, the other 50% being volatilised and internalised in the plants. Iodine content internalised in plants decreased in the order roots > leaves > fruits. High difference of iodine uptake into fruits was noted among the tested varieties (between 1 and 4 mg I/kg dried fruit for the first experimental design and between 3 and 11 mg I/kg dried fruit for the second experimental design).

Conclusions: Only a half of the iodine biofortification dose remains in soil. The iodine biofortification degree in chilli peppers is highly dependent upon the used varieties.

Keywords: biofortification, chili peppers, iodine

***In vitro* and *in vivo* assessment of the antioxidant properties of *Apis mellifera* venom**

Camelia Alina Gîlcescu (Florescu)¹, George Bica¹, Elena Camelia Stănciulescu¹, Loredana Colhon¹ and Cătălina Gabriela Pisoschi¹✉

¹University of Medicine and Pharmacy of Craiova, Craiova, Dolj, Romania;

✉Corresponding author, E-mail: c_pisoschi@yahoo.com

Introduction: The virtues of some bee products (pollen, honey) have been recognized for centuries. Among bee products, the venom has been intensively studied in the last decades to obtain definite scientific data on potential therapeutic properties associated with its complex composition. Research is focused especially on its anti-inflammatory effect, but antioxidant and antimicrobial activities are still under debate. The experiments were designed to assess *in vitro* antioxidant activity of two samples of bee venom (BV) from *Apis mellifera* and its *in vivo* effect on the antioxidant status in a rat model of FCA-induced arthritis.

Materials and methods: 2, 2'-azinobis (3-ethylbenzothiazoline-6-sulfonic acid, ABTS) and 1, 1'-diphenyl-2-picrylhydrazyl (DPPH) assays were used to determine *in vitro* antioxidant activity of BV samples. *In vivo* antioxidant effects of bee venom were evaluated after induction of arthritis on male Wistar rats following an intraarticular injection of 120 µL of Freund's complete adjuvant (FCA). Rats were randomised in four groups: two control groups (negative and positive-arthritis), one treated with methotrexate as a standard drug for rheumatoid arthritis and the fourth group including animals receiving BV (2 mg/kg). Blood reduced glutathione level, glutathione peroxidase and catalase activities as well as serum total antioxidant capacity and lipid peroxides were measured using spectrophotometric standardized methods.

Results: The differences between the antioxidant activity of the two BV samples were statistically significant in both DPPH and ABTS assays. IC₅₀ values for both free radical scavenging methods were lower for sample BV2, this proving to have a better antioxidant effect than sample BV1. Both BV samples proved a free radical scavenging effect more than 50%. Arthritic rats had increased levels of lipid peroxides and decreased blood glutathione, glutathione peroxidase and catalase activities compared to sham and those receiving methotrexate. Bee venom treatment significantly increased the levels of reduced glutathione, glutathione peroxidase and catalase activity and decreased lipid peroxidation.

Conclusions: Bee venom has been shown to improve the antioxidant defence in rats with FCA-induced arthritis due to own antioxidant properties. No doubt, the antioxidant involvement sustains its well-studied anti-inflammatory effect.

Antioxidant and antiproliferative activity of anthocyanin rich extract from roses (*Rosa L.*)

Cosmin-Alin Faur¹✉, Marius Zăhan¹, Gabriela Roman²,
Claudiu Ioan Bunea³, Eugenia Hârșan² and Andrea Bunea¹

¹ Faculty of Animal Science and Biotechnology, University of Agricultural Sciences and Veterinary Medicine, Cluj-Napoca, Romania; ² The Horticultural Research Station, Cluj-Napoca, Romania; ³ Faculty of Horticulture and Rural Development Business, Cluj-Napoca, Romania; ✉ **Corresponding author, E-mail:** alincosminfaur@yahoo.com

Introduction: Rose petals (*Rosa L.*) are a rich source of bioactive compounds, including anthocyanins. Anthocyanins and anthocyanidins are water-soluble compounds well-known for their antiproliferative and antioxidant properties, which are closely related to their structure and redox properties. However, only a limited number of studies have investigated the antiproliferative activity of rose extracts on cell cultures.

The main objective of this study was to perform a biochemical analysis of several rose varieties and select the varieties with the highest anthocyanin content in the petals for testing their antiproliferative activity on two epithelial cell lines.

Materials and methods: In this study, 18 rose varieties were examined to identify anthocyanins, determine total polyphenols, total flavonoids, total lipids and antioxidant activity using specific methods for each class of compounds. The three rose varieties with the highest anthocyanin content were chosen to evaluate their antiproliferative activity on two human skin tissue-derived cell lines. The cell lines used were a tumor cell line (A375), which produces malignant melanoma, and a normal cell line (Hs27), to assess the effect of five different concentrations of anthocyanin-rich extract (200-1000 µg/mL).

Results: The results showed the presence of 9 anthocyanins through HPLC analysis, with the highest concentration of anthocyanins found in the varieties Porta Nigra, Lili Marleen and Schwarze Madonna. These varieties maintained their position regarding total polyphenol and total flavonoid concentrations, as well as antioxidant activity. Moreover, the MTT test conducted to determine antiproliferative activity showed only antiproliferative effects on the A375 tumor cell line, regardless of the varieties and concentrations used. On the other hand, on the normal cell line Hs27, concentrations up to 1000 µg/mL for Porta Nigra and Lili Marleen varieties and up to 600 µg/mL for the Schwarze Madonna variety did not affect the integrity of normal cells.

Conclusions: The anthocyanins from the three rose extracts demonstrated the ability to inhibit cell proliferation in the A375 tumor cell line without affecting cells from the normal Hs27 cell line, in a concentration-dependent manner.

Valorization of carotenoid from sea buckthorn pomace using green solvents and ultrasound-assisted extraction

Cristina Gherasim¹✉ and Adela Pinteau¹

¹ University of Agricultural Sciences and Veterinary Medicine,
Department of Chemistry and Biochemistry, Cluj-Napoca, Romania;
✉Corresponding author, E-mail: cristina.gherasim@usamvcluj.ro

Introduction: Sea buckthorn pomace is a by-product of fruit juice production which still contains large amounts of carotenoids and other lipophilic compounds. In order to limit the negative impact that organic solvents have on the environment and on human health, there is a growing interest for developing new extraction techniques for lipophilic compounds. Besides the use of green solvents, efficient methods like ultrasound-assisted, microwave-assisted or enzyme-assisted extractions are envisaged. Encapsulation of biologically active compounds has gained interest because this method can improve both the stability and the bioaccessibility of natural compounds, providing viable solutions for food and pharmaceutical industry.

Materials and methods: Sea buckthorn fruits were cold pressed, resulting in the juice and the pomace fractions. The resulting pomace was then weighed, dried and ground to produce a powder. Carotenoid extraction was conducted comparatively, using an organic solvent mixture (ethyl-acetate:methanol:petroleum ether) and green solvents (ethyl lactate ethyl acetate, methyl tetrahydrofuran, cyclopentyl methyl ether, sunflower oil). Two extraction methods were applied: maceration (solid-liquid extraction) and ultrasound-assisted extraction. The carotenoid extract was used for encapsulation using alginate and calcium chloride. The capsules (wet or dehydrated) were added to yogurt samples and then subjected to *in vitro* digestion using the INFOGEST method in order to determine the bioaccessibility of carotenoids. Carotenoid content in all samples was determined by spectrophotometry and C30-HPLC-PDA, using external calibration with commercial standards.

Results: The main carotenoids identified in pomace extracts were β -carotene, γ -carotene, lycopene, zeaxanthin, zeaxanthin myristate-palmitate, and zeaxanthin dipalmitate. The highest extraction yield ($99.34 \pm 8.9\%$) was obtained using ultrasound-assisted extraction with MeTHF as extraction solvent. The final extract was dissolved in sunflower oil and used to obtain the alginate microcapsules. The capsules had a mean diameter of 600 μm and the encapsulation efficiency was 99.4%. The retention of carotenoids in microcapsules after 30 days of storage,

at 4°C, was 77 % for wet beads and 74% for dehydrated beads, which indicates a good stability. The bioaccessibility of carotenoids from yogurt samples supplemented with alginate microcapsules was $29.5\pm 3.9\%$ (wet) respectively 40.7 ± 3.8 (dehydrated), compared to control $42.1\pm 4.6\%$ (wet) respectively $40.8\pm 4\%$ (dehydrated). Better results were obtained when yogurt was supplemented with dehydrated capsules compared to wet capsules.

Conclusions: The results presented in this study shows that green solvents and ultrasound-assisted extractions are efficient methods for valorization of sea buckthorn pomace. Encapsulation of carotenoid extract in alginate microcapsules have a protective effect and does not impair their bioaccessibility in a food model.

Acknowledgements: "This work benefited from financial support through the project "Development of the skills of advanced and applied research in STEAM+ Health logic", POCU/993/6/13/153310, project co-financed from the European Social Fund through the Human Capital Operational Program 2014-2020".

Toxicity of Gadolinium on *Stevia rebaudiana* grown *in vitro*

Florina Violeta Scurtu^{1,3}, Doina Clapa¹, Floricuța Ranga², Vasile Coman², Augustin C. Moț³, Sonia Ancuța Socaci², Loredana Florina Leopold² and Cristina Coman²✉

¹ Life Sciences Institute, University of Agricultural Sciences and Veterinary Medicine, 3-5 Calea Mănăstur, 400372, Cluj-Napoca, Romania; ² Faculty of Food Science and Technology, University of Agricultural Sciences and Veterinary Medicine, 3-5 Calea Mănăstur, 400372, Cluj-Napoca, Romania; ³ Faculty of Chemistry and Chemical Engineering, Babes-Bolyai University, Arany János 11, 400028 Cluj-Napoca, Romania; ✉ **Corresponding author, E-mail:** cristina.coman@usamvcluj.ro

Introduction: Lately, there is increasing interest in the potential toxicity of different widely used nanomaterials or chemicals on the environment and on edible plants. Gadolinium (Gd)-based contrast agents (e.g., gadobutrol - GB) are still extensively used for diagnostic purposes in magnetic resonance imaging. However, there are several issues related to their use. For example, after administration, they are excreted and end up in hospital effluents and, consequently, in wastewaters. As wastewater treatment is not flawless, Gd presence in tap water and tap water-based beverages (e.g., Coca-Cola from fast-food franchises in big cities in Germany) has been documented recently.

In this study, we have assessed the accumulation of Gd ions on *Stevia rebaudiana* plantlets grown *in vitro*, and their impact on plant growth and on plant metabolites (chlorophylls, carotenoids, ascorbic and dehydroascorbic acids). The plants were exposed to GB in concentrations up to 3 mM.

Materials and methods: The plant metabolites were quantified using high performance liquid chromatography (HPLC). Oxidative stress was assessed by the malondialdehyde (MDA) assay and electron paramagnetic resonance (EPR).

Results: At the highest doses (1 and 3 mM), GB exposure had detrimental effects, leading to significant inhibition in plant development. The concentrations of carotenoids, chlorophylls A and B (Chl A and B), were severely decreased at these high exposures. For the highest dose, Chl A and B concentrations descended by 52.76% and 58.92%, and the levels of lutein, zeaxanthin, and beta-carotene were inhibited by 38.16%, 54.34%, and 54.34%, respectively. A detrimental effect of the high GB doses was also seen via the increase in free radical species detected by EPR, which was negatively correlated with the evolution of antioxidants (i.e.,

ascorbic acids). The 0.1 mM dose of GB can be considered a threshold, below which the plant defense system is functional, and the GB toxicity seemed to be low or moderate.

Conclusions: Given all these findings, the photosynthesis at high concentrations of GB was impacted significantly. Such pronounced changes in plant morphology and levels of antioxidant molecules can be related to the plant's stress response, which could be sometimes unnoticeable at low exposures and harmful above certain thresholds.

Acknowledgements: This work was supported two Grants of the Romanian Ministry of Education and Research, CNCS-UEFISCDI, project number PN-III-P4-ID-PCE-2020-1847, within PNCDI III.

***Allium sativum* and *Allium ursinum* extracts: antimicrobial activity and phytochemical characterization**

Ioana Andreea Barbu^{1,2,3✉}, Alexandra Ciorîță^{1,4}, Rahela Carpa^{1,3,5},
Augustin Catalin Moț⁶, Anca Butiuc-Keul^{1,2,3} and Marcel Pârvu^{1,3}

¹Faculty of Biology and Geology, Babeș-Bolyai University, Cluj-Napoca, Romania; ²Doctoral School of Integrative Biology, Babeș-Bolyai University, 400015 Cluj-Napoca, Romania; ³Center for Systems Biology, Biodiversity and Bioresources, Babeș-Bolyai University, Cluj-Napoca, Romania;

⁴National Institute for Research and Development of Isotopic and Molecular Technologies, Cluj-Napoca, Romania; ⁵Institute for Research-Development-Innovation in Applied Natural Sciences, Babeș-Bolyai University, Cluj-Napoca, Romania; ⁶Faculty of Chemistry and

Chemical Engineering, Babeș-Bolyai University, Cluj-Napoca, Romania;

✉ **Corresponding author, E-mail:** ioana.barbu@ubbcluj.ro

Introduction: *Allium* plants have been known for their antimicrobial properties since ancient times. Recent studies have shown that the leaves and bulbs of these plants are rich in phenols, flavonoids and thiosulfinates, compounds that have proven antimicrobial, antioxidant or antitumor activity. Naturally, in *Allium* bulbs or leaves, allicin is formed after crushing or cutting the plant organs under the action of the allinase enzyme. The chemical composition of the extracts depends on the species.

Materials and methods: The antimicrobial activity of the extracts was determined by the agar disk diffusion method. The minimum inhibitory concentration (MIC) and minimum bactericid concentration (MBC) were also determined. Through the phytochemical analysis of the extracts, the determination of three classes of compounds was followed: the total thiosulfinates content, the total phenolic content and the total flavonoid content.

Results: The antimicrobial activity of *A. sativum* and *A. ursinum* extracts against *Escherichia coli*, *Staphylococcus aureus*, *Candida albicans* and *Candida parapsilosis* can be correlated with the presence of large amounts of thiosulfinates. Both extracts have shown better results against *Candida* species (inhibition zones of 20–35 mm) and against Gram-positive bacteria, *Staphylococcus aureus* (inhibition zones of 15–25 mm) compared to the other two species tested. The MICs for the tested microbial species were similar to the MBCs. There were also discrepancies between MICs and MBCs, e.g., for the, *A. ursinum* extract on *C. parapsilosis* (MIC = 6.25 and MBC = 25) and for the *A. sativum* extract on *E. coli* (MIC = 6.25 and MBC = 25). The two extracts have a similar content of

thiosulfinates compounds. The *A. sativum* extract has double the amount of flavonoids compared to that of *A. ursinum*, while the total phenolic content is higher in *A. ursinum*.

Conclusions: These results demonstrate the antimicrobial effect of the extracts suggesting their use as adjuvant treatment for microbial infections.

Acknowledgements: This research was funded by Babes-Bolyai University, under the doctoral grant of Ioana Andreea Barbu.

Assessing the risks of nanoplastic exposure to plants: Implications for growth and steviol glycoside production

Loredana F. Leopold^{1,2}✉, Florina V. Scurtu², Doina Clapa²,
Nicolae Leopold³, Stefania D. Iancu³, Floricuța Ranga¹,
Sonia A. Socaci^{1,2} and Cristina Coman^{1,2}

¹Faculty of Food Science and Technology, University of Agricultural Sciences and Veterinary Medicine, Cluj-Napoca, Romania; ²Life Sciences Institute, University of Agricultural Sciences and Veterinary Medicine, Cluj-Napoca, Romania; ³Faculty of Physics, Babeș-Bolyai University, Cluj-Napoca, Romania; ✉Corresponding author, E-mail: loredana.leopold@usamvcluj.ro

This study aims to investigate the toxicity of polystyrene nanoplastic (NP) on *Stevia rebaudiana* plants and develop a quick detection method for NP accumulation in plant tissues using dark field microscopy with hyperspectral imaging (HSI). The research focuses on the potential risks associated with NPs exposure to plants. For this, *in vitro* and *in vivo* *Stevia rebaudiana* plants were exposed to NPs at concentrations up to 250 mg/L to evaluate their impact on plant growth, morphology, and metabolites. High-Performance Liquid Chromatography (HPLC) was used to quantify the *Stevia rebaudiana* metabolites, and the results indicated that the concentration of various plant metabolites decreased with the NP dose (up to 250 mg/L NP), which can be attributed to the stress response of the plant caused by NPs.

The growth of *Stevia rebaudiana* plantlets was negatively impacted by polystyrene NP. However, the production of steviol glycosides, the natural sweeteners in stevia, exhibited a biphasic dose-response, suggesting hormesis, with the highest values at 250 mg/L NP (a 1.3-fold increase compared to controls).

These findings highlight the potential risks associated with NP exposure to plants and suggest the need for further research on the effects of NPs on plant growth and productivity.

Acknowledgements: This work was supported by two grants of the Romanian National Authority for Scientific Research and Innovation, CNCS-UEFISCDI, project number PN-III-P1-1.1-TE-2021-1585 and PN-III-P4-ID-PCE-2020-1847

Antioxidant and cytoprotective effects of *Sorbus aucuparia* L. fruit extract in gentamicin-induced nephrotoxicity on mice renal cells

Mara Aurori¹✉, Daniela Hanganu², Eموke Pall¹,
Mihai Cenariu¹ and Sanda Andrei¹

¹ Faculty of Veterinary Medicine, University of Agricultural Sciences and Veterinary Medicine, Cluj-Napoca, Romania; ² Department of Pharmacology, Faculty of Pharmacy, University of Medicine and Pharmacy "Iuliu Hațieganu", Cluj-Napoca, Romania;
✉ **Corresponding author, E-mail:** mara.aurori@usamvcluj.ro

Introduction: *Sorbus aucuparia* L., also referred to as mountain ash or European rowanberry, has lately been identified as a significant source of several bioactive components, being historically used in the treatment of various ailments. As such, these berries contain great concentrations of organic acids (particularly ascorbic acid), polyphenols (especially phenolic acids - chlorogenic and neochlorogenic acids), carotenoids and microelements. Gentamicin is an antibacterial drug that is frequently utilized in medical facilities due to its extensive range of activity against gram-negative bacteria. It additionally causes unfavorable adverse reactions, such as ototoxicity and nephrotoxicity. Therefore, the aim of this study was to investigate the *in vitro* antioxidant and nephroprotective effects of rowanberries, with the latter potentially leading to the discovery of novel therapeutics for kidney disease.

Materials and methods: Firstly, two types of ethanolic extracts were obtained. They were characterized by employing chromatographic methods. The antioxidant capacity was evaluated using DHPP and FRAP assays. As for cytotoxic activity, primary renal cell cultures were obtained from mouse fetuses' renal tissue, which was further treated using a mixed method including tissue explants and enzymatic treatment. The obtained cell cultures were treated with gentamicin (100 µg/µL), *Sorbus aucuparia* extract in three distinct concentrations (4.8 µg/µL, 10.7 µg/µL and 19.1 µg/µL) and with a combination of both. Furthermore, MTT colorimetric assay and Annexin V-FITC cell apoptosis detection kit were employed to determine the extract's potential cytoprotective effect.

Results: The analysis of the *Sorbus aucuparia* ethanolic extracts revealed that the total phenolic content was 1.003 ± 0.046 mg GAE/mL and the total carotenoid content was 95.68 ± 0.297 µg/g. The antioxidant capacity of *Sorbus*

aucuparia showed a significant activity, with DHPP = 24.51 mg/mL and FRAP = 0.016 μ mol Trolox/mL extract. The MTT and Annexin V-FITC tests revealed that the extract-treated groups had higher cell viability than the antibiotic-treated group at the first two concentrations. Additionally, increased viability was observed in the groups treated with extract and antibiotic, which was comparable to the extract-treated cells. In contrast, a significant decline in cell viability was observed at the highest concentration (19.1 μ g/ μ L) when compared to untreated cells. Moreover, this concentration registered a significant lower viability in extract-treated and extract+antibiotic-treated groups in comparison to cells that received gentamicin alone. These results could be attributed to the extract and gentamicin's additive pro-oxidant effects.

Conclusions: The *Sorbus aucuparia* fruit extract demonstrated a significant *in vitro* antioxidant capacity and, with the exception of the highest dose, it also demonstrated cytoprotective effects in gentamicin-induced stress on mice renal epithelial cells.

The Effect of *Rhizophagus irregularis* on Phenolics and Essential Oil of the *Echinacea purpurea* (L.) Moench

Martin Jakab^{1,2}, Erzsébet Domokos², Csilla Albert³,
Béla Biró-Janka² and Francisc V. Dulf¹

¹ University of Agricultural Sciences and Veterinary Medicine, Faculty of Agriculture, Cluj-Napoca;

² Sapientia Hungarian University of Transylvania, Faculty of Technical and Human Sciences

Târgu Mureş, Târgu Mureş; ³Sapientia Hungarian University of Transylvania,
Faculty of Economics, Socio-Human Sciences and Engineering, Miercurea Ciuc;

 **Corresponding author, E-mail:** jakab.marton@ms.sapientia.ro

Introduction: The majority of studies conducted on *Echinacea purpurea* regarding elicitor (e.g. arbuscular-mycorrhizal fungi – AMF) induction have been carried out *in vitro*, using controlled conditions. The application of elicitors had conducted to elevated levels of various secondary metabolites. The aim of this study was to test the competitive ability of *Rhizophagus irregularis* on different substrates (greenhouse and open field conditions) in the presence of local microorganism communities, in order to induce quantitative and qualitative changes in the active principles of *E. purpurea*.

Materials and methods: Greenhouse and an open field experiment were conducted with *E. purpurea* inoculated with *R. Irregularis* and control plants. In the greenhouse experiment three different soil types and sterile peat were used. HPLC analyses for phenolic compounds were made on dried leaves of *E. purpurea* plants. The dried *herba* was analysed with GC-MS for volatile oil composition.

Results: According to the HPLC analyses six phenolic acids were detected. The two dominant compounds were chicoric and chlorogenic acids. Control plants presented significantly higher values in phenolic content compared to treated plants, on sterile peat and open field stagnic Luviosol in case of caftaric, chlorogenic, caffeic, chicoric acids, and echinacoside. AMF colonization rate favored caftaric, chlorogenic and chicoric acids content on several substrates. The quantitative analyses of the essential oil showed significantly higher yield for potted control plants on stagnic Luviosol. The qualitative analyses revealed 35 constituents, the most abundant were caryophyllene oxide and germacrene D. According to the PCA analyses the essential oil obtained from treated plants contained γ -cadinene and humulene epoxide 2 in higher proportions, while the essential oil of the control plants was abundant in spatulenol and shyobunol.

Conclusions: Observations on AMF effect on root essential oil yield and composition would be of high interest. Further studies with other AMF species in combination with growth-promoting bacteria should be carried out, to assess their competitive behavior with the native microorganisms.

Antioxidant supplementation and its impact on inflammatory and oxidative stress parameters in diet-induced obesity rats

Mihaela Cotul¹✉, Daria-Antonia Dumitraș¹, Alexandra Dreancă¹,
Andrei Paul Ungur¹ and Sanda Andrei¹

¹ Faculty of Veterinary Medicine, University of Agricultural Sciences and Veterinary Medicine, Cluj-Napoca, Romania; ✉ **Corresponding author, E-mail:** mihaela.cotul@usamvcluj.ro

Introduction: Obesity represents a significant public health challenge, associated with the development of various chronic conditions, such as diabetes, cardiovascular disorders, and cancer. In response to this escalating issue, dietary supplements, particularly antioxidants, have gained attention for their potential role in obesity prevention and treatment. Nonetheless, the precise efficacy of these supplements in mitigating or attenuating obesity remains uncertain.

The primary objective of this investigation was to induce obesity in six distinct groups of rats and assess the impact of antioxidant supplementation within two distinct dietary regimens: a normal diet (ND) and a high-fat diet (HFD). Specifically, the diets were supplemented with either plain flaxseed oil or flaxseed oil enriched with powdered antioxidants sourced from *Calendula officinalis* and *Ribes nigrum*.

Materials and methods: In this experimental study, 32 male Sprague-Dawley rats were selected and subjected to an 8-week duration experiment. The experimental animals were divided into six groups and subjected to specific dietary interventions. Three groups received a normal diet (ND), while another three groups were fed a high-fat diet (HFD). Within each diet group, subgroups were further established, with some animals receiving antioxidant powder in flaxseed oil at doses of 200 mg/kg *Calendula officinalis* (CO) and 200 mg/kg *Ribes nigrum* (RN). The administration of the antioxidant powder in flaxseed oil was performed daily via gavage the entire experimental period.

At the end of the study, whole blood and tissue samples were obtained from the rats for the assessment of various markers associated with inflammation (interleukin IL-6 and TNF- α) and oxidative stress (total antioxidant capacity-TAC, catalase activity-CAT, lipids peroxides-LPO, superoxide dismutase-SOD and 8-hydroxy-2'-deoxyguanosine-8-OH-dG). Subsequently, a comparative analysis

was performed to evaluate the differences in these markers between the groups receiving antioxidant supplementation and the non-supplemented control groups.

Results: The consumption of a high-fat diet (HFD) resulted in a substantial elevation in body weight, as indicated by an increased body mass index (BMI) ranging from 0.84 to 0.92. Additionally, the HFD led to a notable accumulation of adipose tissue, reflected by an adiposity index ranging from 2.8% to 3.5%. These changes were accompanied by significantly heightened levels of oxidative stress and inflammation. However, the administration of antioxidants demonstrated a significant mitigating effect on the HFD-induced body weight gain, reducing it by 14% along with a decrease in BMI (0.3 g/cm^2). Furthermore, the antioxidant powder exhibited favorable effects on the inflammatory status, manifesting a significant reduction in inflammation. Moreover, it exerted a notable antioxidant effect by modulating the activity of catalase (CAT) and reducing the levels of lipid peroxidation (LPO) and 8-hydroxy-2'-deoxyguanosine (8-OH-dG).

Conclusions: The findings of this investigation have offered valuable elucidation regarding the prospective role of antioxidant supplementation in the prevention or mitigation of obesity.

The impact of silica nanoparticles (SiNPs) on some biochemical parameters in *Silybum marianum* seedlings

Lucia-Florina Popovici¹✉ and Lăcrămioara-Anca Oprică²

¹Angelmed Laboratory, 700127 Iasi, Romania; ²Faculty of Biology, Alexandru Ioan Cuza University of Iasi, Iasi, Romania; ✉Corresponding author, E-mail: lucia.florina97@yahoo.ro

Introduction: Currently, agricultural productivity is declining due to the negative effects of climate change, rising global temperatures and increased environmental stress. Increased soil salinity is known to be one of the most devastating processes leading to a drop in agricultural productivity, causing major reductions in cultivated area and limiting the productivity and quality of crop plants, due to increased osmotic stress, nutritional disorders and toxicity. Therefore, finding methods to combat salt stress in plants is very important. One of the most promising methods capable of neutralizing the harmful effects of soil salinity is the creation, selection and use of nanoparticles (NPs) with strong antioxidant effects. In this sense, numerous studies suggest that Silicon Nanoparticles (SiNPs) can penetrate into plant cells and influence their metabolic activities.

Materials and methods: For this study, we used 60 seeds of *Silybum marianum* (Secuieni Agricultural Research and Development Station, Neamț, Romania) which were divided into 6 experimental groups of ten seeds each (Control; Control + 50 mM NaCl; Control + 100 mM NaCl; SiNPs; SiNPs + 50 mM NaCl; SiNPs + 100 mM NaCl). Immediately after applying the first treatment, their growth was monitored for 22 days. After that, the seedlings were homogenized and processed to determine the activity of some biochemical parameters like Superoxide dismutase (SOD), Catalase (CAT), Peroxidase (POD), the Malonaldehyde level (MDA), as well as the content of assimilatory pigments in the leaves.

Results: The results of our study indicate that salt stress in concentrations of 50 mM and 100 mM, together with SiNPs, intensifies the antioxidant defense system in *S. marianum* seedlings, compared to variants treated only with NaCl. In contrast, the treatment with SiNPs managed to successfully reduce the oxidative damage of NaCl treatment on *S. marianum*, by restoring the activity of antioxidant enzymes (SOD, CAT, POD) and by down-regulating the level of MDA. Also, the total amount of assimilatory pigments (chlorophyll a, chlorophyll b and carotenes) from the leaves, at the thistle,

showed a notable decrease, under the action of the applied treatments, which seem to inhibit their biosynthesis.

Conclusions: The changes in the physiological and biochemical parameters obtained by determinations at the foliar level, of the *S. marianum* species, constitute an important starting point for the standardization of some toxicity tests in the evaluation of the SiNPs treatment of plants. Further study is needed to elucidate how SiNPs initiate these effects.

Acknowledgements: This work was funded from bilateral scientific project Romania - Belarus competition AR-FRBCF-2020-2021 (National Academy of Sciences of the Republic of Belarus and Foundation of the Republic of Belarus for Fundamental Research)

The GC-MS analysis of some volatile oils and the evaluation of their antibacterial properties against *S. aureus* and *E. coli* bacterial strains

Roberta Tripon^{1,3}, Cristina Gașpar², Dorin Camen¹, Mihaela Enea^{1,3},
Ramona Românu^{1,3} and Camelia Tulcan^{1,3}

¹Faculty of Engineering and Applied Technologies, University of Life Sciences "King Michael I" from Timișoara; ²Faculty of Veterinary Medicine, University of Life Sciences "King Michael I" from Timișoara; ³ULST Research Institute for Biosafety and Bioengineering (ICBB) Timișoara;

 **Corresponding author, E-mail:** roberta.tripon@usvt.ro

Introduction: During the last decade, the use of natural products for their pharmacological properties has gained great attention worldwide. This increased interest in some phytoproducts is correlated especially with their ability to limit antibiotic resistance, being a great alternative to some conventional antibacterial products. In this context, this study aimed to analyze by GC-MS the chemical composition of some volatile oils and to evaluate their antibacterial potential against two bacterial strains of great interest, *Escherichia coli* DK0336 and *Staphylococcus aureus* CP8150.

Materials and methods: The tested volatile oils were represented by thyme volatile oils (*Thymus sepyllum* and *Thymus vulgaris*) and grapefruit volatile oils (*Citrus × paradisi*), all of which were purchased from authorized bio-producers from Romania. For the identification of the biologically active volatile compounds in the composition of the oils, GC-MS chromatographic analysis was carried out, using a 7890A gas chromatograph (Agilent Technologies, USA) coupled with a triple quadrupole mass detector, 5975C (Agilent Technologies, USA) and equipped with a HP-5MS capillary column (30m × 0.25mm × 0.25m). The determination of the inhibition percent (IP%) of these oils on the *E. coli* DK0336 strain, respectively *S. aureus* CP8150 strain, was carried out by the broth microdilution method in microtitre plates. This method is one of the most widely used techniques for assessing the susceptibility of bacteria to certain products with bacteriostatic and/or bactericidal effects.

Results: *T. vulgaris* and *T. sepyllum* volatile oils demonstrated a remarkable effect on the two bacterial strains (*S. aureus* CP8150 and *E. coli* DK0336), indicating inhibition percentages (IP%) of up to 99.36%. These high values of the IP (%) were manifested especially at small volumes of oil (0.5 and 1.0 μL). Regarding the *Citrus × paradisi* oils, however, the inhibition percentages

did not exceed the value of 45.42%. At higher volumes (1.5 and 2.0 μL) a potentiation of bacterial development was observed on the *S. aureus* CP8150 bacterial strain.

Conclusions: The tested volatile oils showed important values of the inhibition percent (PI%), especially at small volumes. Due to the presence of terpenic structures such as thymol and carvacrol in their composition, *T. vulgaris* oils demonstrated the highest PI (%) values, respectively 99.36% for the *E. coli* strain and 99.31% for the *S. aureus* strain.

Acknowledgments: This research was conducted with technical support from the Antioxidant Systems Research Laboratory (A1c) team, part of the Institute for Biosafety and Bioengineering Research (ICBB), University of Life Sciences "King Mihai I" from Timisoara as well as the Veterinary Hygiene and Environmental Protection laboratory research team, Faculty of Veterinary Medicine, ULST Timișoara.

Polyphenols and antimicrobial activity in glycerol *Sanguisorba officinalis* L. and *Sanguisorba minor* Scop. Roots extracts

Alexandra-Cristina Tocai (Moțoc)^{1✉} and Simona Ioana Vicas²

¹ Doctoral School of Biomedical Science, University of Oradea, Oradea, Romania;

² Faculty of Environmental Protection, University of Oradea, Oradea, Romania;

✉ Corresponding author, E-mail: tocai.alexandra@gmail.com

Introduction: *Sanguisorba officinalis* L. and *Sanguisorba minor* Scop. are wild edibles species belonging to the Rosaceae family used frequently in traditional medicine but even now they are being researched more and more. From our previous study, where we characterized and compared the ethanolic extracts of *Sanguisorba* species to highlight which species is more valuable according to the phenolic profile and antimicrobial activity we wanted to find an alternative method, more environmentally friendly for the polyphenols extraction. The main aim of this research was to investigate if glycerol is an efficient solvent for extraction polyphenols from the roots of *S. officinalis* L. and *S. minor* Scop. The antibacterial activity of glycerol extracts of medicinal plants was also investigated.

Materials and methods:

The selected medicinal plants were collected from Bihor and Cluj country, Romania. *S. officinalis* L. roots were collected in August 2021 from Săcădat village, Bihor county and *S. minor* Scop. Roots were collected in May 2021 from Bucea village, Cluj county. A specimen of each *Sanguisorba* ssp. was kept in the Herbarium of the faculty of Medicine and Pharmacy Oradea, Romania, registered in NYBG Steere Herbarium, under the code: Uop 05 367-*S. minor* Scop. and Uop 05 368- *S. officinalis* L. An alcohol-free extract based on *Sanguisorba officinalis* roots purchased commercially was also investigated.

One gram each of *S. officinalis* and *S. minor* was macerated in a water-glycerol combination (60%) at room temperature for 20 days, with daily shaking for 10 minutes, twice a day, to extract the phenolic compounds. All experiments were conducted in triplicate. The phenolic profile of glycol extracts from the roots of the two medicinal plants, as well as the commercial product, was determined using HPLC-DAD-ESI-MS (ESI⁺). The spectral values were recorded in the 200-600 nm range for all peaks. The chromatograms were recorded at the wavelength $\lambda = 280, 340$ and 520 nm. For MS, full scan ESI

positive ionization mode was used in the following working conditions: capillary voltage 3000 V, temperature 350 °C, nitrogen flow 7 l/min and m/z 120-1200. A variation of the Kirby-Bauer diffusion was used for evaluation of antimicrobial activity against *Staphylococcus aureus*, *Escherichia coli* and *Pseudomonas aeruginosa*.

Results: According to the HPLC analysis, ellagic acid and catechin are the major components of the *Sanguisorba* extracts, with higher amounts detected in the root extract of *S. minor* Scop. In terms of antimicrobial activity, the glycerol extract of *S. minor* Scop. roots shown high antibacterial activity against all tested bacteria, particularly *E. coli*, with an inhibition zone of 12.03 ± 0.35 mm. Glycerin extract from *S. minor* Scop. had the highest polyphenol concentration and antibacterial activity, followed by *S. officinalis* L. glycerin extract, and the commercial product investigated.

Conclusions: The potential of water/glycerol combinations to efficiently extract polyphenols from the roots of *Sanguisorba* species was demonstrated in this study, highlighting the fact that the roots of *S. minor* Scop. are rich in phenolic compounds, and the glyceric extract has an effective antibacterial action against *E. coli*.

In vitro* antioxidant and antigenotoxic potential of *Viscum album* L. subsp. *album

Simona Ioana Vicas¹✉, Vasile Laslo¹, Eva Klezken², Adriana Ramona Memete¹, Tudor Emanuel Fertig^{3,5}, Daciana Silvia Marta^{3,4}

¹ Faculty of Environmental Protection, University of Oradea, Oradea, Romania; ² University of Oradea, Doctoral School of Biomedical Science, Oradea, Romania; ³ Ultrastructural Pathology and Bioimaging Lab, Victor Babeș National Institute of Pathology, Bucharest, Romania; ✉ **Corresponding author, E-mail:** svicas@uoradea.ro

Introduction: Nowadays, the mistletoe (*V. album* L.) continues to attract a lot of interest, particularly for research into the bioactivity of its components. A variety of chemical substances, ranging from small molecules like phenolic acids and flavonoids to proteins with high molecular weights like lectins and viscotoxins, are found in the *V. album*. The greater part of mistletoe research is focused on cancer treatment. Most oncological patients apply *V. album* L. extracts to alleviate symptoms related with the disease and therapy, as well as to improve quality of life. Mistletoe extracts have been shown to have anticancer, pro-apoptotic, anti-proliferative, and immune-modulatory properties. Recent researches have also indicated that the antioxidant capacity of mistletoe extracts is affected by the host tree. The major aim was to emphasize the reduction of genotoxicity caused by hydrogen peroxide in normal human dermal fibroblasts (NHDF). Furthermore, the ability of mistletoe aqueous extract to synthesize selenium nanoparticles (SeNPs) has been highlighted.

Materials and methods: Mistletoe leaves have been collected from apple (*Malus domestica*) (host tree) in May 2022 and characterised in terms of polyphenols content using HPLC-MS-ESI. Antioxidant capacity of mistletoe leaves was evidence by four different methods such as DPPH, FRAP, TEAC and CUPRAC. The characterization of SeNPs was performed by UV-Vis spectrum, and DLS, while morphological details were observed by TEM analysis (Negative-Stain). NHDF and the specific culture kit (Fibro-blast Growth Medium-2 BulletKit) were used for the cell culture treatments. Neutral single cell gel electrophoresis, known as Comet assay, was performed according to Purcarea *et al.* (2022).

Results: Twenty-one compounds have been separated and tentatively assigned based on their retention durations, UV absorption spectrum, m/z values, and major fragments. In mistletoe leaves, hydroxycinnamic acids dominate hydroxybenzoic acids. Chlorogenic acid was the major phenolic acid

in mistletoe leaves (1.413 ± 0.11). Twelve molecules were found from the flavonoids class, from which quercetin derivatives were predominant. Among the four antioxidant methods used, it was evident that mistletoe extract has antioxidant properties. In addition, the synthesis of SeNPs was confirmed by the appearance of red color confirming the reducing ability of mistletoe. The SeNPs showed a maximum absorption at 270 nm and the apparent zeta potential was recorded at a maximum value of -24.5 mV, which indicates that these nanoparticles do not form aggregates in solution leading to a stable dispersion. According to TEM, the spherical shape was confirmed and the diameter of SeNPs was around 130 nm. To highlight the potential of mistletoe extract to reduce genotoxicity induced by hydrogen peroxide, two types of treatments were implemented: one of them was pre-treatment to highlight the possible role of DNA protection before the application of hydrogen peroxide (75 μ M) and another, post-treatment to highlight DNA repair potential. Our results showed a significant reduction in the frequency of DNA damage, quantified by %DNA tail, in cells treated with mistletoe extract (25 and 50 μ g/ml) in both treatment, suggesting a bioantimutagenic behavior of the extracts

Conclusions: Mistletoe is a medicinal plant that has significant health benefits. The ability of the extract to reduce the selenite salt to elemental selenium has been demonstrated in this work for the first time in the literature. The mistletoe's protecting but also repairing impact on DNA from fibroblasts degraded by H₂O₂ exposure opens up novel opportunities to explore the molecular mechanisms underlying these features.

Acknowledgements: This work was funded by the University of Oradea through the grant competition "Excellent scientific research related to the priority fields with the goal of technology transfer: INO-TRANSFER-UO", project number 309/21.12.2021.

Strategy for deorphanizing G-protein coupled receptor 75 using brain extract fractions

Cosmin Trif¹✉ and Sorin Tunaru¹

¹ *Institute of Biochemistry of the Romanian Academy, Romania, Cell Signaling Group;*
✉ *Corresponding author, E-mail: trifcosmin@gmail.com*

Introduction: G-protein coupled receptors (GPCRs) are a large superfamily of transmembrane proteins that convert extracellular stimuli into cellular effects. Given their vast implication in physiological and pathological processes they are targeted by almost a third of FDA approved drugs. G-protein coupled receptor 75 (GPR75) is member of this family with high expression in the retina, brain and pancreas and with implications in metabolic syndrome, diabetes and obesity. Although some studies suggest as endogenous ligands for GPR75, 20-Hydroxyeicosatetraenoic acid (20-HETE) and the chemokine RANTES, the receptor is still considered orphan. Given its expression pattern in human and mouse, we devised it is a good strategy for its deorphanization by using brain extracts.

Materials and methods: The brain extracts were obtained by homogenizing mouse brains in 10 volumes of a solution containing 70% V/V acetone 1 M acetic acid, and 20 mM HCl. The homogenate was then delipidated with diethyl ether. The aqueous phase was loaded into a reverse phase column Waters Sep-Pak C18 20 cc Vac Cartridge and we eluted the fractions using an acetonitrile gradient ranging from 0% to 100%. The fractions and the lipid phase was lyophilized and diluted into HBSS and their biological activity was tested in HEK 293T cells transfected with empty vector or GPR75 and a genetic probe for measuring intracellular calcium and cAMP.

Results: Using our pharmacological approach we could not detect 20-HETE and RANTES as ligands for GPR75. The brain extract fractions contained a good yield of protein ranging from 0.5 mg/ml up to more than 5 mg/ml. Some of this fractions were biological active in calcium and cAMP assays but not selective for GPR75.

Conclusions: In this study we optimized a method for obtaining biological active fractions from mouse brain that can be used to discover novel endogenous ligands for orphan GPCRs like GPR75.

Acknowledgements: EEA-RO-NO-2018-0535" New Generation of Drug Targets for Schizpophrenia (NEXTDRUG)

Interactions between transient receptor potential subfamily ankyrin member 1 (TRPA1) and the epidermal growth factor receptor (EGFR) in glioblastoma

David-Ionuț Băcioiu¹✉, Florentina Piciu¹,
Alina-Ana-Maria Botezatu¹ and Dana Cucu¹

¹Department of Anatomy, Animal Physiology and Biophysics,
Faculty of Biology, University of Bucharest, Bucharest, Romania;

✉Corresponding author, E-mail: bacioiu.david-ionut22@s.bio.unibuc.ro

Introduction: Cancer is one of the leading causes of worldwide mortality, alongside diabetes and cardiovascular diseases. Although not as common as other malignant neoplasms (2-3 cases per 100,000 people), glioblastoma makes up for the relative lack of incidence in its severity. This disease is characterized by a low survival rate upon diagnosis, a favorable switch of microglial genetic mechanisms, as well as upregulation and mutations within key proteins (PDGFR, EGFR, EGFRvIII, PTEN, p53). EGFRvIII, for example, renders a resistant tumoral phenotype, taking into account that EGFRvIII cells promote the growth of neighboring wtEGFR cells in an IL-6, LIF and gp130-dependent mechanism. Transient Receptor Potential (TRP) channels emerge as tumor markers and putative therapeutic targets from this barren landscape. The mammalian TRP channel superfamily encompasses six families with 28 members, translating into 27 proteins and one pseudogene (TRPC2). Among them, TRPA1 stands out as one of the most versatile receptors. The channel's activity can be modulated by a wide range of compounds and stimuli, including Ca²⁺ ions, pro-inflammatory mediators, ROS and RNS, xenobiotics, and temperature. Regarding its *modus operandi* in tumor cells, the channel does not follow a prototypical model, inducing somewhat different effects depending on the cancer subtype. It appears to be involved in lung cancer development, whereas TRPA1 activation in PDAC cell lines reduces motility. Factors like the polymodal character and the ubiquitous expression turn the family of TRP channels into a fertile research topic.

Materials and methods: To fully understand the interaction between EGFRvIII and TRPA1 in the glioblastoma landscape, our research group will resort to a battery of assays. We shall address the functionality of TRPA1 in the U-87MG_WT and U-87MG_EGFRvIII cell lines electrophysiologically, with a series of whole cell patch clamp recordings in the presence of specific agonists

and antagonists (AITC, ROS, and A-967079). Furthermore, the wound healing assay will be used to evaluate cell motility of tumor cells treated with adequate EC50 AITC, ROS, and A-967079 concentrations.

Results: Considering the duality of activated TRPA1 in tumoral subtypes, its role in glioblastoma cell lines must be experimentally addressed first. However, certain clues in the scientific literature point to an anti-tumoral function of TRPA1. It should be observed that both WT and EGFRvIII^{+/+} cells express slower migration patterns in the wound healing assay, with some speculative differences attributable to EGFRvIII. TRPA1 might also become upregulated after ROS stimulation or by still undescribed EGFR/EGFRvIII - TRPA1 interactions, statement which allows for further investigations.

Conclusions: Our theories, if proven true, hint at the involvement of TRPA1 in glioblastoma cell apoptosis. Given that TRPA1 activation reduces glioblastoma cell motility, pharmacological targeting of TRPA1 could become a noteworthy option.

Molecular aggregation pathway of cataract-associated γ D-crystallin p23T congenital defect

Elena Matei¹✉, Alina Filip², Călin Gabriel Floare¹,
Adrian Pirnau¹, and Mihaela Mic¹

¹ National Institute for Research and Development of Isotopic and Molecular Technologies, Cluj-Napoca, Romania; ² Enzymology and Applied Biocatalysis Research Centre, Faculty of Chemistry and Chemical Engineering, Babeș-Bolyai University of Cluj-Napoca, Cluj-Napoca, Romania; ✉ **Corresponding author, E-mail:** elena.matei@itim-cj.ro

Introduction: Cataract, the most common cause of blindness, which represents a disturbance of the delicate balance required for transparency, either because of age-related degenerative modifications, or genetic mutations, causing abnormal aggregation of eye lens crystalline proteins. In order to understand how structural changes in the P23T variant of human γ D-Crystallin ($h\gamma$ D-Crys) lead to congenital cataract, we carry out comparative protein-protein interaction studies between wild-type $h\gamma$ D-Crys, and $h\gamma$ D-P23T, with small heat shock chaperone α B-Crys, by solution NMR. We plan to get new insights into the structure of $h\gamma$ D-P23T aggregates, and its interaction mechanism inside the eye lens, with potential interference in protein aggregation by small molecules. These valuable findings will provide alternatives to reduce the severity, delay, or treat congenital cataract.

Materials and methods: The synthetic DNA encoding the wild-type $h\gamma$ D-Crys, the $h\gamma$ D-p23T mutant, and α B-Crys were individually inserted into the pET-14b expression vector, and transformed into BL21(DE3) cells. Proteins were expressed either in LB culture medium, or modified M9 medium for isotopically ¹⁵N-labeled $h\gamma$ D-Crys, the $h\gamma$ D-p23T mutant, and α B-Crys. Proteins were purified by ion exchange, and size-exclusion chromatography using Q-FF, SP-FF, and Superdex columns, attached to the FPLC-Åkta system. For protein-protein interaction study we used ¹H-¹⁵N HSQC NMR pulse sequence.

Results: For studying $h\gamma$ D/ $h\gamma$ D-p23T: α B-Crys complex, we monitor the chemical shift perturbations in the ¹H-¹⁵N HSQC spectra of ¹⁵N-labeled $h\gamma$ D-Crys/ $h\gamma$ D-p23T in complex with unlabeled α B-Crys. The superposition of ¹⁵N- $h\gamma$ D-p23T HSQC spectra in the absence and presence of unlabeled α B-Crys, provides the first quality control of the complex, in addition to exchange regime, and binding interface. The spectral changes on HSQC spectra of ¹⁵N- $h\gamma$ D-Crys/ $h\gamma$ D-p23T upon addition of unlabeled α B-Crys, does not indicate a visible

perturbation of the chemical shifts, only a reduction in the intensity of the NH signals is observed, as a result of the broadening effect of the resonance lines. This fact indicates a non-specific interaction between h γ D-Crys, respectively h γ D-p23T, with the chaperone protein α B-Crys.

Conclusions: Therefore, the soluble (monomeric) fraction of the h γ D-p23T mutant interacts non-specifically with the chaperone protein α B-Crys, in a manner similar to the wild-type h γ D-Crys, suggesting only a transient interaction. This is the first NMR study to highlight the protective role of the chaperone protein α B-Crys, ensuring proper three-dimensional folding of partner proteins (crystallins) present in the (human) eye lens. However, this non-specific interaction is not sufficient to prevent the aggregation process of the h γ D-p23T mutant, under physiological conditions. Apparently, the macromolecular self-association process of the h γ D-p23T mutant is a pronounced one, so that it manages to escape from the supervision of the chaperone α B-Crys, causing cataract.

Acknowledgements: This work was funded by UEFISCDI through the project PN-III-P4-PCE-2021-0316.

Modelling of MHC-I Peptide Loading Complex

Floriana Sibel Bectas^{1✉}, Teodor Asvadur Șulea¹,
Laurentiu Spiridon¹ and Andrei J. Petrescu¹

¹*Department of Bioinformatics and Structural Biochemistry,
Institute of Biochemistry of the Romanian Academy, Bucharest, Romania;*

[✉]*Corresponding author, E-mail: floriana.bectas@biochim.ro*

Introduction: The major histocompatibility complex class-I (MHC-I) peptide-loading complex (PLC) is a critical multi-protein complex of the immune system composed of no less than 5 proteins forming one module that dimerize into the endoplasmic reticulum. Each of the two modules of the PLC complex consists of five components: Tapasin, Calreticulin, ERp57 and the two proteins, namely Human Leukocyte Antigen (HLA) and β 2-microglobulin that together form the Major Histocompatibility Complex Class-I (MHC-I). In this dimeric form the PLC controls the selection and loading of peptides onto MHC-I. After loading, the stable peptide-MHC-I complex is released and leaves the ER through the secretory pathway to reach the cell surface for antigen presentation. Here it is recognized by killer T cells which ensures the detection of infected or mutated cells by the immune system. The process flow that takes place in the PLC during loading is barely known due to the complexity and size of this system and its specific dynamics. However some breakthroughs have been recently made by Cryo-EM which resulted in several low-resolution structural descriptions of this molecular machine. Based on these templates, we present a model of the PLC starting from the HLA-B sequence (IMGT/HLA Acc No: HLA00132) in order to gain a more precise view of the HLA-B based PLC complex and investigate the dynamic events that take place during the loading of Tyrosinase antigenic peptide 280-EEYNHQSL-288.

Materials and methods: The structure of one PLC module was built by homology modelling with Modeller. This module was then duplicated and the two objects were assembled using constrained docking based on the experimentally identified contacts as joining links between the two monomers in order to generate the overall PLC heterodimer. Two N-glycans were further added using Glycopack (Paduraru *et al.* 2006): (1) the immature high-mannose G1M9 oligosaccharide added to N86 (MHC-I) and (2) a high-mannose glycan linked to N233 (Tapasin). The system was subjected to both implicit and explicit solvent molecule simulations. Implicit solvent was used for Hamiltonian Monte Carlo

simulations coupled with Gibbs sampling implemented in the Robosample software package. For the explicit solvent simulations the transmembrane helices were anchored into a POPC membrane and the system was solvated and immersed in a water box with 15Å padding and a concentration of 0.15M Na⁺/Cl⁻.

Results: In order to gain insights into the molecular interactions within the PLC structural model, each protein was independently subjected to electrostatic potential calculations using APBS. Subsequently, the calculated potential was mapped onto their surfaces to detect potential enthalpic contributions to their binding affinity. Furthermore, an assessment of putative hydrophobic patches at their interfaces was conducted to evaluate possible additional contributions to interaction stability.

Following the molecular simulation, an analysis of Root Mean Square Deviation (RMSD) and Root Mean Square Fluctuation (RMSF) was conducted to evaluate the stability of the system and identify potential hotspots on the interaction surfaces. Based on the aforementioned analysis, a ranking was established to identify and prioritize the significant contacts observed at the protein contact surfaces.

Conclusions: Comprehending the dynamic nature of the PLC complex holds paramount importance in gaining insights into its functional behavior and potential conformational changes occurring during the peptide loading process. This understanding plays a vital role in elucidating the complex's structure, dynamics, and functionality, particularly within the context of peptide loading onto Major Histocompatibility Complex (MHC-I) molecules.

Acknowledgements: This work was funded from: PNCIII P4, code PN-III-P4-ID-PCE-2020-2444, acronym CYBORG.

High-throughput screening to identify inhibitors of RAGE-S100B interaction

Ioana Popa¹✉, Carmen Tanase¹, Bernhard Ellinger²,
Jeanette Reinshagen² and Philip Gribbon²

¹ Institute of Biochemistry of the Romanian Academy, Bucharest, Romania; ² Fraunhofer Institute for Translational Medicine and Pharmacology ITMP ScreeningPort, Germany;

✉ **Corresponding author, E-mail:** ipopa@biochim.ro

Introduction: Receptor RAGE is an immunoglobulin-like transmembrane protein. Discrete sites on RAGE extracellular domains (V, C1 and C2 domains) bind various ligands, among which are advanced glycation end products, members of the S100 protein family, high mobility group box protein 1, amyloid β oligomers and fibrils, complement component C1q. Enhanced RAGE signalling pathways leading to pro-inflammatory and pro-oxidative cellular responses are induced by high concentrations of ligands and have been associated with pathological modifications in diabetes, peripheral neuropathy, cardiovascular diseases, chronic inflammation, cancer and neurodegeneration. Therefore, RAGE has been proposed as a promising disease modifying drug target for these pathologies. Growing evidences point to a role for RAGE and its ligand S100B in the pathophysiology of the brain, as active participants in the cellular processes which can have neurodegenerative effects. So far, screening campaigns to identify RAGE inhibitors focused on its interaction with amyloid β . Giving the prominent role of S100B as a cytokine in the nervous system, we initiated a high-throughput screen (HTS) to target S100B binding to RAGE.

Materials and methods: A time-resolved fluorescence resonance energy transfer (TR-FRET) assay was employed to measure RAGE-S100B interaction. The TR-FRET assay consisted of a His tagged VC1 fragment of RAGE coupled with anti-His antibodies labeled with Terbium as FRET donor and an FITC-labeled S100B protein as acceptor. Optimization of the TR-FRET reaction was done to select the most suitable assay set-up which was further used for the screening of a small commercial library of natural compounds (137 natural products), and for the HTS of an EU-OPENSSCREEN chemical library (~100,000 compounds).

Results: The proteins used in the study (VC1-His, S100B, His-S100B) were expressed in bacteria and purified by affinity chromatography. Free amines of S100B and His-S100B were labeled with FITC. The buffer composition and the concentration of binding proteins and of the Terbium-labeled antibodies were optimized for both 96 well and 384 well microplate platforms. The affinity of

S100B-FITC/ VC1-His binding was determined from the titration curves. The minimal concentrations that gave a signal-to-background ratio > 3 and a Z' factor > 0.7 were further used in competition experiments. Unlabeled-S100B, and an antagonistic RAGE peptide, but not BSA competed for the binding of S100B-FITC to VC1-His, proving that the assay set-up was specific for the interaction measurement. Our method was further tested in a small screen of a natural product and we identified three putative candidate inhibitors of RAGE/S100B interaction. The transfer of technology and further optimization of the protocol were done at the EU-OPENSREEN site. The HTS was performed using $10\mu\text{M}$ of the tested compounds, and led to the initial identification of 875 hits. Of these, the active hits were validated in an additional confirmation run and in the counter-screen with His-S100B-FITC. Dose-response curves for all the identified compounds were profiled.

Conclusions: We developed a specific, robust and fast fluorescence-based method suitable for HTS which allowed the identification of small molecule candidates as new inhibitors of RAGE/S100B interaction. These compounds will be further tested in a relevant cell culture model for RAGE activation.

Acknowledgements: This work was funded from EU-OPENSREEN Small Molecules Screening Call (PID 9521/2019)

RP-HPLC studies on chiral separations of racemic nonapeptides sulfoxides

Lucian-Mihai Stănescu¹✉, Corina Aramă¹,
Stefana Petrescu² and Cristian V.A. Munteanu³

¹ University of Medicine and Pharmacy, Carol Davila, Faculty of Pharmacy, Bucharest, Romania;

² Department of Molecular Cell Biology, Institute of Biochemistry of the Romanian Academy (IBRA), Bucharest, Romania; ³ Department of Bioinformatics and Structural Biochemistry,

Institute of Biochemistry of the Romanian Academy (IBRA), Bucharest, Romania;

✉ **Corresponding author, E-mail:** mihai.stanescu@umfcd.ro

Introduction: The asymmetry is an intrinsic property of life. The biogenic molecules, with asymmetric carbon, the peptides and the proteins consist of mostly L-amino acids; only few contain D-amino acids in the structure. A particular example is related to the asymmetric sulphur atom, for peptides oxidised at methionine that form racemic sulfoxides with different biological properties comparing to unoxidised ones at methionine. Previous studies reported chromatographic chiral separation for racemic R and S FMOC-L-methionine sulfoxide by supercritical fluid chromatography and for crosslinked cysteine sulfoxide peptides, but not for underivatized peptides as is the case in this study. The aim of our study is to develop and validate a RP-HPLC enantioseparation method for the racemic mixture of the oxidised YM(Ox)DGTM(Ox)SQV, a linear nonapeptide containing two sulfoxide chiral centres, and to obtain enantiomeric pure fractions for further biological investigations.

Materials and methods: The analyte - the racemic peptide YM(Ox)DGTM(Ox)SQV oxidised at both methionines, (noted M(Ox)) was obtained by chemical synthesis. A JASCO HPLC equipped with a quaternary pump PU-2089 plus and a circularly dichroism detector CD-2095 plus was used for all the chromatographic experiments. The stationary phases used in the investigations of chiral separations were Lux i-Cellulose 5, Lux Cellulose 4 and Pirkle Covalent (R,R) Whelk O-1. The mobile phases contained high percent of water and the organic solvents were acetonitrile, methanol, and isopropanol. The modifiers selected were CF₃COOH and HCOOH as usually used for peptides separation in reversed-phase liquid chromatography. The experimental parameters were optimised to obtain the highest enantioselectivity.

Results: The chiral discrimination varies, depending on the stationary phase type, the organic solvent and the concentration of acid modifier. A partial separation of two of the 4 diastereomers was obtained with the stationary phase Lux Cellulose 4.

Conclusions: The obtained results can be optimised in order to collect the fraction of each enantiomers and then to test the potential use in therapeutics.

Acknowledgements: This work received financial support through the Project of Institutional Development EURO-MEDEx –Contract 33 PFE/2021

The first complex of cobalamin with an organic peroxide

Maria Lehene¹✉, Radu Silaghi-Dumitrescu¹

¹Department of Chemistry, Babeș-Bolyai University, Cluj-Napoca, Romania;

✉Corresponding author, E-mail: maria.lehene@ubbcluj.ro

Introduction: Until recently, the reactivity of cobalamin with oxidizing agents has been confined to processes where, especially with strong oxidizing agents, the corrin ring is covalently modified by oxygenation or halogenation, or where Co(I) or Co(II) are oxidized to Co(III) in an outer-sphere manner. Aqua(III)cobalamin reacts m-chloroperoxybenzoic acid (MCPBA) to form a distinct and stable complex.

Materials and methods: UV-vis spectra were performed on a Cary 50 UV-vis spectrophotometer (Varian, Inc., Foster City, CA, USA). Stopped-flow spectra were collected on a Biologic SFM-300 system equipped with three syringes and sequential mixing, with a high-speed diode array detector. The NMR spectra were recorded at 22°C unless otherwise stated, after diluting the sample with D₂O (1:1 volume ratio), on a 400 MHz Bruker instrument. Raman spectra were measured at 22°C on a Renishaw inVia Raman spectrometer coupled with a Leica microscope. For DFT calculations, the Gaussian09 software package¹⁷ was employed following the methodology previously tested and described for related Cbl complexes.

Results: Upon reaction with MCPBA the UV-vis spectrum of aquacob(III)alamin (H₂OCbl⁺) undergoes bathochromic shifts reminiscent of the hydroperoxocob(III)alamin adduct. Isosbestic points at 461 nm, 340 and 367 nm suggest formation of a single new product, which can in principle be assigned as a peroxyacid(MCPBA)-Cbl(III) complex analogous to the previously-reported cobalamin(III)-hydroperoxy. complex.

Conclusions: To conclude, Cbl(III) forms a relatively stable peroxyacid complex with deprotonated m-chloroperoxybenzoic acid, with distinct UV-vis and ¹H-NMR signatures. By contrast, tBuOOH does not appear to be able to form a peroxy complex with Cbl(III). These findings suggest that the peroxide coordination chemistry of cobalamin does extend beyond simply hydrogen peroxide,⁵ but that not all peroxy compounds should be expected to bind to Cbl(III).

Synthesis, degradation and trafficking processes of the GPR75 receptor

Ramona M. Tecucianu^{1✉}, Sorin Tunaru² and Ștefana M. Petrescu³

¹ Institute of Biochemistry of the Romanian Academy, Bucharest, Romania;

²Institute of Biochemistry of the Romanian Academy, Bucharest, Romania; ³Institute of Biochemistry of the Romanian Academy, Bucharest, Romania;

✉ *Corresponding author, E-mail: teqram2605@yahoo.com*

Introduction: G Protein-Coupled Receptor 75 is a receptor from the GPCR family, which represents the largest family of membrane proteins and the richest source of targets for the pharmaceutical industry. Recent studies have suggested that GPR75 has extremely high potential to be a drug target for diseases such as metabolic syndrome, obesity, dyslipidemia, diabetes, cardiovascular disease, and cerebrovascular disease. Over time, several molecules such as RANTES (Regulated upon Activation, Normal T Cell Expressed and Presumably Secreted)/CCL5 (C-C Motif Chemokine Ligand 5) and 20-HETE (20-Hydroxyeicosatetraenoic acid) have been proposed as GPR75 receptor ligands. However, the Nomenclature and Standards Committee of the International Union of Basic and Clinical Pharmacology (NC-IUPHAR) continues to classify GPR75 as an orphan receptor. One of the most interesting finding related to GPR75 is that certain truncated variants of GPR75 (especially the truncated form at Gln234 of GPR75) were associated with a 1.8 kg/m² lower body mass index (BMI), a higher body weight 5.3 kg less and 54% less chance of obesity in heterozygous carriers. GPR75 might be involved in insulin secretion, potentiating secretion and preventing glucotoxicity-induced beta cell dysfunction. So, we set out to study the processes of synthesis, trafficking and degradation of the GPR75 receptor and to investigate its role in insulin secretion.

Materials and methods: Firstly, the cellular localization of the GPR75 receptor was determined by an immunofluorescence experiment. In order to determine if the GPR75 receptor is glycosylated digestion with Endo H and PNGase F was performed. Then, the GPR75 receptor half-life was established by a cycloheximide chase assay. Furthermore, the degradation pathways of the GPR75 receptor were investigated by treatment with lysosomal/proteasomal inhibitors. Finally, the role of the GPR75 receptor in insulin secretion was explored through ELISA and Western Blotting techniques.

Results: The fluorescence microscope images revealed that the GPR75 receptor is predominantly present at the plasma membrane, but is also present in intracellular compartments. Treatment with Endo H and PNGase F of Hek293T cells transfected with GPR75 showed that most of the GPR75 receptor is glycosylated and transported to its final destination, while some remains retained in the ER. Treatment with cycloheximide led to the determination of the half-life of the GPR75 receptor, which is 4 hours. Moreover, it has been confirmed that the GPR75 receptor is degraded by the lysosomal pathway, but also by the proteasomal pathway. In addition, a decrease in the high-mannose form of GPR75 and an increase in the peptide form of GPR75 were observed with MG132 treatment. Regarding the role of GPR75 in insulin secretion, the results of the glucose stimulation experiments showed that in the case of silencing the GPR75 receptor there is an increase in the expression and secretion of proinsulin, respectively insulin.

Conclusions: This research investigated the processes of synthesis, trafficking and degradation of the GPR75 receptor and its role in insulin secretion. Future studies are needed to better understand the trafficking of the GPR75 receptor, such as identifying the cell organelles in which the receptor is present, as well as studying receptor internalization and recycling.

Acknowledgements: This work was funded from “EEA-RO-NO-2018-0535 New Generation of Drug Targets for Schizophrenia (NEXTDRUG)” project

Study on the interactions between icaricide II and whey protein concentrate

Róbert Szabó¹✉, Csaba Pál Rácz² and Francisc Vasile Dulf¹

¹Department of Environmental and Plant Protection, University of Agricultural Sciences and Veterinary Medicine Cluj-Napoca, Cluj-Napoca, Romania; ²Faculty of Chemistry and Chemical Engineering, Babeș-Bolyai University of Cluj-Napoca, Cluj-Napoca, Romania;

✉Corresponding author, E-mail: robert.szabo@student.usamvcluj.ro

Introduction: In the realm of health and wellness, the quest for natural compounds with significant health-promoting properties is a constant endeavor. Icariside II (ICS), derived from the *Herba Epimedii*, has emerged as a compound of great importance for health promotion. With its diverse range of benefits and potential implications for various physiological processes, such as cardiovascular diseases, osteoporosis, or sexual dysfunction. Icariside II is known to have relatively low bioavailability, meaning that it is not easily absorbed and utilized by the body when ingested. The cause is that ICS is not highly soluble in water, which hinders its absorption in the gastrointestinal tract. Low solubility limits its ability to dissolve and be transported into the bloodstream for systemic distribution. To overcome the challenges associated with the poor bioavailability of Icariside II, recent studies have explored various strategies. These include the use of drug delivery systems, such as nanoparticles or micelles, to enhance solubility and protect the compound from rapid metabolism. In our previous studies we have formed icaricide II and whey protein concentrate (WPC) complexes, with the goal of achieving a higher water solubility, consequently significantly increase the bioavailability of ICS. This paper focuses on exploring binding mechanism of ICS-WPC complex.

Materials and methods: A pure batch of icaricide II was sourced from Xi'an Day Natural Inc. (China). Our whey protein concentrate (80%) was purchased from Foodcom S.A. (Warsaw, Poland). All the other solvents used had analytical grade purity. All other reagents were of analytical grade.

The binding mechanism of the above-mentioned complexes was studied by X-ray powder diffraction, Fourier-transform infrared spectroscopy, and Differential scanning calorimetry and Molecular docking.

Results: In order to analyze the thermal profile of the ICS, WPC, and ICS-WPC physical mixtures and complexes, a Differential Scanning Calorimeter (DSC) was employed. From the DSC curves of the physical mixture the endothermic peak of the ICS can be spotted, while in the case of the complex

this is not present. This indicates the success of the formation of ICS-WPC complexes. These findings were backed up with the XRD measurements, where similarly to the DSC, the intense peaks of ICS have disappeared in the complex. The difference between the physical mixture of ICS-WPC and the complex can be observed from the FTIR spectra. In this case between the ICS-WPC complex and the physical mixture a significant difference in the width of their peak in the 3600-3300 cm^{-1} can be observed. The peak in the case of the complexes are wider, meaning hydrogen bonds were formed. With the means of the molecular docking the interactions between the icariside II and β -lactoglobulin were investigated. As result the conformation with the lowest free energy was considered. This showed that three H-bonds were formed between the ICS and the protein, specifically the PRO-38 and LYS-69 amino acid residues. These are consistent with the results of FTIR measurements.

Conclusions: Measurements of XRD and DSC confirmed the formation of amorphous ICS-WPC complexes. The results of the FTIR and molecular docking showed evidence for the existence of H-bonds between the ICS and protein. Consequently, the formation of ICS-WPC complexes can be considered as a viable solution for increasing the bioavailability of the icariside II.

Acknowledgements: This work was supported by the Collegium Talentum Programme of Hungary

Population dynamics of *Euphyllura olivina* Costa, 1857 (Psyllidae: Hemiptera) in olive trees in the semi-arid region of Djelfa (Algeria)

Nassima Chaabane^{1,2}, Smail Chafaa^{3,4}✉, Frah Naama^{1,2},
Yassine Noudjem⁵ and Fateh Mimeche⁶

¹Department of Agronomy, Institute of Veterinary and Agronomic Sciences University of Batna 1, Batna, Algeria; ²Laboratory Improvement of Agricultural Production and Resource Protection in Arid Zones, University of Batna 1, Batna, Algeria; ³Department of Ecology and Environment, University of Batna 2, Batna, Algeria; ⁴Laboratory of Cellular and Molecular Physiotoxicology-Biomolecules, Faculty of Science of Nature and Life, Department of Biology of Organisms, University of Batna 2, Batna, Algeria; ⁵Yassine Noudjem, Department of Natural and Life Sciences, University of M'Sila, M'Sila, Algeria; ⁶Department of Agricultural Sciences, University of M'Sila, M'Sila, Algeria; ✉ **Corresponding author: E-mail: s.chafaa@univ-batna2.dz**

Article history: Received: 16 March 2023; Revised: 14 December 2023;
Accepted: 15 December 2023; Available online: 28 December 2023.

©2023 Studia UBB Biologia. Published by Babeş-Bolyai University.



This work is licensed under a [Creative Commons Attribution-NonCommercial-NoDerivatives 4.0 International License](https://creativecommons.org/licenses/by-nc-nd/4.0/).

Abstract. We studied the population dynamics of the olive psyllid *Euphyllura olivina* Costa, 1857 in a semi-arid region (Djelfa, central Algeria) during a year, from December 2017 to November 2018. The visual control approach and the striking method were used to monitor the different stages of this pest. The species had two generations per year: a spring generation from March to June and a fall generation from September to November. The first generation of eggs is laid in March and continues through May. The second generation begins in late August and early September and continues through November. The statistical study of the impact of the researched climatic factors (minimum, maximum, and average temperatures; precipitation and frost) on the various stages differs from one stage to the next.

Keywords: *Euphyllura olivina*, population dynamics, *Olea europaea*, climatic factors, Algeria.

Introduction

Olive cultivation is gradually spreading throughout the world. Several non-Mediterranean countries have developed and tended to this crop in specific regions of their territory in recent years. From the Americas (California, Mexico, Brazil, Argentina, and Chile) to Australia and China, as well as Japan and South Africa, olive-growing worldwide is estimated to cover 8,600,000 hectares-95% of which are located in the Mediterranean basin (Chafaa, 2013).

Average production is 10 million tons a year; of which 92% is dedicated to oil extraction whilst the rest goes for table consumption (Zouiten *et al.*, 2001). Mediterranean countries constitute more than 95% of olive oil production and 90% of its consumption (FAO, 2003).

Recently, countries south of the Mediterranean have showed a significant interest in boosting their olive producing industry through improved yielding techniques.

In Tunisia, olive cultivation has a critical socioeconomic role. It covers an area of about 1.7 million hectares (one third of the total of fertile lands) with a population of 67 million trees, (Dibou *et al.*, 2010). In Morocco, constituting 55% of the entirety of trees, the olive tree occupies a central role (MADRPM, 2008). The culture of olive growing occupies a vital and privileged status in Algerian agriculture, with the yield obtained during the last two years (2009-2010) amounting to 13.1 quintals per hectare for all varieties. Furthermore, olive groves cover an area of 178,000 hectares with a production of 300,000 tons per year (Mendil, 2009). The wilaya of Djelfa experienced, for some years, a tremendous rise in olive growing-with olive growing areas going from 150 ha in 2000 to 11000 ha in 2015) (DSA, 2016). Algerian olive growing is characterized by aging trees and / or a lack care for the majority of plantations. This renders the latter vulnerable to alternation-related issues and diseases. We cite the *Verticillium* (*Verticillum dahliae*), Tuberculosis (*Pseudomonassa vastanoi*). On a similar note, the devastating species that tend to lay havoc on olive wood, foliage, flowers and fruits are as follows: the Otiorhynchus (*Otiorhynchus cribricollis*: Curculionidae: Coleoptera), the Moth (*Praysoleae*; Plutellidae: Lepidoptera), the Olive Psyllid (*Euphyllura olivina*: Psyllidae: Hemiptera), the Olive Fly (*Bactrocera oleae*: Tephritidae: Diptera) and the Purple Scale (*Parlatoria oleae*: Diaspididae: Hemiptera) (Arambourg, 1986; Biche, 1987; Biche, 1988; Zerkhefaou, 1988; Jardak and Ksantini, 1996;11;Chafaa *et al.*, 2013; Chafaa *et al.*, 2017).

E. olivina is a pest found in all olive-growing countries. It preys on new stems and flower clusters. According to Chermiti (1992), an infestation rate of 5 larvae per flower cluster causes a 32% fall of inflorescences and a loss of 46 fruits per 100 clusters. Tajnari (1992) estimated that with a density of 30 larvae/flower cluster, production is entirely compromised. This particular

species was first recorded by Costa in 1839 as *Thrips olivina* (Zouiten *et al.*, 2001). Following that, Balachowsky and Mensil (1935) discovered this species on Phyllirea. Arambourg (1985) reported, on the other hand, that *E. olivina* is closely linked to olive trees. However, *Euphyllura phyllirea*, a species extremely similar to *E. olivina*, appears to operate similarly. This makes it often confused with *E. olivina* (Zouiten *et al.*, 2001). Several studies have been carried out on the biology and population dynamics of olive psyllids and their natural enemies, notably in Tunisia, Morocco, Algeria, Iran, Italy, the United States of America and Egypt (Chermiti, 1989; Zouiten *et al.*, 2001, Boukir and Mimoun, 2003; Khaghaninia, 2009; Percy *et al.*, 2012, Meftah *et al.*, 2014). These studies came to the conclusion that this biopest has 2 to 6 generations every year, with the ecological characteristics of different locations being the cause of this variation. In Algeria, studies on this pest are very limited- a study in Tizi-Ouzou by (Boukir and Mimoun, 2003) and in Batna (Chafaa *et al.*, 2017). With that said, and considering the olive tree's economic and social value, cultivation has been the subject of research and experimentation for some time, with the goal of improving output. The aim of this study is to investigate the psyllid's dynamics in order to determine the number of generations of this bio-aggressor in the semi-arid bioclimatic stage, as well as to emphasize the effect of climatic conditions on the population of this insect.

Materials and methods

Study area

The Wilaya of Djelfa is located in central Algeria, in the transition zone between the highlands and the Saharan Atlas. The region's climate is defined by cold, harsh winters on the one hand and scorching, dry summers on the other. The experimental orchard was created in 1999 on clay-limestone soil with a surface of 5 hectares that contain 800 relatively homogeneous trees (varieties: Chemlal and Sigoise). The tree heights ranged from 1.5 to 3 meters, with a planting density of 3 x 5 meters. During the study period, the study orchard received no phytosanitary treatment.

Sample collection

Two sampling techniques were used in this study: Visual control and Threshing. Visual control is the most widespread sampling method used in studying the population dynamics of the psyllid. The latter grows, depending on the season, on young shoots, flower buds, and leaves (Laoudi, 2012). It is a generally a non-destructive mean of control, which allows for the possibility of

following the evolution of populations of auxiliaries and pests (Reboulet, 1986). Our work consists of making field trips every fifteen days in order to conduct sampling via taking a branch from each direction of the tree at human height with the aid of pruning shears. Our sample consists of 10 trees chosen randomly for each variety (Chemlala, Sigoise), covering the entire surface of the orchard. A total of 40 branches were taken, and were put in labeled paper bags, bearing the date, the direction, and the variety. Samples were taken between December 2017 and November 2018. In the laboratory, observations under a binocular magnifying glass are made in order to examine the different life stages of the insects, as well as their appearance dates, and their peak dates.

Threshing Method: According to McGavin (2007), Frah *et al.* (2015) and Chafaa *et al.* (2017), threshing is a simple method that allows for the simultaneous estimation of pest population and the auxiliaries present on the tree or the branches, whether they are winged or not. In our work, we carried out a threshing on the same trees previously selected in the visual control method—during the same time period and with two trees for each variety. Using a stick, only from top to bottom, we strike a branch on each of the four directions in order to recover psyllid adults (male and female). The latter fall on the canvas where they are easily observed and counted; they are then retrieved using a pair of pliers, and are then kept in plastic Petri dishes, labelled with all necessary information such as date, olive variety, and direction. The both methods will be counted together.

Statistical Analysis

Principal component analysis (PCA) was performed to decompose the original matrix into multiplication of loading (environmental factors) and scores (the abundance of the species' larval stages) matrices. PCA is an unsupervised method of model recognition in that no grouping of data is to be known prior to analysis. PCA method explains the maximal amount of variance in the data described by the observed variables based on linear combinations of those groups for the abundance of the species' larval stages samples. Analyses were performed using the software XLSTAT version 5.03 (2014) for MS Windows.

Results

Population dynamics of *Euphyllura olivina*

Two generations are present annually, according to research on the dynamics of the *E. olivina* population. The first generation is a spring one that lasts from March to June, and the second is an autumn one that begins in September 2018 and lasts until late November 2018 or early December 2017.

POPULATION DYNAMICS OF *EUPHYLLURAOLIVINA* IN OLIVE TREES (ALGERIA)

The first generation's egg laying begins in March and lasts until May, whereas the second generation's oviposition begins in late August or early September and lasts until November (Fig. 1).

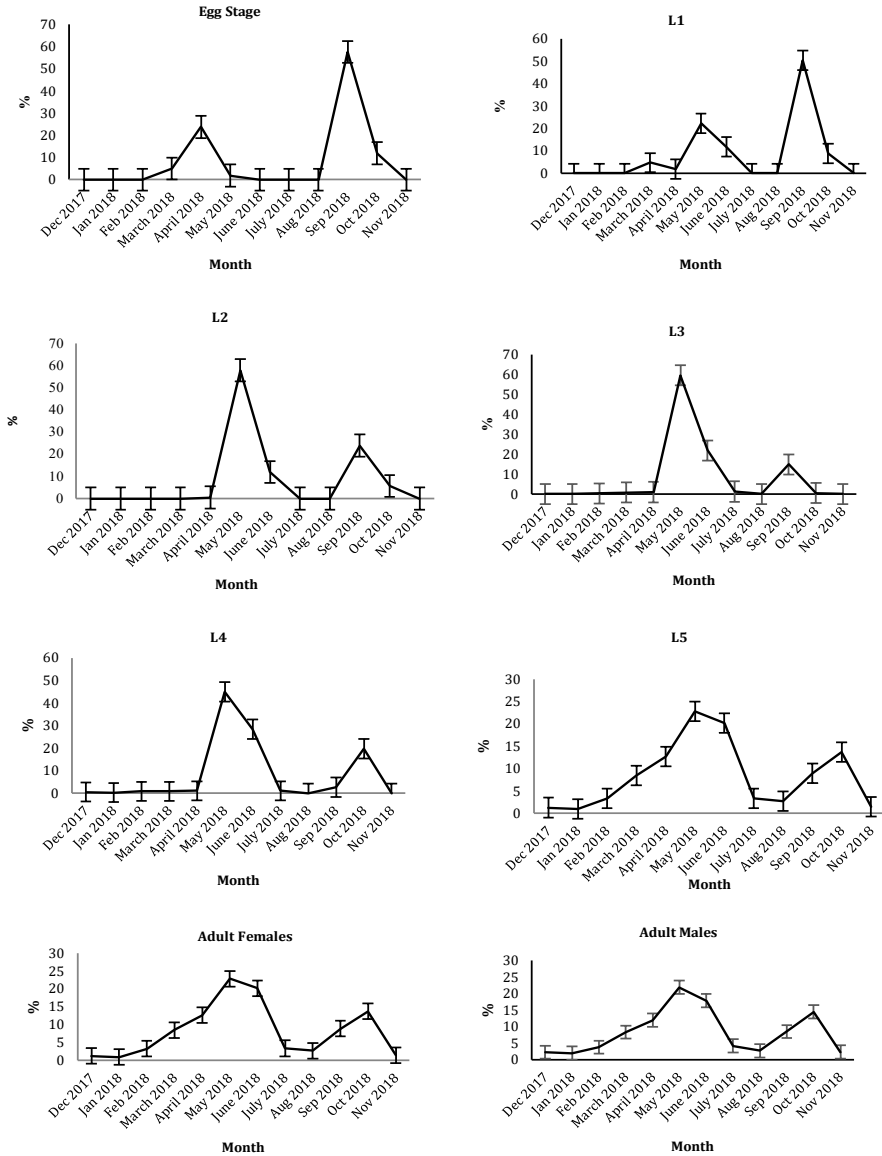


Figure 1. Evolution of the percentages of the different stages of *Euphyllura olivina* in an olive orchard of the semi-arid region Djelfa, Algeria

The first larval stage, for the spring generation takes place between April 2018 and May 2018 and between September 2018 and October 2018 for the fall generation. The second larval stage occurs between May 2018 and June 2018 for the first generation and between September 2018 and November 2018 for the second (Fig. 1). Between April and June for the first generation, and between September and October for the second generation, are when the third and fourth larval stages appear. Beginning in early May and lasting until the end of June for the first generation, and from September until the end of October for the second, the fifth larval stage is visible (Fig. 1). Although adult females are present all year round, they are most frequently seen between March and June for the first generation and beginning in September for the second generation. Between March and June, the males of the first generation leave. When it comes to the second generation, it is seen between September and October (Fig. 1).

The impact of climatic factors on the population dynamics of E. olivina

According to the results of the principal component analysis, the first two axes account for 75.0% of the variation in how climatic conditions affect the species' larval stages. The variance of the F1 axis is 50.96%, whereas that of the F2 axis is 24.03%. Two groups -groups 1 and 2- were determined using PCA. The factorial axes reveal that the eggs, L1, rainfalls (m/m), and T°C together created group 1 (cluster 1). (Mean, min and max) (Fig. 2).

As a result, the cluster records mean wind speed (m/s), as well as the rest of the species' larval stages and adults (L2, L3, L4, L5, adult females and adult males). The effect of the climatic *variables considered on the number of different developmental stages of E. olivina* varies from one developmental stage to the next.

While rainfall and T°C had an impact on eggs and the L1 (Mean, min, and max), the influence of these factors was determined to be statistically significant ($r > 0.5$ for all). When other developmental stage phases (L2, L3, L4, L5, adult male, and adult female) are also involved, the effect of the mean wind speed is quite substantial ($r > 0.5$ and $P < 0.05$ for all).

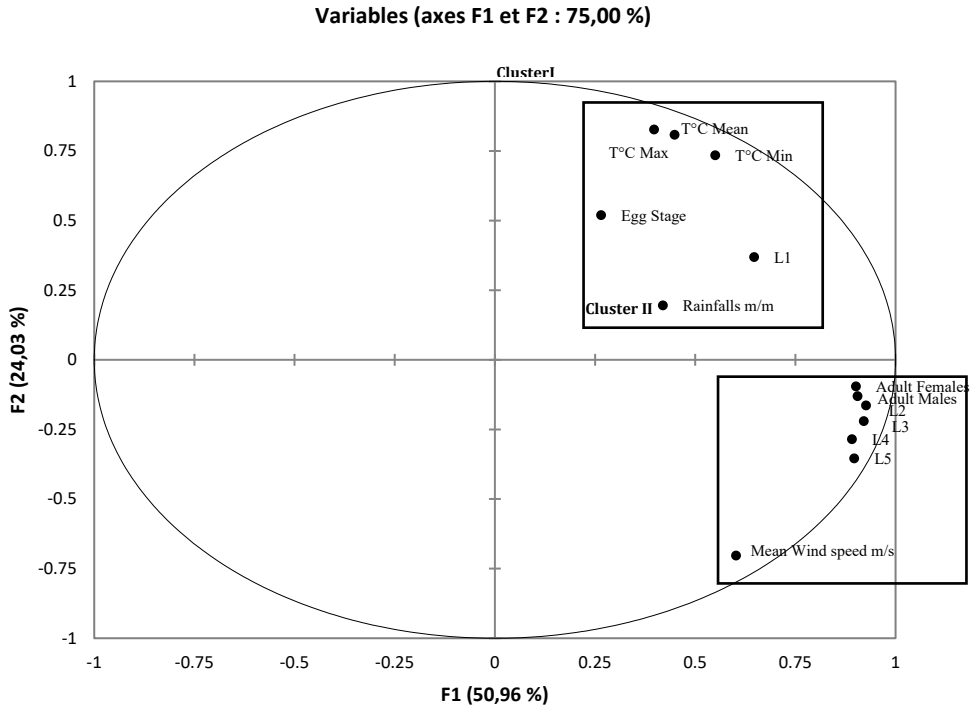


Figure 2. Principal Component Analysis (PCA) illustrating relationship between climatic factors and developmental stage phases

Discussion

This study focused on the question of how life-history traits respond to different climatic factors in *E. olivina*. The *E. olivina* comes in two generations in the Djelfa region: spring and autumn. They hibernate as adult females and males throughout the winter, with larvae of various stages present in small numbers. Eggs are observed in March and September, while first stage larvae emerge in April and September. The first larval stage population peaks in May and September, while the second stage population peaks in late May and late September. The remaining larval stages (L3, L4 and L5) go through several successive molts and become adult females and males in May-June and in October-November.

The rainfalls and temperatures (Mean, min, and max) recorded during this period had an effect on the eggs and L1 stages (P 0.05). The mean wind speed, on the other hand, had a significant impact on the developmental stages of *E. olivina* (L2, L3, L4, L5, adult females and adult males) with P 0.05.

These results are consistent with those of Chafaa *et al.* (2017), who claimed that this bio-pest develops in two annual generations in the Batna region (semi-arid climate of northeastern Algeria) and that this psyllid overwinters in several forms with low percentages.

Two generations were recorded by Tajnari (1992) in Morocco's El-Haouz region. The results are similar since this area, in particular, has numerous climatic similarities to Djelfa. The first generation begins to emerge in April and corresponds with the olive tree's budding cycle. Three recurring and one sporadic generations were observed in Tunisia's Sahel area of Sfax (Arambourg, 1964; Chermiti, 1983; Ksantini, 1997). Two spring generations and one sporadic were reported by Chermiti (1989) in the olive-growing region of the Côte d'Azur coast (France). In Jordan, two generations were recorded by Mustaph (1989).

Generally, three generations of psyllids tend to be the annual norm in many places in olive-growing countries. The first begins in March (Alford, 2014). The second in May, but enters an aestivation period as soon as temperatures exceed 27.2°C (Alford, 2014; Johnson, 2009). The third of these generations appears in September and October (Zalom *et al.*, 2014). Our data, however, support the presence of just two generations. This might be explained by the Wilaya of Djelfa's climate, where summer highs reach 30 °C. Different rates are used by adult females to signal their presence throughout the year. Prophetou *et al.* (1976) in Greece, Meftah *et al.* (2014) in central Morocco, and Chafaa *et al.* (2017) in Batna, Algeria all made similar observations. The olive psyllid evolves on *Olea europaea* in Djelfa throughout the course of a year-long study in two annual generations. Each region's climate has an impact on its dynamics.

Conclusions

The development of a monitoring and control system appears to require a complete understanding of the evolution of the olive psyllid in semi-arid regions of Algeria. In the Djelfa region, the olive psyllid has two generations per year, with oviposition starting in March and ending in June for the first generation. Egg laying for the second generation starts in the first week of September and ends by the end of October or the beginning of November.

The overwintering population is generally made up of adult females and a small proportion of the different stages.

References

- Alford, D. V. (2014). Pests of Fruit Crops: A Colour Handbook. Second edition. *CRC Press* New York, pp.462.
- Arambourg, Y. (1964). Characteristics of the entomological population of olive tree in the Sahel of Sfax. *Ann. Int. Nat. Rech. Agron. Tunisia*, 37, 1 - 140.
- Arambourg, Y. (1985). Fiches synoptiques: lépidoptères (Pyrilidae). [in French]. *Olivae*, (6),21- 24.
- Arambourg, Y. (1986). Traité d'entomologie oléicole. [in French]. *International Olive Council. Juan Bravo Madrid*, pp. 360.
- Baggiolini, M., & Wildbolz, T.H. (1965). Comparison of different population censuses of arthropods living at the expense of the apple tree. *Federal Agricultural Research Station, Switzerland*, pp. 264.
- Balachowsky, A., & Mesnil L. (1935). Les insectes nuisibles aux plantes cultivées leurs moeurs et leur destruction. [in French]. *Etablissement Buisson Paris, T.I*, pp.627.
- Benyeza, Z. (2011). Bioecological study of the olive fly *Bactrocera oleae* GMEL (Diptera, Tephritidae) in the regional station of plant protection of Ain Touta, Batna. Dissertation. University of Batna.
- Biche, M. (1987). Bio-ecology of the purple olive scale, *Parlatoria olea* (Homoptera, Diaspididae) and biological study of its external parasite *Aphytis maculicornis* (Hymenoptera, Aphelinidae) in the Cap Djinet region. Dissertation. University of Nice.
- Biche, M. (1988). Etude Biologique *Aphytis maculicornis* Masi (Hym. Aphelinidae) parasite externe de *Parlatoria oleae* Colvée (Hom. Diaspididae) Ravageur de l'olivier dans la région du Cap-Djinet pour une éventuelle lutte biologique.[in French]. *Ann. Ins. Nat. Agron. El Harrach*, Alger, 12, 119-163.
- Boukir, Z., & Mimoun K. (2003). Contribution to the bioecological study of the olive psyllid *Euphyllura olivina* COSTA (1839) (Homoptera-Psyllidae), in an olive orchard in Tizi-Ouzou. [in French]. Dissertation. University of Tizi-Ouzou.
- Bouktir, O. (2003). Contribution to the study of the entomofauna in three olive groves in Tizi Ouzou and study of some bioecological aspects of the olive fly *Bactrocera oleae* Gmelin et Rossi, 1788 (Diptera-Tephritidae). Dissertation. National Superior School of Agronomy, El Harrach.
- Chafaa, S. (2013). Contribution to the study of the entomofauna of olive tree, *Olea europaea* and the population dynamics of the purple scale *Parlatoria oleae* Colvée, 1880 (Homoptera: Diaspididae) in the region of Batna. Dissertation Docterat. National Superior School of Agronomy, El Harrach.
- Chafaa, S., Biche, M., Sellami, M., Chanchouni, H. & Si Bachir, A. (2013). Life cycle of *Parlatoria oleae* (Hemiptera: Diaspididae) infested with olive groves in an arid region. *Can. Entomolo*,145, 398 - 405.

- Chafaa, S., Dembri, B., & Chabri H. (2017) First data on the life cycle and population dynamics of the olive psyllid (*Euphyllura olivina* csta (1839) Hemiptera: psyllidae) in the region of Ain touta - wilaya of Batna- northeast Algeria. AFPP – 11 e-conference internationale sur les ravageurs et auxiliaires en agriculture Montpellier - 25 et 26 octobre 2017, 186-195p.
- Chermiti, B. (1983). Contribution to the bioecological study of the olive psyllid *Euphyllura olivina* Costa (Hom; Psyllidae) and its endoparasite *Psyllaephagus euphyllurae* Silv. (Hym. Encyridae). Dissertation Doctoral. University of Aix-Marseille.
- Chermiti, B. (1989) Population dynamics of the olive psyllid *E. olivina*, under Mediterranean conditions. Dissertation Doctorat Es-Sciences. University of Aix-Marseille.
- Chermiti, B. (1992). Approach to the evaluation of the harmfulness of the olive psyllid *Euphyllura olivina* Costa 1839 (Hom: Psyllidae). *Olivae*, 43, 34-42.
- Cross, J.V. (1997). The current status of integrated fruit protection of pomaceous crops in Western Europe and its achievements. *Adalia*, 34, 12 -21.
- D.S.A. (2016). Agricultural statistics: olive growing. D.S.A. Djelfa (Algeria).
- Dibou, A, Ksantini, M, & Raptopoulos, D. (2010).Efficacy trials of the bio-insecticide tetrastop for biological control of the olive psyllid *Euphyllura olivina* Costa (Homoptera, Psyllidae). *Revue Ezzaitouna*, 11(1), 1-10.
- FAO (2003). Chapter 2 Food security: Concepts and measurement. In: Trade reforms and food security, FAO.(ed.), Rome, pp. 25-34.
- Frah, N., Baala, H. & Loucif, A. (2015). Étude de l'arthropodofaune dans un verger d'olivier à Sefiane (w. Batna est-algérien). [in French]. *Leban. sci. j.*, 16(2), 37-45.
- Hamiche, A. (2005). Entomofaune dans deux oliveraies de Boudjima et de Maatkas (Tizi Ouzou) ; bioécologie de la mouche de l'olivier *Bactrocera oleae* Gmelin et Rossi 1788 (Diptera R Tephritidae). [in French]. Dissertation, École Nationale Supérieure Agronomique, El Harrach.
- Jardak, T., & Ksantini, M. (1996). L'aménagement de la protection phytosanitaire de l'olivier en Tunisie : Eléments de base et nécessité économique et écologique.[in French]. *Olivae*, 261-309.
- Johnson, M.W. (2009). Olive psyllid, *Euphyllura olivine* (Costa) (Hemiptera: Psyllidae). Center for Invasive Species Research, University of California, Riverside. [Accessed 21 January 2023] <https://cistr.ucr.edu/invasive-species/olive-psyllid>
- Khaghaninia, S. (2009). Effect of emulsifiable oil on overwintering adults of olive psyllid *Euphyllura olivine* (Costa) (Hemiptera: Aphalaridae) and its phytotoxicity on olive trees in Tarom region-Iran. *Mun. Ent. Zool.*, 4(2), 486-492.
- Ksantini, M. (1997). Contribution à l'étude du psylle de l'olivier *Euphyllura olivina* Costa(Homoptera, Aphalaridae) dans la région de Sfax : Relation Plante Hôte-Insecte. [in French].Dissertation, University de Sfax.
- MADRPM (2008). Ministère de l'Agriculture, du Développement Rural et de la Pêche Maritime, direction du conseil général du développement agricole. [in French].
- McGavin, G. (2007). Larousse nature en poche. [in French].Larousse. France, 224 p.

- Meftah, H., Boughdad, A., & Bouchelta, A. (2014). Infestation et cycle biologique d'*Euphyllura olivina* Costa (Homoptera, Psyllidae) au centre du Maroc. *ScienceLib Éditions Mersenne*, 6, 2111-470
- Mendil, M. (2009). Situation de l'oléiculture dans le monde et dans la région méditerranéenne. *Filaha Innove*, 4, 3-7.
- Mustafa, T.M. (1989). Bionomics of the olive psylla, *Euphyllura olivina* Costa (Hom, Psyllidae) in Jordan. *J. Biol. Sc. Res.*, 20(1), 159-166.
- Oussalah, N. (2008). Contribution à l'étude biologique de *Parlatoria oleae* (Colvée, 1832) dans une oliveraie à Bordj Bou Arréridj. [in French]. Dissertation. École Nationale Supérieure Agronomique, El Harrach.
- Percy, D. M., Rung, A., & Hoddle, M. S. (2012). Erratum: Diana M. Percy, Alessandra Rung & Mark S. Hoddle (2012) An annotated checklist of the psyllids of California (Hemiptera: Psylloidea). *Zootaxa*, 3193, 1-27. *Zootaxa*, 3256(1), 64-64.
- Prophetou, D. A., Tzanakis, M. E. (1976). Seasonal development and number of generations of *Euphyllura olivina* Costa in Halkidiki (N. Greece). *Annals. Entomol. Soc. Amer.*, 70 (5), 707-709.
- Reboulet, J. N. (1986). Le contrôle visuel. Groupe de travail ANPP. Les organismes auxiliaires présents dans les conditions naturelles. [in French]. *Acta*, 1 - 13.
- Tajnari, H. (1992). Étude bio-écologique d'*Euphyllura olivina* Costa (Hom. Psyllidae) dans les régions du Haouz et d'Essaouira : mise en évidence d'un état de diapause ovarienne., Maroc. [in French]. Dissertation. École nationale d'agriculture Meknès.
- Zalom, F.G., Vossen, P.M., Van Steenwyk, R.A., & Johnson, M.W. (2014). UC Pest Management Guidelines: *Olive Psyllid*. Statewide Integrated Pest Management Program. University of California Agriculture and Natural Resources. [Accessed 16 January 2023] <https://www.ipm.ucanr.edu/agriculture/olive/Olive-psyllid/>
- Zerkhefaou, K. (1988). Etude de la dynamique des populations de la Mouche de l'olive *Bactrocera oleae* Gmel. (Diptera, Tephritidae) et estimation de ses dégâts dans les régions de Béni Douala (Tizi Ouzou). [in French]. Dissertation. École Nationale Supérieure Agronomique, El Harrach.
- Zouiten, N., & EL Hadrami, I. (2001). Le psylle de l'olivier: Etat des connaissances et perspectives de lutte. [in French]. *Cahiers d'études et de recherches francophones/Agricultures*, 10, 4, 225-232.

First notes on plant diversity, finding sites and sex ratio in natural populations of *Thrips tabaci* Lindeman (Thysanoptera: Thripidae) in Algeria (Biskra province)

Rima Rechid^{1,2}✉, Malik Laamari^{2,3} and Arturo Goldarazena⁴

¹Department of Natural Sciences and Life, University Mohamed Khider, Biskra, Algeria ; ²Laboratoire d'Amélioration des Techniques de Protection Phytosanitaires en Agro-Système Montagneux (LATPPAM), University of Batna, Batna, Algeria; ³Department of Agronomy, University of Batna, Batna, Algeria ; ⁴Laboratorio Nacional de Referencia de Nemátodos y Artrópodos, Departamento de Biodiversidad y Ecología Evolutiva, Museo Nacional de Ciencias Naturales, Madrid, Spain; ✉Corresponding author, E-mail: rima.rechid@univ-biskra.dz, rimarechid@gmail.com

Article history: Received: 20 March 2023; Revised: 14 December 2023;
Accepted: 14 December 2023; Available online: 28 December 2023.

©2023 Studia UBB Biologia. Published by Babeş-Bolyai University.



This work is licensed under a [Creative Commons Attribution-NonCommercial-NoDerivatives 4.0 International License](https://creativecommons.org/licenses/by-nc-nd/4.0/).

Abstract. *Thrips tabaci* Lindeman (Thysanoptera: Thripidae), commonly known as onion thrips, is a serious global pest of commercial onion, causing direct and indirect important damages. This survey carried out in natural areas of Biskra province (Algeria) during two periods, 2008/2009 and 2011/2012, aims to review the plant species harbouring *T. tabaci* in this region.

Algerian and Spanish researchers confirmed twenty-three thrips species. *T. tabaci* is the most abundant and polyphagous. Studies have indicated that it settled in fifty one plant species belonging to nineteen botanical families. The most important are Asteraceae, Brassicaceae, Fabaceae, and Amaranthaceae. In Biskra, *T. tabaci* was found in sites between -32 m and 1000 m of sea level. The results also indicate the presence of sexual and asexual populations.

This study shows that *T. tabaci* is ubiquitous in the natural habitat of Biskra province. Further research is needed to confirm its host plants and the most common mode of reproduction in this region by studying the largest number of plants in various environments and demonstrating the sex ratio over a broad survey spectrum.

Keywords: *Thrips tabaci*, ubiquitous, natural area, finding sites, plant diversity, sex ratio, Biskra region, Algeria.

Introduction

Onion thrips, *Thrips tabaci* (Thysanoptera: Thripidae), is harmful pest thrips vector of tospoviruses (Mound, 2002; Diaz-Montano *et al.*, 2011). The feeding behavior of this species causes severe damage (Mound, 2002; Diaz-Montano *et al.*, 2011). It is believed to have originated in the Mediterranean region. *T. tabaci* was firstly reported by Russian entomologist Karl Eduard Lindeman, represented by specimens collected in Bessarabia, Russia, which caused serious damage to tobacco plants (genus *Nicotiana*) (Diaz-Montano *et al.*, 2011). Later studies reported the presence of *T. tabaci* in more than 120 countries and territories (LoredoVarela and Fail, 2022). *T. tabaci* is extremely electic and cosmopolitan species because of its small size, polyphagy, presence of sexual and asexual populations (Bournier, 1983; LoredoVarela and Fail, 2022), great capacity for reproduction, short generation time, and its ability to disseminate to adjacent fields (LoredoVarela and Fail, 2022). Its host plants range from 355 flowering plants (Gill *et al.*, 2015) to 391 plant species (LoredoVarela and Fail, 2022). Some onion thrips populations have been found to utilize a single plant, such as tobacco, while others can be detected to exploit multiple species from different plant families (Fedorov, 1930; Gill *et al.*, 2015). The current genetic evidence suggests a cryptic species complex of three lineages within the species (LoredoVarela and Fail, 2022).

In North Africa, two interesting studies on thrips were carried out in Egypt by Priesner (1960) and Wafy *et al.* (2021). *T. tabaci* was mentioned among the Thysanoptera fauna list. However, in the Maghreb region, studies in this field are still very limited. They were mainly achieved in the cultivated regions. In Morocco, this species was reported by Le Gall (1961) on cotton. The author indicated that the Egyptian varieties reduced seed cotton production by 15 to 20 %. In Tunisia, *T. tabaci* was found in citrus (Elimem and Chirmiti, 2013; Belaam-Kort and Boulahia-Kheder 2017; Attia *et al.*, 2019; Elimem *et al.*, 2019a; Belaam-Kort *et al.*, 2020; Hached *et al.*, 2020) and on two vine grape orchards (Elimem *et al.*, 2019b).

In Algeria, despite their importance, studies on thrips remain scarce. Until now, little is known about their biodiversity and biology. Few studies on thrips have been conducted in natural areas, except for Pelikan's (1988) first contact with 21 species complementary to the 20 previously recorded (a total of 41 species inventoried on the Algerian territory). Later studies focused solely on *T. tabaci* in some vegetable crops. Djebara *et al.* (2018) investigated this species in greenhouse-grown tomatoes, and Koutti *et al.* (2017) on citrus varieties: Thomson Navel and Clementine. In the Biskra region, it was collected on tomatoes by Laamari and Houamel (2015). Furthermore, it was recorded by

Razi *et al.* (2017, 2019) and Allache *et al.* (2020) on 16 vegetable crops. In this content, the present study aims to record the plant species harboring *T. tabaci* in natural area and to know its distribution in this region characterized by its particular climatic conditions (Sahara) and the endemism of its plant cover.

Materials and Methods

Study region

This study was carried out in Biskra province, a transition and arid region between the Northern and southern parts of Algeria. It is located in the south of the Saharan Atlas Mountains. According to Ozenda (1991) the major part of this region is the desert, where the vegetation is adapted to the different conditions (hot climate and saline soil). The natural vegetation is dominated by steppe plants in the north with high elevations reaching more than 1000 m of sea level and by Saharan plants in the south with very low elevations, reaching - 32 m (Fig. 1) and (Tab. 1). Collection locations were selected based on accessibility, and vegetation diversity in different sites, including the highest or lowest altitudes.



Figure 1. The geographical location of sampling sites in the study region.

Surveys were completed during two periods, 2008/2009 and 2011/2012, in the spring season when spontaneous plants are more abundant, from February, March, and April in 2009 and during March and May in 2012.

Table 1. GPS coordinates of sampled sites in Biskra region.

Localities	Sites	Altitudes (m)	Latitudes and longitudes
Sidi Okba	Sidi Okba	57	N:34°46'04", E:5°52'37"
Oumache	Oumache	49	N:34°41'29", E:5°41'54"
El-Hadjeb	El-Hadjeb	147	N:34°47'11", E:5°35'23"
	Bordj Enos	151	N: 34°45'59", E: 5°32'21"
		149	N:34°46'04", E :05°33'42"
Biskra	Feliach	87	N: 34°49'26", E:5°46'07"
El Outaya	Fontaine des Gazelles	385	N: 35°07'44", E:5°36'32"
Foughala	Foughala	150	N: 34°43'39", E: 5°19'54"
Tolga	Tolga	139	N: 34°42'40", E: 5°23'36"
Branis	Dar Arous	198	N: 34°56'27", E:5°41'53"
Sidi Kaled	Lehouimel	217	N: 34°22'53", E:4°59'8.2"
Ouled Djellal	Marmotha	188	N: 34°26'39", E: 5°6'2.8"
Lioua	Lioua	107	N: 34°38'12", E:5°24'11"
M'ziraa	Tadjemout	865	N:34°59'65", E :06°24'38"
	Djemina	786	N:34°57'52", E :06°24'25"
		719	N:34°57'19", E :06°24'23"
	Kharboucha	126	N:34°47'53", E :06°22'09"
	Oued Romane	298	N:34°53'02", E :06°24'37"
El Haouch	Sidi Med Ben Moussa	- 32	N:34°34'40", E :06°09'72"
Mlili	Mohit Essarig	45	N:34°40'61", E:05°39' 44"
Lichana	Lichana	171.8	N: 34°44'21", E:05°27'10"
Djemorah	Beni Souik	560	N:35°05'68", E:05°52'64"
	Guedila	390	N:35°03'01", E:05°45' 39"
El Kentara	El Kentara	550	N:35°15'09", E:05°42' 56"
Mchouneche	Mchouneche	315.6	N:34°57'30", E:06°00' 41"
		322	N:34°57'29", E:06°00' 45"
Ain Zaatout	Ain Zaatout	970	N:35°15'09", E:05°49' 51"

Collection and morphological identification of specimens

The floral and vegetative parts of different plant species were sampled over two periods, during which 91 plants were sampled weekly. It should be noted that due to the size of the survey area and the distance of some sites, it was impossible to visit these sampling sites at the same pace and on the same dates.

At each visit, a maximum number of new plant species available and characteristic of each site harbouring *T. tabaci* from which a maximum number of individuals of this thrips were shaken over a plastic beating tray. This is particularly effective because the pretarsal bladder of thrips adheres to the smooth surface of a picnic tray collector (Mound *et al.*, 1976). We also beat the maximum of plants of the same species present at the same site. Inflorescences of plants are also taken in a dense bags separated according to plant species (Priesner, 1960). At collection, thrips must be brought back alive or selected on site (Priesner, 1960).

The specimens were recovered in tubes containing 90% ethanol with a fine brush. In the laboratory, the thrips were sorted under a stereo-microscope (Carl Zeiss, Germany) based on certain morphological characteristics; similar individuals were placed separately in vials. The specimens were prepared according to the procedure reported by Mound and Marullo (1996). The best specimens of each species were mounted in permanent slides with Canada Balsam and the others in semi-permanent slides in Hoyer ringed and sealed. The identification of adult thrips was made using the keys of Moritz (1994); Zur-Strassen (2003), and Moritz *et al.* (2004). The majority of the specimens sampled were morphological identification performed on slides, with the exception of a few dozen, and some larvae were left preserved in alcohol, particularly those found on plants with large numbers of individuals. The larvae of thrips were also identified according to Vierbergen *et al.* (2010); in this study *T. tabaci* larvae do not appear to be among the larvae of other thrips. Reference collection of slides is deposited in the collection of the LATPPAM laboratory, Department of Agronomy, University Batna 1 (Algeria).

Statistical exploitation of results

Statistical analyses were performed to assess the effect of environmental variables on the activity of *T. tabaci* species sampled during two periods in different habitats in the study area.

The data were subjected to a multiple correspondence analysis (MCA) to determine the impact of inertia of environmental factors and the correlation between them on the activity of this thrips.

All analyses were performed using SPSS Software version 20.0.

Results

This survey constitutes the most important contribution to the knowledge on *T. tabaci* in the natural environment of Biskra province, Algeria. It was sampled in mountainous and steppe sites at different altitudes. It has been found in 27 sites belonging to 19 localities in this region (Tab. 1 and Fig. 1).

Analyzing environment factors that affect thrips activity, it revealed that systematic plant, sampling regions, and habitat types greatly influenced *T. tabaci* life (Tab. 2) and (Fig. 2 a, b).

In the (Tab. 2) the two dimensions are represented on the two horizontal and vertical axes by dimension 1 and dimension 2 (Fig. 2 a, b) while the 3rd column means the average of the values of the variables (environmental factors) of the two dimensions between (0-1) (Tab. 2). The Percentage of variance explained is significant by more than 50% in both dimension 1 and 2 (Tab. 2) and (Fig. 2 a, b).

Table 2. Inertia of environment factors on *T. tabaci* activity in Biskra region in 2008/2009 and 2011/2012.

Discrimination measures			
	Dimension		Mean
	1	2	
Sampling regions	.959	.970	.965
Habitat types	.808	.835	.821
Individual number	.340	.367	.354
Individual colors	.130	.004	.067
Individual sex	.040	.002	.021
Systematic plant	.993	.993	.993
Active total	3.271	3.171	3.221
Percentage of Variance explained	54.509	52.851	53.680

In (Fig. 2 a, b) the most discriminating environmental factors on the activity of *T. tabaci* are systematic plant (.993), sampling region (.965) and habitat type (.821) which represent an inertia of 86.27 % (Tab. 2) and (Fig. 2a) on the activity of this thrips from the total of the other factors (active total: 3.221) especially in the natural environment that is 84.57% of the individuals of this thrips were collected on the natural environment where there is the greatest number of plants sampled, i.e. 64.7% of the total plant species sampled in all habitats (i.e. 4 groups) (Fig. 2b).

The impact of the inertia of the environmental factors on the activity of *T. tabaci* in this region we found four populations, of which the largest group represents the natural habitat followed by the population that represents the adjacent cultivated-urban and natural adjacent habitat and the last group by urban adjacent habitat (Fig. 2b).

In the first population (natural population) it was found that the environmental factors sampling regions and systematic plant are positively correlated with habitats types with a value of 0.9 (90%). The number of individuals has a moderately positive correlation with systematic plant with a value of almost (0.5) 50%. Furthermore, adult color and sex have no correlation with the other factors mentioned above, but the first factor (color) is weakly influenced or correlated with plant systematic by a value of 30% (Tab. 3).

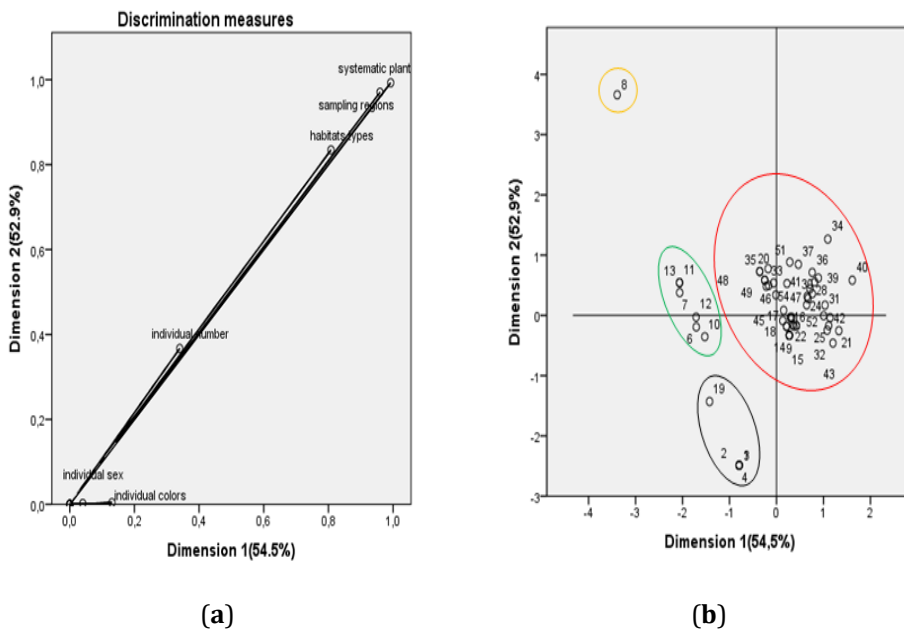


Figure 2. (a, b) : MCA ordination plot of different factors influencing *T. tabaci* activity (Red color: natural habitat, Green color: adjacent crop-urban habitat, Black : adjacent natural habitat, Orange color: adjacent-urban habitat).

Table 3. Correlation between environmental factors affecting *T. tabaci* activity in the study area.

Correlations of transformed variables

Dimension: 1	sampling regions	habitats types	individual number	individual colors	individual sex	systematic plant
sampling regions	1.000	.918	.486	.279	.222	.974
habitats types	.918	1.000	.291	.138	.119	.902
individual number	.486	.291	1.000	.134	-.092	.559
individual colors	.279	.138	.134	1.000	-.065	.359
individual sex	.222	.119	-.092	-.065	1.000	.207
systematic plant	.974	.902	.559	.359	.207	1.000
Dimension	1	2	3	4	5	6
Eigenvalue	3.271	1.124	.888	.672	.036	.009

T. tabaci was sampled on fifty (51) plant species belonging to nineteen (19) different botanical families (Tab. 4).

Table 4. Variations in numbers of *Thrips tabaci* on the different host plants founded in the Biskra region during the periods 2008/2009 and 2011/2012.

Families	Plant species	Individual number
Asteraceae	† <i>Anvillea radiata</i> Coss. and Durieu	10 ♀☀
	<i>Sonchus oleraceus</i> L.	1 ♀♣
	<i>Volutaria lipii</i> (L.) Cass.	1 ♀♣
	○ <i>Scorzonera undulata</i> Vahl	1 ♀(☀)
	<i>Calendula arvensis</i> M. Bieb.	1 ♀☀
	■○†▲ <i>Artemisia herba alba</i> Asso.	(44 ♀+1 ♂) ☀
	<i>Rhantherium adpressum</i> (Desf.) Coss. and Dur.	1 ♀☀
	<i>Scolymus hispanicus</i> L.	1 ♀☀
	<i>Pallenis spinosa</i> (L.) Cass.	2 ♀☀
	<i>Cynara cardunculus</i> L.	2 ♀♣
* <i>Erigeron canadensis</i> (L.) Cronquist	2 ♀☀	
Brassicaceae	<i>Rapistrum rugosum</i> (L.) All.	1 ♀♣
	<i>Diplotaxis eruroides</i> (L.) DC.	1 ♀♣
	<i>Diplotaxis virgata</i> (Cav.) DC.	3 ♀☀
	<i>Moricandia arvensis</i> (L.) DC.	1 ♀☀
	○ <i>Eruca vesicaria</i> (L.) Thell	1 ♀♣
	○ <i>Crambe cralikaii</i> (Coss.)	2 ♀♣
	<i>Muricaria prostrata</i> (Desf.) Desv	1 ♀♣
<i>Eruca sativa</i> (Link.)	1 ♀(☀)	

Families	Plant species	Individual number
Fabaceae	<i>Vicia sativa</i> L.	2 ♀♣
	<i>Ononis natrix</i> L.	5 ♀☼
	<i>Melilotus infesta</i> Guss.	3 ♀♣
	○† <i>Medicago truncatula</i> Gaertn.	8 ♀☼
	♂ <i>Retama raetam</i> Webb and Berthel.	1 ♀☼
	<i>Astragalus gombo</i> Coss. and Dur.	4 ♀☼
	<i>Hedysarum pallidum</i> Desf.	1 ♀☼
	<i>Genista microcephala</i> Coss. and Durieu	1 ♀☼
Amaranthaceae	<i>Chenopodium album</i> L.	2 ♀♣ and 1 ♀☼
	<i>Nucularia perrini</i> Batt.	2 ♀☼
	■ <i>Beta vulgaris</i> L.	4 ♀♣
	<i>Suaeda mollis</i> (Desf.) Del	1 ♀♣
Resedaceae	<i>Reseda lutea</i> L.	2 ♀♣
	<i>Reseda alba</i> L.	4 ♀☼
	<i>Reseda alphonсии</i> (Coss) Mull Arg.	2 ♀☼
Apiaceae	○ <i>Thapsia garganica</i> L.	7 ♀☼
	<i>Daucus carota</i> L.	2 ♀☼
Scrophulariaceae	<i>Linaria aegyptiaca</i> (L.) Dum.	1 ♀☼
	○ <i>Scrophularia hypericifolia</i> Wudl	2 ♀☼
Boraginaceae	<i>Echium parviflorum</i> Moench	1 ♀♣
	<i>Heliotropium undulatum</i> (Vahl.)	1 ♀♣
Liliaceae	<i>Asphodelus refractus</i> Boiss.	1 ♀♣
Plantaginaceae	* <i>Plantago lanceolata</i> L.	1 ♀☼
Juncaceae	<i>Juncus articulatus</i> L.	2 ♀☼
Thymelaeaceae	<i>Thymelaea hirsuta</i> (L.) Endl.	6 ♀☼
Primulaceae	<i>Anagallis arvensis</i> L.	1 ♀♣
Zygophyllaceae	↑ <i>Peganum harmala</i> L.	34 ♀☼
Tamaricaceae	<i>Tamarix Africana</i> Poir.	4 ♀☼
Caryophyllaceae	<i>Silene velutinoides</i> Pomel.	1 ♀(☼)
Labiaceae	<i>Marrubium alysson</i> (L.)	1 ♀(☼)
Plombaginaceae	<i>Limonium fallase</i> (Miller.)	1 ♀(☼)
Poaceae	<i>Phalaris brachystachys</i> (Link.)	1 ♀♣
Total = 19	51	188 (187 ♀ + 1 ♂)

*Plant hosted only *T. tabaci*, ▲ First record of males in Algeria, ↑ largest number of individuals, ■ Black body color, ○ white body color, ♣ adjacent habitat in 2008/2009, (☼) natural habitat in 2008/2009, ☼ natural habitat in 2011/2012.

This species was found more numerous in Asteraceae with 11 plant species, 8 plant species in Fabaceae and Brassicaceae and 4 plant species in Amaranthaceae (Tab. 4). Among these plants it was collected in 3 weeds of Asteraceae, 5 of Brassicaceae, 2 of Fabaceae and 3 of Amaranthaceae (Tab. 4), and (Fig. 2b). The latter family includes one plant species common between wild plants and weeds in two different habitats (Fig. 2b). The Asteraceae, Fabaceae, and Brassicaceae families are the most attractive to *T. tabaci* in the desert and mountainous regions of Biskra.

188 specimens of this species were collected in this study, the majority of them was sampled in the natural habitat where the most plant species were sampled. Over 100 plant species were examined for thrips during the study.

A total of 187 females (♀) and one male (1 ♂) of *T. tabaci* were sampled in the natural habitat and its adjacent environment. One male with 158 females were found in the natural environment. However, 29 females were collected in adjacent habitats to natural, crop, or urban areas (Tab. 4). In 2008/2009, this thrips was collected from 24 plants belonging to 12 botanical families at 12 sites, 4 of which are part of the natural environment. In this period 05 females of *T. tabaci* harboured 05 different plants belonging to 05 different botanical families, of which two females were collected on the same site (Tab. 4).

This is the adjacent environment regarding the samples taken, especially in 2008/2009. The cases of *C. album* was collected in a natural environment at Tadjemout and in Feliach near of crop plant, and *E. parviflorum* was sampled at El Hadjeb near the urban environment that is closer to the natural habitat. In Oumache, the available plants were sampled in the adjacent-urban environment (Tab. 4, Fig. 2b).

On the other hand, some plant species were swept in adjacent-cropfields, especially in Sidi Okba near the bean field and in 6 sites near the date palms (Feliach, Oumache, Foughala, Tolga, Marmotha, and Lehouimel) (Tab. 4, Fig. 2b).

For the second and third population (the adjacent cultivated-urban and adjacent natural habitat). These populations are represented by the presence of the environment adjacent to the cultivation of date palms which represent the sites cited above where *T. tabaci* was collected on the weeds between the plots of date palms while for the third group (the environment adjacent to the natural environment) which includes the sites of Marmotha and Sidi okba whose spontaneous plants collected a little closer to the natural environment, in the last site the Asteraceae family is the most important surveyed. In the fourth population which is characterized by a single plant *E. parviflorum* was found at El Hadjeb near the urban environment that is closer to the natural habitat.

Very low numbers of adults collected (70 % of plants had no more than 2 females; indeed 50% of plants had only one female (Tab. 4).

We have recorded higher number of larvae of Thripidae, Aeolothripidae and one larvae of Phlaeothripidae present on *M. truncatula* but show not larvae of *T. tabaci*.

Forty plants and 10 botanical families surveyed in the study area not inhabited by this species (Tab. 5).

Table 5. Surveyed plants not inhabited *T. tabaci* in 2008/2009 and 2011/2012 in Biskra region.

Families	Plants species
Asteraceae	<i>Leontodon mulleri</i> (Ball.)
	<i>Senecio gallicus</i> (L.)
	<i>Anacyclus clavatus</i> (Desf.)
	<i>Leontodon hispidus</i> (L.)
	<i>Phagnalon saxatile</i> (L.) Cass.
	<i>Matricaria chamomilla</i> L.
	<i>Launaea nudicaulis</i> (L.) Hook. fil.
	<i>Cotula cinerea</i> Del.
	<i>Carduus microcephalus</i> Ten.
	<i>Centaurea nicaeensis</i> All.
Brassicaceae	<i>Pseudorucaria teretifolia</i> (Desf.)(DE)
	<i>Sinapis arvensis</i> L.
	<i>Diplotaxis harra</i> (Forssk.)Boiss.
Fabaceae	<i>Hedysarum cornosum</i> (Desf.)
	<i>Hedysarum naudinianum</i> Coss. & Durieu
Amaranthaceae	<i>Suaeda fructicosa</i> (Forsk.)
	<i>Atriplex halimus</i> (L.)
	<i>Salsola tetragona</i> (Delile)
	<i>Bassia muricata</i> (L.)
	<i>Halocnemum strobilaceum</i> (Pall.) Bieb.
Plumbaginaceae	<i>Limonium sinuatum</i> (L.) Miller
	<i>Limoniastrum guyonianum</i> Coss. & Dur.
Caryophyllaceae	<i>Polycarpaea prostrata</i> (Dec.)
► Renonculaceae	<i>Adonis annua</i> (L.)
► Aizoaceae	<i>Aizoon hispanicum</i> (L.)
Resedaceae	<i>Reseda luteola</i> L.

Families	Plants species
▶ Malvaceae	<i>Malva cretica</i> (Cav.)
▶ Urticaceae	<i>Forsskaolea tenacissima</i> (L.)
Apiaceae	<i>Ridolfia segetum</i> (L.) Morris
Scrophulariaceae	<i>Antirrhinum ramosissimum</i> Coss. & Dur.
▶ Convolvulaceae	<i>Convolvulus arvensis</i> (L.)
▶ Rosaceae	<i>Crataegus monogyna</i> Jacq.
Juncaceae	<i>Juncus maritimus</i> Lam.
Thymelaeaceae	<i>Thymelaea microphylla</i> Coss. et Dur.
▶ Lamiaceae	<i>Ballota hirsuta</i> Benth.
Zygophyllaceae	<i>Zygophyllum cornutum</i> (Coss.)(DR)
▶ Apocynaceae	<i>Nerium oleander</i> L.
Poaceae	<i>Stipa parviflora</i> Desf.
▶ Pinaceae	<i>Pinus halepensis</i> Mill.
▶ Cupressaceae	<i>Juniperus phoenicea</i> L.
Total = 23	40

- ▶ Botanical families on which the presence of onion thrips *T. tabaci* has not been observed.

Sampling by altitude

The highest individual number of this pest species were collected during May 2011/2012 in three sites with an altitude of more than 300 m, particularly in Beni Souik (560 m) on *A. herba alba* (Asteraceae), Ain Zaatout (970 m) on *P. harmala* (Zygophyllaceae) and in Mchouneche (322 m) on *M. truncatula* (Fabaceae). *A. herba alba* sheltered the largest individual number with (44 females and 1 male) followed by *P. harmala* with (34 females) and *M. truncatula* with (8 females). The latter plant and *A. herba alba* which is harboured only by this species of thrips while *P. harmala* was sheltered by 4 other species of thrips. In addition, at the same altitude, some plant species were sheltered only by the onion thrips as *R. raetam* and *P. lanceolata* in Tadjmout, *E. canadensis* in Guedila. However, at a lower altitude (126 m) in Kharboucha and during March 2011/2012, only 10 females were collected on *A. radiata* (Asteraceae) dispersed over a large area (Tab. 4).

Color variations

In our study, we found three colors; white, brown, and black. In March 2011/2012 the white color of this species was found in Lichana on *T. garganica*, *S. hypercifolia*, and on *R. raetam* in Tadjemout. In May 2011/2012, some

individuals with black color were found among light and brown females in Beni Souik on *A. herba alba* and other white individuals were found in Mchouneche on *M. truncatula*. In this study, the adult male is smaller and paler than females. In 2008/2009, all individuals collected had a brown to black body color during the months of February, March and April. Black individuals were collected at Feliach on *B. vulgaris* in March, but a few very light colored individuals were collected at Fontaine des Gazelles on *S. undulata* in the same month; in April, other white individuals were collected at Lehouimel on *Crambe craliki* and on *E. vesicaria* (Tab. 4).

Sex ratio

In this study, one male were sampled for the first time in Algeria in a natural environment in 2011/2012; this individual was detected on the Wadi plant species, it was collected among 44 females on *A. herba alba* in Beni Souik (Tab. 4).

Discussion

The present study showed that *T. tabaci* was sampled in mountainous and steppe sites at different altitudes. Ecologically, it is a very plastic thrips species (Fedorov, 1930). Lewis (1973) noted that it is a cosmopolitan pest of onion grown until 2000 m of sea level (Diaz-Montano *et al.*, 2011; Gill *et al.*, 2015).

The obtained results show that environment factors affect thrips activity, it seemed that systematic plant, sampling regions, and habitat types greatly influenced *T. tabaci* life.

Our results confirm that plant diversity in different habitats seems to play an important role in the ubiquitous behavior of *T. tabaci*. 84.57% of the individuals of this thrips were collected on the natural environment where there is the greatest number of plants sampled, about 64.7% of the total plant species sampled in all habitats.

In our samples very low numbers of adults collected (70 % of plants had no more than 2 females; indeed 50% of plants had only one female). It therefore seems likely that the individuals had drifted from some of the plants on which they had reproduced; rather than actually living on the plants from which we collected them. Our data is not a reliable measure of "polyphagy" host plants.

Adult thrips can be found on many plants (Mound *et al.*, 1976). Plant species provide an important feeding or behavioral resource (Mound, 2013)

but are not used for breeding (Mound *et al.*, 1976; Mound, 2013). Not all of them are suitable for the food of larvae; only the adult stage, which occasionally feeds on them (Fedorov, 1930).

For this reason, it is not easy to consider the sampling plant species in our study, which are the true hosts of *T. tabaci* species. When it comes to adult of this thrips, hundreds of various plant species have provided samples (LoredoVarela and Fail, 2022).

Most crucially, it is usually impossible to tell the difference between the terms "finding site" and "host plant" in published data of onion thrips and other Thysanopteran species (LoredoVarela and Fail, 2022; Mound, 2013). Only adult thrips are discovered at the sites, and their existence may be explained by a variety of circumstances, such as an accidental landing or the plant serving solely as an occasional feeding source (LoredoVarela and Fail, 2022; Mound, 2013).

The morphological identification of immature stages is another factor influencing the incorrect association of thrips species with the host plant. The identification of immature stages is frequently overlooked while identifying different species of thrips since adult stages are prioritized (LoredoVarela and Fail, 2022; Mound, 2013).

Due to the weak association between the larvae and the plant species sampled in our study, especially those of the Thripidae collected from *M. truncatula*, they do not show all the morphological criteria of those of *T. tabaci* (Vierbergen *et al.*, 2010), with the presence and absence of other morphological characters, it cannot be affirmed that it is a host plant of this thrips.

According to LoredoVarela and Fail (2022) the onion thrips' hosts must use a variety of techniques, such as frequent sampling of the intended plants. Many samples of the target plants are taken, morphological and genetic identification techniques are used, and host preference research is done in controlled environments.

In Tunisia it was the most abundant species as it was collected from 9 plant species belonging to 7 botanical families out of 23 plant species referred to 15 botanical families listed (Belaam-Kort *et al.*, 2020).

Most of these plants' yellow color and flower structure are probably responsible for this preference. Usually, thrips inhabit medium-sized flowers with sweet scents with or without nectar, and the petal may be lightly shaded, ranging from white to yellow (Varatharajan *et al.*, 2016). These floral features have been observed in some plants belonging to the basal angiosperm families, such as Asteraceae (Varatharajan *et al.*, 2016).

It can actively participate with other pollinating insects in the ecology of the fragile desert vegetation cover. Further studies can confirm this ecological role.

Although it has a wide range of hosts due to its polyphagous nature, onions are a favorite host and one of the few crops that the same species attacks over the world (Diaz-Montano *et al.*, 2011).

Most available work treats onion thrips as a single species with a wide range of host plants (LoredoVarela and Fail, 2022). According to Diaz-Montano *et al.* (2011) *T. tabaci* has a wide host range compared with other thrips species. Some reports mention *T. tabaci* out of 141 plant species belonging to 41 families, while others list it on 355 plant species (Gill *et al.*, 2015), but the last one reveals the presence of three *T. tabaci* species lineages on 391 plants species from 46 families (LoredoVarela and Fail, 2022). Plant species on which selection and development of *T. tabaci* occur include the Asteraceae, Fabaceae, Brassicaceae, Poaceae, and Solanaceae (LoredoVarela and Fail, 2022).

For the second and third population (the adjacent cultivated-urban and adjacent natural habitat) where *T. tabaci* was collected on the weeds between the plots of date palms while for the third group which includes the sites of Marmotha and Sidi okba whose spontaneous plants collected a little closer to the natural environment.

According to Bournier (1983) since *T. tabaci* is the most polyphagous and widespread species of the thrips. Many weeds are food plants for the Tobacco Thrips (Fedorov, 1930).

Although there were some marginal effects, indicating some movement into the field from surrounding areas, the distribution pattern of onion thrips between plants was random (Diaz-Montano *et al.*, 2011).

T. tabaci was also discovered on various weed species. These plants have developed adaptations to cope with constantly shifting habitats (Diaz-Montano *et al.*, 2011). The weeds that grow along the fields' edges make up the grass where the thrips hibernate (Fedorov, 1930).

LoredoVarela and Fail (2022) noted that the list of most important plants includes wild and weedy species. According to Belaam-Kort *et al.* (2020) *T. tabaci* is common on citrus trees and herbaceous wild plants in Tunisia.

In the fourth population which is characterized by a single plant *E. parviflorum* was found at El Hadjeb near the urban environment that is closer to the natural habitat.

Thrips must develop coping mechanisms for continuously changing habitats (Diaz-Montano *et al.*, 2011). This generalist insect has access to various food resources, allowing them to move more easily from one habitat to another

(Pizzol *et al.*, 2017). Polyphagous species, which were present throughout the year long and used a variety of food sources depending on the plants in season, tended to have large populations (Pizzol *et al.*, 2017).

According to Smith *et al.* (2015), insects may be transported long distances at different altitudes with good wind conditions. These authors indicated that *T. tabaci* dispersal behaviors are classified as “long-distance” or short-distance “trivial”. The altitude at which winged insects travel can reveal whether they are engaged in long-distance or short-distance dispersal. It is unknown what effect immediate weather conditions have on *T. tabaci* dispersal activities.

According to our results, altitude has no effect on these four populations, The most activity of *T. tabaci* was recorded in the mountainous sites with more than 300 m of altitude in May 2011/2012 as well as at a low altitude of 126 m in March 2011/2012. In this period it recorded its maximum number with (44 females and 1 male) found on *A. herba alba* followed by *P. harmala* with (34 females). Only 10 females were collected on *A. radiata* dispersed over a large area.

In our sample we found three colors of *T. tabaci*. The great variability of body and antennae colors has been reported, and several forms have been described. These colors are very light yellow to dark brown (Bournier, 1983). These intraspecific structure and color variations might be explained by food quality or quantity (Mound, 2005a; 2005b). It seemed that the color variations of *T. tabaci* are not strongly influenced by temperature fluctuation, as the different colors were observed on the same plant and in the same site. According to Kirk (2002) the rearing temperatures of *Frankliniella occidentalis* do not specify whether the colored forms were reared at the same or different temperatures. In both cases, the dark and light forms were likely obtained in different sites, rather than color forms coexisting in the same place (Kirk, 2002). Males are smaller and paler than females (Diaz-Montano *et al.*, 2011). All this color variation was seen on the *A. herba alba* with the highest number of this thrips. It seems likely that males will be collected only where there is a large population particularly in the naturel habitat. According to Loredovarela and Fail (2022) in sympatric populations of onion thrips lineages, the low male proportion may thus be undetected during sampling, especially with small sample sizes, and as a result, an inaccurate inference is made based on the samples' solely including females.

Our results indicate the presence of sexual and asexual populations in the study region, it was confirmed for the first time in our country, allowing Algeria to reach number forty and to be added to the list of countries reported by the study conducted by Loredovarela and Fail (2022). Onion thrips can reproduce

asexually (parthenogenesis) and sexually (Bournier 1983; Gill *et al.*, 2015). Thelytoky is parthenogenesis in which females are created from unfertilized eggs, the most prevalent reproductive mode (Nault *et al.*, 2006; Gill *et al.*, 2015). In Arrhenotoky reproduction, males are formed from unfertilized eggs, and females are produced from fertilized eggs (Nault *et al.*, 2006; Gill *et al.*, 2015). It is also used by *T. tabaci* lineages that generate both sexes' progeny throughout the growing season. Their sex ratio varies with the season; latitude, longitude, elevation (m), and food supply (Woldemelak *et al.*, 2021). Most found specimens are females, while males are rare (Mound and Walker, 1982; Chatzivassiliou, 2002).

Lewis (1973) mentioned that in the eastern Mediterranean and Iran, known as the area of origin of *T. tabaci*, the sex ratio is about 1:1 (Chatzivassiliou, 2002; Diaz-Montano *et al.*, 2011), whereas, in most parts of the world, the males are unknown (Chatzivassiliou, 2002). In the colder parts of the earth, significantly lower ratios have been seen (Woldemelak *et al.*, 2021). In southern France, no male was identified by Pizzol *et al.* (2017) of this thrips species. Male onion thrips are described in 33 countries and territories. Therefore, their existence is revealed in 39 countries and regions when combining the information from these records with the information on distribution collected (LoredoVarela and Fail, 2022). In Iran, sex ratio progeny revealed no presence of males. Only females emerged on cucumber (var. Soltan) in laboratory conditions (Pourian *et al.*, 2009). Several studies show that *T. tabaci* males are present in the Western Hemisphere, and the factors determining the presence of the parthenogenetic and the bisexual form of this species are quite ambiguous (Chatzivassiliou, 2002). The same author noted that *T. tabaci* forms a complex of two biotypes or subspecies, one, denoted *T. tabaci spp. tabaci* consists of males and females and the other, *T. tabaci spp. communis*, which include populations composed only of females. The parthenogenetic mode of reproduction and the foliar-feeding (rather than feeding on pollen) habits in hot and dry weather provide *T. tabaci* an ecological advantage to increase its populations over the other thrips species (Shelton *et al.*, 2006).

Several life history studies of *T. tabaci* have been published, but little is known about the impact of a wide range of temperatures on development and reproduction (Murai, 2000). Several studies have investigated the influence of the host plant on the life cycle (Murai, 2000).

Numerous causes of the large variation in observed sex ratios in natural populations and the impact on mating systems must be understood (Woldemelak *et al.*, 2021). Comprehension of the mechanisms that influence the natural sex ratio is crucial for carrying biocontrol techniques that interrupt *T. tabaci* reproduction (Woldemelak *et al.*, 2021).

Conclusions

Most collected specimens of *T. tabaci* are related to Asteraceae (11 plant species). It was collected on 8 plant species of Brassicaceae and Fabaceae. It was detected on 4 plant species of Amaranthaceae. All samples were taken in 27 sites belonging to 19 localities with different altitudes. Six plant species, including 3 plant species of Asteraceae and 2 plant species of Fabaceae, were inhabited only by the onion thrips. Five were sampled in mountainous regions with an altitude of over 300 m. Plant diversity greatly influenced *T. tabaci* life; 84.57% of the individuals of this thrips were collected on the natural environment where there is the greatest number of plants sampled, about 64.7% of the total plant species sampled in all habitats.

One male and 158 females among 187 females were found in the natural environment during sampled periods. However, 29 females were collected in adjacent habitats to natural, crop, or urban areas. Despite the rarity of males of onion thrips, we have been able to find one individual among 44 females on *A. herba alba* plant species, especially in a natural environment. The presence of sexual and asexual populations was confirmed for the first time in our country. In some cases, three kinds of colors were found, and the body color varies from very light yellow (white) to dark brown, all this color variation was seen on the last plant with the highest number of this thrips. More research is needed to confirm the host plants and the most common way of reproduction in our region by surveying the greatest number of plants in various mediums and demonstrating the sex ratio across a broad spectrum of prospection.

Acknowledgements. The authors would like to express their gratitude to Prof. Oudjehih Bachir (Department of Agronomy, Institute of Veterinary and Agronomic Sciences, University of Batna 1, Algeria) for his help in identifying thrips host plants. We would like to thank Dr. Souad Tahar Chaouche (*Centre de Recherche Scientifique et Techniques sur les Régions Aride (CRSTRA)*, Biskra, Algeria) for his help in data analysis.

References

- Allache, F., Demnati, K., & Razi, S. (2020). Thrips diversity and *Frankliniella occidentalis* trends on three melon cultivars at Biskra, Algeria. *Entomol. Faun. – Faun. Entomol.*, 73, 191-206.
- Attia, S., Khouja, S., Belaam-Kort, I., Limam, E., Ammar, M. & Grissa Lebdi, K. (2019). Pest thrips infesting citrus orchards in the South-East region of Tunisia. *J. Entomol. Zool. Stud.*, 7, 1078-1081.

- Belaam-Kort, I. & Boulahia-Kheder, S. (2017). Thrips in citrus orchards, emerging pests in Tunisia. *Entomol. Faun. – Faun. Entomol.*, 70, 77-87.
- Belaam-Kort, I., Marullo, R., Attia, S., & Boulahia-Kheder, S. (2020). Thrips fauna in citrus orchard in Tunisia: an up-to-date. *Bull. Insectol.*, 73, 1-10.
- Bournier, A. (1983). Les Thrips : Biologie, Importance Agronomique. *InraParis* pp. 128.
- Chatzivassiliou, E. K. (2002). *Thrips tabaci*: an ambiguous vector of TSWV in perspective. In *Thrips and Tospoviruses. Proceedings of the 7th International Symposium of Thysanoptera*, Italy, 2-7 July 2001, Marullo, R. and Mound, L. A. (ed.), Australian national insect collection, Canberra, pp. 69 -75.
- Djebara, F., Benzahra, A., Mimeche, F. & Saharaoui, L. (2018). Diversity of entomofauna associated with greenhouse-grown tomatoes in Algiers (North Algeria). *Studia UBB Biologia*, 63, 139-151.
- Diaz-Montano, J., Fuchs, M., Nault, B. A., Fail, J., & Shelton, A. M. (2011). Onion Thrips (Thysanoptera: Thripidae): A Global Pest of Increasing Concern in Onion. *J. Econ. Entomol.*, 104, 1-13. doi:10.1603/ec10269.
- Elimem, M. & Chermiti, B. (2013). Thrips species composition and seasonal dynamic populations in an organic citrus orchard in the central eastern coast of Tunisia. *Integrated Control in Citrus Fruit Crops IOBC-WPRS Bull.*, 95, 77-82.
- Elimem, M., Guesmi, M., Lahfef, C., Jammeli, B., Bessouda, B., & Fersi, R. (2019a). A preliminary checklist and survey of the diurnal entomofauna associated to Citrus orchards in the region of Mograne (Zaghouan) in Tunisia within environmental parameters. *J. N. Sci.*, 11, 231-241.
- Elimem, M., Karouia, W., Lahfef, C., Ben Othmen, S., Limem-Sellemi, E., & Mliki, Y. (2019b). Thrips species composition, biodiversity and seasonal dynamic populations in two vine grape orchards in the north-eastern region of Tunisia. *J. N. Sci. Agricul. Biotechnol.*, 64, 4028-4039.
- Fedorov, S. M. (1930). Tobacco Thrips (*Thrips tabaci* Lind.) as a pest of Tobacco plant in Crimea. *Entomological Section of the Governmentn Botanical Garden Yalta Crimea*, 229-248.
- Gill, H. K., Garg, H., Gill, A. K., Gillett-Kaufman, J. L. & Nault, B. A. (2015). Onion Thrips (Thysanoptera: Thripidae) Biology, Ecology, and Management in Onion Production Systems. *J Integ Pest Mngmt*, 6, 1-9. doi :10.1093/jipm/pmv006.
- Hached, W., Sahraoui, H., Attia, S. & Grissa-Lebdi, K. (2020). Importance of Thrips (Thysanoptera: Thripidae) in Tunisian citrus groves. *J. N. Sci. Agricul. Biotechnol.*, 77, 4493-4498.
- Kirk, W. D. J. (2002). The pest and vector from the West: *Frankliniella occidentalis*. In *Thrips and Tospoviruses. Proceedings of the 7th International Symposium of Thysanoptera*, Italy, 2-7 July 2001, Marullo, R. and Mound, L. A. (ed.), Australian national insect collection, Canberra, pp. 33-42.
- Koutti, A., Bounaceur, F. & Razi, S. (2017). Diversité et distribution spatiale des thrips sur différentes variétés d'agrumes en Algérie. *Rev. Agrobiol.*, 7, 263-273.

- Laamari, M. & Houamel, S. (2015). Première observation de *Thrips tabaci* et de *Frankliniella occidentalis* sur les cultures sous serre en Algérie. *EPPO Bull.*, 45, 205-206. doi:10.1111/epp.12202.
- Le Gall, J. (1961). Les problèmes phytosanitaires posés par la culture du cotonnier. *Al Awamia*, 1, 75-105.
- Lewis, T. (1973) Thrips- Their biology, ecology and economic importance. *Academic Press* London, U K, NY, USA, pp. 349.
- Loredo Varela, R. C. & Fail, J. (2022). Host Plant Association and Distribution of the Onion Thrips, *Thrips tabaci* Cryptic Species Complex. *Insects*, 13, 298. doi:10.3390/insects13030298.
- Moritz, G. (1994). Pictorial key to the economically species of Thysanoptera in central Europe. *Bull. OEPP\EPPO Bull.*, 24, 181-208. doi:10.1111/j.1365-2338.1994.tb01060.x.
- Moritz, G., Mound, L. A., Morris, D. C. & Goldarazena, A. (2004). Pest thrips of the world, visual and molecular identification of pest thrips. *Australie University of Queensland, Center for Biological Information Technology AUD*, Lucid, CD-ROM.
- Mound, L. A. (2002). So many Thrips – so few tospovirus?. In *Thrips and Tospoviruses. Proceedings of the 7th International Symposium of Thysanoptera*, Italy, 2-7 July 2001, Marullo, R. and Mound, L. A. (ed.), Australian national insect collection, Canberra, pp. 15-18.
- Mound, L. A. (2005a). Fighting, flight and fecundity: behavioural determinants of Thysanoptera structural diversity. In: *Insects and Phenotypic Plasticity* Ananthkrishnan, T.N., Whitman, D. (ed.), Enfield, NH Science, pp 81-105.
- Mound, L. A. (2005b). Thysanoptera: Diversity and interactions. *Annu Rev Entomol*, 50, 247-269. doi: 10.1146/annurev.ento.49.061802.123318.
- Mound, L. A. (2013). Homologies and host-plant specificity: recurrent problems in the study of thrips. *Florida Entomol*, 96, 318-322. doi:10.1653/024.096.0250.
- Mound, L. A., Morison, G. D., Pitkin, B. R. & Palmer, J. M. (1976). Thysanoptera: Handbooks for the Identification of British Insects. *Department of Entomology British Museum (Natural History)* London pp. 79.
- Mound, L. A. & Marullo, R. (1996). The thrips of Central and South America: an introduction. *Mem Entomol Int*, 6, 1-488.
- Mound, L. A. & Walker, A. K. (1982). Terebrantia (Insecta: Thysanoptera). *Fauna of New Zealand. Wellington, Dsir New Zealand*, pp.1, 120.
- Murai, T. (2000). Effect of temperature on development and reproduction of the onion thrips, *Thrips tabaci* Lindeman (Thysanoptera: Thripidae), on pollen and honey solution. *Appl Entomol Zool*, 35, 499- 504. doi:10.1303/aez.2000.499.
- Nault, B. A., Shelton, A. M., Gangloff-Kaufmann, J. L., Clark, M. E., Werren, J. L., Cabrera-La Rosa, J. C. & Kennedy, G. G. (2006). Reproductive modes in onion Thrips (Thysanoptera: Thripidae) Population from New York onion fields. *Environ. Entomol*, 35, 1264-1271. doi:10.1093/ee/35.5.1264.
- Ozenda, P. (1991). Flore et végétation du Sahara. *CNRS Paris, France* pp. 662.

- Pelikan, J. (1988). Records, notes and list of Thysanoptera from Algeria. *Acta Entomol. Bohemoslov.*, 85, 21-27.
- Pizzol, J., Reynaud, P., Bresch, C., Rabasse, J. M., Biondi, A., Desneux, N., Parolin, P. & Poncet, C. (2017). Diversity of Thysanoptera species and associated host plants in Southern France. *J. Mediterr. Ecol.*, 15, 13-27.
- Pourian, H. R., Mirab-balou M., Alizadeh, M., & Orosz, S. (2009). Study on biology of onion thrips, *Thrips tabaci* Lindeman (Thysanoptera: Thripidae) on cucumber (var. Sultan) in laboratory condition. *J. P. Protec. Resear.*, 49, 390-394. doi: 10.2478/v10045-009-0061-x.
- Priesner, H. (1960). A monograph of the Thysanoptera of the Egyptian deserts. *Institut du Désert d’Egypte* El Mataria, pp. 541.
- Razi, S., Bernard, E. C. & Laamari, M. (2017). A survey of thrips and their potential for transmission of viruses to crops in Biskra (Algeria): First record of the species *Frankliniella intonsa* and *Thrips flavus*. *Tunis. J. P. Protec.*, 12, 197-205.
- Razi, S., Ouamen, S. & Bernard, E. C., Laamari, M. (2019). Thysanoptera of date palm: First records from Biskra (Algeria). *Agr Nat Resour*, 53, 33–37.
- Shelton, A. M., Zhao, J. Z., Nault, B. A., Plate, J., Musser, F. R., & Larentzaki, E. (2006). Patterns of Insecticide Resistance in Onion Thrips (Thysanoptera: Thripidae) in Onion Fields in New York. *J Econ Entomol*, 99, 1798-1804. doi :10.1603/0022-0493-99.5.1798.
- Smith, E. A., Fuchs, M., Shields, E. J., & Nault, B. A. (2015). Long-Distance Dispersal Potential for Onion Thrips (Thysanoptera: Thripidae) and Iris yellow spot virus (Bunyaviridae: Tospovirus) in an Onion Ecosystem. *Environ Entomol*, 1–10. doi:10.1093/ee/nvv072.
- Varatharajan, R., Maisnam, S., Shimray, V. C. & Rachana, R. R. (2016). Pollination Potential of Thrips (Insecta: Thysanoptera) – an overview. *Zoo’s Print*, 31, 6-12.
- Vierbergen, G., Kucharczyk, H., & Kirk, W. D. J. (2010). A key to the second instar larvae of the Thripidae of the Western Palaearctic region (Thysanoptera). *Tijdschr. Voor Entomol.*, 153, 99- 160. doi: 10.1163/22119434-900000294.
- Wafy, M. E., El- Sebaey, I. I. & Henaish, M. Y. H. (2021). Revision of the thysanopterous (Terebrantia: Thripidae) in Egypt. *Egypt J Plant Prot Res Inst*, 4, 64 –83.
- Woldemelak, W. A., Ladányi, M., & Fail, J. (2021). Effect of temperature on the sex ratio and life table parameters of the leek-(L1) and tobacco-associated (T) Thrips *tabaci* lineages (Thysanoptera: Thripidae). *Pop. Ecol.*, 63, 230–237. doi:10.1002/1438-390X.12082.
- Zur-Strassen, R. (2003). Die terebranten Thysanopteren Europas und des Mittelmeer-Gebietes. In *Die Tierwelt Deutschlands*; Dahl, F. (ed.), Goecke & Evers, Keltern, Germany, 74, pp. 1–277.

Good news from newts: distribution, population size, and dynamics of two protected newt species in the Jiu Gorge National Park, Romania

Severus-Daniel Covaciu-Marcov¹✉, Denisa-Marina Pop²,
Felicia-Nicoleta Sucea³, George-Adelin Ile^{4,5},
Alfred-Ștefan Cicort-Lucaciu¹ and Sára Ferentő¹

¹University of Oradea, Faculty of Informatics and Sciences, Department of Biology, Oradea, Romania; ²Dent AS MED Oradea, DiaSer Laboratory, Oradea, Romania; ³Jiu Gorge National Park; Bumbăști-Jiu, Romania; ⁴Technological High School "Toma Socolescu", Ploiești, Romania; ⁵National Military College "Dimitrie Cantemir" Breaza, Breaza de Sus 105400, Romania; ✉Corresponding author, E-mail: severcovaciu1@gmail.com

Article history: Received: 27 March 2023; Revised: 30 November 2023;
Accepted: 18 December 2023; Available online: 28 December 2023.

©2023 Studia UBB Biologia. Published by Babeș-Bolyai University.



This work is licensed under a [Creative Commons Attribution-NonCommercial-NoDerivatives 4.0 International License](https://creativecommons.org/licenses/by-nc-nd/4.0/).

Abstract. Long-time monitoring studies recently indicated that newts are in decline in many regions. Motivated by the above-mentioned, in the year 2019, we started monitoring the newt populations from the Jiu Gorge National Park (JGNP) in the Romanian Carpathians, 10 years after the previous study on the same topic. Compared with other areas where newts are in decline, we identified new distribution locations of the two newt species which are present in the park. Also, the previously known populations have greatly increased. Thus, the *Lissotriton vulgaris* population increased 2.58 times in 10 years, and the *Triturus cristatus* increased 1.80 times in 10 years. At the same time, in areas from JGNP affected by human activities in the past (abandoned quarry and areas adjacent to the railway), the newts extended their range in the last years and occupied artificial aquatic habitats. In the case of the populations from the natural habitat, the temporal dynamics and the ratio between sexes and species followed the same evolution as in the case of other populations from Romania. The increase of newt populations from JGNP in the last 10 years was most probably a consequence of the reduced human pressure, corroborated with the large surface occupied by native forests in the

park. Thus, in natural areas, probably the best management measures for both newt species are not represented by direct (invasive) human interventions but by the conservation of the natural habitats used by the newts. A protected area should maintain the conservation status at least at the present level, and if the region is natural, this fact will maintain and also increase the newt and probably other amphibian populations.

Keywords: *Triturus cristatus*, *Lissotriton vulgaris*, habitats, forests, Carpathian Mountains, natural protected area.

Introduction

Newt decline is a well-known fact, as it was documented in numerous regions (see Denoël, 2012). Usually, this is a consequence of habitat alteration (e.g., Ficetola and De Bernardi, 2004; Arntzen *et al.*, 2017; Cupșa *et al.*, 2020). Nevertheless, recent data have shown that newt decline also occurs in stable habitats (Falaschi *et al.*, 2022). Thus, in northern Italy, in the case of two newt species, the population reduction was between 57% and 63% and was caused in the first place by invasive fish and crayfish (Falaschi *et al.*, 2022). Besides these, there are other studies that document reductions in newt populations (e.g., Griffiths *et al.*, 2010; Samraoi *et al.*, 2012; Arntzen *et al.*, 2017; Sinsch *et al.*, 2018; von Bülow and Kupfer, 2019). Nevertheless, newts decline seems to be more documented in Western Europe (see Denoël, 2012). Unlike this, in Romania, there are numerous distribution records of newts (see Cogălniceanu *et al.*, 2013), even recent ones (e.g., Bogdan *et al.*, 2013, 2014; Bondar *et al.*, 2018; Cupșa *et al.*, 2020). Besides these, there are also several studies regarding the effective of some newt populations in western Romania, populations which generally seem larger and stable (Cicort-Lucaciu *et al.*, 2009, 2010, 2011; Bogdan *et al.*, 2012; Dobre *et al.*, 2009). But these studies only present the status of some populations at a certain moment, without having any comparison base in the past, in the conditions in which the decline of newts was registered in studies that aimed longer time periods (e.g., Arntzen and Thorpe, 1999; Arntzen *et al.*, 2017; von Bülow and Kupfer, 2019; Falaschi *et al.*, 2022). A region in Romania with some data regarding the effective of two newt species populations is the Jiu Gorge National Park - JGNP (Dobre *et al.*, 2009). Nevertheless, the status of newts in JGNP does not seem exactly favorable, as in the region, only one habitat is able to sustain a large newt population because of the extremely steep relief, which, as a consequence, is unfavorable to aquatic habitats (Covaciu-Marcov *et al.*, 2009). Thus, in the year 2009, in that habitat were present 89 *Triturus cristatus* (Laurenti, 1768) individuals and 486 *Lissotriton vulgaris* (Linnaeus, 1758)

individuals (Dobre *et al.*, 2009). Due to the rarity of aquatic habitats, newts in JGNP ended up using even artificial habitats such as the settling ponds of a stone quarry (Ile and Sucea, 2018). Even if it is considered that the occurrence pattern of *T. cristatus* can be indicated by the aspect of the terrestrial habitats (Gustafson *et al.*, 2011), this fact is probably true in areas with numerous aquatic habitats available to the newts, which is not the case in JGNP (Covaciu-Marcov *et al.*, 2009). In JGNP, there are numerous terrestrial habitats favorable for the newts as a consequence of the large surface occupied by natural, deciduous forests (Theme no.11.RA/2004). Nevertheless, this fact had no influence upon the aquatic habitats, which are rare because of the relief (Covaciu-Marcov *et al.*, 2009), and newts need both (e.g., Müllner, 2011; Denoël and Lehmann, 2006; Denoël and Ficetola, 2008; Gustafson *et al.*, 2011). Moreover, in the last years, the droughts narrowed the few aquatic habitats available to the newts; therefore, in the JGNP, *T. cristatus* ended up frequently consuming *L. vulgaris* individuals (Sucea *et al.*, 2014). This was even worsened by the fact that the last years were warmer and drier in southern Romania (e.g., Bogdan and Marinică, 2010; Marinică and Marinică, 2012; Pravalie *et al.*, 2014). Thus, we hypothesized that the drought further negatively affected the newts in JGNP in the time since the previous studies (Covaciu-Marcov *et al.*, 2009; Dobre *et al.*, 2009). Knowing that newts are declining (e.g., Denoël, 2012; Arntzen *et al.*, 2017; von Bülow and Kupfer, 2019; Falaschi *et al.*, 2022), that JGNP is a natural protected area and that newts are protected (Law 49 / 2011), we aimed to monitor the newts in JGNP 10 years after the previous study from the region (Dobre *et al.*, 2009). For this, in the year 2019 we studied the newts in JGNP with the following objectives: **1.** identifying potential new distribution records, **2.** monitoring the populations in the habitat which was previously investigated with the same methods (Dobre *et al.*, 2009).

Material and Methods

The fieldwork was made in the warm season of the year 2019. Thus, starting with March and until October, we made each month a field trip in JGNP. In spring, the activity took two days, but subsequently, only one day was enough in the field. The studied region is situated in south-western Romania, in the western part of the Southern Carpathians, as JGNP is a mountainous area covered with extensive, mainly beech, forest (Theme no.11.RA/2004).

Because our study had two objectives, the methods that we used differed according to them. When we aimed to record new distribution records of newts in JGNP, we made transects through different areas of the park that we considered suitable for newts' aquatic habitats, especially for

T. cristatus, which is related to larger aquatic habitats (e.g., Fuhn, 1960; Skei *et al.*, 2006). The same method was used in the case of the herpetofauna in other protected areas in Romania (e.g., Covaciu-Marcov *et al.*, 2009, 2020). Because the alpine newt was previously recorded only in a very small area of JGNP, at altitudes above 1100 meters (Covaciu-Marcov *et al.*, 2009), this species was not especially searched, but it wasn't either identified in any habitat. If we encountered suitable aquatic habitats, newts were directly observed in the case of clear and shallow waters without being captured. In deeper and more turbid waters, newts were captured with a round net mounted on a two-meter-long metal handle; this dip net was used in other studies (e.g., Covaciu-Marcov *et al.*, 2020; Cupșa *et al.*, 2020). Newts were released in their habitats immediately after their capture.

The evaluation of the population size of *T. cristatus* and *L. vulgaris* took place firstly in the habitat from Comandă, which is considered the only one from JGNP that shelters large populations of both species (Covaciu-Marcov *et al.*, 2009; Dobre *et al.*, 2009). This is the most important (relatively permanent) aquatic habitat available for newts in JGNP; thus, it was repeatedly described previously (Covaciu-Marcov *et al.*, 2009; Dobre *et al.*, 2009; Sucea *et al.*, 2014). The size of this habitat varied depending on the rainfall regime, both between different years and in the case of the studied year seasons. Just like in the past (Dobre *et al.* 2009), the water depth reached an average of 40-50 de cm, rarely reaching 1 m; the length of the habitat was 7-10 m at its spring maximum after the snow melt, and the width was of 4-5m. The water surface reduced a lot during the warm season. The other habitats had smaller surfaces and depths, as they generally dried up faster. With the exception of the Meri quarry settling ponds which is a permanent habitat, the other was temporary and artificial habitats, which modifies from year to year. Thus, at Meri railroad station, the old habitat had a length of 3 m, a width of 1 m, and a depth of 30-40 de cm, with a lot of mud in the substratum and alders on the shores. The new habitat from Meri railroad station has a surface of more m², but it reached a depth of only 10-20 cm. In Vulcan Pass, the habitat was a puddle formed in wheel tracks on a mountain peak, without aquatic vegetation, with turbid water with only 20 depths. The habitats from the Meri Quarry settling ponds were also previously described (Ile and Sucea, 2018), as they are two artificial basins with 9 m length and 6 m wide and a half a meter depth, with a lot of mud in the substratum. In the Meri Quarry technological area, there were more puddles with a diameter between 1 and 6 m², and a depth of 30-40 cm, with crushed stones on the bottom and without vegetation, as they were described previously (Covaciu-Marcov and Sucea 2021). Finally, in the Meri quarry extraction area there were two ponds of 6 - 7 m in length, 2 - 3 m in width, and 30 - 40 cm in depth with rocky substratum and with no aquatic vegetation.

Population parameters (population size, sex ratio, etc.) were studied after capturing all individuals from the habitat at the time of the study, as in other cases (Cicort-Lucaciu *et al.*, 2009, 2010, 2011; Dobre *et al.*, 2009). The newts were captured with two dip nets, identical to the one described above. Each time, the nets were operated by the same two people, both from the shore and from the water. Similar methods of capturing newts were previously used, both in Romania (e.g., Covaciu-Marcov *et al.*, 2020; Cupşa *et al.*, 2020) and in other regions (Vuorio *et al.*, 2013). Each month we allocated an hour for capturing newts, time that was roughly sufficient to generally investigate the entire habitat. Subsequently, all newts captured during the study hour were determined, numbered, and their sex was established. After that, all newts were released into the habitat. During the summer, we monitored the presence of larvae. Also, in the case of other, smaller aquatic habitats from JGNP, we counted the newts and their sex.

Results

During 2019, we identified 10 amphibian species (including two newt species) in several distribution locations in JGNP (Tab. 1). Among newts, *T. cristatus* was the most widespread species, and among Anurans, *Bombina variegata* (Linnaeus, 1758) and *Rana dalmatina* Bonaparte, 1840 were the most widespread species (Tab. 1). The abandoned areas (at least at the time of the study) belonging to Meri quarry sheltered a high number of amphibian species (nine).

Table 1. Amphibian species observed in the investigated habitats in JGNP

	Comandă	Vulcan Pass	Meri railroad station - old	Meri railroad station - new	Meri quarry - settling ponds	Meri quarry - technological area	Meri quarry - extraction area
<i>Salamandra salamandra</i> (Linnaeus, 1758)	-	-	X	-	X	-	-
<i>Lissotriton vulgaris</i> (Linnaeus, 1758)	X	-	X	X	X	X	X
<i>Triturus cristatus</i> (Laurenti, 1768)	X	X	X	X	X	X	X

	Comandă	Vulcan Pass	Meri railroad station - old	Meri railroad station - new	Meri quarry - settling ponds	Meri quarry - technological area	Meri quarry - extraction area
<i>Bombina variegata</i> (Linnaeus, 1758)	X	-	X	-	X	X	X
<i>Hyla arborea</i> (Linnaeus, 1758)	-	-	-	-	-	X	-
<i>Bufo bufo</i> (Linnaeus, 1758)	X	-	-	-	X	X	X
<i>Bufo viridis</i> (Laurenti, 1768)	-	-	-	-	X	X	-
<i>Rana dalmatina</i> Bonaparte, 1840	X	-	X	X	X	X	-
<i>Rana temporaria</i> Linnaeus, 1758	x	-	X	-	X	X	-
<i>Pelophylax ridibundus</i> (Pallas, 1771)	-	-	-	-	X	X	X
Total no. of species	6	1	6	3	9	9	5

The largest newt populations in JGNP are still present in the habitat at Comandă; the other habitats in JGNP shelter a much lower number of newts (Tab. 2). Nevertheless, also in most of the other habitats, newt populations seem viable, a fact indicated by the presence of larvae (Tab. 2). In the habitat from Comandă, the maximum number of newts was registered on 20 April 2019, when in the habitat, 1419 newts from both species were present (Tab. 3). Most of them were *L. vulgaris* (1258); *T. cristatus* was represented by 161 individuals. Compared to April, in March and May, the number of newts present in the habitat was lower (Tab. 3). Nevertheless, the fact that in May, a high number of newts were present in the water compared to March indicated that their reproduction period had not been finished yet. The reproduction peak, indicated by the maximum number of individuals present in the water,

was registered in April. In June, newts from both species were still present in the water in high numbers. Because of the very high number of larvae (which are very sensitive), we did not capture newts in that month but just observed them from the shoreline. Nevertheless, judging by the large number of individuals observed from the shores compared with the ones observed in the previous month in the same way, in June, approximately 400-500 newts from both species were still present in the water. Adults from both newt species were observed in very small numbers (few individuals) both in June and July. Newts' larvae were encountered in the habitat from Comandă between June and August. In August, the water level was very low, and in September and October, the pond dried out completely.

Table 2. Newt population size in the investigated habitats in JGNP in 2019 (data from 2009 after Dobre *et al.*, 2009)

	Comandă		Vulcan Pass	Meri railroad station - old	Meri railroad station - new	Meri quarry - settling ponds	Meri quarry - technological area	Meri quarry - extraction area
	2009	2019						
<i>L. vulgaris</i>	486	1258	-	12	39	16	1	3
<i>T. cristatus</i>	89	161	1	10	2	10	8	30

In the case of both newt species, in the habitat from Comandă in March, males were more numerous than females, but subsequently, in the case of both species, the sex ratio turned in favor of females (Tab. 3). In the case of *L. vulgaris*, the decrease in the number of individuals of both sexes present in the water was faster than in the case of *T. cristatus*. Unlike this natural habitat with large populations, in the other habitats that are artificial by origin and generally recently colonized by newts, the sex ratio presented higher and random differences between periods (Tab. 3). At Comandă, in the natural habitat, the sex ratio was approximately equal in the case of both species (Tab. 3). In the artificial habitats, this ratio was different, and also differed between the habitats (Tab. 3).

Table 3. Population size and sex ratio dynamics of newts in the investigated ponds in JGNP in 2019 (III – X : March – October, M – males, F – females, J – juveniles, L – larvae, -- – not investigated because of the presence of larvae in the pond, *with italic* – visual investigation).

Habitat	Month	<i>L. vulgaris</i>				<i>T. cristatus</i>				Habitat	Month	<i>L. vulgaris</i>				<i>T. cristatus</i>			
		M	F	J	L	M	F	J	L			M	F	J	L	M	F	J	L
Comandă	III	517	327	-	-	71	42	-	-	Meri quarry – settling ponds	III	7	9	-	-	3	2	-	-
	IV	612	646	-	-	72	89	9	-		IV	8	5	-	-	-	9	1	-
	V	395	583	-	-	63	87	-	-		V	5	1	-	-	-	2	-	-
	VI	--	--	--	x	--	--	--	x		VI	1	--	--	x	--	2	--	x
	VII	<i>10</i>		--	x	<i>5</i>		--	x		VII	1	--	--	2	--	2	--	4
	VIII	--	--	--	x	--	--	--	x		VIII	--	--	--	2	1	--	--	x
	IX	pond dried out									IX	--	--	--	2	1	--	--	--
	X	pond dried out									X	-	-	-	-	-	-	-	-
Meri railroad station – old	III	7	2	-	-	6	1	-	-	Meri quarry – technological area	III	-	-	-	-	-	-	-	-
	IV	6	6	-	-	2	2	-	-		IV	-	1	-	-	-	5	1	-
	V	1	1	-	-	4	6	-	-		V	-	-	-	-	8			
	VI	--	--	--	x	--	--	--	x		VI	--	--	--	--	--	--	--	x
	VII	-	-	-	-	5	-	-	-		VII	-	-	-	-	-	-	-	-
	VIII	-	-	-	-	-	-	-	-		VIII	-	-	-	-	-	-	-	-
	IX	pond dried out									IX	pond dried out							
	X	pond dried out									X	-	-	-	-	-	-	-	-
Meri railroad station – new	III	17	22	-	-	1	-	-	-	Meri quarry – extraction area	III	-	-	-	-	-	-	-	-
	IV	13	12	-	-	1	1	-	-		IV	2	1	-	-	30			
	V	--	--	--	x	--	--	--	--		V	2		6					
	VI	--	--	--	x	--	--	--	--		VI	--	--	--	x	--	--	--	x
	VII	-	-	-	-	-	-	-	-		VII	-	-	-	-	-	-	-	-
	VIII	pond dried out									VIII	-	-	-	-	-	-	-	-
	IX	pond dried out									IX	pond dried out							
	X	pond dried out									X	-	-	-	-	-	-	-	-

Discussion

Although numerous recent studies clearly indicated that newts are in an obvious decline (e.g., Denoël, 2012; Samraoi *et al.*, 2012; Arntzen *et al.*, 2017; von Bülow and Kupfer, 2019; Falaschi *et al.*, 2022), our results indicated that in JGNP both species register important increases in their populations. Thus, in the habitat from Comandă, *T. cristatus* population increased by 1.80 times in 10 years, and *L. vulgaris* population increased by 2.58 in the same time interval, compared with the previous data (Dobre *et al.*, 2009). Not only the previously known populations have increased, but the two newt species were also identified in new locations in JGNP, a fact that increases even more their number in the park. The new distribution records are situated both in the close vicinity of

areas where the presence of the species was previously established, like the Meri quarry and the railway station (Covaciu-Marcov *et al.*, 2009; Ile and Sucea, 2018), as well as several kilometers from them. The favorable evolution of the newts in JGNP could be a consequence of the reduced and constant human impact that manifests in most of the park surface. At the same time, JGNP is covered almost completely by forests (Theme no.11.RA/2004), habitats that are extremely important for newts in their terrestrial phase (e.g., Müllner, 2001; Gustafson *et al.*, 2011). Thus, except for the areas surrounding the European road, which was recently modernized, and a gas pipeline that was installed near the limit of the park, JGNP experienced little human activity with disturbing potential in the 10 years that passed since the previous study (Dobre *et al.*, 2009). Nevertheless, in the year 2022, the Meri quarry resumed activity, and obviously, that had a negative impact on the newts in its area. Our results from JGNP seem to indicate that in regions with no increase in human activity (regions where habitats were not destroyed, fragmented, etc.), the newt populations can increase by themselves without any special management measures. The new distribution records highlight once again that JGNP still shelters unexplored habitats, a fact already indicated in the case of other terrestrial (Sucea, 2019) and aquatic species (Sucea *et al.*, 2022).

Although some of the new distribution records are only partially new, as newts were not searched in those regions previously (Covaciu-Marcov *et al.*, 2009), in other cases, the newts expanded their range between studies. Thus, in May 2019, *T. cristatus* was identified in Vulcan Pass, in the immediate vicinity of the JGNP limit (but with a few tens of meters off limits), at an altitude of 1428 m, but that region was not included in the previous study (Covaciu-Marcov *et al.*, 2009). Nevertheless, in the Vulcan Pass, we identified only one female at an altitude near the maximum altitude reached by this species in Romania (Cogălniceanu *et al.*, 2013). Probably, the female accidentally reached that habitat as it was the only newt present in it. The habitat was represented by a puddle formed in wheel tracks on a forest road on the top of the mountain. Moreover, the water level was low, and the puddle was totally devoid of vegetation, while *T. cristatus* prefers deep aquatic habitats with vegetation (e.g., Fuhn, 1960; Skei *et al.*, 2006). Thus, either in the region, there are other more suitable habitats for newts, or the encountered individual was a relict of former populations.

The other new distribution records of newts in JGNP were situated in the vicinity of some previously known habitats, in areas where the newts' presence was already established (Covaciu-Marcov *et al.*, 2009; Ile and Sucea, 2018). First, this is the case of the Meri quarry, where although newts were not mentioned in the past (Covaciu-Marcov *et al.*, 2009), they were recently

encountered in the settling ponds (Ile and Sucea, 2018). In 2019, both newt species were recorded in the settling ponds and in other abandoned areas in the quarry. Thus, newts were identified in several large puddles, with little vegetation in the technological areas of the quarry, where the crushed stone was loaded in trucks, but also at approximately 1 km upstream, in an area where the stone was recently exploited. Probably, the presence of newts in different areas of the quarry has the same explanation as previously in the case of the settling ponds (Ile and Sucea, 2018). Thus, the newts present in the area occupied different suitable habitats for a period after the cessation of human activity, coming from the neighboring natural areas (Ile and Sucea, 2018). At least in the case of *T. cristatus*, juveniles remain in the close vicinity of the aquatic habitat (Jarvis, 2016), but the adults were observed moving even over 1.5 km during the breeding season (Haubrock and Altrichter, 2016). Thus, they can move easily during a single year between different aquatic habitats from the Meri area. Probably, the human impact that existed in the region over time changed the number, type, and position of the habitat, as well as the newt population size. Probably, even in 2019 the newts moved often between those habitats, a fact indicated by the sex ratio different from the one registered at Comandă, by the shorter length of the aquatic period compared with Comandă, and also by the reduced number of individuals. Also, in other regions, the expansion of the newt population was related to the creation of new aquatic habitats, which newts usually colonize in only a few years (Arntzen and Teunis, 1993; Glesener *et al.*, 2022).

During the study, the Meri quarry was not in operation; thus, the entire range of habitats from the quarry was practically available to the newts. Nevertheless, in the year 2022, the quarry activity partially resumed a fact that surely had a negative impact on newts. The same fact was observed in the vicinity of the Meri railway station, where besides the previously known habitat (Covaciu-Marcov *et al.*, 2009), we identified a new habitat also resulted from human activities. The new habitat was less deep and completely exposed to the sun, thus drying faster. The new habitat was populated almost exclusively by *L. vulgaris*. Both the quarry and the railway station from Meri offer relatively flat areas in a region where the steep slopes are the cause of the rarity of aquatic habitats available for newts (Covaciu-Marcov *et al.*, 2009). The quarry and the railway leveled the ground, which made possible the formation of aquatic habitats subsequently used by newts. Therefore, the data from JGNP confirms the fact that abandoned quarries could be valuable for different amphibian species (e.g., Wirga and Majtyka, 2015; Caballero-Diaz *et al.*, 2020; Kettermann and Fartmann, 2023), including newts (e.g., Arntzen and Teunis, 1993; Arntzen and Thorpe, 1999). However, quarries replaced different

natural habitats, whose value for biodiversity is unknown (and virtually impossible to be known). Indeed, the quarry offers habitats for newts, but what if, before, on the slopes that were replaced by the quarry, there were good habitats for plants, insects, or reptiles? Thus, the high number of records regarding the value of quarries for biodiversity (e.g., Wirga and Majtyka, 2015; Caballero-Diaz *et al.*, 2020; Kettermann and Fartmann, 2023) should rather be considered a result of the high number of such artificial habitats that appeared in the landscape. The situation of newts in JGNP is a particular one because of the relief (Covaciu-Marcov *et al.*, 2009), and even this apparently favorable trend could be reversed as a consequence of resuming the quarry activity.

Compared with the previous studies regarding newt populations from Romania (Cicort-Lucaciu *et al.*, 2009, 2010, 2011; Bogdan *et al.*, 2012), it seems that the habitat from Comandă sheltered in 2019 the second largest *L. vulgaris* and *T. cristatus* populations known in the country, after the ones from Măru, in Banat region (Bogdan *et al.*, 2012). Probably the same explanations as in Măru is also true in JGNP; thus, the reduced number of available aquatic habitats attracts a large number of newts in a small area (Bogdan *et al.*, 2012). At the same time, the ratio between the two species was the one previously registered, as *L. vulgaris* was generally more numerous than *T. cristatus* (Cicort-Lucaciu *et al.*, 2009, 2011; Dobre *et al.*, 2009; Bogdan *et al.*, 2012). Although, at Comandă *T. cristatus* consumed in certain situations numerous *L. vulgaris* individuals (Sucea *et al.*, 2014), the *L. vulgaris* population from this habitat increased more compared to the *T. cristatus* population. Regarding the sex ratio, in the case of both species, their temporal dynamic was, at Comandă, similar to the one described previously, with the prevalence of males at the beginning of the aquatic season and a subsequent increase in female percentage abundance (e.g., Cicort-Lucaciu *et al.*, 2011; Bogdan *et al.*, 2012). Unlike Comandă, in artificial habitats, this dynamic was no longer observed. This fact indicates either the importance of large aquatic habitats for newts or the fact that artificial aquatic habitats from JGNP were only recently populated by newts, and the populations from those habitats are not yet stabilized. In the case of other crested newt species, it was proven that even aquatic habitats of the same type offer different conditions to the newts, but the larger ones offer more stable conditions (Lukanov *et al.*, 2021). Also, in other cases, the breeding period (the aquatic phase) of newts was shorter in artificial habitats compared with natural habitats (Cicort-Lucaciu *et al.*, 2010).

For newts, the importance of forests with rich herbaceous vegetation in the substrate close to their aquatic habitats was previously indicated, at least in the case of *T. cristatus* (Vuorio *et al.*, 2013). But forests are generally preferred by both species rather than grassy areas (Müllner, 2001). JGNP is a region with

numerous forests (Theme no.11.RA/2004), many of them being native with a rich and diverse litter fauna, even if there are many recoveries and plantations (Cicort-Lucaciu *et al.*, 2020). Although it is considered that the distribution of *T. cristatus* could be indicated by the aspect of the surrounding terrestrial habitats (Gustafson *et al.*, 2011), in JGNP, they are generally favorable to newts and occupies most of the park. Thus, the above-mentioned (Gustafson *et al.*, 2011) is probably valid in regions with numerous aquatic habitats available for newts, which is not the case in JGNP, where the steep slopes make them very rare (Covaciu-Marcov *et al.*, 2009). Thus, in JGNP, newts frequently use, in large numbers, different artificial aquatic habitats left behind by human activities in the quarry and in the railway vicinity. At the same time, in JGNP, forests are usually native, deciduous forests (Theme no.11.RA/2004), and at least for *T. cristatus* coniferous plantations was proved to be unfavorable (Gustafson *et al.*, 2011), a fact repeatedly indicated also in JGNP for different animal groups (Covaciu-Marcov *et al.*, 2009; Tomescu *et al.*, 2011; Cicort-Lucaciu *et al.*, 2020). Thus, in JGNP, the newt's distribution is rather indicated by the presence of aquatic habitats. We agree that *T. cristatus* management should focus to a greater extent on terrestrial habitats (Gustafson *et al.*, 2011), which in this case are represented by the forested areas from JGNP surrounding the aquatic habitats. Thus, JGNP should be preserved in the future as much as possible as it is nowadays, a fact that will guarantee that 10 years later, the newts will still be present here in large numbers. At a small scale, it is difficult to stop the climatic changes which will negatively affect amphibians in the future (e.g., McMenamian *et al.*, 2008; Cohen *et al.*, 2019; Souza *et al.*, 2023), but we can try to preserve habitats at least at their present status. Thus, in similar situations, the best management measure seems to be non-intervention (at least directly) because there were cases when pond restoration caused the decline of some newt populations (Sinsch *et al.*, 2018).

Although our study targeted newts in the first place, almost all amphibian species previously recorded in JGNP (Covaciu-Marcov *et al.*, 2009) were identified in the studied habitats, and in some cases, they were identified in new distribution locations. Thus, it is relevant that new results can be brought, even regarding the geographical distribution from an area considered a sampling effort hot spot (Cogălniceanu *et al.*, 2013). This fact highlights the necessity of future studies, even in regions considered to be well studied, and even more in areas not so well known, under the conditions in which in Romania, even nowadays, many regions have only a few amphibian records (Cogălniceanu *et al.*, 2013), although nothing explain their absence from the region, except for the absence of appropriate studies.

Acknowledgments. Our study was made at the request and with the support of the Jiu Gorge National Park administration, as it is part of the monitoring programs of species with conservation importance from the natural protected area. In this way, we want to thank the parks rangers, Ion Dan Iacobescu, Roland Eduard Mihuț, Tiberiu Laszlo Feczko, and Dan-Mihail Roșca, for their assistance during the fieldwork.

References

- Arntzen, J. W., & Teunis, S. F. M. (1993). A six year study on the population dynamics of the crested newt (*Triturus cristatus*) following the colonization of a newly created pond. *Herpetol. J*, 3, 99-110.
- Arntzen, J. W., & Thorpe, R. S. (1999). Italian crested newts (*Triturus carnifex*) in the Basin of Geneva: distribution and genetic interactions with autochthonous species. *Herpetologica*, 55, 4, 423-433.
- Arntzen, J. W., Abrahams, C., Meilink, W. R. M., Iosif, R., & Zuiderwijk, A. (2017). Amphibian decline, pond loss and reduced population connectivity under agricultural intensification over a 38 year period. *Biodivers. Conserv*, 26, 1411-1430.
- Bogdan, O., & Marinică, I. (2010). Considerations upon the droughts of Oltenia and their effects. *Balwois 2010*, Orhid, Republic of Macedonia – 25, 29 May 2010: 1-10.
- Bogdan, H. V., Badar, L., Goilean, C., Boros, A., & Popovici, A. M. (2012). Population Dynamics of *Triturus cristatus* and *Lissotriton vulgaris* (Amphibia) in an aquatic habitat from Banat region, Romania. *Herpetologica Romanica*, 6, 41-50.
- Bogdan, H. V., Ilieș, D., & Gaceu, O. (2013). Conservation implications on present distribution of herpetofauna from plain areas of the Western Banat region, Romania. *North-West. J. Zool*, 9, 1, 172-177.
- Bogdan, H. V., Sas-Kovács, I., & Covaciu-Marcov, S. D. (2014). Herpetofaunistic diversity in Lipova Hills, western Romania: Actual and past causes. *Bihorean Biologist*, 8, 1, 48-52.
- Bondar, A., Cicort-Lucaciu, A. Ș., & Sas-Kovács, I. (2018). New distribution records of the Danube crested newt *Triturus dobrogicus* (Kiritzescu, 1903) in southern Romania. *Oltenia. Studii și Comunicări Științele Naturii*, 34, 1, 145-148.
- Caballero-Díaz, C., Sánchez-Montes, G., Butler, H. M., Vredenburg, V. T., & Martinez-Solano, I. (2020). The role of artificial breeding sites in amphibian conservation: a case study in rural areas in central Spain. *Herpetol. Conserv. Bio*, 15, 1, 87-104.
- Cicort-Lucaciu, A. Ș., David, A., Lezău, O., Pal, A., & Ovlachi, K. (2009). The dynamics of the number of individuals during the breeding period of more *L. vulgaris* and *T. cristatus* populations. *Herpetologica Romanica*, 3, 19-23.
- Cicort-Lucaciu, A. Ș., Paina, C., Serac, C. P., & Ovlachi, K. B. (2010). Population dynamics of *Lissotriton montandoni* and *Triturus cristatus* species in two aquatic habitats. *South-Western Journal of Horticulture, Biology and Environment*, 1, 1, 67-75.

- Cicort-Lucaciu, A. Ș., Radu, N. R., Paina, C., Covaciu-Marcov, S. D., & Sas, I. (2011). Data on population dynamics of three syntopic newt species from western Romania. *Ecologia Balkanica*, 3, 2, 49-55.
- Cicort-Lucaciu, A. Ș., Cupșa, D., Sucea, F. N., Ferenti, S., & Covaciu-Marcov, S. D. (2020). Litter-dwelling invertebrates in natural and plantation forests in the southern Carpathians, Romania. *Baltic For*, 26, 1, 323.
- Cogălniceanu, D., Székely, P., Samoilă, C., Iosif, R., Tudor, M., Plăiașu, R., Stănescu, F., & Rozyłowicz, L. (2013). Diversity and distribution of amphibians in Romania. *ZooKeys*, 296, 35-57.
- Cohen, J. M., Civitello, D. J., Venesky, M. D., McMahon, T. A., & Rohr, J. R. (2019). An interaction between climate change and infectious disease drove widespread amphibian declines. *Global Change Biol*, 25, 3, 927-937.
- Covaciu-Marcov, S. D., & Sucea, F.-N. (2021). Altered breeding behaviour in some amphibians from an artificial habitat in Jiu Gorge National Park, Romania. *Herpetology Notes*, 14, 1353-1356.
- Covaciu-Marcov, S. D., Cicort-Lucaciu, A. Ș., Dobre, F., Ferenti, S., Birceanu, M., Mihuț, R., & Strugariu, A. (2009). The herpetofauna of the Jiului Gorge National Park, Romania. *North-West. J. Zool*, 5, Supplement 1, S01-S78.
- Covaciu-Marcov, S. D., Popovici, P. V., Cicort-Lucaciu, A. Ș., Sas-Kovacs, I., Cupșa, D., & Ferenti, S. (2020). Herpetofauna diversity in the middle of the Southern Carpathians: data from a recent survey (2016-2018) in Cozia National Park (Romania). *Eco Mont*, 12, 2, 11-21.
- Cupșa, D., Telcean, I. C., Cicort-Lucaciu, A. Ș., Sas-Kovács, I., Ferenti, S., & Covaciu-Marcov, S. D. (2020). Newts and fish in the remnants of former wetlands from north-western Romania in front of the same enemy. *Oltenia. Studii și Comunicări Științele Naturii*, 36, 1, 100-108.
- Denoël, M. (2012). Newt decline in Western Europe: highlights from relative distribution changes within guilds. *Biodivers. Conserv*, 21, 2887-2898.
- Denoël, M., & Lehmann, A. (2006). Multi-scale effect of landscape process and habitat quality on newt abundance: implications for conservation. *Biol. Conserv*, 130, 4, 495-504.
- Denoël, M., & Ficetola, G. F. (2008). Conservation of newt guilds in an agricultural landscape of Belgium: the importance of aquatic and terrestrial habitats. *Aquat. Conserv*, 168, 714-728.
- Dobre, F., Cicort-Lucaciu, A. Ș., Dimancea, N., Boroș, A., & Bogdan, H. V. (2009). Research upon the biology and ecology of some newt species (Amphibia) from the Jiu River Gorge National Park. *Analele Universității din Craiova, Seria Biologie, Horticultură, Tehnologie prelucrării produselor alimentare, Ingineria mediului*, 14, 475-480.
- Falaschi, M., Muraro, M., Gibertini, C., Delle Monache, D., Lo Parrino, E., Faraci, F., Belluardo, F., Di Nicola, M. R., Manenti, R., & Ficetola, G. F. (2022). Explaining declines of newts abundance in northern Italy. *Freshwater Biol*, 67, 1174-1187.

- Ficetola, G. F., & De Bernardi, F. (2004). Amphibians in a human-dominated landscape: the community structure is related to habitat features and isolation. *Biol. Conserv*, 119, 219-230.
- Fuhn, I. (1960). "Fauna R.P.R.", vol. XIV, Fascicola I, Amphibia. *Editura Academiei R.P.R.*, Bucharest, pp. 288. [in Romanian].
- Glesener, L., Gräser, P., & Schneider, S. (2022). Conservation and development of great crested newt (*Triturus cristatus* Laurenti, 1768) populations in the west and south-west of Luxembourg. *Bulletin de la Société des Naturalistes Luxembourgeois*, 124, 107-124.
- Griffiths, R. A., Sewell, D., & McCrea, R. S. (2010). Dynamics of a declining amphibian metapopulation: survival, dispersal and the impact of climate. *Biol. Conserv*, 143, 2, 485-491.
- Gustafson, D. H., Malmgren, J. C., & Mikusiński, G. (2011). Terrestrial habitat predicts use of aquatic habitat for breeding purposes – a study on the great crested newt (*Triturus cristatus*). *Ann. Zool. Fenn*, 48, 295-307.
- Haubrock, P. J., & Altrichter, J. (2016). Northern crested newt (*Triturus cristatus*) migration in a nature reserve: multiple incidents of breeding season displacements exceeding 1 km. *Herpetological Bulletin*, 138, 31-33.
- Ile, G. A., & Sucea, F. N. (2018). Artificial habitats serving as shelters for amphibians in rich biodiversity areas: a case in the Jiu Gorge National Park, Romania. *South-Western Journal of Horticulture, Biology and Environment*, 9, 2, 91-96.
- Jarvis, L. E. (2016). Terrestrial ecology of juvenile great crested newts (*Triturus cristatus*) in a woodland area. *Herpetol. J*, 26, 287-296.
- Kettermann, M., & Fartmann, T. (2023). Quarry ponds are hotspots of amphibian species richness. *Ecol. Eng*, 190, 106935.
- Law 49 / 2011. Lege nr. 49 din 7 aprilie 2011 privind aprobarea Ordonanței de urgență a Guvernului nr. 57/2007 privind regimul ariilor naturale protejate, conservarea habitatelor naturale, a florei și faunei sălbatice. Publicată în Monitorul Oficial nr. 262 din 13 aprilie 2011. [in Romanian, Romanian law].
- Lukanov, S., Doncheva, T., Kostova, N., & Naumov, B. (2021). Effects of selected environmental parameters on the activity and body condition of Buresch's crested newt (*Triturus ivanbureschi*) with notes on skin secretions. *North-West. J. Zool*, 17, 1, 34-38.
- Marinică, I., & Marinică, A. F. (2012). Excessively droughty autumn in the south-west of Romania during 2011. *Aerul și Apa. Componente ale mediului*, 2012, 351-358.
- McMenamian, S. K., Hadly, E. A., & Wright, C. K. (2008). Climatic change and wetland desiccation cause amphibian decline in Yellowstone National Park. *PNAS*, 105, 44, 16988-16993.
- Müllner, A. (2001). Spatial patterns of migrating Great Crested Newts and Smooth Newts: the importance of the habitat surrounding the breeding pond. *RANA*, 4, 279-293.
- Pravalie, R., Sîrodoev, I., & Pepteanu, D. (2014). Changes in the forest ecosystems in areas impacted by aridization in south-western Romania. *J. Environ. Health Sci*, 12, 2.

- Samraoui, B., Samraoui, F., Benslimane, N., Alfarhan, A., & Al-Rasheid, K. A. S. (2012). A precipitous decline of the Algerian newt *Pleurodeles poireti* Gervais, 1835 and other changes in the status of amphibians of Numidia, north-eastern Algeria. *Rev. Ecol. - Terre Vie*, 67, 1, 71-81.
- Sinsch, U., Kaschek, J., & Wiebe, J. (2018). Heavy metacercariae infestation (*Parastrigea robusta*) promotes the decline of a smooth newt population (*Lissotriton vulgaris*). *Salamandra*, 54, 3, 210-221.
- Skei, J. K., Folmen, D., Rønning, L., & Ringsby, T. H. (2006). Habitat use during the aquatic phase of the newts *Triturus vulgaris* (L.) and *T. cristatus* (Laurenti) in central Norway: proposition for a conservation and monitoring area. *Amphibia-Reptilia*, 27, 309-324.
- Souza, K. S., Fortunato, D. S., Jardim, L., Terribile, L. C., Lima-Ribeiro, M. S., Mariano, C. Á., Pinto-Ledezma, J. N., Loyola, R., Dobrovolski, R., Rangel, T. F., Machado, I. F., Rocha, T., Batista, M. C. G., Lorini, M. L., Vale, M. M., Navas, C. A., Maciel, N. M., Villalobos, F., Olalla-Tarraga, M. A., Rodrigues, J. F. M., Gouveia, S. F., & Diniz-Filho, J. A. F. (2023). Evolutionary rescue and geographic range shifts under climate change for global amphibians. *Front. Ecol. Evol*, 11, 1038018.
- Sucea, F. N. (2019). The second record of a rare lizard species, *Darevskia praticola* (Eversmann, 1834), in the Jiu Gorge National Park, Romania. *Ecologia Balkanica*, 11, 1, 239-241.
- Sucea, F., Cicort-Lucaciu, A. Ș., Covaciu, R. F., & Dimancea, N. (2014). Note on the diet of two newt species in Jiului Gorge National Park, Romania. *Herpetologica Romanica*, 8, 11-27.
- Sucea, F. N., Păunescu, E. A., Roșca, D. M., Mihuț, R. E., Feczko, T. L., & Iacobescu, I. D. (2022). Data on the distribution of a protected crayfish, *Austropotamobius torrentium*, in the Jiu Gorge National Park, Carpathian Mountains, Romania. *Biharean Biologist* 16, 1, 21-26.
- Theme no.11.RA/2004 (2004). Studiu privind constituirea Parcului Național Defileul Jiului. Institutul de Cercetări și Amenajări Silvice București. [in Romanian].
- Tomescu, N., Ferenczi, S., Teodor, L. A., Covaciu-Marcov, S. D., Cicort-Lucaciu, A. S., & Sucea, F. N. (2011). Terrestrial isopods (Isopoda: Oniscoidaea) from Jiului Gorge National Park, Romania. *North-West. J. Zool*, 7, 2, 277-285.
- von Bülow, B., & Kupfer, A. (2019). Monitoring population dynamics and survival of northern crested newts (*Triturus cristatus*) for 19 years at a pond in Central Europe. *Salamandra*, 55, 2, 97-102.
- Vuorio, V., Heikkinen, R. K., & Tikkanen, O. P. (2013). Breeding success of the threatened great crested newt in the boreal forest ponds. *Ann. Zool. Fenn*, 50, 158-169.
- Wirga, M., & Majtyka, T. (2015). Herpetofauna of the opencast mines in Lower Silesia (Poland). *Fragmenta Faunistica*, 58, 1, 65-70.

Dual resistance to heavy metals and antibiotics of *Aeromonas hydrophila* isolated from *Carassius carassius* (Linnaeus, 1758) in Lake Tonga, Algeria

Lamia Benhalima¹✉, Sandra Amri¹ and Mourad Bensouilah²

¹Department of Biology, Faculty of the Nature and the Life Sciences and the Earth and the Universe Sciences, 8 Mai 1945 University, Guelma, Algeria; ²Laboratory of Ecobiology of Marine Environment and Coastlines, Faculty of Science, Badji Mokhtar University, Annaba, Algeria;

✉Corresponding author, E-mail: benhalima.lamia@univ-guelma.dz; benhalimalamia300@gmail.com

Article history: Received: 15 August 2023; Revised: 28 November 2023;
Accepted: 4 December 2023; Available online: 28 December 2023.

©2023 Studia UBB Biologia. Published by Babeş-Bolyai University.



This work is licensed under a [Creative Commons Attribution-NonCommercial-NoDerivatives 4.0 International License](https://creativecommons.org/licenses/by-nc-nd/4.0/).

Abstract. *Aeromonas hydrophila*, a bacterium with significant virulence potential, is the predominant pathogenic bacteria naturally infecting fish. This study aims to identify the antibiogram and heavy metal resistance pattern of *Aeromonas hydrophila* obtained from both *Carassius carassius* fish and their surrounding water environment in Lake Tonga, Algeria. A total of 59 strains of *Aeromonas hydrophila* were isolated from 168 *Carassius carassius* samples and 144 waters samples of Lake Tonga. All the strains were tested for resistance to 13 antibiotics and three types of heavy metals (Cobalt, copper and cadmium) using disk diffusion and two-fold agar dilution method, respectively. Clinical macroscopic examination of the fish was also carried out. More than 14% of the examined fishes showed the characteristic clinical signs. Drug screening showed high levels of resistance to β -lactam antibiotics, 100% of the strains were resistant to ampicillin followed by cefalotin (91.53%) and ticarcillin (88.14%). More than 40% of the strains exhibited resistance against gentamicin, amikacin and chloramphenicol. The multiple antibiotic resistance (MAR) indexing of *A. hydrophila* strains showed that all of them originated from high-risk sources. Among tested heavy metals, bacterial isolates exhibited resistant pattern of Co>Cu>Cd. A positive correlation was observed between antimicrobial resistance

and metal tolerance (Odds Ratio>0.1). These resistant profiles could be useful information to avoid unnecessary use of chemical and antimicrobial products in the aquatic environment and to provide a novel approach to manage bacterial infection in fish.

Keywords: *Aeromonas hydrophila*, antimicrobial resistance, *Carassius carassius*, heavy metal, MAR index.

Introduction

The crucian carp (*Carassius carassius*) is a North European freshwater fish that often inhabits small ponds (Sollid *et al.*, 2003). Currently, *Carassius carassius* (*C. carassius*) is a widespread fish in Lake Tonga (northeast Algeria). It is a non-cultivated wild fish that is commonly consumed in the region. Several studies have demonstrated *Carassius carassius*'s ability to withstand exposure to high concentrations of contaminants. However, this species remains vulnerable to bacterial infections (Shuvho *et al.*, 2016).

Aeromonas have been identified as significant pathogens responsible for numerous disease outbreaks in finfish farming worldwide (Lee and Wendy, 2017). The genus *Aeromonas* comprises species that are commonly isolated from the environment, especially from aquatic samples, but also from a variety of foods, such as fish, mussels, meat products, milk and vegetables (Stratev and Odeyemib, 2016). *Aeromonas hydrophila* (*A. hydrophila*) has garnered attention due to its recurrent involvement in infections affecting both humans and fish, and its growing resistance to antimicrobial agents. This bacterium is responsible for causing hemorrhagic septicemia, skin ulcerations, and gastrointestinal tract infections in various fish hosts, including crucian carp (Jiang *et al.*, 2020; Lü *et al.*, 2016).

The presence of drug and heavy metal pollution poses a significant and widespread environmental issue, disrupting microbial ecology. Cobalt, cadmium, and copper are among the major contaminants frequently found in the environment, and at high concentrations, they prove to be extremely toxic to microbes (Benhalima *et al.*, 2020). Nevertheless, bacteria strains possess various mechanisms to cope with elevated levels of these pollutants. The increasing resistance of *A. hydrophila* to antibiotics and heavy metals is a source of concern for public health (Yu *et al.*, 2017). Hence, it is imperative to evaluate the resistance potential of this opportunistic pathogen worldwide in order to help farmers and veterinarians to establish more efficient and suitable chemical management practices for farm operations.

In this study, the main hypothesis posits that a considerable proportion of fish aeromonads in non-aquaculture freshwater environments are likely to exhibit resistance to multiple antibiotics and metals. Furthermore, it is suggested that these resistance traits can be transferred between different genera, thereby posing a significant risk to both consumers and the ecosystem. For this reason, the purpose of the present study was, for the first time, to (i) search for the presence of *A. hydrophila* in water and crucian carp of a non-aquaculture environmental (Lake Tonga), (ii) determine the antimicrobial and heavy metals sensitivity of the isolates, and identify the high-risk source.

Materials and methods

Water and fish samples

Water samples were collected from Lake Tonga (brackish water, 2400 ha; 36°53'N; 08°31'E), Northeastern Algeria (Fig.1). It is designated as a Ramsar site since 1983 and forms an integral part of the El Kala National Park, which is renowned for being one of the primary reservoirs of biodiversity in the Mediterranean Basin (Djamai *et al.*, 2019). All water samples (n = 144) were collected between January and July 2022 at four different sampling points in the system: El Bir (S1; 36.51231 N; 08.31432 E), Chalet (S2; 36.55017 N; 08.26483 E), Maizila (S3; 36.57485 N; 08.35331 E), and Oum jedour (S4; S3; 36.58615 N; 08.35847 E) (Fig.1).

A total of 168 adult crucian carp (*Carassius carassius*) weighing 15-45g were sampled. The fish was trapped and wiped down with a sterile drag-swab to collect samples of the skin's mucus layer. Subsequently, the fish samples were then gathered in sterile plastic bags and sent to the laboratory in a sterile container containing ice blocks, where the analyses were done. The collected fish (n > 30 at each sample site) were clinically examined in situ to identify any potential alterations or lesions. The overall prevalence of affected fish (P %) was then determined using the "pathological code" methodology (Girard and Elie, 2007). Mucus was scraped from the dorsal body of 3 or 4 fish 10-14 cm in length for bacteriological examination; ventral skin mucus was not collected to avoid intestinal tract and sperm contamination. The samples were collected in sterile tubes containing 5 ml of sterile alkaline peptonic water with 1% NaCl (w/v) (Oxoid, UK). The samples were incubated at 37°C for 24h (Harnisz and Tucholski, 2010). Gills and fish flesh were harvested aseptically using normal aseptic technique. Ten grams of each sample were suspended in 90 mL of sterile alkaline peptonic water (Oxoid, UK) containing 1% NaCl (w/v), homogenized for 2 minutes at high speed, and incubated at 37°C for 24 h (González-Fandos and Herrera, 2013).

Isolation and growth conditions of Aeromonas

Water samples and the fluid cultures of mucus, flesh, and gills were inoculated on thiosulfate citrate bile sucrose (TCBS) agar (Oxoid, UK). Bacteria colonies subjected to the Gram stain, oxidase and catalase tests, to identify potential *Aeromonas* spp. Several phenotypic tests (API ID 20E, BioMerieux, France) were also used in order to differentiate members of the aeromonads (Abott *et al.*, 2003).

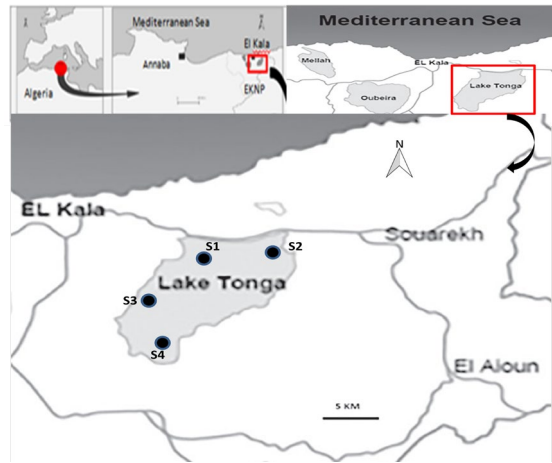


Figure 1. Study area with location of sampling sites.

Antimicrobial susceptibility testing

Antibiotic susceptibility was determined by the standard disk-diffusion method (CLSI, 2015) on Mueller-Hinton (MH) agar plates (Oxoid, UK) using 13 antibiotic disks (Lab. Pvt. Mumbai, India): Ampicillin (AM, 10 µg), ticarcillin (TI, 75 µg), imipenem (IPM, 10 µg), cephalotin (CF, 30 µg), cefotaxim (CTX, 30 µg), tetracycline (TE, 30 UI), gentamycin (GEN, 15 µg), amikacin (AKN, 30 µg), chloramphenicol (C, 30 µg), ciprofloxacin (CIP, 5 µg), nalidixic acid (NA 30 µg), nitrofurantoin (NIT, 300 µg), and fosfomycin (FOS, 15 µg + 50 µg G6P).

The *A. hydrophila* strain was grown overnight in MH broth, the turbidity of the cell suspensions was adjusted to that equivalent of a 0.5 McFarland standard and used to inoculate MH agar plates, which were incubated at 30°C for 24 h. The results were interpreted as susceptible, intermediate, or resistant according to Clinical and Laboratory Standard Institute (CLSI, 2015). Reference strain, *E. coli* ATCC 25922 (Institut Pasteur CIP 7624), was used as antimicrobial susceptibility testing control, according to CA-SFM recommendations.

The MAR index, when applied to a single isolate, is defined as a/b , where "a" represents the number of antibiotics to which the isolate was resistant and "b" represents the number of antibiotics to which the isolate was exposed. MAR index values greater than 0.2 are considered to originate from high risk sources of contamination such as humans, commercial poultry, swine and dairy cattle, where antibiotics are widely used. MAR index value less than or equal to 0.2 is considered to be the origin of the strain from animals in which antibiotics are rarely or never used (Sarter *et al.*, 2007).

Heavy metal tolerance assay

Three metals (cobalt, copper, and cadmium) were selected for the metal resistance assay based on their projected toxicities and presence in water samples. Adjusted bacterial suspensions (10^9 CFU) were subsequently disseminated onto trypticase soy agar medium TSA (Oxoid, UK), which contained various concentrations ranging from 12.5 to 3200 g mL⁻¹ of one of the three metal salts, Co(NO₃)₂, CuSO₄·5H₂O and CdCl₂·2H₂O (Sigma-Aldrich, Germany). The inoculated media was incubated for 24 h at 37°C. The Minimal Inhibitory Concentration (MIC) for each strain for the three toxic metals was determined. The bacteria were considered resistant to the tested heavy metals if they are grown at a higher concentration than the reference strain *Escherichia coli* K12. In this study, the operational definition of tolerance was determined by observing a favorable increase in bacterial growth when the concentration of heavy metals exceeded the specified resistance threshold (Lee and Wendy, 2017).

Statistical analysis

Two way analysis of variance (ANOVA) was performed to determine the significant difference among the proportions of resistant *A. hydrophila* from different sources. The relationship between bacterial strains possessing a MAR index of ≥ 0.2 and their high tolerance to toxic metals was assessed by calculating the odds ratio (OR). The confidence interval used was 95%. An OR value of ≤ 1.0 suggested a negative correlation, indicating a lower probability of the condition in the first group compared to the second or an equal likelihood in both groups. Conversely, an OR value > 1.0 indicated a positive correlation (Resend *et al.*, 2012). All analyses were performed using the software R Development Core Team, 2014 Version 3.1.2. Critical p-value was set at 0.05.

Results

Clinical investigation of fish and bacteriological examination

A clinical macroscopic analysis of *C. carassius* revealed various clinical indications, including hemorrhages, erosions, and necrosis. The findings from the examination of the captured fish are presented in Table 1. The total prevalence (P) of fish with external abnormalities amounts to 14.04%. The highest prevalence values were observed at station S3 in February, April, June, and July. Meanwhile, station S1 exhibited elevated prevalence values in March and July. It is important to note that water and habitat quality were found to be subpar during these specific months and at the mentioned stations.

Table 1: Prevalence of external lesions of *Carassius carassius*.

Sampling period	Station	Number of fish examined	Prevalence of fish affected (%)	Lesions	Disturbance	Water and habitat quality
January	S1	35	14.29	E	Medium	Mediocre
	S2	30	10	N	Medium	Mediocre
	S3	30	13.33	H, E	Medium	Mediocre
	S4	37	8.11	N	Medium	Mediocre
February	S1	40	10	E	Medium	Mediocre
	S2	37	8.11	E	Medium	Mediocre
	S3	45	24.44	H, E, N	High	Poor
	S4	50	12	H, E	Medium	Mediocre
March	S1	34	23.53	H, E	High	Poor
	S2	30	13.33	E	Medium	Mediocre
	S3	42	19.05	N, E	Medium	Mediocre
	S4	53	9.43	N, H	Medium	Mediocre
April	S1	33	12.12	E	Medium	Mediocre
	S2	32	6.25	H, E, N	Medium	Mediocre
	S3	42	21.43	N	High	Poor
	S4	40	12.5	E	Medium	Mediocre
May	S1	38	18.42	E	Medium	Mediocre
	S2	34	8.82	H	Medium	Mediocre
	S3	45	11.11	H, E	Medium	Mediocre
	S4	43	6.98	E	Medium	Mediocre
June	S1	33	9.1	E	Medium	Mediocre
	S2	31	6.45	N	Medium	Mediocre
	S3	40	22.5	H, N	High	Poor
	S4	44	13.64	N	Medium	Mediocre
July	S1	40	22.5	E, H, N	High	Poor
	S2	42	11.9	E, N	Medium	Mediocre
	S3	40	22.5	H, E	High	Poor
	S4	45	13.33	H, E	Medium	Mediocre

H: hemorrhage, E: erosion, N: necrosis.

A total of 28 *A. hydrophila* bacteria were identified in water samples collected from four distinct stations. Among the *A. hydrophila* isolates, 31 were recovered from *C. carassius* fish, with 23 originating from the gills, 5 from the mucus, and 3 from the flesh. However, a significant difference ($p < 0.05$) was observed in the prevalence of *A. hydrophila* among the various fish specimens. All the *A. hydrophila* strains were identified as Gram-negative and non-swarming. They showed positive results in oxidase and glucose-fermentative tests and were found to utilize L-arabinose, D-mannose, D-mannitol, D-lactose, D-sorbitol, and sucrose.

Antibiotic susceptibility

The percentage of *A. hydrophila* strains showing resistance against each antibiotic is given in Figure 2A. All the strains showed the highest resistance rate for beta-lactam and ticarcillin. More than 40 % of the strains were resistant to aminoglycoside and chloramphenicol. All isolates were found to be susceptible to imipinem, ciprofloxacin, nalidixic acid, nitrofurantoin, and fosfomycin. No significant differences in resistance frequencies were found among the strains of both fish and water (ANOVA, $F = 0.26$, $p = 0.532$). The resistance of the *A. hydrophila* pattern isolate toward 13 antimicrobial agents tested is shown in Table 2. Among the 59 selected isolates, 37 % were multiresistant. *A. hydrophila* strains from fish exhibited resistance from 3 to 7 antibiotics, while 75% of the strains from water showed resistance to 3 antibiotics (Fig. 2B). The MAR index ranged from 0.23 to 0.54. Among the isolates 20.34% exhibited MAR indices ≥ 0.4 , while 13.59% had MAR indices > 0.3 . All of isolates indicate high-risk contamination originating from humans or animals where antibiotics are often used.

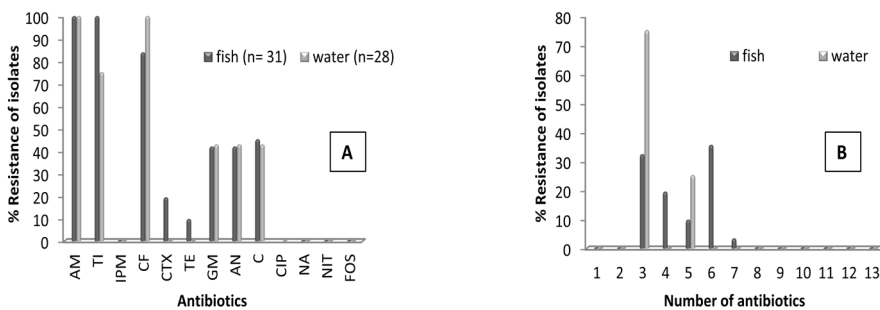


Figure 2. (A) Percentage frequency of antibiotic resistant and (B) multiple antibiotic resistance in *Aeromonas hydrophila* strains from fish (*Carassius carassius*) and water of Lake Tonga. AM: ampicillin; TI: ticarcillin; IPM: imipinem; CF: cephalotin; CTX: cefotaxim; TE: tetracyclin; GEN: gentamycin; AN: amikacin; C: chloramphenicol; CIP: ciprofloxacin; NA: nalidixic acid; NIT: nitrofurantoin, FOS: fosfomycin.

Table 2. Resistance patterns of the *Aeromonas hydrophila* isolates from fish (*Carassius carassius*) and water of Lake Tonga.

Resistance patterns	Origin			Water
	Fish Gill	Mucus	Flesh	
AM/TI/CF	6	2	2	21
AM/TI/CF/CTX	5		1	
AM/CF/GM/AN/C				7
AM/TI/CF/GM/AN	1			
AM/TI/CF/TE/C		2		
AM/TI/CF/GM/AN/C	11			
AM/TI/CF/TE/GM/AN/C		1		

AM: ampicillin; TI: ticarcillin; CF: cephalotin; CTX: cefotaxim; TE: tetracyclin; GEN: gentamycin; AN: amikacin; C: chloramphenicol.

Heavy metal tolerance essay

The bacterial isolates displayed different levels of tolerance to the three metals used in this study. All of the isolates displayed higher tolerance towards Co, while 99.3% of the bacterial isolates in the current study showed resistance to Cu. The MBC showed a similar pattern, indicating that cadmium exhibited the highest bactericidal activity (Tab. 3). Fifty six (94.91%) *A. hydrophila* isolates showed Co/Cu/Cd combination pattern. Positive correlations were observed between multidrug-resistant *Aeromonas hydrophila* (MAR >0.2) recovered from water and fish in Lake Tonga and high tolerance to all toxic metals (OR>1.0; 95% confidence interval).

Table 3. Heavy metal resistance of *Aeromonas hydrophila* strains isolated from water and *Carassius carassius*.

Metal salts	Source	MIC ($\mu\text{g mL}^{-1}$)	MBC ($\mu\text{g mL}^{-1}$)	Resistant strains (%)*
Co(NO₃)₂	Water	1200±1.38	2400±0.75	100
	Mucus	1600±0	3200±0	100
	Gills	1200±1.38	2400±2.75	100
	Flesh	800±0	2400±2.75	100
CuSO₄·5H₂O	Water	1200±1.04	2400±1.35	100
	Mucus	1200±0.68	2400±2.75	98.4
	Gills	1200±0.25	2400±1.35	98.8
	Flesh	800±0	2400±1.35	100
CdCl₂·2H₂O	Water	400±0	1600±0	100
	Mucus	400±0	800±0	100
	Gills	200±0	800±0	100
	Flesh	150±1.56	200±0	66.66

*Resistance Concentration: Co and Cu (200 $\mu\text{g mL}^{-1}$); Cd (100 $\mu\text{g mL}^{-1}$), values obtained with *E. coli* K-12 standard strain.

Discussion

Fish, with their heightened sensitivity to environmental factors, serve as valuable bioindicators in monitoring programs, aiming to assess fish food quality, monitor water and aquatic environment quality, and evaluate the health status of fish populations (Outa *et al.*, 2020). In the present study, approximately a thousand common carp were examined in Lake Tonga, revealing 153 pathological alterations, with 24.18% corresponding to hemorrhages and 75.82% to erosions and necroses of fins. These alterations appear to be more common in fish inhabiting polluted environments, likely caused by a decline in bacteriological quality and chemical contamination of the surroundings. Various bacteria, including *Aeromonas* sp., are involved in causing lesions in freshwater fish, as shown by other studies (Lee and Wendy, 2017; Zhang *et al.*, 2016). According to the 'Pathological code' methodology and integrated diagnoses, the health of fish in the Lake Tonga is considered precarious, with an overall prevalence of lesions well over 5%, indicating impaired habitat quality. Stations S3 and S1 exhibit the highest prevalence of affected fish, possibly due to the increased microbiological contamination of water in these sites (Liu *et al.*, 2020).

In the last two decades, there has been a growing interest in bacteria of the genus *Aeromonas*, mainly because of their pathogenicity to both aquatic organisms and humans. In this study, *A. hydrophila*, which causing many disease outbreaks, were found in water and crucian carp captured from Lake Tonga. According to Atef *et al.* (2016), the bacterial community associated with fish is generally related to the characteristics of the aquatic habitat, such as the bacterial load in the water. Interestingly, *A. hydrophila* were more frequently present in some of the healthy fishes. Zhang *et al.* (2016) suggested that these pathogenic strains are usually present in the healthy fishes and they may act not only as opportunistic pathogens, but also as important players of other functions. However, Cao *et al.* (2022) have reported that *A. hydrophila* is recognized for its high pathogenicity to aquatic animals and is prevalent in diseased aquatic organisms worldwide, affecting a variety of fish species and the primary indications of *A. hydrophila* infection in fish consist of necrosis, ascetic fluid accumulation, darkening of the spleen and kidney, and liver pallor.

The isolation of *A. hydrophila* resistant to beta-lactams in various freshwater environments and from fish was previously reported by several authors. Olumide and Asmat (2015) as well as Shuvho *et al.* (2016) documented complete resistance to ampicillin among all *Aeromonas* species isolated from various aquatic sources. Additionally, the substantial resistance of *A. hydrophila* to cephalotin has been documented in earlier studies (Wickramanayake *et al.*, 2020; Pfeifer *et al.*, 2010). However, the incidence of resistance to chloramphenicol

in our study was less than what was observed in the research conducted by Michel *et al.* (2003), wherein 80% of fish bacteria from brown trout, Atlantic salmon, brook trout, and their hybrids exhibited resistance to chloramphenicol. Conversely, it was higher than the findings of Zdanowicz *et al.* (2020), who reported a lower percentage (5–6%) of *Aeromonas* strains resistant to chloramphenicol. The lower occurrence of tetracycline-resistant strains of *A. hydrophila* was consistent with the findings of Shao-wu *et al.* (2013). Imipenem belongs to the carbapenem class of β -lactams, has a very broad spectrum of activity, and acts mostly on gram-negative and gram-positive bacteria (Cheng *et al.*, 2019). Also, quinolones are synthetic antibiotics used as drugs of choice for the treatment of *Aeromonas* infections in humans (Alcaide *et al.*, 2010). Fortunately, our study showed that *A. hydrophila* was 100% susceptible to imipenem, ciprofloxacin and acid nalidixic, which aligns with the findings of Asadpour *et al.* (2016), and Stratev and Odeyemi (2016). In the case of nitrofurantoin, Shamsun *et al.* (2016) demonstrated that 20% of selected *Aeromonas hydrophila* isolates from fish were resistant to this antibiotic, a result that contrasts with our own findings.

All isolates had MAR indices > 0.2 , which is unexpected, considering that most of the isolates had been previously exposed to antimicrobial agents. This finding is in agreement with the results reported by Vivekanandhan *et al.* (2002). Numerous factors contribute to the presence of multi drug resistance *A. hydrophila* isolates. According to Fang *et al.* (2019), the extensive utilization of antibiotics across medical, agricultural, and livestock sectors leads to the introduction of antibiotic remnants into the ecosystem. Consequently, the interplay of genetic resistance traits between diverse settings becomes possible through direct or indirect interaction, facilitated by mobile genetic components. The rapid surge in the prevalence of antibiotic-resistant and highly resistant aquatic *Aeromonas* species can be traced back to these organisms' ability to propagate antibiotic resistance via mobile genetic components (including plasmids, transposons, IS elements, gene cassettes, and class 1 integrons) within bacterial populations through direct cell-to-cell contact as highlighted by Zdanowicz *et al.* (2020).

Aeromonas hydrophila isolates exhibited high resistance for Co, Cu and Cd. The detected tolerance to toxic metals in *A. hydrophila* strains might be attributed to the presence of these metals in our site, given its location in agricultural and livestock farming areas. Cobalt's resistance is higher than that of other metals, which could be explained by its role as an essential micronutrient for bacteria at low concentrations. Nevertheless, at high intracellular concentration the redox active metal ion Co is highly toxic and when the content of this metallic element surpasses the established limits and persists over extended periods, it has an unfavorable impact on the operational dynamics and assortment of microbial populations. Unfortunately, this phenomenon can lead to the emergence of

bacterial resistance to heavy metals (Jiang *et al.*, 2020). Consistent with our findings, Yi *et al.* (2014) identified a prevalence of 74.4% Cd-resistant *Aeromonas* spp. among farmed fish and imported pet fish in Korea. Moreover, Wei *et al.* (2015) demonstrated that 25% of *Aeromonas* spp. isolated from red hybrid tilapia exhibited resistance to Cu. The variances in bacterial resistance to distinct metals could be elucidated through two interconnected mechanisms: co-resistance, in which genetically linked factors are concurrently expressed, and cross-resistance, where a single factor or gene confers resistance to multiple antimicrobials (Chettri and Joshi, 2022). Similar to many previous studies, resistance of *A. hydrophila* to antibiotics and heavy metals were found to be positively correlated (Lee and Wendy, 2017; Resend *et al.*, 2012). According to Pathak and Gopal (2009), water pollution caused by heavy metals increases the likelihood of bacterial resistance and infection in aquatic macrofauna, particularly fish populations and their consumers, representing a risk to public health. Jiang *et al.* (2020) indicate that the coselection or the coexistence of certain antibiotic resistance genes and heavy metal resistance genes may be beneficial to bacteria for increasing fitness in various environments. In the studies conducted by Wickramanayake *et al.* (2020) and Benhalima *et al.*, (2019), Copper and cadmium in agricultural fields and hospitals select for resistance to these substances and co-select for bacterial resistance to antimicrobials, including beta-lactams, cephalosporin and chloramphenicol.

Conclusion

This study demonstrates the presence of dual antibiotic and metal-resistant *Aeromonas hydrophila* strains in fish and their aquatic environment, which have not been subjected to any aquaculture practices thus far. *Carassius carassius*, serving as a bioindicator, can effectively monitor pollution levels. The MAR index values indicate a significant antibiotic exposure risk source in Lake Tonga. The evident phenotypic resistance to both antibiotics and heavy metals highlights the critical need to manage human activities that may contribute to resistance proliferation within Lake Tonga. The study clearly indicates that the consumption of fish infected with *A. hydrophila* could potentially pose a public health concern.

Ethics Statement

Animal studies involved in this manuscript adhere to the recommendations in the Guide for the Care and Use of Laboratory Animals of the National Institutes of Health and maintained according to the standard protocols. All the experiments were reviewed and approved by the department of Ecology and Environmental Engineering of Guelma University.

References

- Abbott, S.L., Cheung, W.K., & Janda, J.M. (2003). The genus *Aeromonas*: biochemical characteristics, atypical reactions, and phenotypic identification schemes. *J. Clin. Microbiol.*, 41, 2348–2357. <https://dx.doi.org/10.1128/JCM.41.6.2348-2357.2003>.
- Alcaide, E., Blasco, M.D., & Esteve, C. (2010). Mechanisms of quinolone resistance in *Aeromonas* species isolated from humans, water and eels. *Res. Microbiol.*, 161, 40-45. <http://dx.doi.org/10.1016/j.resmic.2009.10.006>
- Atef, H.A., El Shafei, H.M., Mansour, M.K., Snosy, S.A.M., & Abo-zaid K.F. (2016). Effect of microbiological contamination and pollution of water on the health status of fish. *Eur. J. Acad. Es.*, 3(5), 178-192.
- Asadpour, Y., Barzegar, A., Soleimannezhadbari, E., & Hashempour, A. (2016). Identification of antibiotic and heavy metal susceptibility, bacteria isolated from crayfish (*Astacus leptodactylus*) of Aras Dam. *Entomol. Appl. Sci. Lett.*, 3, 2:6-10. Available from: <http://nbn-resolving.de/urn:nbn:de:0000easl.v3i2S.944>.
- Benhalima, L., Amri, S., Bensouilah, M., & Ouzrout, R. (2020). Heavy metal resistance and metallothionein induction in bacteria isolated from Seybouse River, Algeria. *Appl. Ecol. Environ. Res.*, 18, 1721-1737. http://dx.doi.org/10.15666/aeer/1801_17211737
- Benhalima, L., Amri, S., Bensouilah, M., & Ouzrout, R. (2019). Antibacterial effect of copper sulfate against multi-drug resistant nosocomial pathogens isolated from clinical samples. *Pak. J. Med. Sci.*, 35(5), 1322-1328. <https://doi.org/10.12669/pjms.35.5.336>
- Cao, Y., Kou, T., Peng, L., Munang'andu, H.M., & Peng, B. (2022). Fructose promotes crucian carp survival against *Aeromonas hydrophila* Infection. *Front. Immunol.*, 13, 865560. <http://dx.doi.org/10.3389/fimmu.2022.865560>
- Cheng, H., Jiang, H., Fang, J., & Zhu, C. (2019). Antibiotic resistance and characteristics of integrons in *Escherichia coli* isolated from *Penaeus vannamei* at a freshwater shrimp farm in Zhejiang Province, China. *J. Food Prot.*, 82, 470-478. <http://dx.doi.org/10.4315/0362-028X.JFP-18-444>
- Chettri, U., & Joshi S.R. (2022). A first calibration of culturable bacterial diversity and their dual resistance to heavy metals and antibiotics along altitudinal zonation of the Teesta River. *Arch. Microbiol.*, 204, 241. <https://doi.org/10.1007/s00203-022-02858-1>
- CLSI. (2015). M100-S25 Performance standard for antimicrobial susceptibility testing, twenty-fifth informational supplement, Wayne, PA: Clinical and Laboratory Standards Institute.
- Djamai S., Mimeche F., Bensaci E., & Oliva-Paterna F. J. (2019). Diversity of macro-invertebrates in Lake Tonga (northeast Algeria). *Biharean Biol.*, 13 (1), 8-11.
- Fang, J., Shen, Y., Qu, D., & Han, J. (2019). Antimicrobial resistance profiles and characteristics of integrons in *Escherichia coli* strains isolated from a largescale centralized swine slaughterhouse and its downstream markets in Zhejiang, China. *Food Control*, 95, 215–222. <https://doi.org/10.1016/j.foodcont.2018.08.003>

- Girard, P., & Elie, P. (2007). Manual for the identification of the main anatomomorphological lesions and external parasites of eels. CEMAGREF/Association "Health Wild Fish". Cemagref n°110.
- González-Fandos, E., & Herrera, B. (2013). Efficacy of propionic acid against *Listeria monocytogenes* attached to poultry skin during refrigerated storage. *Food control*, 34, 601-606. <https://dx.doi.org/10.1016/j.foodcont.2013.05.034>.
- Harnisz, M., & Tucholski, S. (2010). Microbial quality of common carp and pikeperch fingerlings cultured in a pondfed with treated wastewater. *Ecol. Eng.*, 36, 466-470. <https://dx.doi.org/10.1016/j.ecoleng.2009.11.015>.
- Jiang, M., Yang L-F., Zheng, J., Chen Z.G., & Peng B. (2020). Maltose promotes crucian carp survival against *Aeromonas sobria* infection at high temperature. *Virulence*, 11(1), 877-888. <https://dx.doi.org/10.1080/21505594.2020.1787604>
- Jiang, H., Yu, T., Yang, Y., Yu, S., Wu, J., Lin, R., Li, Y., Fang, J., & Zhu, C. (2020). Co-occurrence of antibiotic and heavy metal resistance and sequence type diversity of *Vibrio parahaemolyticus* isolated From *Penaeus vannamei* at freshwater farms, seawater farms, and markets in Zhejiang Province, China. *Front. Microbiol.*, 11, 1294. <https://dx.doi.org/10.3389/fmicb.2020.01294>
- Lee, S.W. & Wendy, W. (2017). Antibiotic and heavy metal resistance of *Aeromonas hydrophila* and *Edwardsiella tarda* isolated from red hybrid tilapia (*Oreochromis* spp.) coinfecting with motile aeromonas septicemia and edwardsiellosis. *Vet. World*, 10(7), 803-807. <https://dx.doi.org/10.14202/vetworld.2017.803-807>
- Liu, Y.S., Deng, Y., Chen, C.K., Khoo, B.L., & Chua, S.L. (2020). Rapid detection of microorganisms in a fish infection microfluidics platform. *J. Hazard. Mater.*, 431, 128572. <https://doi.org/10.1016/j.jhazmat.2022.128572>
- Lü, A.J., Hu, X.C., Li, L., Sun, J.F., Song, Y.J., Pei, C., Zhang, C., & Kong, X.H. (2016). Isolation, identification and antimicrobial susceptibility of pathogenic *Aeromonas media* isolated from diseased Koi carp (*Cyprinus carpio koi*). *Iran. J. Fish. Sci.*, 15, 760-774. Available from: <https://jifro.ir/article-1-2219-en.html>
- Michel, C., Kerouault, B., & Martin, C. (2003). Chloramphenicol and florfenicol susceptibility of fish-pathogenic bacteria isolated in France: comparison of minimum inhibitory concentration, using recommended provisory standards for fish bacteria. *J. Appl. Microbiol.*, 95, 1008-1015. <http://dx.doi.org/10.1046/j.1365-2672.2003.02093.x>.
- Olumide, A.O., & Asmat, A. (2015). Antibiotic resistance profiling and phenotyping of *Aeromonas* species isolated from aquatic sources. *Saudi J. Biol. Sci.*, 65-70. <http://dx.doi.org/10.1016/j.sjbs.2015.09.016>
- Outa, J.O., Kowenje, C.O., & Avenant-Oldewage, A. (2020). Trace Elements in Crustaceans, Mollusks and Fish in the Kenyan Part of Lake Victoria: Bioaccumulation, Bioindication and Health Risk Analysis. *Arch. Environ. Contam. Toxicol.*, 78, 589-603 <https://doi.org/10.1007/s00244-020-00715-0>
- Sarter, S., Kha Nguyen, H.N., Hung, L.T., Lazard, J., & Montet, D. (2007). Antibiotic resistance in Gram-negative bacteria isolated from farmed catfish. *Food Control*, 18, 1391-1396. <http://dx.doi.org/10.1016/j.foodcont.2006.10.003>

- Shamsun, N., Mizanur Rahman, M., Uddin Ahmed, G., & Reza Faruk M.A. (2016). Isolation, identification, and characterization of *Aeromonas hydrophila* from juvenile farmed pangasius (*Pangasianodon hypophthalmus*). *Int. J. Fish. Aqua. Stud.*, 4, 52-60. Available from: <http://www.fisheriesjournal.com/archives/2016/vol4issue4/PartA/4-3-32-237.pdf>.
- Shao-wu, L., Wang, D., Hong-bai, L., & Tong-yan, L. (2013). Molecular Typing of *Aeromonas hydrophila* Isolated from Common Carp in Northeast China. *J. Northeast Agric. Univ.*, 20, 30-36. [https://doi.org/10.1016/S1006-8104\(13\)60005-7](https://doi.org/10.1016/S1006-8104(13)60005-7)
- Shuvho, C.B., Fabaya, R., Ali Reza, A.K.M., Sharifa Khatun, M., Luthful Kabir, M., Hafizur Rahman, M., & Shirajum Monir, M. (2016). Isolation, molecular identification and antibiotic susceptibility profile of *Aeromonas hydrophila* from cultured indigenous Koi (*Anabus testudineus*) of Bangladesh. *Asian J. Med. Biol. Res.*, 2(2), 332-340. <http://dx.doi.org/10.3329/ajmbr.v2i2.29078>
- Stratev, D., & Odeyemib, O.A. (2016). Antimicrobial resistance of *Aeromonas hydrophila* isolated from different food sources: A mini-review. *J. Infec. Public Health*, 9, 535-544. <http://dx.doi.org/10.1016/j.jiph.2015.10.006>
- Resende, J. A., Silva, V.L., Fontes, C.O., Souza-Filho, J.A., Rocha De Oliveira, T.L., Coelho, C.M., César ,D.E., & Diniz, C.G. (2012). Multidrug-resistance and toxic metal tolerance of medically important bacteria isolated from an aquaculture system. *Microbes Environ.*, 27(4), 449-455. <http://dx.doi.org/10.1264/jsme2.ME12049>
- Pathak, S.P., & Gopal, K. (2009). Bacterial density and antibiotic resistance of *Aeromonas* sp. in organs of metal-stressed freshwater fish *Channa punctatus*, *Toxicol. Environ. Chem.*, 91(2), 331-337. <http://dx.doi.org/10.1080/02772240802098222>
- Pfeifer, Y., Cullik, A., & Witte, W. (2010). Resistance to cephalosporins and carbapenems in Gram-negative bacterial pathogens. *Inter. J. Med. Microbiol.*, 300, 371-379. <http://dx.doi.org/10.1016/j.ijmm.2010.04.005>
- Shuvho, C.B., Fabaya, R., Ali Reza, A.K.M., Sharifa Khatun, M., Luthful Kabir, M., Hafizur Rahman, M., & Shirajum Monir, M. (2016). Isolation, molecular identification and antibiotic susceptibility profile of *Aeromonas hydrophila* from cultured indigenous Koi (*Anabus testudineus*) of Bangladesh. *Asian J. Med. Biol. Res.*, 2(2), 332-340. <http://dx.doi.org/10.3329/ajmbr.v2i2.29078>.
- Sollid, J., De Angelis, P., Gundersen, K., & Nilsson, E. G. (2003). Hypoxia induces adaptive and reversible gross morphological changes in crucian carp gills. *J. Exp. Biol.*, 206, 3667-3673. <http://dx.doi.org/10.1242/jeb.00594>
- Vivekanandhan, G., Savithamani, K., Hatha, A.A.M., & Lakshmanaperumalsamy, P. (2002). Antibiotic resistance of *Aeromonas hydrophila* isolated from marketed fish and prawn of South India. *Int. J. Food Microbiol.*, 76, 165-168. PMID: 12038573
- Wei, L.S., Mustakim, M.T., Azlina, I.N., Zulhisyam, A.K., Anamt, M.N., Wee, W., & Huang, N.M. (2015). Antibiotic and heavy metal resistance of *Aeromonas* spp. isolated from diseased red hybrid tilapia (*Oreochromis* sp.). *Ann. Res. Rev. Biol.*, 6, 264-269.

- Wickramanayake, M.V.K.S., Dahanayake, P.S., Hossain, S., De Zoysa, M., & Heo, G.J. (2020). *Aeromonas* spp. Isolated from Pacific Abalone (*Haliotis discus hannai*) Marketed in Korea: Antimicrobial and Heavy-Metal Resistance Properties. *Curr. Microbiol.*, 77, 1707–1715. <https://doi.org/10.1007/s00284-020-01982-9>
- Yi, S.W., Kim, D.C., You, M.J., Kim, B.S., Kim, W.I., Yi, S.W., & Shin, G.W. (2014). Antibiotic and heavy-metal resistance in motile *Aeromonas* strains isolated from fish. *Afr. J. Microbiol. Res.*, 8, 1793–1797. <https://dx.doi.org/10.5879/AJMR2013.6339>
- Yu, Z., Gunn, L., Wall, P., & Fanning, S. (2017). Antimicrobial resistance and its association with tolerance to heavy metals in agriculture production. *Food Microbiol.*, 64, 23-32. <https://dx.doi.org/10.1016/j.fm.2016.12.009>
- Zdanowicz, M., Mudryk, Z.J., & Perliński, P. (2020). Abundance and antibiotic resistance of *Aeromonas* isolated from the water of three carp ponds. *Vet. Res. Commun.*, 44, 9–18. <https://doi.org/10.1007/s11259-020-09768-x>
- Zhang, D., Xu, D.H., & Shoemaker, C. (2016). Experimental induction of motile *Aeromonas* septicemia in channel catfish (*Ictalurus punctatus*) by waterborne challenge with virulent *Aeromonas hydrophila*. *Aquac. Rep.*, 3, 18-23. <https://doi.org/10.1016/j.aqrep.2015.11.003>